

EARLY GENETIC AND MOLECULAR SIGNALS AND ENVIRONMENTAL  
MODULATORS OF INTESTINAL NEOPLASIA IN THE PIRC RAT

By

Amy A. Irving

A dissertation submitted in partial fulfillment of  
the requirements for the degree of

Doctor of Philosophy  
(Molecular and Environmental Toxicology)

at the

UNIVERSITY OF WISCONSIN-MADISON

2014

Date of final oral examination: 12/5/13

The dissertation is approved by the following members of the Final Oral Committee:

William F. Dove, Professor, Cancer Biology

Christopher Bradfield, Professor, Cancer Biology

Dale Bjorling, Professor, Veterinary Medicine

Mark Cook, Professor, Animal Sciences

Colin Jefcoate, Professor, Cell & Regenerative Biology

Amy Moser, Associate Professor, Human Oncology

© Copyright by Amy A. Irving 2014  
All Right Reserved

	PAGES
TABLE OF CONTENTS .....	i-v
ABSTRACT .....	vi-vii
ACKNOWLEDGEMENTS.....	viii-xi
TABLE OF ABBREVIATIONS .....	xii-xiii
 INTRODUCTION	
I. The Pirc Rat as a Model for Colorectal Cancer .....	1
Modeling colon cancer.....	1
Colon cancer risk and survival.....	3
The Pirc rat.....	5
Table I-1. Tumor multiplicities for the Pirc strains and their F <sub>1</sub> derivatives .....	6
Histopathology of human and rat tumors.....	7
Colon cancer genetics .....	7
II. Environmental Modifiers of Colon Cancer.....	9
Global distribution of incidence.....	9
Modeling inflammatory colon cancer.....	11
III. Early Detection of Colon Cancer.....	14
Visual/Direct detection .....	14
Molecular/Indirect detection.....	17
IV. Summary.....	18
References.....	20

CHAPTER ONE: Dextran sodium sulfate, a model for inflammatory colon cancer,  
enhances tumor multiplicity, growth and stage in the Pirc rat

Contributors .....	26
Abstract.....	27
Introduction.....	28
Materials & Methods .....	30
Figure 1-1. Pathology of adenoma, <i>intramucosal carcinoma</i> and early carcinoma .....	34
Results.....	35
Figure 1-2. Longitudinal body weight measurements .....	36
Figure 1-3. Pathology of colon sections exposed to dextran sodium sulfate.....	37
Table 1-1. Tumor multiplicities of untreated and DSS-treated F <sub>1</sub> Pirc rats .....	40
Figure 1-4. Whole mount colon images of rats given dextran sodium sulfate .....	41
Figure 1-5. Longitudinal tumor counts by endoscopy.....	42

Figure 1-6. Longitudinal tumor fate classification .....	43
Figure 1-7. Histological scoring of tumor stage .....	44
Figure 1-8. Phenotype of wild type rats given dextran sodium sulfate .....	45
Figure 1-9. Immunohistochemistry of $\beta$ -catenin protein expression patterns .....	48
Discussion .....	49
References .....	54

## CHAPTER TWO: Early gene expression signatures of previously inflamed normal colonic tissue may foreshadow tumor development and progression

Contributors .....	57
Abstract .....	58
Introduction .....	59
Materials & Methods .....	61
Results .....	65
Figure 2-1. Gene expression patterns in normal tissue .....	68
Figure 2-2. Gene expression patterns in normal tissue and tumor .....	74
Table 2-1. Gene candidates selected for real-time PCR validation .....	77
Figure 2-3. Real-time PCR results of four priming candidates .....	80
Figure 2-4. Real-time PCR results of most highly expressed candidates .....	81
Figure 2-5. Real-time results of candidates upregulated following DSS .....	82
Figure 2-6. Real-time results of candidates downregulated following DSS .....	83
Figure 2-7. Immunohistochemical analysis of BCAT1 protein .....	84
Discussion .....	85
References .....	92

## CHAPTER THREE: Supplementation by vitamin D compounds does not affect colonic tumor development in vitamin D sufficient murine models

Contributors .....	99
Abstract .....	100
Introduction .....	101
Materials & Methods .....	104
Figure 3-1. Experimental design .....	107
Results .....	111
Table 3-1. Serum measurements .....	112
Figure 3-2. Total intestinal tumor counts .....	113
Table 3-2. Small intestinal and colonic tumor counts .....	114
Figure 3-3. Longitudinal endoscopic tracking of colonic tumors .....	116
Table 3-3. Longitudinal tumor fate classification .....	117
Discussion .....	117
References .....	123

CHAPTER FOUR: Dietary hyper-supplementation with 25(OH)D<sub>3</sub> increases tumor multiplicity, size and net growth rate in the Pirc rat

Contributors.....	128
Abstract .....	129
Introduction .....	130
Materials & Methods.....	132
Results .....	136
Table 4-1. Serum measurements.....	137
Figure 4-1. Longitudinal body weight measurements .....	139
Figure 4-2. Small intestinal and colonic tumor multiplicities.....	141
Figure 4-3. Longitudinal tumor fate classification .....	142
Table 4-2. Small intestinal and colonic tumor multiplicities.....	143
Discussion .....	143
References .....	150

CHAPTER FIVE: A simple, quantitative method to determine rat colonic tumor volume *in vivo* using alginate gel

Contributors.....	153
Abstract .....	154
Introduction .....	155
Materials & Methods.....	158
Figure 5-1. Conversion factor to calculate tumor volume from dental stone weight.....	161
Results .....	162
Figure 5-2. Experimental design to determine the error rate of the alginate molding and dental stone casting procedures.....	163
Figure 5-3. Longitudinal tumor volume measurements.....	165
Figure 5-4. Correlation between dry dental stone weight and tumor weight.....	167
Discussion .....	168
References .....	173

CONCLUSIONS & PROSPECTUS

I. The Power of Modeling Human Colon Cancer in the Rat.....	175
Three genera.....	175
Figure CP-1. Overlap of Entrez IDs differentially expressed between normal tissue and tumor in mouse, rat and human .....	177
Manipulating the rat genome .....	178
Rat Resources.....	180
II. Managing Human Colon Cancer .....	181
Early detection .....	181

Chemoprevention .....	185
III. Summary .....	188
References .....	189
 APPENDIX A: Reciprocal F <sub>1</sub> crosses to investigate the influence of maternal and paternal strain on tumor number and time to emergence .....	 193
Figure A-1. Latency to colonic tumor emergence.....	195
Figure A-2. Colonic tumor multiplicities in reciprocal crosses .....	196
References .....	198
 APPENDIX B: Aspirin does not protect against colonic tumor formation in the Pirc rat in the presence or absence of inflammation induced by dextran sodium sulfate	
Contributors.....	199
Abstract .....	200
Introduction .....	201
Materials & Methods.....	202
Results .....	205
Figure B-1. Experimental design .....	206
Table B-1. Tumor multiplicities in the small intestine and colon.....	207
Figure B-2. Total tumor multiplicities .....	208
Figure B-3. Longitudinal endoscopic tracking of colonic tumors .....	209
Figure B-4. Longitudinal tumor fate classification.....	210
Discussion .....	211
References .....	215
 APPENDIX C: Dextran sodium sulfate does not induce colonic tumorigenesis in the <i>TGF-βR2</i> mutant rat .....	 217
References .....	218
 APPENDIX D: Dextran sodium sulfate does not induce colonic tumorigenesis in the <i>p53</i> <sup>-/-</sup> rat .....	 219
Table D-1. Tumor multiplicities in the small intestine and colon.....	221
Figure D-1. Tumor multiplicities in the small intestine and colon .....	222
References .....	223
 APPENDIX E: Whole genome analysis of Field Cancerization in the Pirc rat .....	 224
Figure E-1. Longitudinal tumor multiplicities in the colon.....	226
Figure E-2. Hierarchical clustering of differentially expressed genes .....	228
References .....	230

APPENDIX F: N <sub>2</sub> backcrosses to investigate kinky tail phenotype in an (ACIxF344)F <sub>1</sub> female and tumor multiplicity in the N <sub>2</sub> generations of ACI and F344 .....	232
Table F-1. Tumor multiplicities in the small intestine and colon .....	234
Figure F-1. Tumor multiplicities in the small intestine and colon .....	235
References .....	236
APPENDIX G: Generation of <i>Apc</i> <sup>Pirc/+</sup> <i>Bcat1</i> <sup>-/-</sup> rats to investigate the Priming Effect Hypothesis .....	237
Table G-1. Bcat1 zinc-finger nuclease mRNA injections .....	241
Figure G-1. PCR genotyping of founder rats .....	242
Figure G-2. Cel-I assay of founder rats .....	243
Table G-2. Sanger sequencing of <i>Bcat1</i> in ZFN-injected embryos .....	244
References .....	246
PROTOCOLS	
Alginate molding of colonic tumors in rodent models .....	247
Fig P-1. Alginate molding procedure .....	251
Dental stone casting of colonic tumor impressions in alginate molds .....	252
SUPPLEMENTARY GENE EXPRESSION TABLES	
Table S-1. Pirc control normal tissue versus all tumors .....	254
Table S-2. Pirc normal tissue: control versus DSS-treated .....	269
Table S-3. Pirc DSS-treated normal tissue versus all tumors .....	276
Table S-4. Wild type normal tissue: control versus DSS-treated .....	281
Table S-5. Pirc tumor: control versus DSS-treated .....	285
Table S-6. Control normal tissue: wild type versus Pirc .....	289
Table S-7. DSS-treated normal tissue: wild type versus Pirc .....	290
Table S-8. Pirc normal tissue: colonic tumor-free versus tumor-plus .....	295

## Abstract

### **“Early genetic and molecular signals and environmental modulators of intestinal neoplasia in the Pirc rat.”**

**Amy A. Irving**

Colon cancer affects 1 in 20 individuals. When an adenoma is removed during colonoscopy, 5-year survival rates can be greater than 70%. However, due to non-compliance or obstacles prohibiting access to endoscopy, 1 in 3 individuals who reach the recommended age for colonoscopy do not have the procedure. These undetected cancers progress, resulting in survival rates in the single digits.

Prevention and early detection are each key to better overall management of the disease. To enhance these efforts, we must first understand the earliest stages of tumorigenesis. Here, we highlight the experimental features of the *Apc*<sup>Pirc/+</sup> rat model for familial colon cancer that allow us to investigate molecular signals in the early adenoma and surrounding normal tissue. At each step, we compare with the human case the phenotypic, histological, and molecular signatures of the Pirc rat. By comparing the untreated Pirc rat with Pirc rats given the inflammatory compound dextran sodium sulfate (DSS), which show enhanced tumor multiplicity, growth and invasion, we have discovered molecular candidates present both in apparently normal tissue from the DSS-treated Pirc rat and in tumor. These alterations occurring during the earliest stages of tumorigenesis may represent targets for prevention, early detection and diagnosis.



The Pirc model has also proven appropriate to test the effects of two important candidate chemopreventive agents, vitamin D and aspirin, on the early colonic adenoma. Notably, a dose-dependent enhancement in tumor multiplicity was seen with vitamin D supplementation- a finding that could not be detected *in vitro*. An extension of these studies will determine under what conditions the benefits of supplementation outweigh the risks.

The experimental features of the Pirc rat, and the similarities with the human disease, provide a unique resource to increase prevention and detection of human colon cancer. Each of these lines of investigation introduce a new facet to our understanding of the earliest processes in tumor development. Where prevention fails, methods that can be carried out as a part of standard medical practice throughout the world will increase early detection efforts. These two avenues will work synergistically to reduce the overall toll of colon cancer.

## Acknowledgements

It takes a village to advance our understanding of the world in which we live. Meaningful science does not happen in a bubble. Rather, it takes the input of those in the basic sciences and those in the clinic, those expert in your field and those more knowledgeable in other arenas, conceptual thinkers and technical minds, those “in the know” and those unfettered by scientific expectations of what “should be”. My “village” encompasses my family, friends, lab mates, McArdle-mates, Toxicology-mates, collaborators, animal care staff, clinicians, Professors and friends-in-research around the globe. The list of people to whom I owe my gratitude could fill the pages of this dissertation. But I’ve learned when something seems too overwhelming, you should just start at the beginning.

First, and absolutely foremost, I thank my parents for the sacrifices they have made and the support they have given to me my entire life. When I was younger, my mother assured me that I would one day be a scientist. I refused to believe that would be my career path, as I found science in the classroom boring, and instead set my sights on becoming a veterinarian. However, as I grew and encountered new ideas and people, the path to my chosen career became muddled. I was thrilled when I was accepted as an undergraduate to the University of Wisconsin-Madison, but struggled to find my path for over a year. Without a declared major, I finally took a position in a laboratory, tending mice and autoclaving dishes. As they say, the rest is history.

It has been a long road from the nights in the laboratory filling tip boxes to transitioning to a full time position at the Medical College of Wisconsin to my return to UW-Madison for graduate school, but it has all been worth it. Recently, my mother was cleaning out her old records and gave me a receipt for the first clarinet my parents purchased for me. Payment after

payment they made, so that fine instrument could be mine alone. I've kept that receipt to remind me that good things take time and are worth waiting – and working – for.

I have been blessed to work with such wonderful, supportive individuals throughout my young career. Without these individuals, I would not have been able to accomplish a fraction of what I have. Nor would I have wanted to. Science and research are filled with perceived failures- experiments that just don't work or make sense, negative results, equipment malfunctions- but the people are the reason we continue. I have been surrounded by individuals who have a passion for what they do, and that passion is contagious. In particular, I must thank Jim Amos-Landgraf, Kathy Krentz, Jennifer Pleiman, Linda Clipson, Tammy Palenski, Melissa Keller, Erin Shanle and Brian Johnson for listening to my rants *ad nauseam* on the days where the last straw finally broke this rat researcher's back- and for helping me to rebound from those days stronger than I was before.

Through others willing to share what they know, I have expanded my horizons to understand, at least on a basic level, genetics, reproductive biology, pathology and biochemistry. The Dove laboratory is deeply rooted in the use of genetics to model disease and I had only the most basic understanding of this topic when I joined. Through the careful explanations of William Dove, Alexandra Shedlovsky and Jim Amos-Landgraf, I have learned to embrace the use of genetics to tease apart observed differences in phenotype. Through my desire to create a knockout model for a gene of interest, I learned from Kathy Krentz that, yes, both a male and a female are needed to generate fertilized embryos (I always seem to forget about the male component when setting up experiments!). The time and energy that Kathy has dedicated to this project, and her availability to examine our animals when something “just doesn't look right”, will make me forever in her debt. Ruth Sullivan has had the patience to answer the question “what kind of cell is

that?" time and again, and I always thoroughly enjoy her perspective on our current studies. Though I had to take a basic biochemistry course not once, but three times for it to begin to make sense, I am glad that I persevered. I finally understood this topic when it was related to nutrition...how could anyone not love a class relating to food? This has helped me to more fully engage in discussions about vitamin D biology with Billy Wardle, Lori Plum and Hector DeLuca. These discussions have allowed me to embrace the vitamin D project, which began as a pilot and evolved into a significant portion of my dissertation.

A laboratory is built upon the basic services that we often don't acknowledge, but could not function without. I thank those in the Histology Department, especially Jane Weeks and Ella Ward, for their eagerness to help me learn new techniques and rapid turn-around of slides. I thank our animal care staff, who cares deeply about the animals that we depend upon to reveal the secrets of biology. I thank all the undergraduate researchers who have been in our lab through the years, especially Elisa Vice, Tony Hunter, Mackenzie Eagen, Lindsay Young and Madeline Ford. Without them, many of the projects discussed here would not have gotten off the ground. Furthermore, they have each helped me in a broader sense to explain our projects more clearly, hone my teaching skills, and especially to think afresh about the science. Both the McArdle and Molecular & Environmental Toxicology office staff are the engines that keep the department and programs running smoothly.

Last, but absolutely not least, I thank my mentors. As I round the corner towards home base, I look back on my graduate career fondly. This experience would not have been the same without the amazing mentors that have guided me. Foremost, my deepest gratitude goes to William Dove and Alexandra Shedlovsky. They took a chance when they accepted me into their laboratory- I had limited comprehension of genetics and mediocre grades, two things they always

strive for when hiring undergraduates. But I had a passion for working with the rat, to understand the biology of why it differed so greatly from the mouse. Beyond the science, their kindness to my family has been unsurpassed. When I was just beginning to find my way as a new parent, they were there to support and encourage me. Though “just” a post-doc when I joined the lab, Jim Amos-Landgraf, has provided an incredible amount of mentoring, from discussing the science to navigating funding sources to introducing me to new collaborators. I knew I could always count on him when I had a question I would be embarrassed to ask anyone else, and he always had a good answer for me. Jim is the reason I am more easily able to communicate ideas I may have been too reserved to in the past. Finally, I thank my Committee members, who have devoted a significant portion of their time over the past five years to listening to me outline my projects and in turn sharing their wisdom with me. I vividly remember my first Committee meeting in March 2009, just five months after officially joining the Dove lab. I went into the meeting feeling terrified, and came out of the meeting thinking, “I have no idea what I am doing”. Now, looking back, I am happy that I chose the diverse group of individuals that I did, and that I quickly learned that their comments were meant to make the science better, for they did.

I must not forget the two people who always make my days brighter, my husband Liang and my son Andrew. No matter how stressful life becomes, I remember that they are the reason for everything I do. Weekends and evenings, nary a gripe when I had to check my rats. I will always remember Andrew’s first experience in the rat room- at twelve months old he just didn’t know where to look, this cage or that one! The wonderment I saw in his eyes that day reminds me of how I felt when I began in science, and that I still feel each time another piece of the biological puzzle falls into place.

## Table of Abbreviations

<b>Abbreviation</b>	<b>Definition</b>
25(OH)D <sub>3</sub>	25-dihydroxy-vitamin D <sub>3</sub>
AALAC	American Association for Laboratory Animal Science
ACF	aberrant crypt focus
AOM	azoxymethane
Apc	Adenomatous polyposis coli
BN	Brown Norway (rat strain)
bp	base pairs
CD	Crohn's disease
cDNA	copy DNA
cLOH	loss-of-heterozygosity at the Pirc locus in copy DNA
cMOH	maintenance-of-heterozygosity at the Pirc locus in copy DNA
CRC	colorectal cancer
CRISPR	Clustered Regularly Interspaced Short Palindromic Repeats
CrI	Charles River (rat strain)
CT	computed tomography
DFMO	D,L-alpha-difluoromethylornithine
DMH	dimethylhydrazine
DNA	deoxyribonucleic acid
DPBS	Dulbecco's phosphate buffered saline
DSS	dextran sodium sulfate
F344	Fisher 344 (rat strain)
FAP	Familial adenomatous polyposis
FDR	false discovery rate
FOBT	fecal occult blood test
gDNA	genomic DNA
GEO	Gene Expression Omnibus
gLOH	loss-of-heterozygosity at the Pirc locus in genomic DNA
gMOH	maintenance-of-heterozygosity at the Pirc locus in genomic DNA
HNPCC	Hereditary nonpolyposis colorectal cancer
HP	High Potency vitamin D analog
HPFS	Health Professionals Followup Study
IBD	inflammatory bowel disease
ICI	intracytoplasmic injection
IOM	Institute of Medicine
IRR	incidence rate ratio
KOMP	Knockout mouse project ( <a href="http://www.komp.org/">www.komp.org/</a> )
MCW	Medical College of Wisconsin
Min	Multiple intestinal neoplasia

MOM-1	Modifier of Min locus
MRI	magnetic resonance imaging
n	indicates the number of animals used in a particular study
N	indicates the generation of the animal
NBRP	National BioResource Project ( <a href="http://www.anim.med.kyoto-u.ac.jp/nbr/">www.anim.med.kyoto-u.ac.jp/nbr/</a> )
NC	Non-calcemic vitamin D analog
NHANES	National Health and Nutrition Examination Survey
NHEJ	non-homologous end joining
NS	not scored
Pirc	Polyposis in rat colon
PNI	pronuclear injection
Px	prevention
RDA	recommended daily allowance
RGD	Rat Genome Database ( <a href="http://www.rgd.mcg.edu">www.rgd.mcg.edu</a> )
RNA	ribonucleic acid
RRRC	Rat Resource and Research Center ( <a href="http://www.rrrc.us">www.rrrc.us</a> )
SD	standard deviation
SI	small intestine
TALENs	Transcription activator-like effector nuclease
TNBS	2,4,6-trinitrobenzenesulfonic acid
Tx	treatment
UC	ulcerative colitis
VC	virtual colonoscopy
VDR	vitamin D receptor
w/v	weight per volume
w/w	weight per weight
WI	Wistar (rat strain)
ZFN	zinc finger nuclease

## Introduction

### I. The Pirc Rat as a Model for Colorectal Cancer

**Modeling colon cancer.** Owing to the complex nature of human tumors, simplified model systems are necessary to study the biology of colon cancer. They allow us to manipulate conditions to better understand how cancer behaves and evolves, something that is seldom possible in the human. While *in vitro* systems tell us a great deal about these aberrant cells, certain phenomena must be tested *in vivo*. This is illustrated by our pursuit to understand the tumor-host relationship regulating the ability of a tumor to grow, remain static or regress. The host likely influences whether or not a tumor grows or progresses. This influence may come from nearby cells or from cells that relocate from other tissues in response to the presence of the tumor. Without prior knowledge of what cell types or molecules are interacting in the tumor microenvironment, it is impossible to recapitulate these conditions *in vitro*.

The first genetic model of intestinal cancer was the *Apc*<sup>Min/+</sup> mouse<sup>46</sup>, now with over 900 publications (Pubmed search 11/15/13). Many other genetic and chemical mouse models are now used to study intestinal cancer<sup>53,62</sup>. Although the deep understanding of mouse genetics and the ability to manipulate the mouse genome has historically made it a model of choice, the rat has recently made dramatic strides and is an increasingly preferred choice to model human disease<sup>23,34,37</sup>. In some cases the rat may recapitulate the human disease more closely than the mouse. For example, mammary cancers in the rat are often estrogen-responsive similar to the human, but unlike most mammary cancers in the mouse<sup>52</sup>. Recently, the ability to readily ma-



nipulate the rat genome through the use of zinc-finger nucleases, transcription activator-like effector nucleases (TALENs), clustered regularly interspaced short palindromic repeats (CRISPR)<sup>42</sup> or other methods have all rapidly accelerated the study and use of genetically modified rat models<sup>27,44</sup>. Genetic analysis is an essential tool for assessing causation in the living animal, and different types of analysis will give different perspectives. In humans, associations between molecular alterations and the presence or absence of cancer can be made. For example, the goal of The Cancer Genome Atlas Consortium, or TCGA, is to identify changes in each cancer's genome<sup>6</sup>. While this is a useful starting point, causation of particular perturbations is often difficult to determine within the patient. If a drug exists to target the molecule of interest, and this causes the cancer to regress, a causative role for that molecule in that particular cancer can be determined. Alternatively, animal models allow manipulation of the genome to assess causation of candidate molecules.

When models in multiple genera are utilized to study a particular disease, the likelihood of finding elements that overlap with the human disease increases. This occurs by two possible avenues. First, by the "or" logic, we may find signals that overlap between human tumors and at least one of our different rodent models. The rat and the mouse are rodents in two different genera, and they differ in their genetic makeup. The rat and mouse each have overlap with the human genome, but the level of conservation differs between the two rodent models. In some areas where the mouse may not reflect what is seen in the human, the rat might, and vice versa. Second, by the "and" logic, signals that are present in both a rat and a mouse model may have a greater likelihood of also appearing in human tumors. For example, the number of genes with differences in expression between normal tissue and tumor in each the rat and the mouse can be daunting. By narrowing down the list of genes to those differentially expressed in both rodent

models, the chance that particular genetic change will be conserved in humans increases. To this end, our lab developed a rat model of colon cancer to complement our existing mouse model.

**Colon cancer risk and survival.** Colon cancer is one of the leading causes of cancer and cancer-related death in the world. Excluding non-melanoma skin cancers, colon cancer ranks third in men and in women, and second overall in the number of patients diagnosed annually. Globally, an estimated 1.2 million new cases of colorectal cancer were diagnosed in 2008, comprising nearly 10% of all cancers<sup>28</sup>. In the United States in 2009, close to 140,000 people were diagnosed with colorectal cancer and over 50,000 people died from the disease. On average, one in every 20 people will develop colon cancer in their lifetime<sup>3</sup>. This translates on a local scale to about 25,000 of the 500,000 residents in Dane county developing the disease sometime within their life.

Survival rate is highly dependent on cancer stage at diagnosis. Typically, nearly 40% of colon cancers are diagnosed while the cancer is still localized to the primary site, 40% are diagnosed after the cancer has spread to regional lymph nodes, and the remaining 20% of cases are diagnosed after the cancer has metastasized<sup>33</sup>. Five-year survival rates are greater than 90% for localized cancer but plunge below 13% once it has metastasized. Without any early detection, the death toll from colon cancer within our Dane County cohort could be as high as 23,500. However, if these cancers are detected at their earliest stages with currently available technology, this number could be cut to 6,250. This still leaves room for a great deal of improvement. New methods for early detection, that are less invasive and more accessible, can further reduce the burden of this disease.

Several additional aspects further underscore the need for new modes of early detection to increase the rate of treatable cancers. The factors with the greatest impact on cancer risk are intrinsic to the patient and cannot be modified. Factors such as age, a family or personal history of polyps or cancer, or having an inflammatory bowel disease impact risk to the greatest extent. Further, while several risk factors for colon cancer are known, likely many more remain unknown. Individual lifestyle factors may each only carry a small risk, but, when combined, can substantially affect risk.

Age has the single greatest impact on sporadic cancer risk. The majority of colorectal cancer (CRC) cases are diagnosed in people over the age of 50; the average age at diagnosis is 69 years of age<sup>33</sup>. Between 2006-2010 almost no colon cancers were diagnosed in individuals under the age of 20, about 40% of cancers were diagnosed in individuals under the age of 64, and 60% of colon cancers were diagnosed in those over the age of 65. Despite their longer average lifespan, risk appears to be slightly lower in females compared to males<sup>33</sup>.

For several decades, the B6-Min mouse has been the predominant model used to study intestinal cancer. The bulk of the tumor burden in these mice develops within the small intestine and not the colon. Tumors of the small intestine are likely very different from those of the colon, and this must be considered when extending these results to the human disease. Further, B6-Min mice develop adenomas throughout the intestine at a rapid rate, resulting in mortality by 3-4 months of age. This does not allow the tumors enough time to progress past the early adenoma stage, limiting study of this aspect of tumor biology. In resistant (SWR x B6)F<sub>1</sub>-Min mice, nearly 90% of tumors were invasive adenocarcinomas at one year of age, but the majority of the tumors were in the small intestine<sup>29</sup>. By contrast, the Pirr rat model develops its tumors primarily

in the colon, can survive 6-12 months and shows a spectrum of tumor stages corresponding to the earliest stages of cancer in the human.

**The Pirc rat.** The *Apc*<sup>Pirc/+</sup> (Polyposis in rat colon) rat was created by ENU-mutagenesis of the Fisher 344 (F344) rat germline and carries a nonsense mutation at nucleotide 3409 of *Apc*<sup>5</sup>. The coisogenic F344-Pirc strain was created by backcrossing to F344 (N19 as of 11/2013). Like the Min mouse this model is highly relevant to the human disease since over 80% of human colon cancers contain mutations in the *Apc* gene<sup>24</sup>. *Apc*, or adenomatous polyposis coli, is a tumor suppressor gene involved in Wnt signaling. Located on chromosome 5 in the human, and chromosome 18 in the mouse and rat, this gene produces the APC protein. Under normal conditions, the APC protein forms a “destruction complex” with Axin and GSK-3; this complex then promotes proteolytic degradation of  $\beta$ -catenin in the cytoplasm. This reduces the amount of  $\beta$ -catenin that enters the nucleus, where it can interact with TCF/LEF family transcription factors to promote gene expression. The Pirc mutation is predicted to cause the APC protein to be truncated within the  $\beta$ -catenin binding domain, rendering it non-functional. The Pirc mutation is embryonic lethal in homozygous form and is thus maintained in heterozygous form, as *Apc* function is essential for development.

The Pirc rat develops the majority of its tumor burden in the colon rather than the small intestine, which recapitulates the phenotype of the human disease. The rat is also similar to the human in that tumors continue to emerge as the animal ages, and older rats have more and larger tumors than younger rats. Like humans, the Pirc rat shows a gender bias for tumor development, towards an increased susceptibility in males over females. Tumors that develop in the Pirc rat look very similar to those in humans<sup>5</sup>. Most tumors that develop in the colon are peduncular, in

contrast to the flat adenomas of the small intestine. In the rat, tumors can reach 1 cm or greater in diameter, allowing enough tissue to be collected for multiple modes of analysis.

On the F344/NTac background, Pirc rats begin to develop colon tumors as early as three months of age, and develop an average of  $9.2 \pm 8.3$  (female) to  $20.0 \pm 9.5$  (male) colonic tumors by 7-8 months of age (Table I-1). Since the creation of the original F344-Pirc strain, the Pirc mutation has been back-crossed on to two additional strains, ACI and Brown Norway (BN). ACI Pirc rats (N19 as of 11/2013) are more susceptible to tumor development than are F344 Pirc rats, harboring over 30 colonic tumors by 6 months of age. By contrast, BN Pirc rats (N10 as of 11/2013) are more resistant to tumor development, often surviving longer than one year without developing any tumors. Tumor regionality within the colon also varies by strain, with tumors developing to a greater extent in the distal two-thirds of the colon in F344-Pirc and ACI-Pirc rats and in the proximal third of the colon in BN-Pirc rats (See Chapter 1, Figure 1-4). This variability in tumor multiplicity and regionality between the three inbred Pirc strains allows one to choose the best tumor distribution demanded by the particular experimental needs.

**Table I-1.** Tumor multiplicities in the small intestine (SI) and colon of each of the Pirc strains and their  $F_1$  derivatives.

Strain	Sex	n of animals	Age (days)	SI (mean $\pm$ SD)	Colon (mean $\pm$ SD)
BN	F	4	180-182	0.0 $\pm$ 0.0	0.0 $\pm$ 0.0
(N6-N10)	M	2	180-182	0.0 $\pm$ 0.0	1.5 $\pm$ 2.1
(BNxF344)F1	F	6	179-360	0.2 $\pm$ 0.4	2.3 $\pm$ 3.4
	M	8	180-359	2.6 $\pm$ 1.4	12.1 $\pm$ 14.9
F344	F	13	212-220	0.9 $\pm$ 1.0	9.2 $\pm$ 8.3
	(N10-N19)	M	38	136-232	16.3 $\pm$ 7.5
(F344xACI)F1	F	31	49-272	1.4 $\pm$ 2.1	5.3 $\pm$ 3.5
	M	18	171-184	12.7 $\pm$ 5.5	25.4 $\pm$ 10.8
ACI	F	1	179	0.0	6.0
	(N10-N19)	M	6	120-179	5.3 $\pm$ 4.5

**Histopathology of human and rat tumors.** Generally, tumors within the Pirc rat align with the earliest stages in the human, making it a useful model in which to study early indicators of colon tumorigenesis. In the F344-Pirc rat, roughly 80% of tumors are considered adenomas, while the remaining 20% are classified as adenocarcinomas, showing local invasion of neoplastic cells into the stalk<sup>5</sup>. Histopathological changes include dysplasia, nuclear enlargement, and crypt expansion with loss of normal columnar architecture. Tumors that develop are positive for cytoplasmic and nuclear accumulation of  $\beta$ -catenin (see Chapter 1, Fig 1-9). Metastasis to other organs has not been seen, though this has not yet been extensively examined.

**Colon cancer genetics.** Beyond *Apc*, human colon cancers show a diverse array of genetic mutations and epigenetic changes. In colorectal cancers, on average about 66 genes per cancer show subtle mutations that would be expected to alter their encoded proteins<sup>58</sup>. Though advances in genomic sequencing have allowed researchers to profile a large number of tumors from many individual patients, difficulties arise when they attempt to discern which events are drivers and which are simply passengers. Statistical analyses conducted on 11 colorectal tumors found that the majority of mutations in a given tumor are bystanders, while only about 15% are drivers of initiation or progression<sup>60</sup>. There are a small subset of mutations that occur frequently in cancers across many individuals, such as *Apc*, *Kras*, and *p53*. Many more infrequently mutated genes exist that show a great deal of variability between individuals. These infrequently mutated genes may play a role in resistance of some tumors to therapeutic agents. Beyond mutations, many other alterations to the transcriptome, such as methylation, or proteome, such as post-translational modifications, can alter the expression of a gene or protein without mutating the gene itself<sup>58</sup>.

The sequence by which mutations commonly occur in colon cancers may also play a role in the tumor behavior. Proposed by Bert Vogelstein, the coined “Vogelgram” shows *Apc* mutations arising early in the dysplastic sequenced, followed by *K-ras*, *DCC*, and eventually *p53* in advanced cancer. However, cancers that are initiated in the presence of inflammation are reported to show *p53* mutations earlier and *Apc* mutations later<sup>49,57</sup>, though this claim is debated<sup>17</sup>. The genetic profile may even differ within a lesion. When a single tumor that contained areas of adenoma and carcinoma was examined for the presence of various mutations, one stark difference was found: the area of carcinoma had one allele of *p53* that was deleted and another allele that was mutated, while the area of adenoma was wild type for *p53*<sup>7</sup>. Somatic TGF- $\beta$  receptor 2 mutations are also present in about 30% of later stage colon cancers<sup>8</sup>. The interaction between *p53* loss (Appendix D) or TGF- $\beta$  receptor mutation (Appendix C) and an inflammatory microenvironment are explored further here using rat models.

Many of the experiments within this dissertation utilize an F<sub>1</sub> design. This increases the power of the Pirc model to investigate the genetics of tumorigenesis in three ways. First, F<sub>1</sub> Pirc progeny often show a phenotype that is a hybrid between the two parental lines. Thus, tumor multiplicity is increased and time to first tumor is decreased in (ACIxF344)F<sub>1</sub>-Pirc progeny compared to F344-Pirc rats, but multiplicity is less than that in ACI-Pirc rats (see Appendix A). This increases efficiency and allows us to complete studies in a shorter period of time, while still allowing the animals to live long enough when treated with compounds that further enhance tumor development (see Chapter 1). Alternatively, when an experiment necessitates animals that have a low tumor multiplicity, we can cross F344 to BN. These resultant F<sub>1</sub> Pirc rats develop very few colonic tumors within a reasonable amount of time (see Appendices A and E). A second reason to utilize the F<sub>1</sub> generation is that these animals display “hybrid vigor”, with a re-

duced impact of recessive traits specific to one inbred rat strain influencing tumor development. This was the case with the *modifier of Min (Mom-1)* locus in the mouse encoding *Pla2g2a*, which alters tumor number from the original strain<sup>20</sup>. Third, by using an F<sub>1</sub> we create a model that is informative at every locus that varies between the two parental strains across the entire genome. This creates the opportunity to investigate genetic and epigenetic changes that occur in the tumor, whether directed or stochastic. We have utilized this strategy with the *Pirc* mutation, which is viable when heterozygous and thus present in one of two alleles in the somatic genome, to show a variety of genetic and epigenetic expression patterns by which the function of the wild type allele is lost in tumors<sup>4</sup> (see Chapter 1).

The myriad of mutations seen in tumors that arise in the colons of humans can be very difficult to study in a systematic manner. Although chemical (eg: azoxymethane) or environmental (eg: high fat diet) models may more closely resemble the heterogeneity of the human disease, the unknown factors attributed to these models may greatly hinder the ability to study the impact of additional factors (eg: inflammation). The *Pirc* rat is useful in these experiments because, although it is a model for familial colon cancer, the mutation of the *Apc* gene is seen in the majority of spontaneous human cancers<sup>24</sup>. This controlled genetic model allows us to more clearly detect modifiers of the tumor lineage, the tumor microenvironment, or the system overall. By reducing noise from uncontrolled variables, the signal to noise ratio is increased, allowing detection of more subtle phenotypes.

## **II. ENVIRONMENTAL MODIFIERS OF COLON CANCER**

**Global distribution of incidence.** Colon cancer varies widely around the globe. Developed regions, such as Australia, New Zealand, Europe and North American, have the highest age-



standardized rates of colon cancer, with incidence rates from about 20-40 per 100,000 people per year<sup>28</sup>. Less developed regions, including Central America and Africa, have the lowest rates of colon cancer, with incidence rates ranging from about 5-10 per 100,000 people per year. Age-standardized mortality rates range from about 12-20 per 100,000 people per year in Europe to about 3 per 100,000 people per year in Africa. Although, it is reasonable to attribute some of the differences in incidence rate to access to endoscopy for early detection, the death rate is only slightly higher in less developed regions (56%) than in more developed regions (42%), indicating that a global disparity in colon cancer risk does exist<sup>28</sup>. Interestingly, within one to three generations of a population migrating from a low-risk area to a high-risk area, the risk approximates that of the new high-risk locale<sup>59</sup>. This emphasizes the importance of environmental factors as a direct cause or contributor to increased risk of colonic neoplasia.

Geographical region is also associated with colon cancer incidence and mortality within the United States. First noted in 1980, colorectal cancer death rates are higher in Southern states along the Appalachian Mountain corridor and lower in the Northeast<sup>26</sup>. Recently, age-adjusted incidence rates have shown a similar pattern, where the lowest rates occur along the Pacific and Atlantic coasts, and in the Western states, and the highest rates occur in the Central states<sup>13</sup>. In the same recent survey, age-adjusted mortality rates tended to correlate with incidence rates. The influence of screening rates on incidence and mortality data remains a question, and indeed in 2010 the states which had lower rates of adults aged 50-75 with up-to-date colorectal cancer screening tended to have higher rates of the disease<sup>14</sup>.

Many factors may explain the apparent association between geography and colon cancer incidence and mortality. The amount of solar radiation, temperature, pollution, access to adequate preventive care, diet, level of physical activity, and presence of pathogens may each play a

role in an individual's risk for developing the disease. One environmental factor that has recently garnered great interest and that may be related to sunlight exposure is vitamin D<sup>10</sup>. Indeed, 25-hydroxy-vitamin D<sub>3</sub> levels tend to be lower in individuals who develop colon cancer<sup>26,38</sup>. However, supplementation of individuals with vitamin D<sub>3</sub> has generally not been shown to reduce risk<sup>11,55</sup>. Whether increased serum 25(OH)D<sub>3</sub> levels by way of 25(OH)D<sub>3</sub> or vitamin D dietary supplementation protect from incidence or growth of early colonic tumors is explored using the Pirc rat model in Chapters 4 and 5.

**Modeling inflammatory colon cancer.** Inflammation is one environmental factor with a known role in some cancers, particularly hepatic cancers. Several lines of evidence also support the association between inflammation and the increased likelihood of developing colon cancer. Greater histological inflammation at colonoscopy is often an indicator for subsequent risk of neoplasia<sup>56</sup>. Adenoma size appears to correlate with the degree of acute and chronic inflammation<sup>9</sup>. Patients that have an underlying inflammatory bowel disease (IBD), such as ulcerative colitis (UC) or Crohn's disease (CD) are at an increased risk of developing colon cancer. Further, IBD patients who take maintenance medication to reduce inflammation tend to have lower risk of developing cancer than patients who do not<sup>56</sup>. In fact, even in non-predisposed populations, the regular use of aspirin has been associated with reduced risk<sup>25</sup>. Since this reduction is only evident after a decade or more of use, the role of aspirin may be important specifically in preventing lesions at an early stage. The use of aspirin as both a chemopreventive and a treatment option are explored with the Pirc rat model in Appendix B.

Though there has been some debate recently regarding whether IBD patients have an increased risk of colon cancer, most evidence suggests that the threat of cancer is real. One study

of patients in Norway found that the risk of colorectal cancer (CRC) among patients with UC was comparable to that of the general population<sup>39</sup>. However, patients with long-standing or widespread disease were at an increased risk. They also found that the overall risk of CRC declined over time in the UC patient population, possibly as a result of improved therapies for treating IBD. Another study with 20 years of follow-up in a Finnish cohort, showed that the risk of CRC was only moderately increased in IBD patients<sup>43</sup>. Some of the discrepancy seen between studies may be derived from IBD patients developing both sporadic and inflammation-associated colon cancers, which may differ. When IBD patients are classified based on the degree of atypia within the adenoma, those with atypical adenomas had a higher risk of developing advanced neoplasias than those with typical adenomas<sup>50</sup>. Survival, regardless of stage, appears to be worse in CRC patients with IBD<sup>1</sup>. A large meta-analysis of 116 studies (over 54,000 IBD patients and 1500 CRCs) demonstrated a 10 year risk of developing CRC of 2%, a 20-year risk of 8% and a 30-year risk of 18% in IBD patients<sup>18</sup>, compared with about a 5% life time risk for the general population.

While the Pirc rat is a good model of familial and spontaneous colon cancer, alone it may not be sufficient to study inflammatory colon cancers. There are multiple methods to induce colonic inflammation in model systems and they include both perturbations to epithelial integrity (chemical models, such as TNBS or DSS) and to the immune system (genetic models, such as the IL-10 knockout); the two are not necessarily mutually exclusive. Because of the similarities with human colonic inflammatory disease upon histological inspection, namely ulcerative colitis, we chose to use the DSS model.

DSS was first used to induce intestinal inflammation and tumors in rats over three decades ago<sup>31</sup>. Animals given DSS in the diet or drinking water develop bloody, loose stools and

watery diarrhea. Pathological changes in the colorectal mucosa of DSS-treated wild type rats include ulceration and squamous metaplasia. While acute colitis is characterized by goblet cell loss and inflammatory cell infiltrates, chronic colitis shows epithelial necrosis, crypt abscesses and diffuse lymphocytic infiltrates<sup>2</sup>. The effects of DSS on tissue pathology and tumorigenesis in the Pirc rat are explored in Chapter 1.

Though DSS is often cited as an ‘inflammatory agent’, the mechanism by which this inflammation occurs remains unclear. Recent studies have begun to shed light on the issue. When colon explant cultures covered in a mucus layer were exposed to 3% DSS (49 kDa MW) in culture, the mucus layer was permeabilized by 2  $\mu\text{m}$  beads- approximately the upper limit for the size of a bacterium- within 15 minutes<sup>41</sup>. Furthermore, when colons from mice given DSS were examined 12 hours after treatment, bacteria had penetrated the inner mucus layer and had reached the underlying epithelium. This occurred before any inflammatory cells were seen. This suggests that the bacteria reaching the epithelial layer is the event that triggers the subsequent inflammatory response. However, this experiment suggests only an association between bacterial presence and the subsequent development of inflammation. Although it has been shown that germ-free Min mice do not significantly differ in their phenotype from Min mice housed in a conventional setting<sup>21</sup>, the effect of DSS treatment on germ free animals has not yet been explored.

Disruption of the inner mucus layer may also be a contributing factor to the development of UC in humans, making the DSS model relevant to the study of this disease. The inner mucus layer of UC colon samples from patients with active disease was found to be highly penetrable, while the majority of patients in remission had an impenetrable mucus layer similar to patients without disease<sup>40</sup>. While some disagreement exists regarding whether the number of goblet cells

is decreased<sup>45</sup> or unchanged<sup>40</sup>, patients with active inflammation have fewer mucus-filled goblet cells, which may explain the difference in quality or thickness of the upper mucus layer. These patients were also shown to have bacteria penetrating the mucus layer to reach the epithelium.

DSS also affects the proliferation rate of cells of the colon. Five days of DSS treatment of wild type mice reduced the number of proliferating cells from 3.2 to 0.4 per crypt<sup>54</sup>. Surprisingly, DSS did not affect the number of cells undergoing apoptosis as compared with untreated mice. Since the gut has a high turnover rate, this dramatic suppression of proliferation could have a rapid effect on gut integrity, even without affecting apoptosis.

The cytokine profiles also differ between acute and chronic colitis. Acute colitis shows upregulation of IL-6, TNF- $\alpha$ , and IL-17, while chronic colitis shows upregulation of IL-4 and IL-10<sup>2</sup>. Others have shown that DSS treatment also increases the chemokine Cxcl2 in the *lamina propria* and submucosa and the production of Mmp-9 and neutrophil elastase<sup>51</sup>. We have found that many changes occur in both the normal mucosa and tumors of DSS-treated Pirc rats. Global gene expression profiling of DSS-treated Pirc rats is explored in detail in Chapter 2. Here, we explore whether expression changes in inflamed normal mucosa can foreshadow the development of tumors.

### **III. EARLY DETECTION OF COLON CANCER**

**Visual/Direct detection.** Rates of colon cancer have decreased dramatically as endoscopic screening has become routine. It is generally recommended that individuals begin colonoscopy screening at the age of 50 and continue until age 75, with one colonoscopy every ten years as long as no polyps are detected<sup>15</sup>. In 2002, roughly 40% of individuals aged 50-75 had reported

having undergone endoscopy in the US<sup>12</sup>. By 2010 the rates had increased to over 65%<sup>19</sup>. Between 2003-2007 both incidence and mortality declined by 3%, which is largely attributed to increased screening rates<sup>12</sup>.

Endoscopy has also become routine for mouse<sup>22,30</sup> and rat<sup>5,35</sup> models of intestinal cancer. Tumors can be visualized by endoscopy in approximately the distal two-thirds of the rat colon, allowing observations regarding time to tumor emergence and tumor growth pattern. Visualizing tumors over time in the living animals allows agents to be tested for both their chemopreventive and therapeutic potential<sup>35</sup> (see Chapters 3 and 4). Though genetic or chemical manipulation may not alter tumor multiplicity, it may affect the tumor's ability to grow and thrive (see Chapter 1). By counting tumors only at study termination this valuable information is lost.

Beyond simple visualization of the tumor, many manipulations can be done *in vivo* during endoscopy. Biopsy samples are routinely obtained from both tumor and normal colonic epithelium both in the human and in rodent models. Even in the rat, these biopsy samples are large enough to be split so that half of the sample can be fixed in formalin and the other half stored for DNA and RNA extraction. Tumor biopsy samples do not maintain the relationship with the underlying and surrounding normal tissue so interpretation of resulting data must be done with care. However, there are benefits of being able to analyze the tumor over time. By obtaining samples when the tumor first appears, molecular or cellular differences that are seen later in tumor development can be examined to determine whether they existed early or occurred only later. This is especially important when investigating differences between growing and static or regressing tumors, as these tumors will eventually differ in size, an unavoidable complication. This technique was utilized in Chapter 1, where early samples of tumors found to differ in stage are analyzed to determine if they express markers that may foreshadow future invasion.

Recently, over-diagnosis has become an important topic in cancer research. Although increased screening has prevented the development of thousands of cancers, it has also caused an increase in the number of healthy adults undergoing unnecessary medical treatment. When a polyp is found at endoscopy, it is generally removed during the procedure and sent for pathological assessment. However, polyps occur in 30-50% of adults<sup>16</sup>, but only about 5% of all individuals will ever develop cancer. This indicates that many individuals are being subjected to the risk of polyp removal in cases where it may not be necessary.

Virtual colonoscopy (VC) is decreasing the number of patients who have their colon polyps removed. VC uses computed tomography (CT) technology to detect colonic polyps and quantify their size. It has been recently recognized that not all early colonic tumors grow, some remain static for years while a few spontaneously regress<sup>48</sup>. Importantly, it appears that the early growth profile of a tumor may correlate with its eventual fate. After biopsy and pathological analysis, about 90% of advanced neoplasms were growing, while about 70% of early adenomas were static or regressing<sup>48</sup>. Accurate determination of tumor volume allows small polyps to be left in place and followed over time. This aspect of tumor biology is a newly emerging area that deserves deeper study.

The Pirr rat demonstrates the same three tumor fates seen in humans: growing, static and regressing (see Chapter 2). Longitudinal monitoring of tumor growth in rodent models can investigate potential determinants of tumor fate. This information can help to reduce the number of patients undergoing polyp resection without necessity, by treating only those patients with lesions predicted to grow and become invasive. In the mouse, microCT colonography can be used to detect a 16% change in tumor volume in the living animal with 95% confidence<sup>22</sup>. However, equipment costs and the need to transfer animals to a shared facility prohibit its routine use in

longitudinal studies. To circumvent these hurdles, we have developed a new method to accurately and quantitatively determine tumor volume *in vivo* in the Pirc rat (see Chapter 5). Accurate tumor volume determination combined with the experimental Pirc rat platform, can allow us to find molecular signals that correlate with eventual tumor fate and to test the causative role of these molecules in tumor growth. Studies of causation often cannot be accomplished in the human or *in vitro* models, but instead depend on the genetics of an animal model.

**Molecular/Indirect detection.** Beyond screening methods that directly visualize a lesion, other methods work by detecting molecules associated with the presence of a tumor or cancer. The fecal occult blood test (FOBT) is a very basic method of screening that detects the presence of blood in the stool. This could result from a number of underlying causes, but forms the basis for further clinical investigation. The detection of mutated or methylated DNA within stool is an emerging method to detect cancers without the use of endoscopy. A meta-analysis of 20 studies comprising over 5500 individuals found that 75% of cancers and 62% of advanced adenomas could be detected by methylated DNA markers in stool<sup>61</sup>. However, nearly 40% of advanced adenomas remain undetected by this method. While this may represent an advancement for individuals willing to undergo stool DNA testing but refusing endoscopy, the sensitivity and specificity are both lacking compared to traditional colonoscopy, especially for early neoplasms.

Recent advances have begun to allow the detection of molecules in the circulating blood that may be associated with a developing cancer. Some researchers believe that any molecules shed from cells of the tumor would be present at a level several orders of magnitude too low for detection in blood<sup>32</sup>. However, the possibility should not be discounted that a systemic response to the presence of a tumor could elicit a molecular change large enough to be measured in blood.



This has indeed been shown to be true in a study utilizing the Min mouse. This study found 40 different proteins to be differentially expressed in the serum between wild type mice and mice with intestinal tumors<sup>36</sup>. Of the top 22 protein candidates, only 9 proteins also showed differential mRNA expression between tumor and normal colonic epithelium in the mice with intestinal tumors, indicating that these signals measured in blood may originate from tissues other than the tumor itself. Although much work lies ahead to determine the sensitivity and specificity of blood-based testing, and to determine whether these tests can detect the very earliest of tumors, the availability, if established, of such tests would greatly increase compliance with colon cancer screening, thereby reducing disease burden and mortality.

Transcriptome analysis within the gut itself may uncover novel early indicators of tumorigenesis. Recently, changes within normal colonic tissue from IBD patients<sup>47</sup> have been found that correlate with the presence or absence of a distant tumor. Although no published data exists for a similar comparison in the general population without an IBD, animal models are actively being utilized to study this. Preliminary data from similar experiments in the Pirc rat are discussed in Appendix E. If these changes foreshadow tumor development but are present at early stages within the normal tissue (see Chapter 2), they could represent targets for early detection and treatment before lesions appear.

#### **IV. SUMMARY**

Animal modeling of colon cancer can greatly increase our understanding of the earliest events in the neoplastic process. Within this dissertation, the experimental features of the Pirc rat are explored. At each step, comparisons are made to the human case. In Chapters 1 and 2,

DSS is utilized to induce cancers associated with inflammation and to explore their relationship with tumors from untreated Pirc rats. Further, we take advantage of changes to the normal mucosa caused by DSS to determine whether these are early indicators of future neoplasia. These results gain significance when compared with similar studies in humans with inflammatory bowel diseases. In Chapters 3 and 4, we use the Pirc model to test whether an environmental factor, supplementation with vitamin D compounds, can affect tumor multiplicity, growth or size. The results of these studies are put into perspective from published human trials involving colonic and other cancers. Finally, in Chapter 5, the use of a new method for quantitatively determining tumor volume allows us to accurately determine tumor fate. This technique will further strengthen longitudinal studies of tumor growth in animal models by eliminating the subjective nature of previous methods used to score tumor fate. In sum, this dissertation represents an intricate dovetailing between rodent modeling of colon cancer and the human disease. Both are necessary to fully understand the early neoplasm, but neither is sufficient alone.

## References

1. **Adams SV, Ahnen DJ, Baron JA, Campbell PT, Gallinger S, Grady WM, Lemarchand L, Lindor NM, Potter JD, Newcomb PA.** 2013. Survival after inflammatory bowel disease-associated colorectal cancer in the Colon Cancer Family Registry. *World Journal of Gastroenterology*. **19**:3241–8.
2. **Alex P, Zachos NC, Nguyen T, Gonzales L, Chen T-E, Conklin LS, Centola M, Li X.** 2009. Distinct cytokine patterns identified from multiplex profiles of murine DSS and TNBS-induced colitis. *Inflammatory Bowel Diseases*. **15**:341–52.
3. **American Cancer Society.** 2013. Colorectal Cancer Facts & Figures 2011-2013.
4. **Amos-Landgraf JM, Irving AA, Hartman C, Hunter A, Laube B, Chen X, Clipson L, Newton MA, Dove WF.** 2011. Monoallelic silencing and haploinsufficiency in early murine intestinal neoplasms. *Proceedings of the National Academy of Sciences USA*. **109**:2060–2065.
5. **Amos-Landgraf JM, Kwong LN, Kendzierski CM, Reichelderfer M, Torrealba J, Weichert J, Haag JD, Chen K-S, Waller JL, Gould MN, et al.** 2007. A target-selected *Apc*-mutant rat kindred enhances the modeling of familial human colon cancer. *Proceedings of the National Academy of Sciences USA*. **104**:4036–41.
6. **The Cancer Genome Atlas (TCGA) Consortium.** <http://cancergenome.nih.gov/> (Accessed 11/15/2013).
7. **Baker SJ, Preisinger AC, Jessup JM, Paraskeva C, Markowitz S, Willson JKV, Hamilton S, Vogelstein B.** 1990. p53 gene mutations occur in combination with 17p allelic deletions as late events in colorectal tumorigenesis. *Cancer Research*. **23**:7717–7722.
8. **Bellam N, Pasche B.** 2010. Tgf-beta signaling alterations and colon cancer. *Cancer Treatment Research*. **155**:85–103.
9. **Bilinski C, Burleson J, Forouhar F.** 2012. Inflammation associated with neoplastic colonic polyps. *Annals of Clinical and Laboratory Science*. **42**:266–70.
10. **Boscoe FP, Schymura MJ.** 2006. Solar ultraviolet-B exposure and cancer incidence and mortality in the United States, 1993-2002. *BMC Cancer*. **6**:264.
11. **Cauley JA, Chlebowski RT, Wactawski-Wende J, Robbins J a, Rodabough RJ, Chen Z, Johnson KC, O’Sullivan MJ, Jackson RD, Manson JE.** 2002. Calcium plus vitamin D supplementation and health outcomes five years after active intervention ended: the Women’s Health Initiative. *Journal of Women’s Health*. **11**:915-929.

12. **Centers for Disease Control.** 2011. Colorectal cancer screening, incidence and mortality-United States, 2002-2010. *Morbidity and Mortality Weekly Report*. 884–889. <http://www.cdc.gov/mmwr/preview/mmwrhtml/mm6026a4.htm> (Accessed 11/15/2013).
13. **Centers for Disease Control.** 2012. Colorectal Cancer Rates by State. <http://www.cdc.gov/cancer/colorectal/statistics/state.htm> (Accessed 11/15/2013).
14. **Centers for Disease Control.** 2012. Colorectal Cancer Screening Rates. [http://www.cdc.gov/cancer/colorectal/statistics/screening\\_rates.htm](http://www.cdc.gov/cancer/colorectal/statistics/screening_rates.htm) (Accessed 11/15/2013).
15. **Centers for Disease Control.** 2013. Colorectal cancer screening guidelines. 2013. [http://www.cdc.gov/cancer/colorectal/basic\\_info/screening/guidelines.htm](http://www.cdc.gov/cancer/colorectal/basic_info/screening/guidelines.htm) (Accessed 11/15/2013).
16. **Charette A, Fletcher R.** 2013. Colon polyps (beyond the basics). <http://www.uptodate.com/contents/colon-polyps-beyond-the-basics> (Accessed 11/15/2013).
17. **Claessen MMH, Schipper MEI, Oldenburg B, Siersema PD, Offerhaus GJA, Vleggaar FP.** 2010. WNT-pathway activation in IBD-associated colorectal carcinogenesis: potential biomarkers for colonic surveillance. *Cellular Oncology*. **32**:303–310.
18. **Connelly TM, Koltun WA.** 2013. The Cancer “Fear” in IBD Patients: Is It Still REAL? *Journal of Gastrointestinal Surgery*. [Epub ahead of print].
19. **Center for Disease Control.** 2013. Colorectal cancer screening rates remain low. <http://www.cdc.gov/media/releases/2013/p1105-colorectal-cancer-screening.html> (Accessed 11/15/2013).
20. **Cormier RT, Hong K, Halberg RB, Hawkins T, Richardson P, Mulherkar R, Dove WF, Lander ES.** 1997. Secretory phospholipase Pla2g2a confers resistance to intestinal tumorigenesis. *Nature Genetics*. **17**:88–91.
21. **Dove WF, Clipson L, Gould KA, Luongo C, Marshall DJ, Moser AR, Newton MA, Jacoby RF.** 1997. Intestinal neoplasia in the Apc Min mouse: independence from the microbial and natural killer (beige locus) status. *Cancer Research*. **5**:812–814.
22. **Durkee BY, Mudd SR, Roen CN, Clipson L, Newton A, Weichert JP, Pickhardt PJ, Richard B.** 2008. Reproducibility of tumor volume measurement at microCT colonography in living mice. *Academic Radiology*. **15**:334–341.
23. **Dwinell M, Lazar J, Geurts A.** 2013. The emerging role for rat models in gene discovery. *Mammalian Genome*. **22**:466–475.

24. **Fearnhead N, Britton M, Bodmer W.** 2001. The ABC of Apc. *Human Molecular Genetics*. **10**:721–733.
25. **Flossmann E, Rothwell PM.** 2007. Effect of aspirin on long-term risk of colorectal cancer: consistent evidence from randomised and observational studies. *Lancet*. **369**:1603–13.
26. **Garland CF, Garland FC.** 1980. Do sunlight and vitamin D reduce the likelihood of colon cancer? *International Journal of Epidemiology*. **9**:227–231.
27. **Geurts AM, Cost GJ, Freyvert Y, Zeitler B, Miller JC, Choi VM, Jenkins SS, Wood A, Cui X, Meng X, et al.** 2009. Knockout rats via embryo microinjection of zinc-finger nucleases. *Science*. **325**:433.
28. **GLOBOCAN.** 2008. Colorectal Cancer Incidence and Mortality Worldwide. <http://globocan.iarc.fr/factsheet.asp> (Accessed 11/15/2013).
29. **Halberg RB, Waggoner J, Rasmussen K, White A, Clipson L, Prunuske AJ, Bacher JW, Sullivan R, Washington MK, Pitot HC, et al.** 2009. Long-lived Min mice develop advanced intestinal cancers through a genetically conservative pathway. *Cancer Research*. **69**:5768–75.
30. **Hensley HH, Merkel CE, Chang W-CL, Devarajan K, Cooper HS, Clapper ML.** 2009. Endoscopic imaging and size estimation of colorectal adenomas in the multiple intestinal neoplasia mouse. *Gastrointestinal Endoscopy*. **69**:742–9.
31. **Hirono I, Kuhara K, Hosaka S, Tomizawa S, Golberg L.** 1981. Induction of intestinal tumors in rats by dextran sulfate sodium. *Journal of the National Cancer Institute*. **66**:579–583.
32. **Hori S, Gabmhir S.** 2011. Mathematical model identifies blood biomarker-based early cancer detection strategies and limitations. *Science Translational Medicine*. **3**:109ra116.
33. **Howlander N, Noone A, Krapcho M, Garshell J, Neyman N, Altekruse S, Kosary C, Yu M, Ruhl J, Tatalovich Z, et al.** 2012. NCI SEER Fact Sheet: Colon and Rectum. <http://seer.cancer.gov/statfacts/html/colorect.html>
34. **Iannaccone PM, Jacob HJ.** 2009. Rats! Disease models & mechanisms. **2**:206–10.
35. **Irving AA, Halberg RB, Albrecht DM, Plum LA, Krentz KJ, Clipson L, Drinkwater N, Amos-Landgraf JM, Dove WF, DeLuca HF.** 2011. Supplementation by vitamin D compounds does not affect colonic tumor development in vitamin D sufficient murine models. *Archives of Biochemistry and Biophysics*. **515**:64–71.
36. **Ivancic MM, Huttlin EL, Chen X, Pleiman JK, Irving AA, Hegeman AD, Dove WF, Sussman MR.** 2013. Candidate serum biomarkers for early intestinal cancer using <sup>15</sup>N

- metabolic labeling and quantitative proteomics in the *Apc<sup>Min/+</sup>* mouse. *Journal of Proteome Research*. **12**:4152–66.
37. **Jacob HJ**. 2010. The Rat: A Model Used in Biomedical Research. In: *Rat Genomics: Methods and Protocols*. **597**:1–11.
  38. **Jacobs ET, Hibler EA, Lance P, Sardo CL, Jurutka PW**. 2013. Association between circulating concentrations of 25(OH)D and colorectal adenoma: A pooled analysis. *International Journal of Cancer*. **12**:2980-2988.
  39. **Jess T, Simonsen J, Jørgensen KT, Bo VP**. 2012. Declining risk of colorectal cancer in patients with inflammatory bowel disease over 30 years. *Gastroenterology*. **2**:375-381.
  40. **Johansson ME V, Gustafsson JK, Holmén-Larsson J, Jabbar KS, Xia L, Xu H, Ghishan FK, Carvalho FA, Gewirtz AT, Sjövall H, et al**. 2013. Bacteria penetrate the normally impenetrable inner colon mucus layer in both murine colitis models and patients with ulcerative colitis. *Gut*. [Epub ahead of print].
  41. **Johansson ME V, Gustafsson JK, Sjöberg KE, Petersson J, Holm L, Sjövall H, Hansson GC**. Bacteria penetrate the inner mucus layer before inflammation in the dextran sulfate colitis model. *PLoS One*. **8**:e12238.
  42. **Li D, Qiu Z, Shao Y, Chen Y, Guan Y, Liu M, Li Y, Gao N, Wang L, Lu X, et al**. 2013. Heritable gene targeting in the mouse and rat using a CRISPR-Cas system. *Nature Biotechnology*. **31**:681–3.
  43. **Manninen P, Karvonen A, Huhtala H, Aitola P, Hyöty M, Nieminen I, Hemminki H, Collin P**. 2013. The risk of colorectal cancer in patients with inflammatory bowel diseases in Finland: a follow-up of 20 years. *Journal of Crohns Colitis*. **11**:e551-557.
  44. **Mashimo T, Kaneko T, Sakuma T, Kobayashi J, Kunihiro Y, Voigt B, Yamamoto T, Serikawa T**. 2013. Efficient gene targeting by TAL effector nucleases coinjected with exonucleases in zygotes. *Scientific Reports*. **3**:1253.
  45. **McCormick DA, Horton LW, Mee AS**. 1990. Mucin depletion in inflammatory bowel disease. *Journal of Clinical Pathology*. **43**:143–6.
  46. **Moser AR, Luongo C, Gould KA, McNeley MK, Shoemaker AR, Dove WF**. 1990. *Apc<sup>Min</sup>*: a mouse model for intestinal and mammary tumorigenesis. *European Journal of Cancer*. **31A**:1061–4.
  47. **Pekow J, Dougherty U, Huang Y, Gometz E, Nathanson J, Cohen G, Levy S, Kocherginsky M, Venu N, Westerhoff M, et al**. 2013. Gene signature distinguishes patients with chronic ulcerative colitis harboring remote neoplastic lesions. *Inflammatory Bowel Diseases*. **3**:461-470.

48. **Pickhardt PJ, Kim DH, Pooler BD, Hinshaw JL, Barlow D, Jensen D, Reichelderfer M, Cash BD.** 2013. Assessment of volumetric growth rates of small colorectal polyps with CT colonography: a longitudinal study of natural history. *The Lancet Oncology*. **14**:711–20.
49. **Risques RA, Rabinovitch PS, Brentnall TA.** 2006. Cancer surveillance in inflammatory bowel disease: new molecular approaches. *Current Opinion in Gastroenterology*. **22**:382–90.
50. **van Schaik FD, Mooiweer E, van der Have M, Belderbos TD, Ten Kate FJ, Offerhaus GJ, Schipper ME, Dijkstra G, Pierik M, Stokkers PC, et al.** 2013. Adenomas in patients with inflammatory bowel disease are associated with an increased risk of advanced neoplasia. *Inflammatory Bowel Diseases*. **19**:342–349.
51. **Shang K, Bai Y-P, Wang C, Wang Z, Gu H-Y, Du X, Zhou X-Y, Zheng C-L, Chi Y-Y, Mukaida N, et al.** 2012. Crucial involvement of tumor-associated neutrophils in the regulation of chronic colitis-associated carcinogenesis in mice. *PloS One*. **7**:e51848.
52. **Shull JD, Spady TJ, Snyder MC, Johansson SL, Pennington KL.** 1997. Ovary-intact, but not ovariectomized female ACI rats treated with 17beta-estradiol rapidly develop mammary carcinoma. *Carcinogenesis*. **18**:1595–601.
53. **Taketo MM, Edelmann W.** 2009. Mouse models of colon cancer. *Gastroenterology*. **136**:780–798.
54. **Tessner TG, Cohn SM, Schloemann S, Stenson WF.** 1998. Prostaglandins prevent decreased epithelial cell proliferation associated with dextran sodium sulfate injury in mice. *Gastroenterology*. **115**:874–82.
55. **Trivedi DP, Doll R, Khaw KT.** 2003. Effect of four monthly oral vitamin D<sub>3</sub> (cholecalciferol) supplementation on fractures and mortality in men and women living in the community: randomised double blind controlled trial. *British Medical Journal*. **326**:1–6.
56. **Velayos FS, Ullman TA.** 2013. Looking forward to understanding and reducing colorectal cancer risk in inflammatory bowel disease. *Gastroenterology*. **106**:1–3.
57. **Vogelstein B, Fearon E, Hamilton S, Kern S, Preisinger A, Leppert M, Nakamura Y, White R, Smits A, Bos J.** 1988. Genetic alterations during colorectal-tumor development. *New England Journal of Medicine*. **319**:525–32.
58. **Vogelstein B, Papadopoulos N, Velculescu VE, Zhou S, Diaz LA, Kinzler KW.** 2013. Cancer genome landscapes. *Science*. **339**:1546–58.
59. **Willett WC.** 2001. Diet and cancer: one view at the start of the millennium. *Cancer Epidemiology, Biomarkers and Prevention*. **1**:3-8.

60. **Wood LD, Parsons DW, Jones S, Lin J, Sjöblom T, Leary RJ, Shen D, Boca SM, Barber T, Ptak J, et al.** 2007. The genomic landscapes of human breast and colorectal cancers. *Science*. **318**:1108–13.
61. **Yang H, Xia BQ, Jiang B, Wang G, Yang YP, Chen H, Li BS, Xu AG, Huang YB, Wang XY.** Diagnostic value of stool DNA testing for multiple markers of colorectal cancer and advanced adenoma: a meta-analysis. *Canadian Journal of Gastroenterology*. **27**:467–475.
62. **Zeineldin M, Neufeld KL.** 2013. More than two decades of Apc modeling in rodents. *Biochimica et Biophysica Acta*. **1836**:80–9.



## Chapter 1

### **Dextran sodium sulfate, a model for inflammatory colon cancer, enhances tumor multiplicity, growth and stage in the Pirc rat**

Amy A. Irving designed these studies (in collaboration with James Amos-Landgraf), performed the majority of the rat endoscopies and dissections, completed all of the data analysis and wrote the final manuscript. Kathleen J. Krentz, Tony Hunter, Mackenzie Eagen, Jennifer K. Pleiman and Madeline R. Ford each assisted with endoscopies, dissections and sample collection. Under the supervision of James Amos-Landgraf, Tony Hunter performed the Sanger sequencing of tumors. Ruth Sullivan performed histological analysis and scoring of tumor stage. William F. Dove served as an advisor.

## **Abstract**

The role for inflammation in cancer initiation, growth and progression is complex and may differ by cancer stage. Environmentally controlled models that accurately reflect the human disease, paired with techniques to manipulate their genome, diet and exposures, can help to elucidate the intricate role played by inflammation. The *Apc*<sup>Pirc/+</sup> rat model for familial colon cancer develops colonic tumors spontaneously. However, this model may not be sufficient to study tumors involving inflammation. To create an inflammatory environment, Pirc rats can be given dextran sodium sulfate (DSS). DSS-treated Pirc rats develop many symptoms similar to those seen in human patients with inflammatory bowel disease, including loose and bloody stools, inflamed mucosa, an increased risk for developing polyps, and increased invasion of advanced lesions.

Not all Pirc rats given DSS are susceptible to its tumorigenic effects. F<sub>1</sub> progeny involving the resistant strain Brown Norway do not show an increase in the number of colonic tumors after DSS treatment. Untreated Pirc rats also show a gender disparity, with males developing significantly more colonic tumors than females. This remains true in the DSS-treated Pirc rat, and is also observed in sporadic human cancer. Both tumors forming spontaneously and those associated with inflammation show diversity in growth potential and staging, similar to human populations. The DSS-treated Pirc rat creates a platform to model human colonic tumors involving an inflammatory aspect, especially the differences in tumor growth patterns, level of invasion and effects of chemopreventives between spontaneous and inflammation-associated tumors.

## **Introduction**

Roughly 1 in 20 individuals will develop colon cancer during their lifetime. This increases dramatically for individuals with an inflammatory bowel disease (IBD). Lifetime risk of cancer in these patients increases with duration and extent of the inflammatory disease, reaching up to 18% by 30 years of active disease<sup>7</sup>. Beyond their increase in risk, IBD patients with cancer tend to show slightly worse prognosis, possibly owing to the cancer being discovered at later stages than sporadic cancers<sup>9,18</sup>. Late detection is unexpected since IBD patients often undergo endoscopy at much more frequent intervals than individuals without an inflammatory disease. The presence of inflammation may either obscure accurate detection of these cancers at an early stage or, more likely, could increase the speed at which invasive cancer develops.

IBD-associated cancers and sporadic cancers differ at the cellular and molecular levels as well, although to what extent is under debate. Of particular interest is whether there is a role for Wnt activity in colitis-associated cancer, as over 80% of sporadic cancers contain mutations in *Apc*, a tumor suppressor of Wnt activation<sup>8</sup>. Recent evidence suggests that Wnt activation does occur during colitis-associated carcinogenesis, as judged by nuclear  $\beta$ -catenin accumulation<sup>3</sup>.

The *Apc*<sup>Pirc/+</sup> (Pirc) rat is a model for familial colon cancer, but it alone may not be sufficient to study the development of colitis-associated cancers. Dextran sodium sulfate (DSS) delivered through the diet or drinking water is a common method to induce colitis that mimics many of the symptoms and pathology seen in human colitis cases<sup>5</sup>. However, DSS-treated wild type animals develop intestinal tumors at a low incidence and with a long latency<sup>10,22</sup>. Tumor incidence can be increased by also giving animals a chemical carcinogen, such as azoxymethane (AOM)<sup>22</sup>. While AOM combined with DSS may usefully model the heterogeneity seen in hu-

man populations exposed to environmental carcinogens, the mutations caused by AOM to lead to cancer are also heterogeneous, adding a random variable to a systematic study of the added effect of the inflammatory microenvironment.

Histological similarities between DSS rodent models and human colitis-associated colon cancer provide further evidence that these models are useful for studying human inflammatory cancers. Although there is some debate, the order and frequency of mutations may differ between sporadic and colitis-associated cancers. For example, inflammatory colon cancers in humans tend to have mutations in p53 early in tumor development, in contrast to sporadic tumors which often acquire this mutation late or not at all<sup>4,6</sup>. Similar observations have been seen in rodent models. In a DSS-treated *Apc*<sup>Min/+</sup> mouse model, cytoplasmic and nuclear staining of  $\beta$ -catenin was found in all tumors regardless of DSS treatment, but strong nuclear staining of p53 was found specifically in tumors from DSS-treated mice<sup>22</sup>.

Colitis-associated cancer also tends to be more poorly differentiated after invasion, resulting in poorer prognosis, compared to their sporadic counterparts<sup>15</sup>. A similar phenomenon has been observed in DSS-treated animals. In addition to increasing tumor multiplicity, DSS has also been shown to increase tumor stage. While only 1 of 5 rats treated with the carcinogen dimethylhydrazine (DMH) alone formed an adenocarcinoma, 12 of 15 rats treated with DMH plus DSS developed adenocarcinomas<sup>17</sup>.

To test whether tumors associated with inflammation could be studied using DSS in the Pirr rat model, treated and untreated rats underwent endoscopy to determine whether there were changes in tumor fate with DSS treatment. Following dissection, terminal tumor multiplicity was determined from formalin-fixed sections. Histological sections of tumor and normal tissue were then examined to score tumor stage, and to analyze  $\beta$ -catenin staining patterns.

Pyrosequencing was also performed to determine whether the process of loss of *Apc* function in DSS-induced Pirc tumors differed from that of sporadic tumors.

## **Materials and Methods**

**Animal Breeding and Maintenance.** Rats were maintained under a protocol approved by the Animal Care and Use Committee of the University of Wisconsin School of Medicine and Public Health and in a facility in the McArdle Laboratory approved by the American Association of Laboratory Animal Care. Rats were individually housed in standard caging with free access to Lab Diet 5020 chow (St. Louis, MO) and acidified water. F<sub>1</sub> generation (ACIxF344)-Pirc rats were generated by breeding female ACI *Apc*<sup>+/+</sup> rats (Harlan, Indianapolis, IN) to male F344 *Apc*<sup>Pirc/+</sup> rats (developed in the laboratory of WFD and now commercially available through Taconic, Hudson, NY)<sup>1</sup>. F<sub>1</sub> generation (BNxF344)-Pirc rats were generated by breeding female BN *Apc*<sup>+/+</sup> (Harlan, Madison, WI) rats to male F344 *Apc*<sup>Pirc/+</sup> rats. F<sub>1</sub> generation rats show an intermediate tumor multiplicity and time to tumor emergence from each parental strain. Congenic ACI-Pirc rats are more susceptible and BN-Pirc rats are less susceptible to colonic tumor development than F344-Pirc rats. (ACIxF344)F<sub>1</sub> rats develop fewer tumors than the ACI-Pirc strain, but in a more rapid timeframe than the F344-Pirc strain. (BNxF344)F<sub>1</sub> rats develop more tumors than the BN-Pirc strain, but over a greater period of time compared to the F344-Pirc strain. A second reason for using the F<sub>1</sub> generation is that it allows genetic and epigenetic events to be examined in each allele across the genome where the sequence differs between the two parental lines.

**DSS Treatment.** Dextran sodium sulfate was purchased from Fisher Scientific (500 kDa; Pittsburgh, PA) or MP Biomedical (36-50 kDa; Solon, OH). Either a 2% (36-50 kDa) or 4% (500 kDa) solution of DSS (wt/vol) mixed with standard acidified drinking water was delivered to DSS-treated rats between 40-47 days of age and again from 54-61 days of age.

**Endoscopy.** Briefly, the animal was anesthetized with 3% isoflurane and placed on a sterile surgical field, ventral side down. The colon was flushed with warm saline to remove any fecal material and to provide lubrication. A 2.7 mm x 18 cm Hopkins Optik 30° endoscope (7219BA, Karl Storz, Tuttlingen, Germany) within a sheath (67065C, Karl Storz) was inserted to the proximal colonic flexure. Illuminated by the Xenon Nova 175 (201315, Karl Storz), still and video images were captured at each visit using the Image 1 hub (22200, Karl Storz) and AidaVet software (692040, Karl Storz). The anatomy of the rat allows the distal two-thirds of the colon to be visualized by endoscopy.

**Assessment of Tumor Growth Patterns.** Three observers blinded to treatment details of the animal determined the longitudinal fate of tumors. Tumors were examined during each endoscopy visit and any tumor that appeared at least twice during the study was given one of four scores: growing, static, regressing or unscorable; those judged to be unscorable were excluded from the longitudinal analysis. A score was generated based on agreement between at least two of the three blinded observers.

**Terminal Tumor Counts.** (ACIxF344)F<sub>1</sub> rats were dissected at 98, 140, 180 and 210 days of age. (BNxF344)F<sub>1</sub> rats were dissected at one year of age. At sacrifice, the small intestine and

colon were opened longitudinally, laid flat, washed with PBS and fixed with formalin; the small intestine was divided into four equal sections before fixation. Formalin-fixed tumors from dissected intestines were counted on a dissecting microscope. Tumor counts were obtained for each of the four small intestinal sections and for the entire colon.

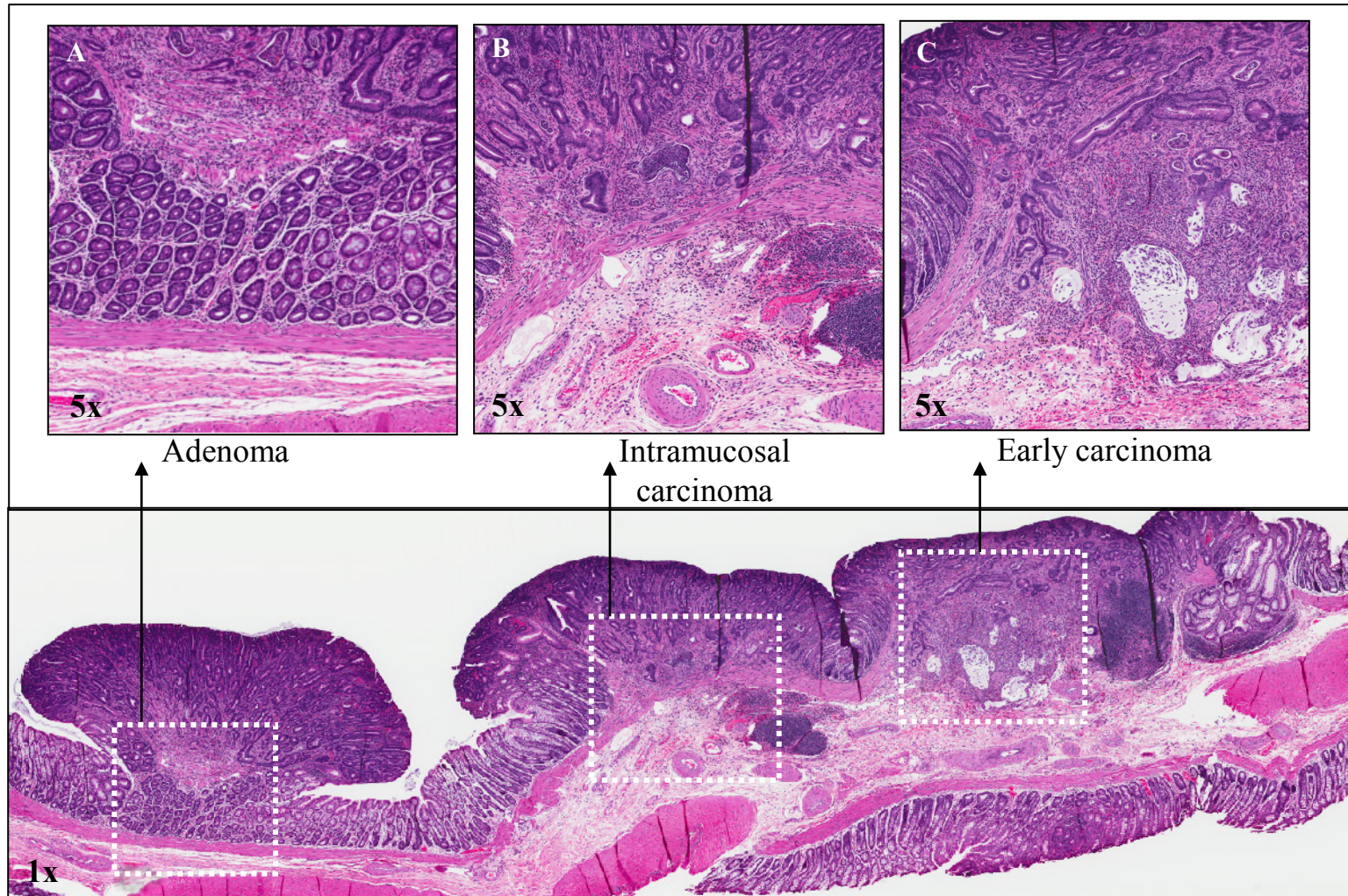
**Sample Collection and DNA/RNA Isolation.** Samples were collected from tumor and normal tissue for DNA and RNA isolation before the colon was exposed to ethanol or formalin. Samples were obtained from tumors by making a vertical cut at the tumor midline down to the center of the tumor. Then a second cut was made horizontal to the first, resulting in one-quarter of the tumor being harvested. This method allows cells to be collected from the outer tumor as well as from the innermost tumor near the stalk, yet allows the remaining tumor to be left securely attached to the stalk. This is important to preserve the relationship with the normal intestinal tissue for future histological analysis. For normal tissue collection, a scalpel blade was used to gently scrape the normal intestinal mucosa in each of the proximal, medial and distal colon. A minimum 2 mm barrier surrounding any tumor was required for normal tissue collection. All samples were homogenized in a tube containing RLTplus buffer (Qiagen, Valencia, CA) and frozen at -80° C until use. DNA and RNA were extracted from the same sample using an Allprep DNA/RNA Mini Kit (Qiagen) following the manufacturer's protocol. DNA contamination of RNA samples was removed by DNase treatment (Qiagen) of the RNA using the on-the-column protocol recommended by the manufacturer. cDNA was generated from isolated RNA using the SuperScript III Reverse Transcriptase Kit (Invitrogen).

**Histological and Immunohistochemical Analysis.** Intestines were fixed for 24-48 hours in formalin and then transferred to 70% ethanol for storage. Samples were embedded in paraffin blocks in one of two ways: either a longitudinal strip was cut the length of the colon and wound into a Swiss roll or short strips of tissue were cut through the center of a tumor(s), including surrounding normal tissue. Five micron sections were used for pathological and immunohistochemical analysis. Tumor stage was judged on hematoxylin and eosin stained sections where the tumor stalk was present. A tumor was judged to be an adenoma if no invasion was present, an intramucosal carcinoma if invasion was present into the stalk or into but not through the *muscularis mucosa*, an early carcinoma if invasion occurred through the *muscularis mucosa* and into but not through the submucosa, and a carcinoma if invasion occurred through the submucosa (Fig 1-1 A-C)<sup>24</sup>.

**Determination of allelic ratios at the *Pirc* site.** Pyrosequencing was used to quantify genetic (gDNA) and epigenetic (cDNA) changes at the *Pirc* site within *Apc* by determining the ratio of *Pirc* mutant allele versus wild type allele. The following final PCR concentrations were used: 1x GoTaq clear buffer, 1.2mM MgCl<sub>2</sub>, 0.2mM dNTPs, 264 pM of each the forward and reverse primer, 0.6 U GoTaq Flexi (Promega), 8 µl sample and ddH<sub>2</sub>O to a final volume of 50 µl. The PCR cycling parameters were 94° C for 3 minutes followed by 50 cycles of 94° C for 15 seconds, 57° C for 90 seconds, 72° C for 2 minutes, and a final elongation step of 72° C for 10 minutes. 40 µl of PCR product was used per well. Pyrosequencing was performed using Pyro Gold Reagents according to the manufacturer's protocol. Each sample was run in duplicate; if the error between duplicates of a single sample was greater than 5% the sample was rerun in duplicate.



**Fig 1-1.** Hematoxylin and eosin staining of a section of colon containing three tumors from a DSS-treated Pirc rat. A tumor was judged to be (A) an adenoma if no invasion was present, (B) an intramucosal carcinoma if invasion was present into the stalk or into but not through the *muscularis mucosa*, or (C) an early carcinoma if invasion occurred through the *muscularis mucosa* and into but not through the submucosa.



**Statistical Methods.** Significant sex differences were observed in the multiplicities of small intestinal and colonic tumors, as described previously for the Pirc rat<sup>1</sup>. Therefore, data from male and female rats were analyzed separately. A 2-sided Wilcoxon rank sum test was employed to test for a difference in tumor multiplicity between male and female Pirc rats or between untreated and DSS-treated rats. Tumors of the small intestine and colon were analyzed separately. Longitudinal analysis of endoscopic images utilized a chi-square test of growing versus non growing tumors. Terminal tumor pathological staging utilized a chi-square test of non-invasive versus invasive lesions. For each of the tests, a p-value  $\leq 0.05$  was considered significant.

## **Results**

**General DSS phenotype.** As reported in the literature for both mice<sup>5</sup> and rats<sup>26</sup>, DSS-treated wild type and Pirc rats develop bloody, loose stools during treatment. These symptoms quickly subside following cessation of treatment. Based on a small subset of female rats, it does not appear that the rate of weight gain is affected in Pirc rats given DSS compared to controls (Fig 1-2). However, once a high tumor burden is reached, weight loss does occur, and this tumor threshold will generally be met earlier in DSS-treated rats.

**Histopathology and influence of molecular weight.** In animals treated with high molecular weight DSS, crypt structure is maintained throughout the colon (Fig 1-3 C-D), similar to controls (Fig 1-3 A-B). A few short colonic segments display mild hyperplasia, there are a small number of inflammatory infiltrates in the *lamina propria*, and a few small sections show possible foci of ulceration. By contrast, following low molecular weight DSS, the epithelium is segmentally de-

**Fig 1-2.** Contemporaneous longitudinal weights of three untreated and three DSS-treated Pirc rats. Litter-matched female rats were weighed at the beginning of each DSS cycle and one week following the second DSS cycle. No differences in weight gain over that interval was seen between untreated and DSS-treated rats.

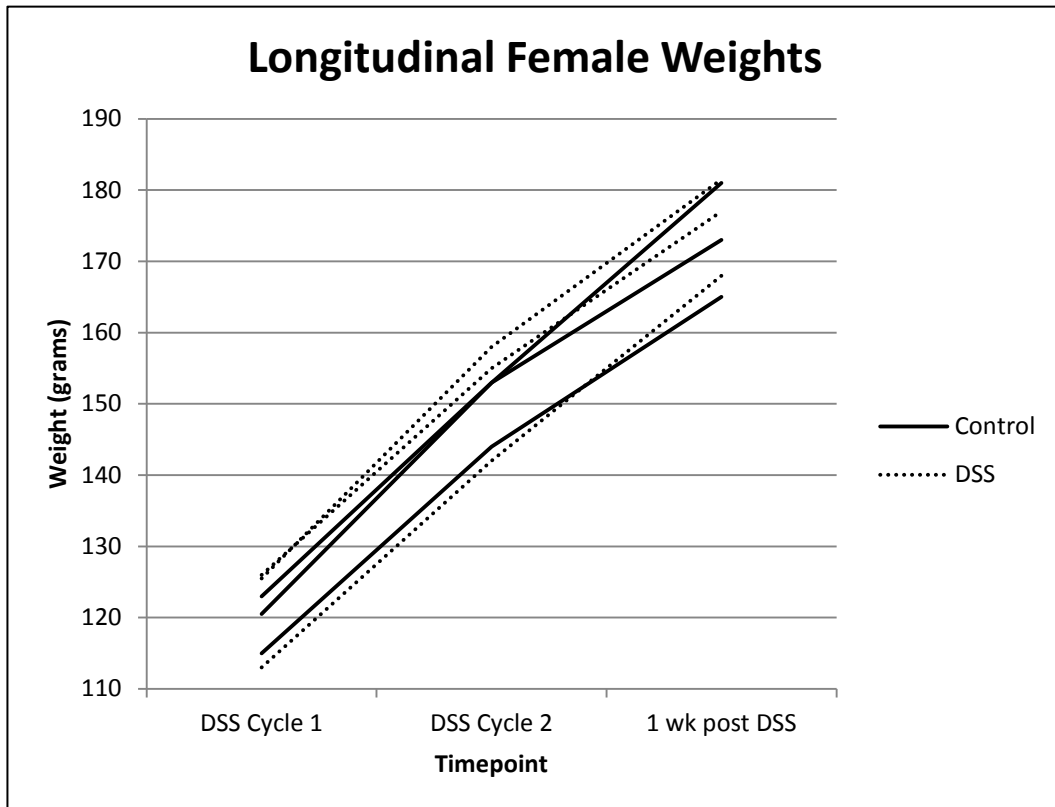
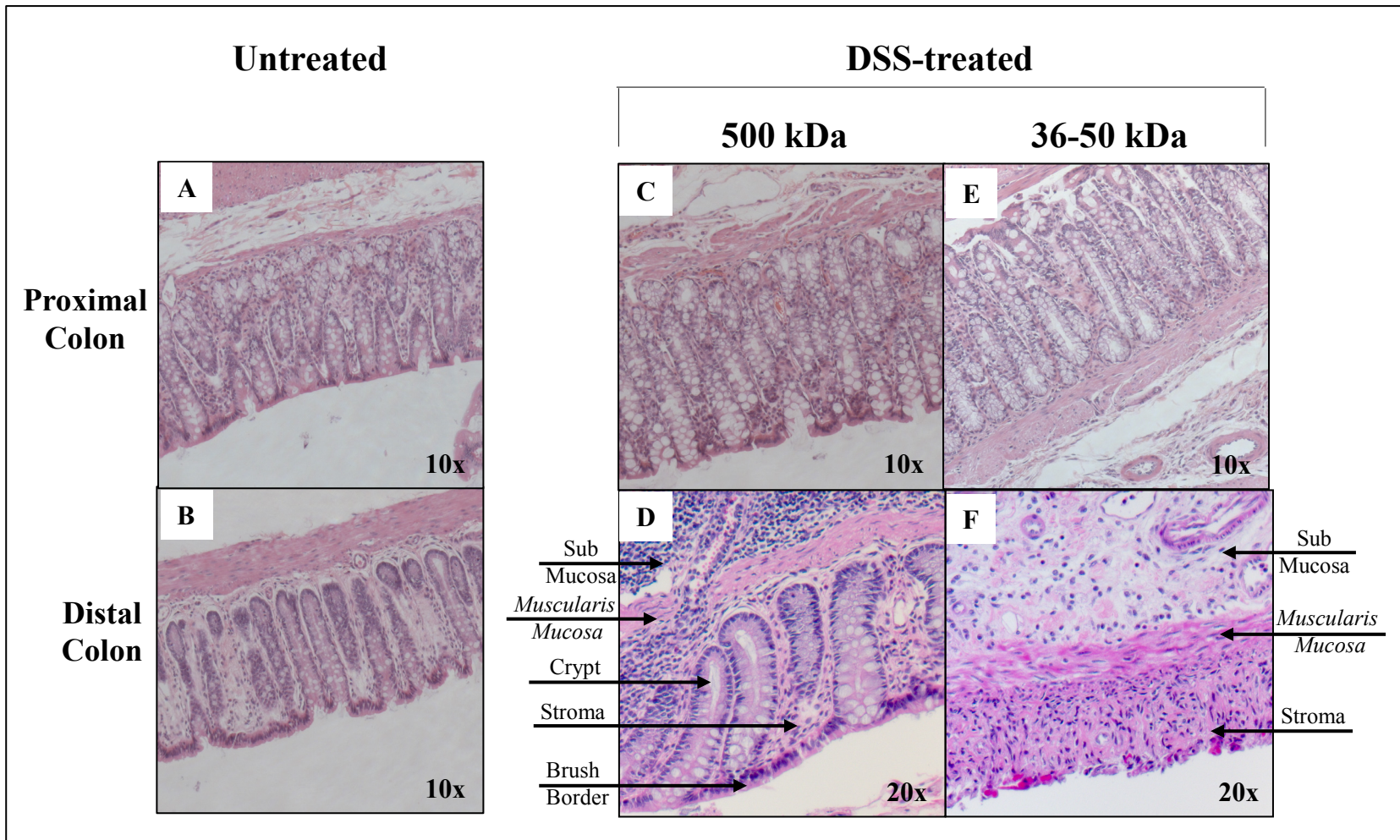


**Fig 1-3.** Histopathology of low versus high molecular weight DSS compared to untreated colon from wild type rats. Hematoxylin and eosin staining demonstrates that similar to controls (A, B), higher molecular weight (500 kDa) DSS does not cause overt structural damage to the colon (C, D), while lower molecular weight (36-50 kDa) DSS causes complete loss of crypt structure in the distal colon (F), though not in the proximal colon (E).



nuded in the distal colon to the extent of complete crypt loss in long sections, there is more substantial hyperplasia and multifocal perturbed crypt architecture, and substantial ulceration is accompanied by inflammatory infiltrates (Fig 1-3 E-F). The effects of DSS appear to be most severe in the distal colon and rectum and less so towards the proximal colon. Interestingly, the distal colon and rectum are where the greatest increase in tumor multiplicity is seen after DSS treatment (Fig 1-4A). These preliminary observations of the differential effects between low and high molecular weight DSS warrant further study. Owing to the severe colonic structural damage caused by low molecular weight DSS, we chose to utilize high molecular weight DSS for the all future studies.

**The gender disparity in (ACIxF344)F<sub>1</sub> Pirc rat tumor multiplicity persists following high**

**molecular weight DSS treatment.** Similar to previous findings in the F344-Pirc rat<sup>1</sup>, (ACIxF344)F<sub>1</sub>-Pirc females have significantly fewer tumors in both the small intestine ( $p < 0.0005$ ) and colon ( $p < 0.0002$ ) than their male counterparts. Upon high molecular weight DSS treatment, this difference persists. At 140 days of age, untreated female (ACIxF344)F<sub>1</sub>-Pirc rats have an average of  $1.4 \pm 2.1$  small intestinal tumors and  $4.2 \pm 1.5$  colonic tumors, while males have an average of  $9.7 \pm 4.3$  small intestinal tumors and  $22 \pm 5.6$  colonic tumors (Table 1-1). At 140 days of age, DSS-treated (ACIxF344)F<sub>1</sub>-Pirc female rats have an average of  $0.4 \pm 0.5$  small intestinal tumors and  $43.8 \pm 9.9$  colonic tumors, while male rats have an average of  $13 \pm 7.6$  small intestinal tumors and  $56.3 \pm 3.4$  colonic tumors. Following DSS treatment, females still have significantly fewer tumors of the small intestine ( $p < 0.0005$ ) and colon ( $p < 0.002$ ) than do male Pirc rats. This remains true until at least 210 days of age.

**Differing effects of high molecular weight DSS treatment in (ACIxF344)F<sub>1</sub> versus**

**(BNxF344)F<sub>1</sub> Pirc rats.** By contrast to (ACIxF344)F<sub>1</sub>-Pirc rats, in female and male (BNxF344)F<sub>1</sub>-Pirc rats tumor multiplicity in both the small intestine and colon is unaffected by DSS treatment (Table 1-1). In female (ACIxF344)F<sub>1</sub>-Pirc rats given high molecular weight DSS, colonic tumor multiplicity was significantly greater at 140 days ( $p<0.007$ ) and 180 days ( $p<0.001$ ), and nearly so at 210 days ( $p=0.1$ ) compared with untreated Pirc rats (Table 1-1). However, small intestinal tumor multiplicity was unaffected at 140 days ( $p=0.51$ ), 180 days ( $p=0.22$ ) and 210 days of age ( $p=1.0$ ). In male (ACIxF344)F<sub>1</sub>-Pirc rats given high molecular weight DSS, colonic tumor multiplicity was significantly greater at 98 days ( $p<0.0001$ ), 140 days ( $p<0.0001$ ) and 210 days ( $p<0.01$ ) compared with untreated male Pirc rats (Table 1-1). Similar to females, small intestinal tumor multiplicity was generally unaffected by DSS. At 98 days, a significant decrease in tumor multiplicity in the small intestine was found upon DSS treatment ( $p<0.0003$ ); however, this difference was gone by 140 days ( $p=0.35$ ) and remained unchanged at 210 days ( $p=0.95$ ).

Whereas the majority of DSS-treated (ACIxF344)F<sub>1</sub>-Pirc rats become moribund by 180 days of age, (BNxF344)F<sub>1</sub>-Pirc rats given DSS routinely survive beyond 1 year of age. The distribution of colonic tumors in (BNxF344)F<sub>1</sub>-Pirc rats is also quite different from that seen in (ACIxF344)F<sub>1</sub>-Pirc rats. Both untreated and DSS-treated (BNxF344)F<sub>1</sub>-Pirc rats form the majority of their tumors in the proximal colon, especially the herringbone region (Fig 1-4B). In (ACIxF344)F<sub>1</sub>-Pirc rats, tumors rarely form in this proximal herringbone region, and the greatest increase in tumor multiplicity upon DSS treatment is seen in the distal colon and rectum (Fig 1-4A).

**Table 1-1.** Tumor multiplicities in untreated and DSS-treated  $F_1$  Pirc rats. The Wilcoxon rank sum test was used to test for a difference in tumor multiplicity between untreated and DSS-treated rats. A  $p$ -value  $\leq 0.05$  is considered significant.

Strain	Age (days)	Sex	Treatment	N of animals	Small Intestine		Colon	
					Mean $\pm$ SD	p-value	Mean $\pm$ SD	p-value
(AxF) $F_1$	98	M	Control	15	8.9 $\pm$ 2.5		10.3 $\pm$ 3.4	
			DSS	13	5.4 $\pm$ 1.4	0.0002	44.2 $\pm$ 10.3	<0.0001
	140	M	Control	23	9.6 $\pm$ 4.3		22.0 $\pm$ 5.6	
			DSS	13	13.0 $\pm$ 7.6	0.35	56.3 $\pm$ 3.4	<0.0001
		F	Control	5	1.4 $\pm$ 2.1		4.2 $\pm$ 1.5	
			DSS	5	0.4 $\pm$ 0.5	0.51	43.8 $\pm$ 9.9	0.007
	180	F	Control	8*	0.0 $\pm$ 0.0		9.9 $\pm$ 4.3	
			DSS	6	1.0 $\pm$ 1.1	0.22	32.8 $\pm$ 9.6	<0.001
	210	M	Control	9	14.4 $\pm$ 5.1		25.9 $\pm$ 12.9	
			DSS	5	16.8 $\pm$ 11.8	0.95	49.0 $\pm$ 11.1	0.009
		F	Control	3	1.5 $\pm$ 2.1		5.0 $\pm$ 2.6	
			DSS	3	3.5 $\pm$ 5.0	1.0	20.7 $\pm$ 3.5	0.10
(BxF) $F_1$	365	M	Control	2	4.0 $\pm$ 1.4		35.0 $\pm$ 11.3	
			DSS	2	3.0 $\pm$ 2.8	1.0	24.0 $\pm$ 21.2	0.67
		F	Control	3	0.3 $\pm$ 0.6		4.7 $\pm$ 3.5	
			DSS	3	0.7 $\pm$ 0.6	0.65	8.3 $\pm$ 1.5	0.30

\*The small intestines of only two of these animals were available for counting.

**The proportion of growing tumors is increased in DSS-treated Pirc rats.** Tumor multiplicity appears to increase in DSS-treated rats soon after the first treatment (especially in male rats), and continues to increase throughout the life span of the animal (Fig 1-5). To determine whether DSS treatment also affected tumor growth potential, 107 spontaneous colonic tumors and 72 DSS-induced tumors were scored as growing, static or regressing by three blinded observers. No difference has been seen in tumor fate between female and male rats<sup>12</sup>; therefore all tumors were combined for analysis. In control Pirc rats, 71% of the tumors grew, 25% were static and 4% regressed (Fig 1-6). A dramatic shift towards growing tumors was seen in Pirc rats treated with DSS, where 95% grew, 4% were static and 1% regressed. Tumors that would otherwise become static appear to be shifted towards the growing fate upon DSS treatment. Thus, the number of growing versus non-growing tumors was significantly greater in DSS-treated Pirc rats compared to Pirc rats not given DSS ( $p < 0.0002$ ).

**Fig 1-4.** Whole mount colons from untreated and DSS-treated Piric male rats. (A) At 97 days of age, DSS treatment significantly enhances the number of colonic tumors in (ACIxF344) $F_1$  male Piric rats, especially in the distal colon (right). (B) By contrast, at 365 days of age, DSS-treatment does not affect tumor multiplicity in (BNxF344) $F_1$  male Piric rats. Further, tumors preferentially form in the proximal colon (left) in (BNxF344) $F_1$  male Piric rats.

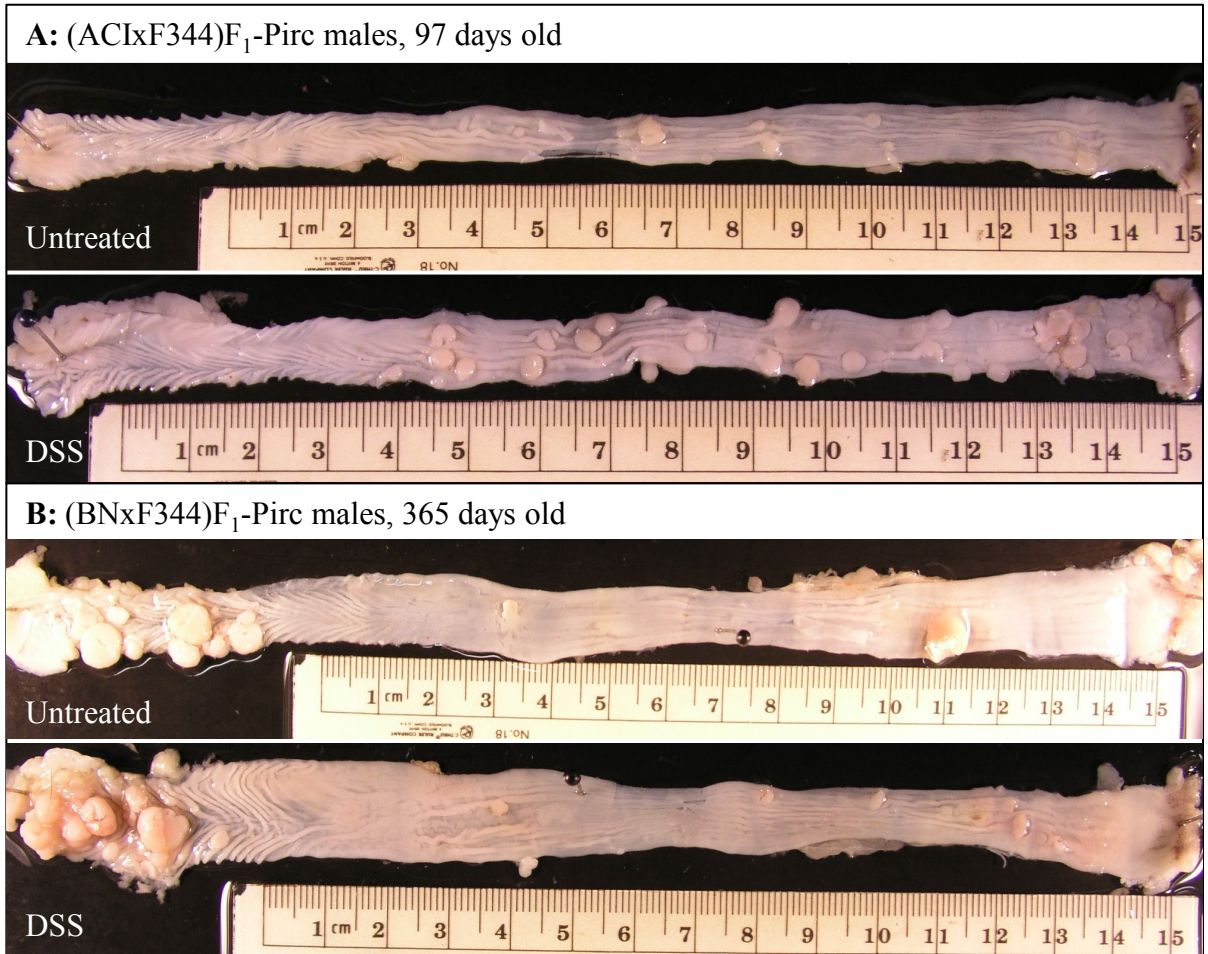




**Fig 1-5.** Longitudinal tumor counts by endoscopy. Tumors were counted by endoscopy for 6 female and 11 male untreated (ACIxF344) $F_1$  Pirc rats and 6 female and 10 male DSS-treated (ACIxF344) $F_1$  Pirc rats at various time points. Endoscopy is generally done before the first DSS treatment (40 days), before the start of the second DSS treatment (54 days) and every 10-14 days thereafter. Error bars represent the biological standard deviation from the mean. Note: endoscopy in the rat can visualize approximately the distal two-thirds of the colon; therefore, tumors that arise in the proximal colon may go undetected until sacrifice.

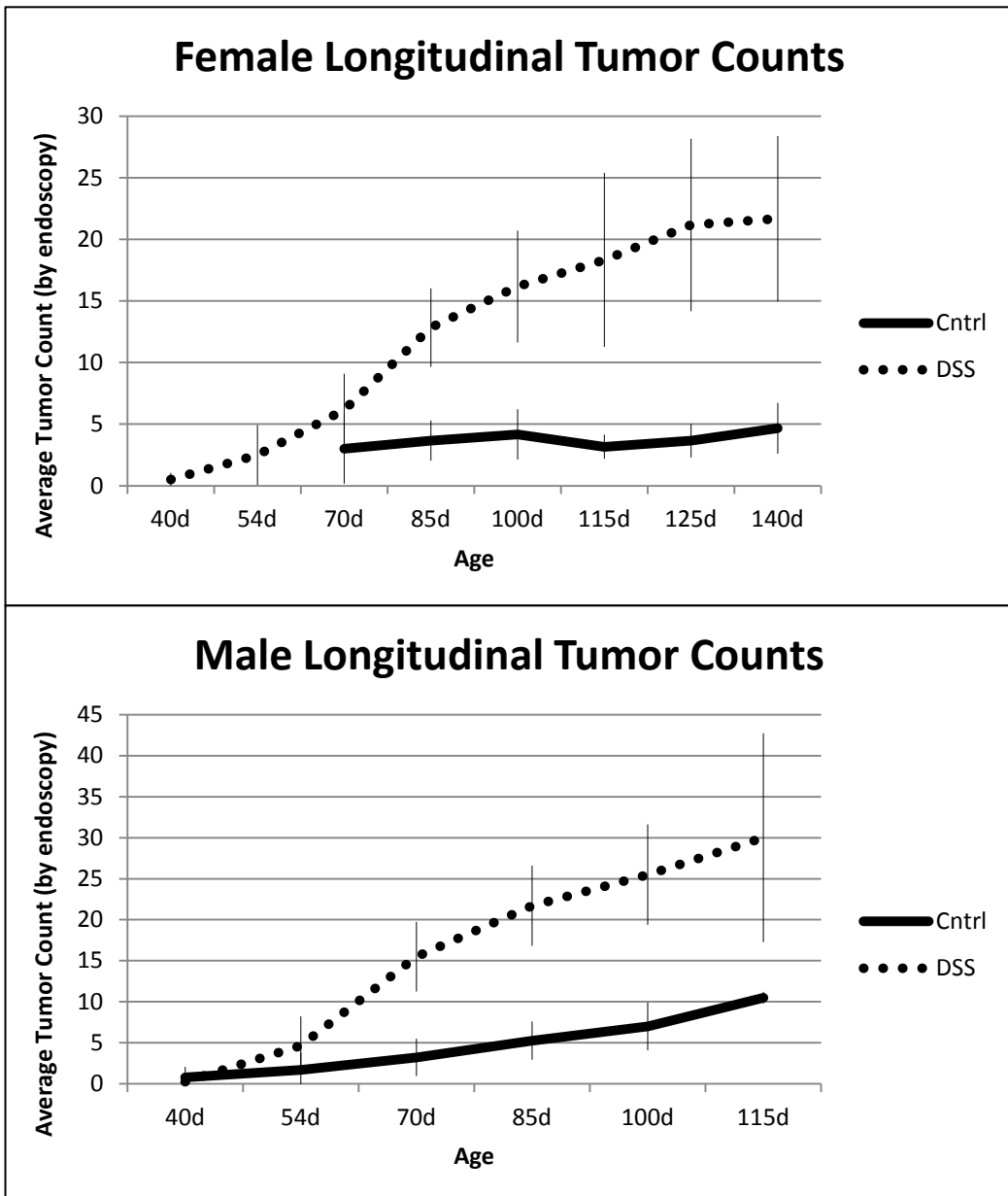


**Fig 1-6.** Longitudinal growth profiles by endoscopy. In control Pirc rats, 71% of tumors grew, 25% were static and 4% regressed. A dramatic shift towards growing tumors was seen in Pirc rats treated with DSS, where 95% grew, 4% were static and 1% regressed. The proportion of growing versus not growing tumors was significantly greater in DSS-treated Pirc rats compared to untreated Pirc rats ( $p < 0.0002$ ).

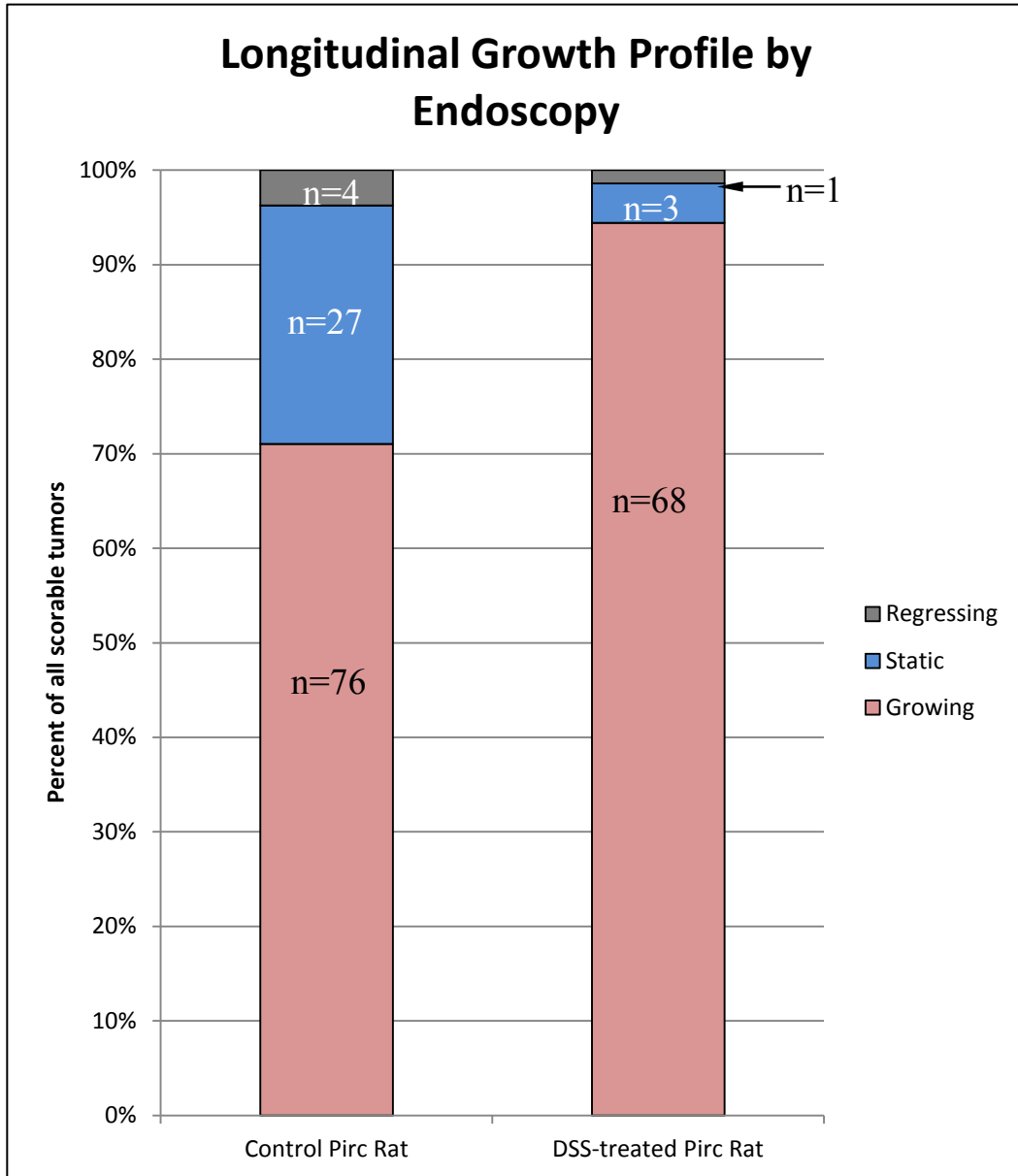


**Fig 1-7.** Histopathological grading of colonic tumors. Histopathological grading of hematoxylin and eosin stained tumor sections revealed that tumor stage is unaffected in female Pirc rats (top panel), but is enhanced in male Pirc rats given DSS (bottom panel).

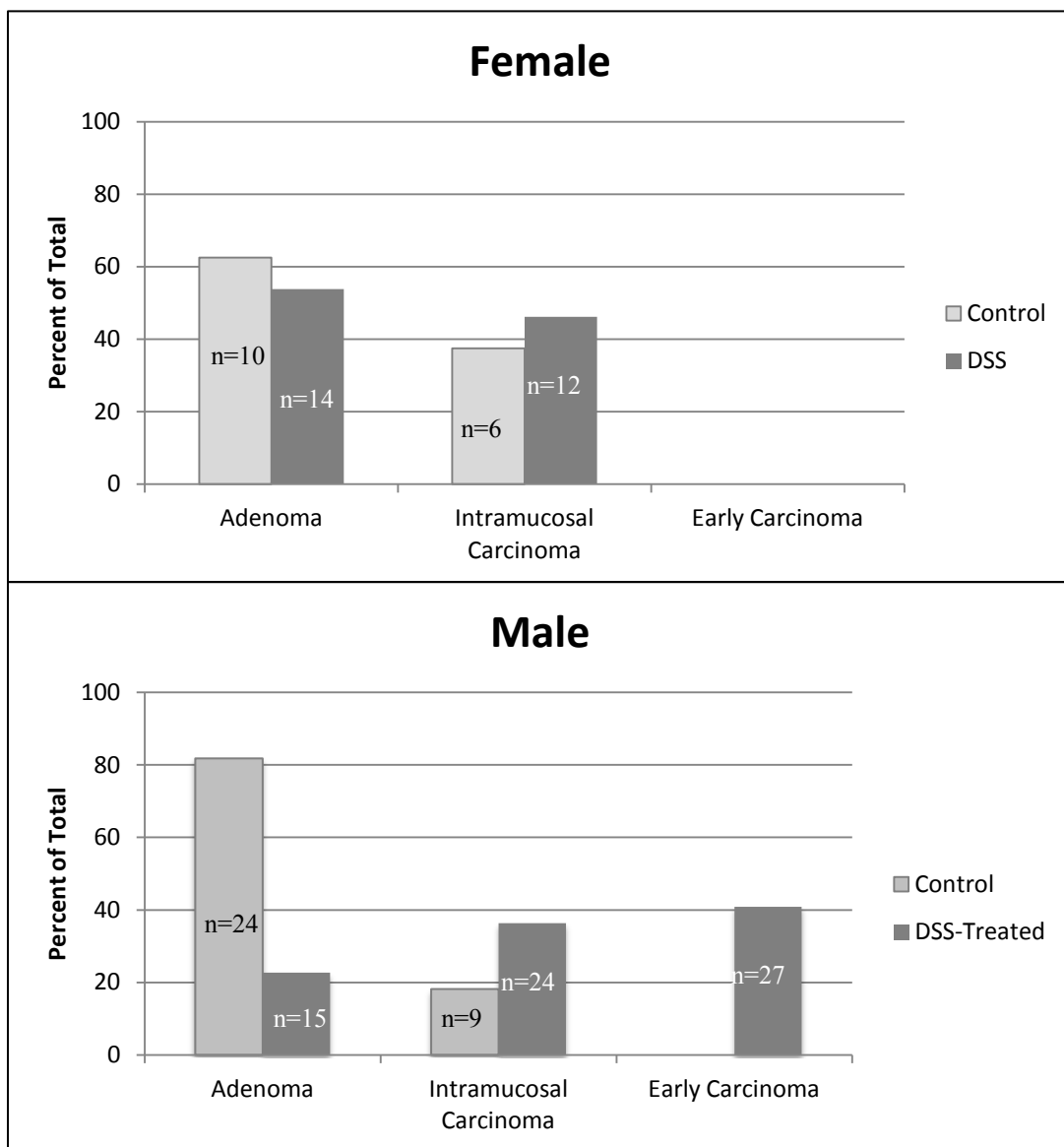
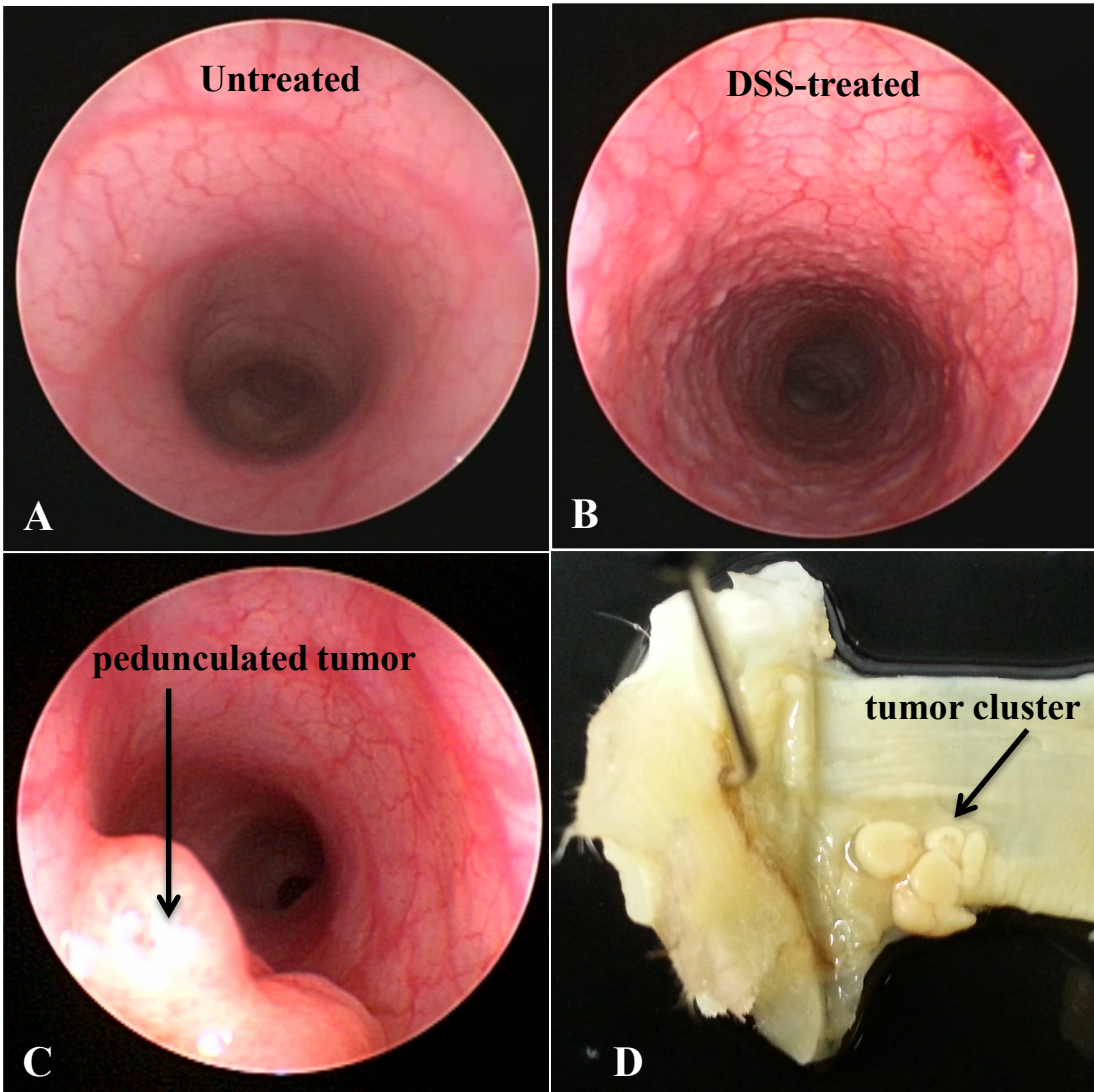


**Fig 1-8.** DSS phenotype in wild type rats. Wild type rats generally have a smooth colonic mucosa with no lesions (A). After DSS treatment, a cobblestone pattern appears (B) and persists until the animal is sacrificed. Untreated wild type rats never develop colonic tumors, while only a single cluster of rectal tumors has been observed upon endoscopy (C) and dissection (D) in one of over thirty wild type rats given DSS.



**Tumor stage is increased in DSS-treated Pirc rats.** Although tumor multiplicity is increased in both female and male Pirc rats given DSS, only male rats show an increase in tumor stage upon DSS-treatment. At 180 days of age, colonic tumor stage did not differ between untreated (n=18) and DSS-treated (n=26) female Pirc rats (p=0.48). In untreated female Pirc rats, 63% of tumors were adenomas, 38% were intramucosal carcinomas and none were early carcinomas (Fig 1-7, top panel). Similarly, in DSS-treated female Pirc rats, 54% of tumors were adenomas, 46% were intramucosal carcinomas and none were early carcinomas.

By contrast, tumor stage is significantly altered in DSS-treated male Pirc rats (n=66) compared to their untreated counterparts (n=33, p<0.00001). Whereas 82% of tumors were adenomas and 30% were intramucosal carcinomas in untreated male Pirc rats, 23% of tumors were adenomas and 36% were intramucosal carcinomas in DSS-treated Pirc rats (Fig 1-7, bottom panel). Further, none of the tumors in untreated male Pirc rats were early carcinomas, while 41% of tumors were early carcinomas in DSS-treated male Pirc rats. This represents a highly significant shift towards invasive tumors within the DSS-treated male Pirc rat.

**DSS treatment in the *Apc* wild type rat.** During DSS treatment, wild type rats develop the same symptoms as Pirc rats, including bloody stool. Commonly, they also develop a “cobblestone” phenotype in the distal colon and rectum following treatment (Fig 1-8B). This cobblestone persists even to one year of age, the oldest age that rats have been examined in our studies.

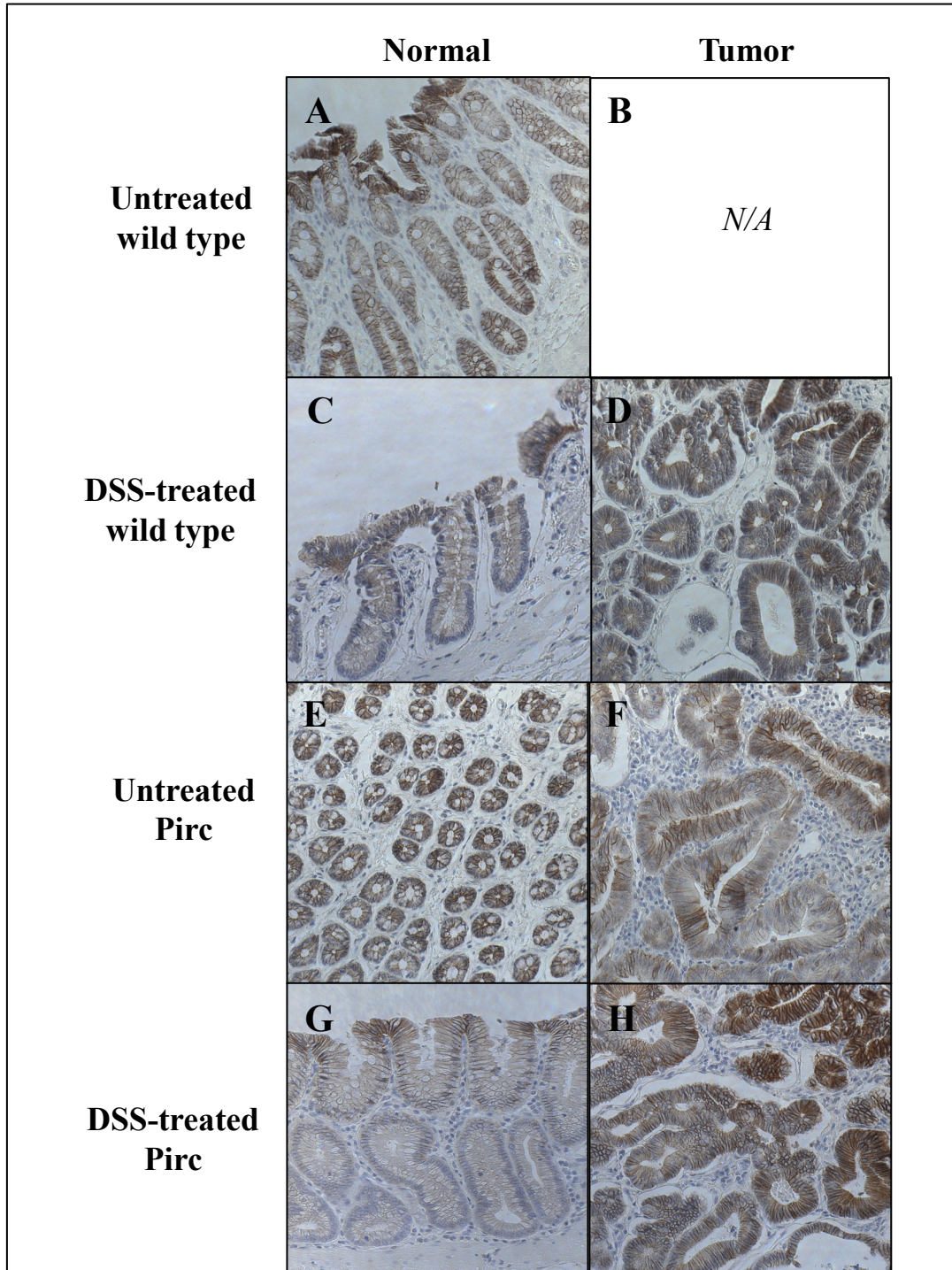
Despite this visible disturbance of the colonic tissue, tumors rarely form in the DSS-treated wild type rat. Of a total 29 male (ACIxF344)F<sub>1</sub> *Apc* wild type rats aged up to 300 days having undergone two or five week-long DSS cycles, only one rat developed a tumor. In this rat, a single rectal tumor appeared 11 weeks after the end of the 2<sup>nd</sup> and final DSS treatment (Fig 1-

8C). This tumor underwent biopsy at several endoscopic visits, and histological evaluation of the biopsy sample revealed that it was indeed neoplastic. At termination, this single tumor appeared instead as a cluster (Fig 1-8D). This could be owing to initiation of a “field” predisposed to tumor formation caused by either DSS treatment or repeat *in vivo* biopsy (see Appendix E).

**$\beta$ -catenin protein localization in normal tissue and tumors from spontaneous and DSS-treated rats.** When *Apc* function is lost within a cell,  $\beta$ -catenin is then able to accumulate in the cytoplasm and translocate to the nucleus.  $\beta$ -catenin is often used as an immunohistochemical marker of cells that have lost *Apc* function, and is a reliable marker of neoplastic lesions. In normal colonic tissue of untreated wild type or Pirc rats,  $\beta$ -catenin protein localizes only to the cell membrane (Fig 1-9A, C, E, G). By contrast, in neoplastic tissue from untreated Pirc rats,  $\beta$ -catenin protein is strongly expressed in the cytoplasm, and occasionally the nucleus, of the cell (Fig 1-9D, F, H).

Tumors from Pirc rats given DSS also show an accumulation of  $\beta$ -catenin protein in the cytoplasm (Fig 1-9H). This may not be surprising given that these tumors are arising in a model where expression of *Apc* has already been lost from one allele. However, the single tumor cluster that developed in a DSS-treated *Apc* wild type rat also showed  $\beta$ -catenin accumulation within the cytoplasm (Fig 1-9D). It is possible that treatment with DSS caused a mutation in *Apc* or *Ctnnb1* ( $\beta$ -catenin). A mutation resulting in a dominant constitutive allele of  $\beta$ -catenin could explain the increase cytoplasmic accumulation of  $\beta$ -catenin protein. Sequencing of both *Apc* and *Ctnnb1* could help to resolve this question.

**Figure 1-9:**  $\beta$ -catenin staining patterns in untreated and DSS-treated wild type and Pirc rats.  $\beta$ -catenin protein normally localized to the cell membrane (A, C, E, G). In both sporadic and DSS-induced lesions in wild type and Pirc rats,  $\beta$ -catenin protein accumulates in the cytoplasm (D, F, H). All images acquired at 20x magnification.



**Enhanced maintenance of heterozygosity at the Pirc locus in tumors from DSS-treated rats.**

To determine whether Pirc rats given DSS developed tumors that were similar to those in untreated Pirc rats, we measured the allelic ratios at the Pirc locus using Pyrosequencing. Of a total 9 colonic tumors from untreated (ACIxF344)<sub>F1</sub> Pirc rats, 100% lost both genomic and cDNA expression of *Apc* (gLOH, cLOH). This contrasts sharply with tumors from DSS-treated (ACIxF344)<sub>F1</sub> Pirc rats: of 24 total tumors, only 67% lost the wild type allele of *Apc* in the genome. In these DSS-treated rats, 25% of tumors maintained heterozygosity of genomic DNA, but lost expression of the cDNA (gMOH, cLOH), and 8% maintained heterozygosity of both the genomic and cDNA (gMOH, cMOH).

**Sequencing of *Apc* and *Ctnnb1* in gMOH/cMOH tumors.** In our small study of 33 sporadic and DSS-induced tumors, we found 8 DSS-induced tumors that maintained heterozygous expression of *Apc*; 2 of these 8 tumors also maintained expression of the cDNA (gMOH, cMOH). Analysis by Sanger sequencing of these two DSS-induced gMOH, cMOH tumors showed that one tumor carried a new mutation in *Apc*, in addition to the Pirc mutation. This mutation occurred in exon 15 of *Apc*. An additional mutation was found in another tumor that was gLOH, cLOH at dissection, but gMOH, cLOH at an earlier biopsy. This mutation occurred in intron 13 of *Apc*. No mutations in exons 2, 3 or 4 of *Ctnnb1* ( $\beta$ -catenin), which contain a mutation hot spot, were found in any of the tumors examined.

**Discussion**

Colon cancers that arise in a field of inflammation may be even more complex than those arising sporadically. Individuals with an inflammatory bowel disease may develop some tumors



that resemble the sporadic case and others that depend upon the surrounding inflammation. Furthermore, the mechanisms underlying these two scenarios may be additive or even counteract one another. This was shown to be true in a rare case of a patient with both familial adenomatous polyposis (FAP), an inherited syndrome where *Apc* is mutated, and concomitant ulcerative colitis. Polyps were seen in this patient only in the area lacking active inflammation, and these polyps were classified as adenomatous<sup>20</sup>. FAP patients have hundreds to thousands of polyps form along the length of the colon, so an area devoid of polyps is generally not seen. Mosaicism was ruled out as a cause for this lack of polyps. The authors posit that the inflammation may have suppressed the polyps, and that any suppression would have needed to occur early, as they were unable to detect even an aberrant crypt focus, a controversial early indicator of neoplasia, in this region. While this case is unique and counter to the general observation that patients with colonic inflammation have an increased risk of cancer, it nonetheless illustrates the complex nature of cancers arising in an inflammatory field.

The phenotype of the DSS-treated Pirc rat has many similarities to those seen in IBD patients with cancer. While all (ACIxF344)F<sub>1</sub> Pirc rats will develop tumors and therefore a change in risk cannot be measured, the multiplicity of tumors in DSS-treated rats is increased. Further, we have never detected a tumor in a wild type rat, except when it has first been given DSS. The cancer risk for males is greater than females in the general population<sup>16</sup>. This gender disparity further extends to patients with IBD. In a population-based study of over 7000 patients with IBD, 8% of males developed colon cancer, while only 3% of females did over a surveillance period of 40 years<sup>21</sup>.

The stage of tumors associated with inflammation is also greater in both human patients and in our rat model. Interestingly, this increase in tumor stage following DSS treatment is only

evident in male Pirc rats. In humans, there is a greater prevalence of Crohn's disease in females, though the incidence of ulcerative colitis does not differ by gender<sup>2</sup>. Although the age-standardized mortality rate from colon cancer is consistently higher in men than woman<sup>14</sup>, studies restricted to the subset of patients with concomitant IBD are lacking.

Examining the DSS-treated Pirc rat can expand our understanding of the involvement of the Wnt pathway in inflammatory cancer. While the *Apc* mutation present in Pirc rats causes many more tumors to form after DSS treatment than in wild type rats, it appears that loss of the second allele, either in genomic or cDNA, is not always required for tumor formation. Knudson's two-hit hypothesis, which states that a single genetic "hit" would be insufficient to initiate tumorigenesis, may not be true in the case of inflammation<sup>13</sup>. Indeed, one-hit effects have been detected in the proteome of FAP patients heterozygous for an *Apc* mutation. Of the 1695 proteins identified, 13% were abnormally expressed in apparently normal crypts, and these abnormal proteins were often consistent with at least a partial loss of *Apc* function<sup>25</sup>. This finding is supported further by a study in the *Apc*<sup>Min/+</sup> mouse showing that cell shape at the base of the crypt is altered even in heterozygous colonic tissue, which may contribute to tumorigenesis<sup>19</sup>.

Pyrosequencing of whole tumors has caveats<sup>23</sup>, which may be especially pronounced in the DSS model. A tumor is not comprised purely of neoplastic cells, and likely contains pathologically normal cells as well. Furthermore, DNA or RNA is isolated from the admixture of cells that comprises the tumor, including epithelial, stromal and immune contributions. An increase in immune cells related to the inflammatory microenvironment, or an increase in stromal cells owing to increased invasion may each result in a shift towards a tumor appearing to have maintained expression at either the genomic or cDNA levels. It is possible that our results from these studies of allelic loss are affected by these caveats. It is unknown whether the distribution of al-

lelic ratios in apparently normal colonic tissue from DSS-treated rats differs from the expected gMOH, cMOH in normal colonic tissue from untreated rats. Even with the caveats of the assay of allelic ratios, this could give insight into whether the loss of *Apc* function is sufficient (loss of function in apparently normal tissue) or necessary (intact function within tumors) for tumor development.

A second interesting aspect of the interaction between the Wnt pathway and inflammation comes from the observation that the tumor from the DSS-treated wild type rat had increased cytoplasmic  $\beta$ -catenin accumulation. No  $\beta$ -catenin mutations were found in tumor tissue from DSS-treated Pirc rats; however, it is unknown whether  $\beta$ -catenin mutations are present in normal tissue or tumor from DSS-treated wild type rats.

*Apc* may also play a role in colonic inflammation and healing apart from its regulation of the Wnt pathway. The Kyoto *Apc* Delta, or KAD rat, contains a mutation causing premature termination at codon 2523 of APC<sup>27</sup>. By contrast to the Pirc rat model, the KAD is homozygous viable and will not develop tumors unless also given both AOM and DSS. Additionally, the regulation of the Wnt pathway by the Kyoto c-terminal truncation mutant APC appears to be intact<sup>26</sup>. However, compared to DSS-treated wild type rats, when the KAD rat is given DSS alone, defects are seen in the ability of the colonic mucosa to heal following the inflammatory insult. After DSS treatment, KAD rats show reduced angiogenesis, a longer latency to crypt repopulation, and a longer duration with elevated levels of several cytokines and inflammatory mediators<sup>26</sup>. This is similar to what is seen in IBD patients, and suggests that *Apc* function may contribute directly or indirectly to IBD pathogenesis. This dual role for *Apc* in both the inflammatory process and subsequent tumorigenesis make it a relevant candidate for understanding colorectal cancer associated with inflammation.

In our experiments we chose to use a molecular weight of DSS different from that generally reported in the literature. In wild type ACI rats the 54,000 Da molecular weight was reported to be the most carcinogenic<sup>11</sup>. The most commonly utilized form is approximately 40,000 Da in molecular weight, but even at lower concentrations, this form causes severe disturbances to crypt structure, with complete loss of crypts seen even in wild type rats<sup>26</sup>. Instead, we have chosen to utilize the 500,000 Da molecular weight for the majority of our studies. This molecular weight allows crypt structure to maintain intact, while still causing a dramatic increase in tumor multiplicity, proportion of growing tumors and tumor stage in the Pirc rat.

Since both spontaneous and DSS-induced tumors will occur in DSS-treated Pirc animals, it may be difficult within this mixed model to detect any differences between the sporadic and inflammation-associated pathways. However, effects of DSS on normal colonic mucosa in the rat, especially those also occurring in wild type animals, will increase our understanding of inflammation in the gut and how it affects the tumorigenic process. Perturbations caused by DSS to the normal mucosa that foreshadow tumor development may give insights into the earliest processes of tumorigenesis.

## References

1. **Amos-Landgraf JM, Kwong LN, Kendzierski CM, Reichelderfer M, Torrealba J, Weichert J, Haag JD, Chen K-S, Waller JL, Gould MN, et al.** 2007. A target-selected Apc-mutant rat kindred enhances the modeling of familial human colon cancer. *Proceedings of the National Academy of Sciences USA*. **104**:4036–41.
2. **Brant SR, Nguyen GC.** 2008. Is there a gender difference in the prevalence of Crohn's disease or ulcerative colitis? *Inflammatory Bowel Diseases*. **14 Suppl 2**:S2–3.
3. **Claessen M, Schipper M, Oldenburg B, Siersema P, Offerhaus G, Vleggaar F.** 2010. WNT-pathway activation in IBD-associated colorectal carcinogenesis: Potential biomarkers for colonic surveillance. *Cellular Oncology*. **32**:303–10.
4. **Claessen MMH, Schipper MEI, Oldenburg B, Siersema PD, Offerhaus GJA, Vleggaar FP.** WNT-pathway activation in IBD-associated colorectal carcinogenesis: potential biomarkers for colonic surveillance. *Cellular Oncology*. 2010;**32**:;303–310.
5. **Cooper H, Murthy S, Kido K, Yoshitake H, Flanigan A.** 2000. Dysplasia and cancer in the dextran sulfate sodium mouse colitis model. Relevance to colitis-associated neoplasia in the human: a study of histopathology, B-catenin and p53 expression and the role of inflammation. *Carcinogenesis*. **21**:757–68.
6. **Dirisina R, Katzman RB, Goretsky T, Managlia E, Mittal N, Williams DB, Qiu W, Yu J, Chandel NS, Zhang L, et al.** 2011. p53 and PUMA independently regulate apoptosis of intestinal epithelial cells in patients and mice with colitis. *Gastroenterology*. **141**:1036–45.
7. **Eaden J a, Abrams KR, Mayberry JF.** 2001. The risk of colorectal cancer in ulcerative colitis: a meta-analysis. *Gut*. **48**:526–35.
8. **Fearnhead N, Britton M, Bodmer W.** 2001. The ABC of Apc. *Human Molecular Genetics*. **10**:721–733.
9. **Freeman H.** 2001. Colorectal cancer complicating Crohn's Disease. *Canadian Journal of Gastroenterology*. **15**:231–36.
10. **Hirono I, Kuhara K, Hosaka S, Tomizawa S, Golberg L.** 1981. Induction of Intestinal Tumors in Rats by Dextran Sulfate Sodium. *Journal of the National Cancer Institute*. **66**:579–583.
11. **Hirono I, Kuhara K, Yamaji T, Hosaka S, Golberg L.** 1983. Carcinogenicity of dextran sulfate sodium in relation to its molecular weight. *Cancer Letters*. **18**:29–34.

12. **Irving AA, Halberg RB, Albrecht DM, Plum LA, Krentz KJ, Clipson L, Drinkwater N, Amos-Landgraf JM, Dove WF, DeLuca HF.** 2011. Supplementation by vitamin D compounds does not affect colonic tumor development in vitamin D sufficient murine models. *Archives of Biochemistry and Biophysics*. **515**:64–71.
13. **Knudson A.** 1996. Hereditary cancer: two hits revisited. *Journal of Cancer Research and Clinical Oncology*. **122**:135–140.
14. **Koo JH, Leong RWL.** 2010. Sex differences in epidemiological , clinical and pathological characteristics of colorectal cancer. *Gastroenterology and Hepatology*. **25**:33–42.
15. **Mikami T, Yoshida T, Numata Y, Kikuchi M, Araki K, Nakada N, Okayasu I.** 2011. Invasive behavior of ulcerative colitis-associated carcinoma is related to reduced expression of CD44 extracellular domain: comparison with sporadic colon carcinoma. *Diagnostic Pathology*. **6**:30.
16. **Nguyen S, Bent S, Chen Y, Terdiman J.** 2009. Gender as a risk factor for advances neoplasia and colorectal cancer: a systematic review and meta-analysis. *Clinical Gastroenterol and Hepatol*. **7**:676–81.
17. **Onose J, Imai T, Hasumura M, Ueda M, Hirose M.** 2003. Rapid induction of colorectal tumors in rats initiated with 1,2-dimethylhydrazine followed by dextran sodium sulfate treatment. *Cancer Letters*. **198**:145–152.
18. **Ouaïssi M, Maggiori L, Alves A, Giger U, Sielezneff I, Valleur P, Sastre B, Panis Y.** 2011. Colorectal cancer complicating inflammatory bowel disease: a comparative study of Crohn’s disease vs ulcerative colitis in 34 patients. *Colorectal disease: the official journal of the Association of Coloproctology of Great Britain and Ireland*. **13**:684–8.
19. **Quyn AJ, Appleton PL, Carey FA, Steele RJC, Barker N, Clevers H, Ridgway RA, Sansom OJ, Näthke IS.** 2010. Spindle orientation bias in gut epithelial stem cell compartments is lost in precancerous tissue. *Cell Stem Cell*. **6**:175–81.
20. **Samadder NJ, Gornick M, Everett J, Greenson JK, Gruber SB.** 2013. Inflammatory bowel disease and familial adenomatous polyposis. *Journal of Crohn’s & Colitis*. **7**:e103–7.
21. **Söderlund S, Granath F, Broström O, Karlén P, Löfberg R, Ekblom A, Askling J.** 2010. Inflammatory bowel disease confers a lower risk of colorectal cancer to females than to males. *Gastroenterology*. **138**:1697–703.
22. **Tanaka T, Kohno H, Suzuki R, Yamada Y, Sugie S, Mori H.** 2003. A novel inflammation-related mouse colon carcinogenesis model induced by azoxymethane and dextran sodium sulfate. *Cancer Science*. **94**:965–73.

23. **Tomlinson IPM, Lambros MBK, Roylance RR.** 2002. Loss of heterozygosity analysis: practically and conceptually flawed? *Genes, Chromosomes & Cancer.* **34**:349–53.
24. **Washington MK, Powell AE, Sullivan R, Sundberg J, Wright N, Coffey RJ, Dove WF.** 2013. Pathology of Rodent Models of Intestinal Cancer: Progress Report and Recommendations. *Gastroenterology.* **4**:705-17.
25. **Yeung AT, Patel BB, Li X, Seeholzer SH, Coudry RA, Cooper HS, Bellacosa A, Boman BM, Zhang T, Litwin S, et al.** 2008. One-Hit Effects in Cancer: Altered Proteome of Morphologically Normal Colon Crypts in Familial Adenomatous Polyposis. *Cancer.* **18**:7579–7586.
26. **Yoshimi K, Tanaka T, Serikawa T, Kuramoto T.** 2013. Tumor suppressor APC protein is essential in mucosal repair from colonic inflammation through angiogenesis. *The American Journal of Pathology.* **182**:1263–74.
27. **Yoshimi K, Tanaka T, Takizawa A, Kato M, Hirabayashi M, Mashimo T, Serikawa T, Kuramoto T.** 2009. Enhanced colitis-associated colon carcinogenesis in a novel Apc mutant rat. *Cancer Science.* **100**:2022–7.

## Chapter 2

### **Early gene expression signatures of previously inflamed normal colonic tissue may foreshadow tumor development and progression**

Amy A. Irving designed the studies (in collaboration with James Amos-Landgraf), performed the majority of the rat endoscopies and dissections, completed all of the data analysis and wrote the final manuscript. Kathleen J. Krentz, Tony Hunter, Mackenzie Eagen, Jennifer K. Pleiman and Madeline R. Ford each assisted with endoscopies, dissections and/or sample collection. William F. Dove served as an advisor.



## **Abstract**

Although many association studies have identified an increased risk of colorectal cancer among patients with an inflammatory bowel disease, the specific molecular or cellular players that cause this increase in risk remain to be elucidated. Studies are beginning to examine differences between uninflamed and inflamed tissue from patients with and without an inflammatory bowel disease and with and without neoplasia. However, these human studies are generally restricted to small cohorts that may lack the power to detect differences above background in the face of the uncontrolled variables within human populations.

Here, we have harnessed the power of the Pirc rat to discover molecular players in inflammation-associated carcinogenesis using a controlled experimental model of colorectal cancer. By treating Pirc rats with dextran sodium sulfate (DSS), an inflammatory microenvironment is created to allow us to study how inflammation affects both apparently normal tissue as well as the tumors that arise within this field. Furthermore, although DSS-treated wild type rats rarely develop even a single tumor, untreated and DSS-treated wild type rats allow us to discover molecular markers that are differentially expressed in normal tissue independently of the Pirc mutation. Taken together, these data can help us to begin to understand what events are occurring early following an inflammatory event that may predispose to tumor formation in the future. Finally, these early markers may foreshadow changes that occur later in inflammation-associated tumors that drive them to grow and become more invasive than their spontaneous counterparts.

## **Introduction**

Inflammation is strongly associated with the tumorigenic process, but a great deal remains to be understood regarding the specific role played by the several classes of cells that contribute to a tumor, and the timing, tissue localization and interactions between each of these cellular and molecular players. Patients with an inflammatory bowel disease have increased risk of developing colon cancer<sup>13</sup>. However, not all of these individuals will develop cancer. Further, in patients with widespread inflammation, tumors generally arise focally rather than as a field of tumors. Often though, these tumors become more invasive than those arising in patients without an inflammatory disease<sup>39</sup>. These phenomena lead us to ask whether there are genetic or molecular markers within inflamed tissue that foreshadow the development of a tumor. Additionally, do these markers differ between spontaneous tumors and tumors present in an inflamed environment?

Studies in humans report differences in apparently normal tissue between asymptomatic patients and patients with an inflammatory bowel disease (IBD). One particular pathway of interest is the Wnt pathway, as Wnt activation is involved in a majority of sporadic colorectal cancers<sup>21</sup>. If patients with inflammatory bowel disease have an over-activated Wnt pathway in apparently normal tissue, this may in turn lead to tumor development. Indeed, it has been shown that in apparently normal colonic tissue, ulcerative colitis (UC) patients have a level of Wnt activation (measured by  $\beta$ -catenin expression) intermediate between that seen in normal tissue from asymptomatic patients and that in frank cancer<sup>52</sup>. Further, levels of nuclear  $\beta$ -catenin expression increase, and levels of membranous expression decrease, as tumors progress from inflamed normal tissue to dysplasia to colorectal cancer<sup>12</sup>.

Interestingly, when inflamed tissue is segregated into two classes- that from UC patients and that from Crohn's disease (CD) patients-  $\beta$ -catenin levels are altered in normal tissue only from UC and not from CD patients<sup>55</sup>. Generally colitis occurs in patches in CD patients compared with the extensive colitis in UC patients. Although, CD patients typically having a higher cancer risk than UC patients<sup>23</sup>, the risk for synchronous tumors is higher in UC patients. While 55% of UC patients have synchronous dysplasia and 14% have synchronous tumors, only 30% of CD patients have synchronous dysplasia and 4% have synchronous tumors<sup>33</sup>. Since gene expression patterns in inflamed mucosa are very similar between UC and CD patients<sup>25</sup>, the extent or duration of inflammation alone may account for these differences<sup>19</sup>.

Though molecular differences occurring between uninflamed tissue in asymptomatic patients and inflamed tissue from IBD patients is not surprising, differences also exist in uninflamed tissue between asymptomatic patients and IBD patients. When non-inflamed tissue from 24 asymptomatic patients was compared to non-inflamed tissue from 25 ulcerative colitis patients by microarray, 706 probes were significantly differentially expressed (GEO Dataset GDS3268, FDR 1%)<sup>43</sup>. Changes that are occurring in apparently normal tissue, even after the inflammation has subsided, may predispose to tumor development.

In our studies, we want to determine what molecular changes occur in apparently normal colonic tissue following an inflammatory insult. Further, we sought to determine whether these molecular changes correlate with changes that occur in early adenomas. Finally, we want to understand whether these molecular candidates can give insight regarding the future fate of the tumor. To accomplish this, a subset of wild type and Pirc rats were given the inflammatory stimulus dextran sodium sulfate (DSS). Tissues from normal colon (wild type and Pirc) and tumor (Pirc) were harvested after inflammation from DSS treatment had subsided, but before differ-

ences in tumor pathology were seen. These tissues were compared by whole genome microarray analysis to determine molecular signatures in the apparently normal mucosa from DSS-treated wild type and Pirc rats that correlated with changes observed in the tumor.

## **Materials and Methods**

**Animal Breeding and Maintenance.** Rats were maintained under a protocol approved by the Animal Care and Use Committee of the University of Wisconsin School of Medicine and Public Health and in a facility in the McArdle Laboratory approved by the American Association of Laboratory Animal Care. Rats were individually housed in standard caging with free access to Lab Diet 5020 chow (St. Louis, MO) and acidified water. F<sub>1</sub> generation (ACIxF344)-Pirc rats were generated by breeding female ACI *Apc*<sup>+/+</sup> rats (Harlan, Indianapolis, IN) to male F344 coisogenic *Apc*<sup>Pirc/+</sup> rats (developed in the laboratory of WFD and now commercially available through Taconic, Hudson, NY)<sup>1</sup>. F<sub>1</sub> generation Pirc rats show tumor multiplicity and time to tumor emergence intermediate between each parental strain. Congenic ACI-Pirc rats are more susceptible to colonic tumor development than F344-Pirc rats. (ACIxF344)F<sub>1</sub> Pirc rats develop fewer tumors than the ACI-Pirc parental strain, but more rapidly than the F344-Pirc parental strain. (ACIxF344)F<sub>1</sub> wild type rats from these litters develop no intestinal tumors and were used to find transcripts altered in normal tissue upon DSS treatment independent of the Pirc mutation.

**DSS Treatment.** A 4% solution (wt/vol) of dextran sodium sulfate (DSS; Fisher Scientific (500,000 Da; Pittsburgh, PA) was mixed with standard acidified drinking water and delivered to

a subset of Pirc and wild type rats from 40-47 days of age and again from 54-61 days of age. Following DSS treatment the rats were returned to normal acidified drinking water for the remainder of the experiment.

**Sample Collection and DNA/RNA Isolation.** Untreated and DSS-treated Pirc and wild type rats were aged to 97 days and sacrificed for sample collection. Samples were collected from tumor and normal tissue for DNA and RNA isolation before the colon was exposed to ethanol or formalin. Samples were obtained from tumor by making a vertical cut at the tumor midline down to the center of the tumor. Then a second cut was made perpendicular to the first, resulting in one-quarter of the tumor being harvested. This method allows cells to be collected from the outer tumor as well as from the innermost tumor near the stalk, yet allows the remaining tumor to be left securely attached to the stalk. This is important to preserve the relationship with the normal intestinal tissue for future histological analysis. For normal tissue collection, a scalpel blade was used to gently scrape the normal intestinal tissue in the distal colon. These scrapings contain many cell types including epithelial, stromal and immune components. This must be taken into consideration when interpreting any resultant data from these samples. A minimum 2 mm barrier surrounding any tumor was required for normal tissue collection. All samples were homogenized in a tube containing RLTplus buffer (Qiagen, Valencia, CA) and frozen at -80° C until use. DNA and RNA were extracted from the same sample using an Allprep DNA/RNA Mini Kit (Qiagen) following the manufacturer's protocol. DNA contamination of RNA samples was overcome by DNase treatment of the RNA using the protocol recommended by the manufacturer. cDNA was generated from isolated RNA using the SuperScript III Reverse Transcriptase Kit (Invitrogen).

**Microarray Design.** All microarray experiments follow the nomenclature, descriptions, and data sharing recommended by the MIAME Guidelines<sup>5</sup>. The microarray data discussed in this publication have been deposited in NCBI's Gene Expression Omnibus<sup>19</sup> and are accessible through GEO Series accession number GSE54036. Only male rats were utilized for the microarray studies to eliminate the potential confounder of the estrus cycle of female rats. A 12:12 hour light:dark cycle was maintained throughout the experiments, and rats were all dissected within a four-hour window in the afternoon to control for any transcripts that could vary according to circadian cycles. For both single and two-color arrays, total RNA (100 ng) isolated from normal colonic tissue and tumors from untreated and DSS-treated Pirc and wild type rats was labeled with a Low Input Quick Amp kit with Cy3 dye (Agilent, Santa Clara, CA) according to the manufacturer's instructions. For two-color arrays, the control channel was comprised of RNA collected from normal tissue from a cohort of rats labeled with Cy5 dye. Samples were evenly distributed and hybridized to a total of 24 Agilent Whole Genome 4x44k microarrays (Pirc samples, two color; 6 biological samples each of control normal tissue matched to control tumors, and DSS-treated normal tissue matched to DSS-treated tumors) or 16 Agilent Whole Genome 8x60k microarrays (Pirc and wild type normal tissue samples, single color; 4 biological samples each of control normal tissue and DSS-treated normal tissue from each genotype). Following incubation, arrays were scanned on an Agilent High-Resolution Microarray Scanner at 3  $\mu$ m resolution with a 20 bit data format.

**Microarray Analysis.** Files were extracted using Agilent Feature Extraction version 10.7. Data were then imported into Partek Genome Suite software for analysis (St. Louis, MO). Functional

annotation was done using DAVID<sup>29</sup> and protein interactions were determined using STRING<sup>2</sup>, using lists of genes differentially expressed equal to or greater than 2-fold with a false discovery rate (FDR) equal to or less than 5%.

**Real-Time PCR Analysis.** All real time PCR experiments follow the nomenclature and descriptions recommended by the MIQE Guidelines<sup>8</sup>. Taqman hydrolysis probes labeled with FAM dye for four genes were purchased from Applied Biosystems Incorporated (Grand Island, NY): *CD44* (Rn00681157\_m1), *Ism1* (Rn01337005\_m1), *Mmp7* (Rn00689241\_m1), *Tnfrsf12a* (Rn00710373\_M1). Primetime hydrolysis probes labeled with FAM dye for 14 other genes were purchased from IDT (Coralville, IA): *ApoE* (Rn.PT.49.22182496), *Bcat1* (Rn.PT.49.7992966), *Calm4* (Rn.PT.49.7249560), *Cxcl1* (Rn.PT.49.9564322), *Ednra* (Rn.PT.49.6603748), *Epdr1* (Rn.PT.49.6743538), *Gcgr* (Rn.PT.49.17907728), *Ifi204* (Rn.PT.49.5504837), *Igfbp4* (Rn.PT.49.10650256), *Ppargc3* (Rn.PT.49.13222597), *Sh3kbp1* (Rn.PT.49.10281227), *Steap4* (Rn.PT.49.12263308), *Vcan* (Vcan ex12-13), and *RGD1559482* (Rn.PT.49.18400461). *GAPDH* labeled with VIC (4352338E) from Applied Biosystems was used as a reference gene.

**Histological and Immunohistochemical Analysis.** Intestines were fixed for 24-48 hours in formalin and then transferred to 70% ethanol for storage. Samples were embedded in paraffin blocks in one of two ways: either a longitudinal strip was cut the length of the colon and wound into a Swiss roll or short strips of tissue were cut through the center of a tumor(s), including surrounding normal tissue. Five micron sections were used for pathological and immunohistochemical analysis. Tumor stage was judged on hematoxylin and eosin stained sections where the tumor stalk was present. A tumor was judged to be an adenoma if no invasion

was present, an intramucosal carcinoma if invasion was present into the stalk or into but not through the *muscularis mucosa*, an early carcinoma if invasion occurred through the *muscularis mucosa* and into but not through the submucosa, and a carcinoma if invasion occurred through the submucosa (see Chapter 1, Fig 1-1)<sup>61</sup>.

A rabbit polyclonal antibody to BCAT1 was purchased from Abgent (San Diego, CA). Heat mediated antigen retrieval using citrate buffer at pH 6.0 was followed by blocking with 10% normal goat serum. Primary antibody was mixed with 10% normal goat serum at a dilution of 1:500 and incubated at 4°C overnight. After washing, samples were incubated with an anti-rabbit secondary antibody for 30 minutes at room temperature. BCAT1 was visualized with DAB and slides were counterstained with hematoxylin.

**Statistical Methods.** After input of data from the Agilent Extraction files into Partek Genomics Suite, variables including Chip ID, Sample Type, Treatment and Genotype were associated with each array. For single color arrays, samples were quantile normalized before analysis. Unless otherwise indicated, gene lists were created from microarray data where expression levels differed by at least 2-fold between any two tissue classifications, and with a false discovery rate (FDR) of no more than 5%.

## **Results**

**Histological analysis of spontaneous and DSS-induced tumors.** At 97 days of age, 4 sporadic tumors and 15 DSS-induced tumors from three untreated and two DSS-treated male Pirc rats were scored for pathological stage and graded as either an adenoma, intramucosal carcinoma, or



early carcinoma. Between sporadic versus DSS-induced tumors, the percentage of adenomas (75% versus 79%, respectively) and intramucosal carcinomas (25% versus 21%, respectively) did not differ significantly at this early 97-day time point. Therefore, any treatment-related difference in gene expression found in subsequent study of the two tumor types at this time point is not owing to differences in tumor stage.

**Microarray Data Analysis.** All microarray analyses were performed from whole homogenized tissue. Therefore, any change in the level of expression could either indicate an actual change in transcript level or instead could indicate a change in the number or localization of a particular cell type. At 97 days of age, microarray analysis found no difference between tumors from untreated Pirc rats and those from their DSS-treated counterparts until the false discovery rate was increased to 40%. Therefore, to improve statistical power, all tumors were combined for subsequent comparison against other groups.

The biggest differences in gene expression, as expected, were between untreated normal tissue and tumors (Supplementary Table S-1). A total of 4630 probes were differentially expressed between normal tissue from untreated Pirc rats and all tumors. Of these, 2177 were expressed at a higher level in tumor than normal tissue, and 2453 were expressed at a lower level in tumor than normal tissue. Based on published literature, several genes, including *Cd44*<sup>11</sup> and *Mmp7*<sup>36</sup>, expected to show increased expression in tumors did so in our data set.

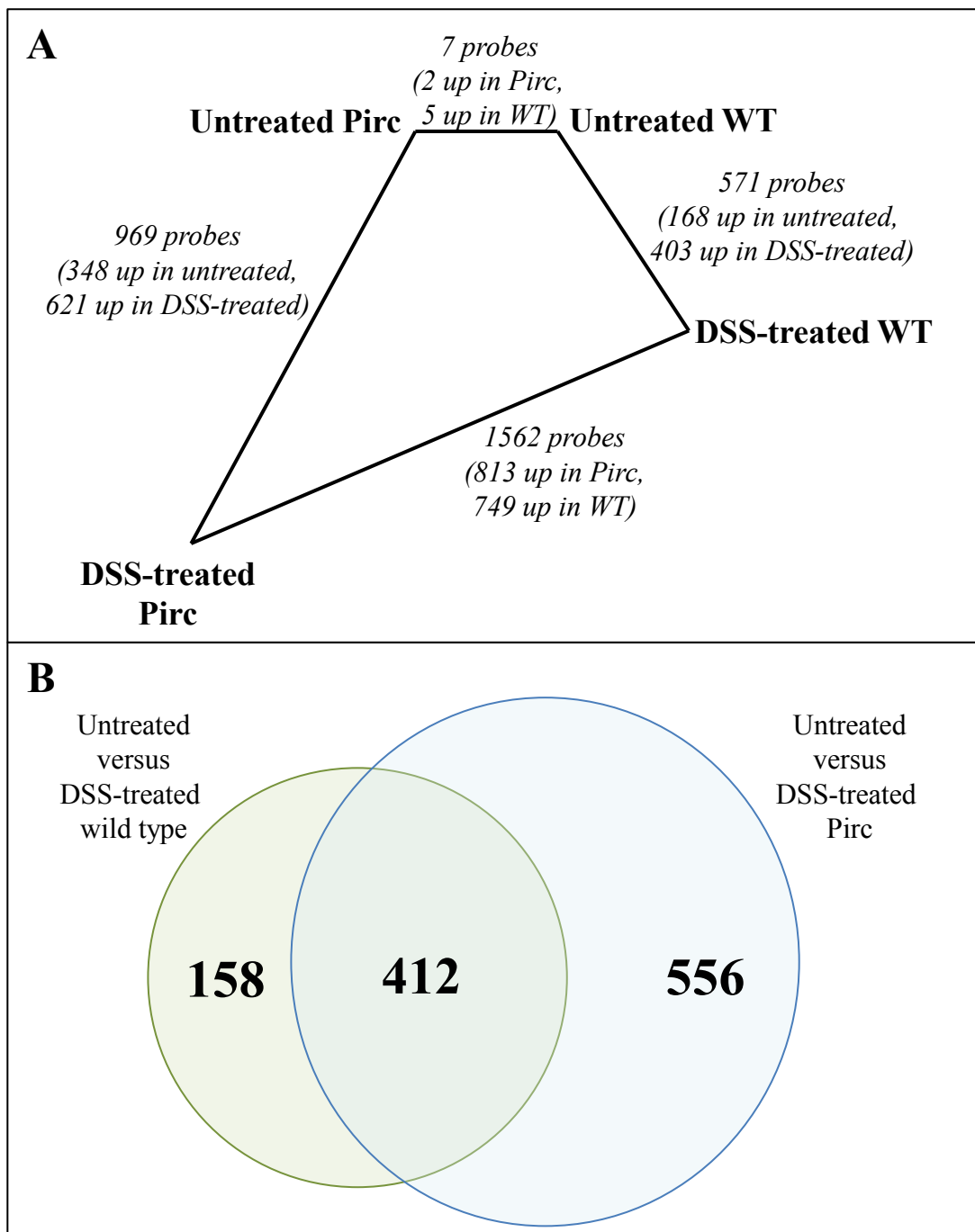
Since DSS treatment is known to increase tumor multiplicity, growth and stage (see Chapter 1), we compared untreated normal tissue to normal tissue from DSS-treated rats to determine whether we could detect any molecular differences (Supplementary Table S-2). A total of 969 probes were differentially expressed between normal tissues from untreated versus DSS-

treated Pirc rats. Of these, 621 were expressed at a higher level in DSS-treated normal tissue and 348 were expressed at a higher level in spontaneous normal tissue. These results support our hypothesis that molecular changes can be detected in apparently normal tissue of DSS-treated rats.

Next, we sought to determine whether the molecular changes seen in DSS-treated normal tissue could be early indicators of the neoplastic process, and whether these tissues more closely resemble tumors. Indeed, the comparison between untreated normal tissue and tumor yields a set of differentially expressed genes about 65% greater than between DSS-treated normal tissue and tumors (1613 probes, Supplementary Table S-3). Of these, 679 were expressed at a lower level in tumors than in DSS-treated normal tissue, and the remaining 934 were expressed at a higher level in tumors than in DSS-treated normal tissue. This observation may indicate that normal tissue exposed to DSS is already on its way to becoming tumorigenic.

Although the use of the Pirc rat was necessary to permit comparison with tumor tissue, changes in these genetically predisposed rats may not reflect the general process of inflammation associated with tumorigenesis in individuals not already genetically predisposed. To determine which of the genes altered in normal tissue following DSS treatment were independent of the Pirc genotype, untreated and DSS-treated normal tissue from wild type rats were compared. A much smaller list of probes were differentially expressed in untreated versus DSS-treated wild type rats than in the same comparison made in Pirc rats (Supplementary Table S-4). A total of 571 probes were differentially expressed between normal tissue from untreated and DSS-treated wild type rats. Of these, 168 were more highly expressed in untreated normal tissue and 403 were more highly expressed in DSS-treated normal tissue. In total, 412 probes are differentially expressed in normal mucosa between untreated and DSS-treated rats, regardless of genotype (Fig 2-1A). When this subset of 412 probes is compared against genes differentially expressed in tumors, the overlap is narrowed to a list of 147 probes (Fig 2-1B).

**Fig 2-1.** Analysis of gene expression in normal colonic tissue from untreated and DSS-treated Pirc and wild type rats. (A) The number of genes differentially expressed in normal mucosa following DSS-treatment compared with untreated tissue is greater in Pirc rats than in wild type rats. (B) Of the total 571 probes differentially expressed in wild type rats, and the 969 probes differentially expressed in Pirc rats, 412 probes appear in both lists. These genes are considered as Pirc-independent candidate genes.



**Pathway Analysis.** Additional analytic methods can be used to narrow candidates for further investigation. Pathway analysis is one method to accomplish this. Kegg Pathways is a collection of pathway maps representing current knowledge of molecular interplay between genes.

DAVID, or the Database for Annotation, Visualization and Integrated Discovery, is an open-source online tool that allows for basic pathway analysis. Kegg Pathway Analysis showed an enrichment for differential gene expression between untreated normal tissue and tumors from Pirc rats in 55 different pathways from the 2502 probes matched in DAVID. These include cytokine-cytokine receptor interaction (58 probes), pathways in cancer (58 probes), focal adhesion (49 probes), chemokine signaling (45 probes) and, not surprisingly, the Wnt signaling pathway (30 probes). A greater number of pathways showed gene expression enrichment between untreated normal tissue and tumors than between DSS-treated normal tissue and tumors. This may indicate that DSS-treated normal epithelium is closer to tumor biologically than is untreated normal epithelium. 13 pathways were significantly enriched including calcium signaling (16 probes), drug metabolism (15 probes), Wnt signaling (15 probes), and metabolism of xenobiotics by cytochrome P450 (9 probes).

Pathways significantly altered in normal tissue upon DSS treatment could give insights into the early stages of tumorigenesis. Between untreated and DSS-treated normal tissue in Pirc rats, 13 Kegg pathways were enriched for differentially expressed genes from the 617 probes matched in DAVID. In particular, Wnt signaling (11 probes), MAPK signaling (17 probes), cytokine-cytokine receptor interaction (17 probes) and p53 signaling (6 probes) pathways were enriched. Despite the smaller number of differentially expressed genes in untreated versus DSS-treated normal tissue from wild type rats, a greater number of Kegg pathways were enriched in wild type rats (23 pathways) compared to the same contrast in Pirc rats (13 pathways). This dif-

ference could be owing to the different array densities used for the two sets (40k probes in the Pirc studies and 66k probes in the wild type studies). Interestingly, in untreated versus DSS-treated normal tissue from wild type rats the Wnt and p53 signaling pathways were not enriched, while MAPK signaling and cytokine-cytokine receptor interaction pathways were. Other Kegg pathways affected uniquely in wild type rats given DSS include cell adhesion molecules (14 probes), chemokine signaling (13 probes) and focal adhesion (12 probes) pathways.

**Protein Interaction Analysis.** STRING, or Search Tool for the Retrieval of Interacting Genes/Proteins, is a biological database of both known and predicted protein-protein interactions. This mode of analysis lets us further examine what may be occurring on a molecular basis in tumors associated with inflammation. Although no direct study of proteins was conducted in these experiments, computational analysis can attempt to predict what would happen to proteins transcribed by mRNA differentially expressed under various conditions.

The largest set of protein interaction enrichment is, as expected, between untreated normal tissue and tumors. STRING protein analysis shows that, when the list of proteins is narrowed down to the 357 with greatest statistical significance, the network is highly enriched with 322 protein-protein interactions. Not unexpectedly, the greatest enrichment occurs around those proteins known to be involved in cancer processes, including CD44 and MMP7.

A large number of interactions are also seen in proteins potentially affected by DSS-treatment. Of the top 131 proteins corresponding to the most statistically significantly differentially expressed genes, 35 protein-protein interactions are observed. These interactions are highly involved in metabolic functions, including drug and xenobiotic metabolism by cytochrome

P450s, cysteine and methionine metabolism, retinol metabolism, nitrogen metabolism, and arachadonic acid metabolism.

When only normal mucosa is examined from untreated and DSS-treated *Pirc* rats, the top 200 genes, corresponding to 88 mapped proteins, again show an enrichment of protein-protein interactions (23 interactions). ICAM1 showed the greatest number of primary interactions, with connections to APOE, PLA2G2A, IL1a, CXCL1, PLAU, CD44 and PLAT. Both APOE and CD44 themselves each interacted with four proteins. CD44 had interactions with MADCAM1, PLAU, MMP7 and ICAM1, and APOE interacted with PLAT, ICAM1, IDE and PLA2G2A. The APOE and CD44 pathways appear to be greatly altered in DSS-treated normal tissue, as they are in tumors. This finding reinforces the biological proximity of DSS-treated normal tissue to the tumor.

Protein interactions were then studied in untreated and DSS-treated wild type rats to determine which alterations did not depend on the *Pirc* mutation. More protein-protein interactions were found between untreated and DSS-treated normal tissue in wild type rats (92 interactions) compared to the same comparison in *Pirc* rats (23 interactions). APOE showed the greatest number of primary protein-protein interactions, with linkage to GSTA3, CLU, TGFB1, MMP2 and PLA2G2A. MMP2 showed the second greatest number of primary protein-protein interactions, with linkage to APOE, TGFB1, CCL7 and EDNRA. To determine the greatest differences between wild type and *Pirc* rats caused by DSS-treatment, we determined what protein networks were most enriched in this comparison. In DSS-treated normal tissue between wild type and *Pirc* rats, several interactive networks were highly enriched. In particular the defensins (Defensins 6, 8, 9, 10, 24 and DEFA-RS1) were greatly enriched in *Pirc* tissue. The transcripts for each of the

genes encoding the defending proteins are all expressed at significantly higher levels in DSS-treated tissue from Pirc rats compared with wild type rats.

Although at our standard stringency (2-fold and 5% FDR) no differences could be found in gene expression between spontaneous and DSS-induced tumors, increasing the FDR to 50% resulted in a list of 160 differentially expressed probes (Supplementary Table S-5). Of these, 57 corresponded to proteins in STRING. However, only 2 protein-protein interactions were evident. These included interactions between CYP4F4 and CYP2J4 and between KRT12 and KRT24. Each of these four candidates is more highly expressed in DSS-treated tumors, except for CYP2J4, which is more highly expressed in tumors from untreated rats. KRT12 and KRT24 are genes that encode for two keratin proteins, an important component of the cellular cytoskeleton. Although the expression levels of these candidates were not tested by real-time PCR, differences at this early 97-day time point may foreshadow differences in tumor stage in the future, and further study is warranted.

**Effect of DSS treatment on the Wnt signaling pathway.** Normal tissue previously exposed to DSS shows expression changes in several regulators and target genes of the Wnt pathway. Importantly, these changes occur only in Pirc rats, which already have defects in Wnt signaling. Antagonists of Wnt activation include Wnt inhibitory factor 1 (*Wif-1*), secreted Frizzled-related protein (*Sfrp*) and Dickkopf (*Dkk*). Compared with untreated normal tissue, mRNA expression levels for *Wif-1*, *Sfrp1* and *Dkk4* are upregulated 5-fold, 5-fold and 6-fold in DSS-treated normal tissue and 22-fold, 4-fold and 56-fold in tumor, respectively. The downstream target of Wnt signaling matrix metalloproteinase 7 (*Mmp7*) is upregulated 17-fold in DSS-treated normal tissue and 52-fold in tumors compared with untreated normal tissue. Interestingly the transcript levels

of neither *Apc* nor *Ctnnb1* ( $\beta$ -catenin) are altered in any of the tissue types, despite originating from an *Apc*-mutant model.

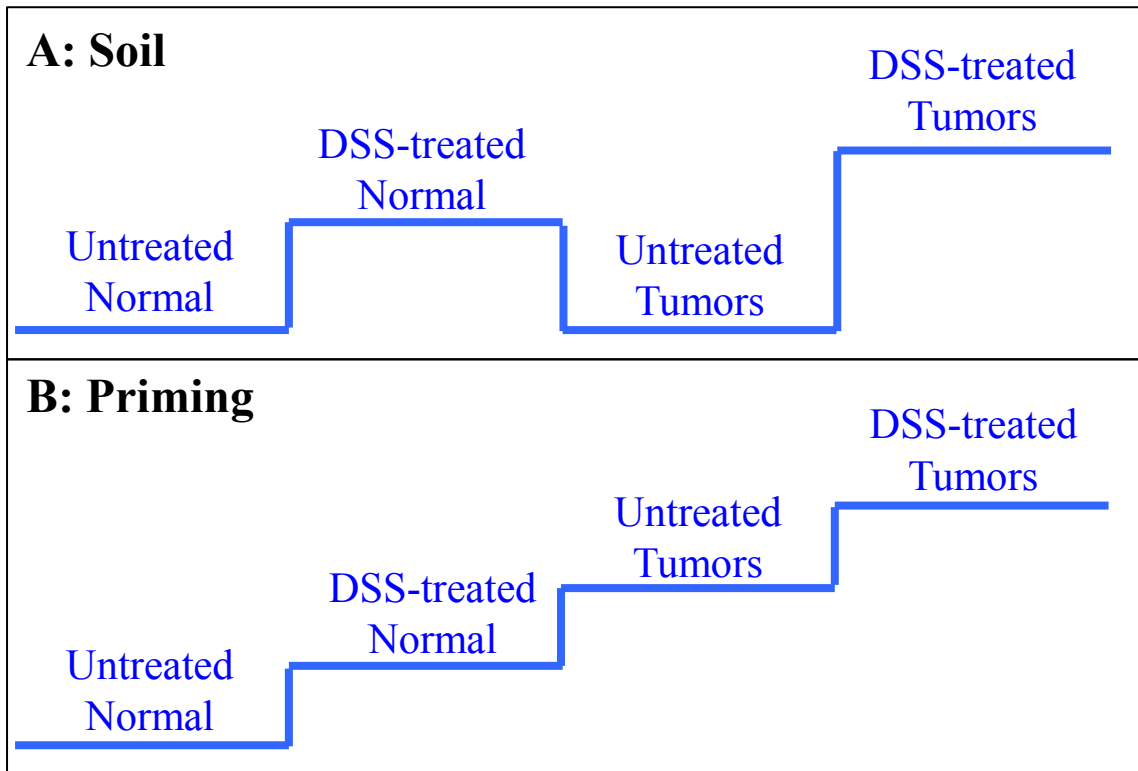
**Selecting candidates for real time PCR validation.** Candidates were classified into two categories depending on their expression patterns in the various tissue types. Candidates were classified as “soil” candidates if they were differentially expressed between untreated and DSS-treated normal tissue, but expression was not different between DSS-treated normal tissue and spontaneous tumor, while expression did differ between DSS-treated normal tissue and DSS-treated tumor (Fig 2-2A). These candidates may be associated with surrounding tissue that allows the DSS-treated tumors to become more invasive than their spontaneous counterparts. The “soil” candidates selected for validation include *ApoE*, *Cxcl1*, *Ednra*, *Epdr1*, *Ifi204*, *Igfbp4*, *Lilrb4*, *Ppapdc3*, *Steap4*, *RGD1559482* and *Vcan*.

Candidates were classified as “priming” candidates if they were differentially expressed between untreated and DSS-treated normal tissue, and also between DSS-treated normal tissue and spontaneous tumor, and even further between DSS-treated normal tissue and DSS-treated tumor (Fig 2-2B). These candidates may be associated with processes within the tumor tissue that allow the DSS-treated tumors to become more invasive than their spontaneous counterparts. The “priming” candidates selected for validation include *Bcat1*, *CD44*, *Ism1*, *Mmp7*, *Sh3kbp1* and *Tnfrsf12a*.

Despite appearing to be a “priming” candidate based on microarray analysis, *Gcgr* shows a pattern different from either of these classifications by real time PCR, where DSS-treated normal tissue does not significantly differ from untreated normal tissue. Although *Gcgr* expression is higher in all tumors compared to normal tissue, its expression also does not differ between un-



**Fig 2-2.** Two gene expression patterns were discovered when comparing normal mucosa and tumor in untreated and DSS-treated Pirc rats. A) “Soil” gene candidates, while not differentially expressed between untreated normal mucosa and untreated tumor, are differentially expressed between DSS-treated normal mucosa and untreated normal mucosa, and are further differentially expressed between untreated normal mucosa and DSS-treated tumors. B) “Priming” gene candidates are differentially expressed between DSS-treated normal mucosa and untreated normal mucosa, and then further differentially expressed in untreated tumors and even further yet in DSS-treated tumors.



treated and DSS-treated tumors. Therefore, *Gcgr* was not further considered as an early player specific to inflammation-associated neoplasia.

Candidates were also evaluated as to whether their expression differences in normal tissue upon DSS-treatment required the *Pirc* mutation. All candidates examined showed a response of gene expression in DSS-treated normal epithelial tissue from wild type rats in the same direction as was seen in *Pirc* rats. This indicates that each of the genes expression changes seen in the normal tissue after DSS-treatment did not depend on the *Pirc* mutation.

**Real-time PCR confirmation of candidates from microarray analysis.** All samples were collected at 97 days of age, 36 days after the final day of DSS treatment. Transcript levels for all candidates were measured by real-time PCR for both normal tissue and tumors in 3-4 biological replicates from each untreated and DSS-treated *Pirc* rats. Additionally, transcript levels were also measured in normal tissue in 3-5 biological replicates from each untreated and DSS-treated wild type rats for all hydrolysis probes purchased from IDT.

Reproducibility of technical replicates was very high. Therefore, the standard deviation within a sample group is due either to biological variability or potentially to variability in the amount of input RNA for the cDNA reaction. However, the latter is unlikely since replicate measures of RNA concentration on the Nanodrop were made for a subset of samples and these measurements were also highly reproducible (data not shown). Note that the standard deviation is no larger in samples obtained from *Pirc* rats than that from wild type rats. Although apparently normal tissue collected from *Pirc* rats may contain nascent tumors or aberrant crypt foci, this is not true in wild type animals. The similar margin of error within each of the groups suggests

that biological variability does not significantly differ between untreated and DSS-treated rats or between Pirc and wild type rats.

Within our set of 18 candidate genes, proteins encoded by five of the soil candidates interact: CD44 interacts with both MMP7 and VCAN, while CALM4 and IFI204 interact with one another. Each of our candidates was chosen based on its individual merits in our dataset as well as on information available in published literature. Further, all of these candidates show a high degree of conservation of sequence from the rat to both mouse and human, and many have supporting evidence for a role in human colon cancer.

Three of the soil candidates, *Calm4*, *Ppapdc3*, and *RGD1559482*, have not been previously described in any cancer. However, based on what is currently known about each candidate, a role in cancer is plausible. Calmodulin-like 5 is linked to breast carcinogenesis in premenopausal women<sup>14</sup>. *Ppapdc3* is a nuclear envelope protein that functions as a negative regulator of differentiation, specifically in myoblasts<sup>38</sup>. No publications regarding *RGD1559482* exist, but this candidate is similar to other immunoglobulin superfamily members which play a role in the host immune response to the presence of a tumor<sup>15</sup>.

Each of the other fifteen candidates is associated with some form of cancer. Six soil candidates (*ApoE*, *Cxcl1*, *Ednra*, *Igfbp4*, *Steap4*, and *Vcan*) and three priming candidates (*Bcat1*, *Cd44* and *Mmp7*) have specific links to colon cancer (see Table 2-1). *Epdr1* (soil) has been shown to be upregulated in dysplastic epithelium in vocal fold lesions<sup>4</sup>, and *Epdr1* genotype has been associated with risk for prostate cancer<sup>56</sup>. Upregulation of *Ifi204* (soil) reduces tumor cell proliferation in a mouse model of prostate cancer<sup>48</sup>. Interestingly, *Ism1* (priming) is overexpressed specifically in tumors harboring mutations in  $\beta$ -catenin<sup>18</sup>. This may explain its increased expression in our model, where  $\beta$ -catenin protein accumulates in the cytoplasm and nucleus due

**Table 2-1.** Gene candidates of the priming and soil hypotheses chosen for real time PCR confirmation, in alphabetical order. Functions are summarized from Entrez Gene for each candidate. Relevant publications are not exhaustive, but highlight some of the roles for each candidate. Unknown indicates that the function or relevance to cancer have not been previously reported.

Class	Candidate	Gene	Function	Relevance to Cancer
Priming	Bcat1	Branched Chain Amino transferase 1, Cytosolic	Catalyzes the first reaction in the catabolism of the essential branched chain amino acids leucine, isoleucine, and valine.	Promotes cell proliferation in gliomas <sup>57</sup> . Over-expression induces cell proliferation, migration and invasion in nasopharyngeal carcinoma <sup>66</sup> . Biomarker for metastasis in colorectal cancer <sup>44</sup> .
	Cd44	CD44 molecule (Indian blood group)	Cell-surface glycoprotein involved in cell-cell interactions, cell adhesion and migration, and lymphocyte activation. Receptor for hyaluronic acid and can also interact with other ligands, such as osteopontin, collagens, and matrix metalloproteinases (MMPs).	Highly expressed in colorectal cancers, correlates closely with clinical features and pathological diagnosis <sup>9</sup> .
	Ism1	isthmin 1, angiogenesis inhibitor		Overexpressed in adrenocortical tumors harboring mutations in CTNBN1 <sup>18</sup> .
	Mmp7	matrix metalloproteinase 7	Involved in breakdown of extracellular matrix in normal and disease processes. Degrades proteoglycans, fibronectin, elastin and casein. Involved in wound healing; studies in mice suggest that it regulates the activity of defensins in intestinal mucosa.	Biomarker of colon cancer initiation and progression <sup>36</sup> . Loss of expression reduces tumor burden in Min mice <sup>63</sup> . Putative immunologic target in colon cancer prevention <sup>7</sup> .
	Sh3kbp1	SH3-domain kinase binding protein 1	Facilitates protein-protein interactions and implicated in numerous cellular processes including apoptosis, cytoskeletal rearrangement, and cell adhesion.	Promotes EGFR endocytosis and loss of expression may increase drug resistance in ovarian carcinoma <sup>45</sup> .
	Tnfrsf12a	tumor necrosis factor receptor superfamily, member 12A	Unknown.	Elevated expression correlates with non-small cell lung cancer migration and invasion <sup>62</sup> . Expression greatly enhanced in benign and malignant skin pathologies associated with an inflammatory component <sup>51</sup> .
Soil	Apoe	Apolipoprotein E3	Mediates the binding, internalization, and catabolism of lipoprotein particles. Serves as a ligand for LDL receptor and for the specific apo-E receptor.	The same genotypes associated with increased risk of coronary heart disease influence colon cancer development <sup>53</sup> .
	Calm4	calmodulin 4	Unknown.	Unknown. Calmodulin-like protein 5 is linked to breast carcinogenesis in premenopausal women <sup>14</sup> .
	Cxcl1	chemokine (C-X-C motif) ligand 1 (melanoma growth stimulating activity, alpha)	The encoded protein is a secreted growth factor that signals through the G-protein coupled receptor, CXC receptor 2. This protein plays a role in inflammation and as a chemoattractant for neutrophils.	Increased protein expression in aggressive bladder cancers <sup>40</sup> . Transcript level higher in colorectal cancers than in dysplastic adenomas <sup>22</sup> .

**Table 2-1. Continued.**

<b>Class</b>	<b>Candidate</b>	<b>Gene</b>	<b>Function</b>	<b>Relevance to Cancer</b>
Soil	Ednra	Endothelin Receptor Subtype A	Receptor for endothelin-1. Mediates its action by association with G proteins that activate a phosphatidylinositol-calcium second messenger system.	High levels in colorectal tumors correlate with poor prognosis <sup>50</sup> .
	Epdr1	ependymin related 1	The protein encoded by this gene is a type II transmembrane protein that is similar to two families of cell adhesion molecules, the protocadherins and ependymins. This protein may play a role in calcium-dependent cell adhesion.	Upregulated in dysplastic keratotic epithelium in vocal fold lesions <sup>4</sup> . Defined as a “risk genotype” for prostate cancer <sup>56</sup> .
	Gcgr	glucagon receptor	The protein encoded by this gene is a glucagon receptor that is important in controlling blood glucose levels.	Defective signaling causes pancreatic neuroendocrine tumors in a mouse model <sup>65</sup> . Mutation is associated with islet cell tumors <sup>67</sup> .
	Ifi204	interferon activated gene 204	Unknown.	Association between upregulation and a reduction in tumor cell proliferation in a mouse model of prostate cancer <sup>48</sup> .
	Igfbp4	insulin-like growth factor binding protein 4	This gene is a member of the insulin-like growth factor binding protein (IGFBP) family. The protein binds both insulin-like growth factors (IGFs) I and II, prolonging the half-life of the IGFs and altering their interaction with cell surface receptors.	Targeted gene therapy in the colon increases apoptosis and decreases tumor cell mitosis by altering Bcl-2 and Bax proteins <sup>16,17</sup> .
	Ppapdc3	phosphatidic acid phosphatase type 2 domain containing 3	Unknown.	Unknown.
	Steap4	Six transmembrane epithelial antigen of prostate family member 4	The protein encoded by this gene functions as a metalloreductase that has the ability to reduce both Fe(3+) to Fe(2+) and Cu(2+) to Cu(1+), using NAD(+) as acceptor.	Overexpressed in many cancers, including colon <sup>24</sup> . Potential involvement in prostate cancer progression <sup>35</sup> .
	RGD1559482	similar to immunoglobulin superfamily, member 7	Unknown.	Unknown.
	Vcan	versican	The protein encoded is a large chondroitin sulfate proteoglycan and is a major component of the extracellular matrix. This protein is involved in cell adhesion, proliferation, migration and angiogenesis and plays a central role in tissue morphogenesis and maintenance.	Posttranslational modifications associated with colon carcinoma <sup>58</sup> .

to the loss of expression of *Apc*. *Sh3kbp1* (priming) may play a role in drug resistant cancers by promoting EGFR endocytosis<sup>45</sup>. Lastly, *Tnfrsf12a* (priming) shows elevated expression in association with inflammation<sup>51</sup>, and correlates with tumor invasion in lung cancer<sup>62</sup>.

By real time PCR, expression of *Calm4* was too low to detect in any of our samples. Since all 17 other candidates could be readily detected in at least one sample type, we did not further pursue *Calm4* as a soil candidate. Six candidates with the highest transcript levels overall include *Ism1*, *Mmp7*, *Bcat1*, *Cxcl1*, *Ednra* (all upregulated in tumors) and *Gcgr* (downregulated in tumors, Figs 2-3 and 2-4). Six candidates expressed at lower levels were upregulated in tumors: *CD44*, *Tnfrsf12a*, *ApoE*, *Vcan*, *Igfbp4* and *Ppapdc3* (Figs 2-3 and 2-5). Five soil candidates (*Steap4*, *Epdr1*, *Ifi204*, *Lilrb4* and *RGD1559482*) and one priming candidate (*Sh3kbp1*) expressed at lower levels were downregulated in tumors (Fig 2-6).

Although global microarray analysis did not find any differences in expression between untreated and DSS-treated tumors until the FDR was adjusted to 40%, many of the candidates evaluated individually by real-time PCR did show differences between the two tumor classes. Candidates that were more differentially expressed between normal tissue and DSS-treated tumor than between normal tissue and spontaneous tumor include two priming candidates (*Bcat* and *Ism1*) and seven soil candidates (*Ednra*, *Cxcl1*, *Steap4*, *Epdr1*, *Ifi204*, *Lilrb4* and *RDG1559482*). Candidates that were more differentially expressed between normal tissue and spontaneous tumor than between normal tissue and DSS-treated tumor is limited to the soil candidate *Ppapdc3*.

**Immunohistochemical analysis of BCAT1 protein.** Initial studies of the BCAT1 protein were pursued because of an available antibody validated for rat FFPE tissue and of the proven zinc-

**Fig 2-3.** Real time PCR results for candidates differentially expressed in Pirc rats given DSS. Only those comparisons not significantly different from untreated Pirc normal tissue are indicated (NS, not significant). \* p-value  $\leq 0.05$  between tumors from untreated and DSS-treated Pirc rats. NE, normal epithelium; Tum, tumor.

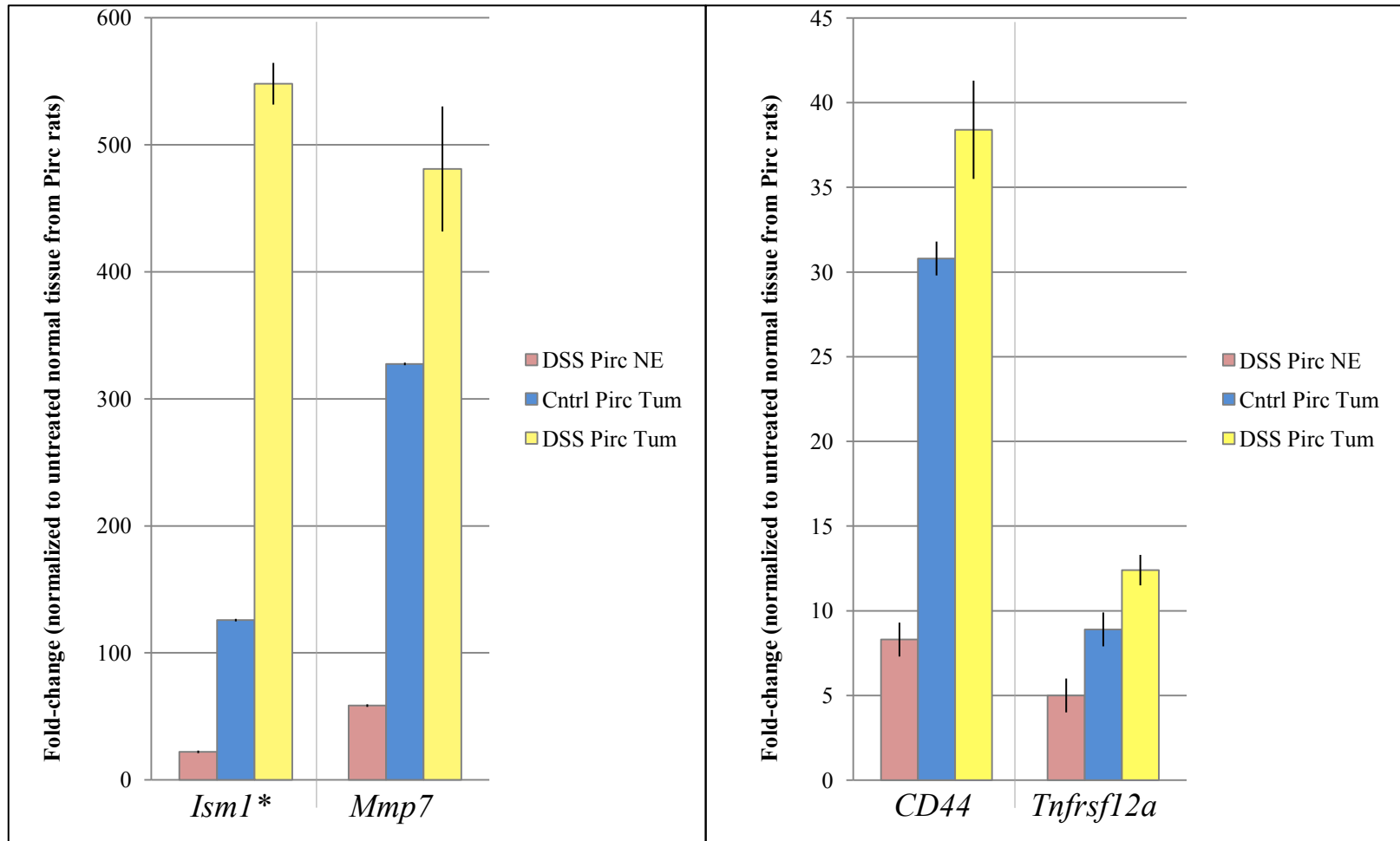


**Fig 2-4.** Real time PCR results for highly expressed candidates. *Bcat1* is a priming candidate, while *Ednra* and *Cxcl1* are soil candidates. *Gcgr* is similar to a priming candidate, however no differential expression is seen between untreated and DSS-treated tumors. Only those comparisons not significantly different from untreated Pirc normal tissue are indicated (NS, not significant). \* p-value  $\leq 0.05$  between tumors from untreated and DSS-treated Pirc rats. † p-value  $\leq 0.05$  between untreated and DSS-treated normal tissue from wild type rats. WT, wild type; NE, normal epithelium; Tum, tumor.

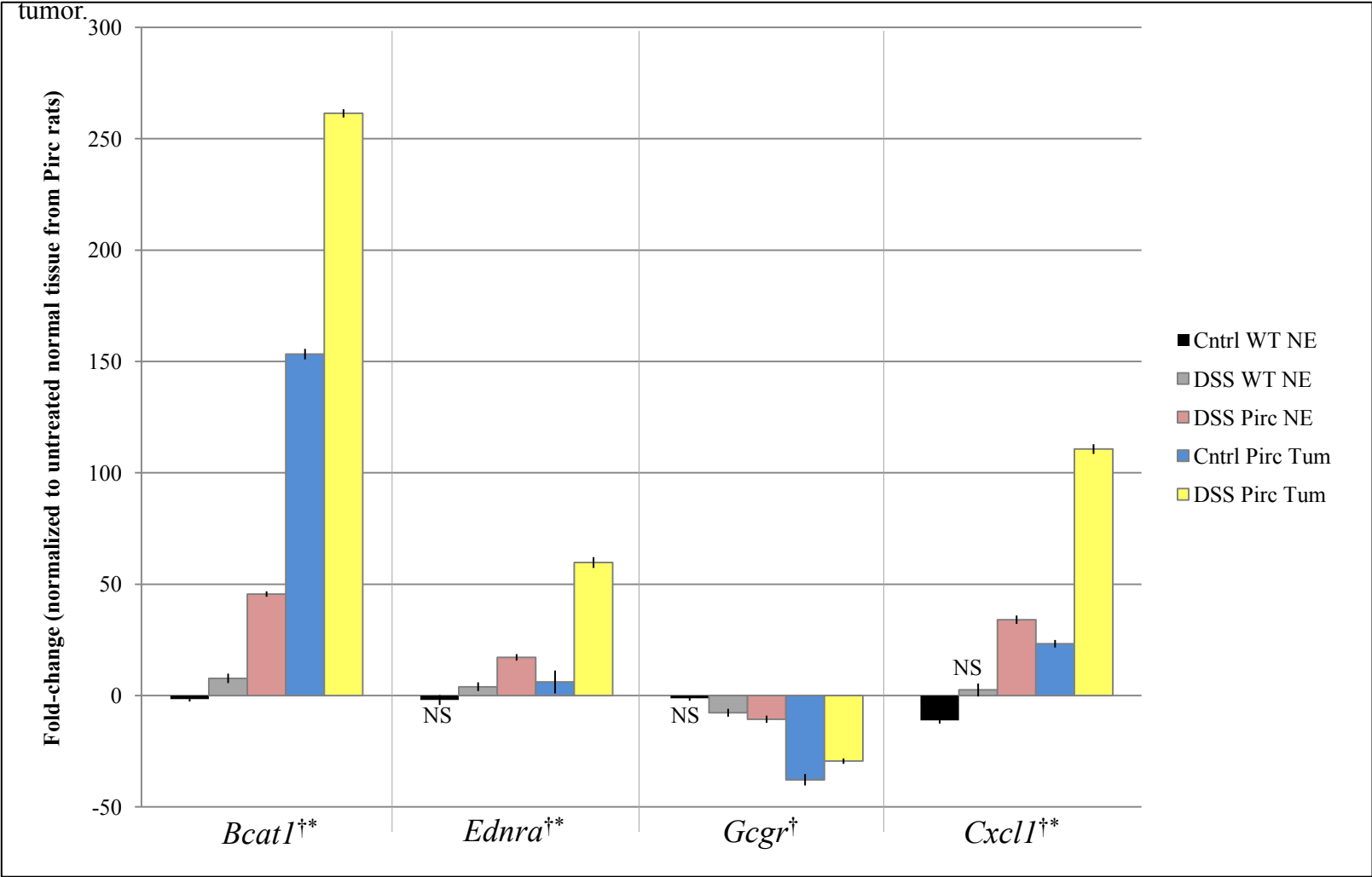




**Fig 2-5.** Real time PCR results for candidates upregulated with DSS treatment. *Apoe*, *Vcan*, *Igfbp4* and *Ppapdc3* are soil candidates. Only those comparisons not significantly different from untreated Pirc normal tissue are indicated (NS, not significant). \* p-value  $\leq 0.05$  between tumors from untreated and DSS-treated Pirc rats. † p-value  $\leq 0.05$  between untreated and DSS-treated normal tissue from wild type rats. WT, wild type; NE, normal epithelium; Tum, tumor.

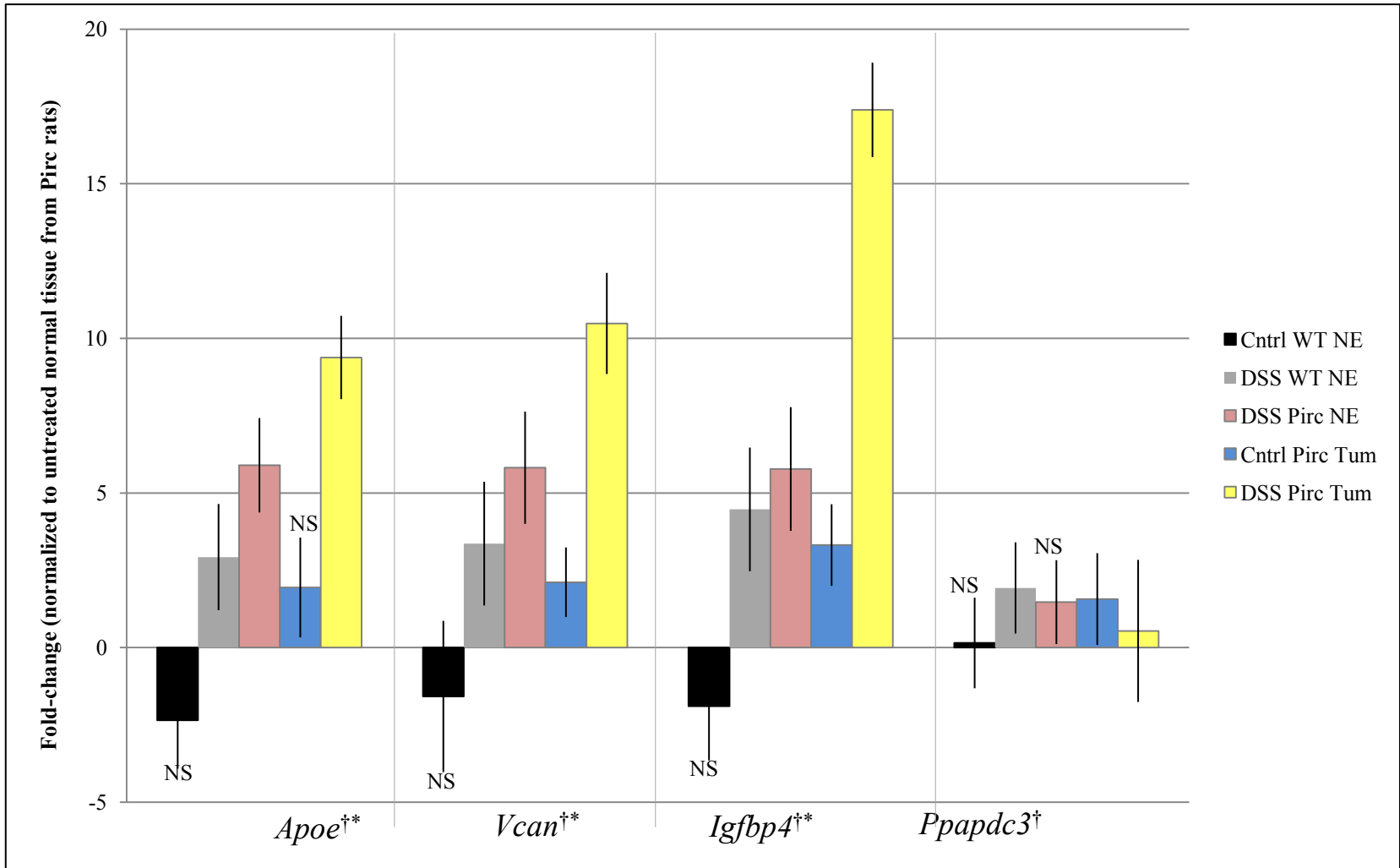


**Fig 2-6.** Real time PCR results for candidates downregulated with DSS treatment. *Sh3kbp1* is a priming candidate. *Steap4*, *Epdr1*, *Ifi204*, *Lilrb4* and *RGD1559482* are soil candidates. Only those comparisons not significantly different from untreated Pirc normal tissue are indicated (NS, not significant). \* p-value  $\leq 0.05$  between tumors from untreated and DSS-treated Pirc rats. † p-value  $\leq 0.05$  between untreated and DSS-treated normal tissue from wild type rats. WT, wild type; NE, normal epithelium; Tum, tumor.

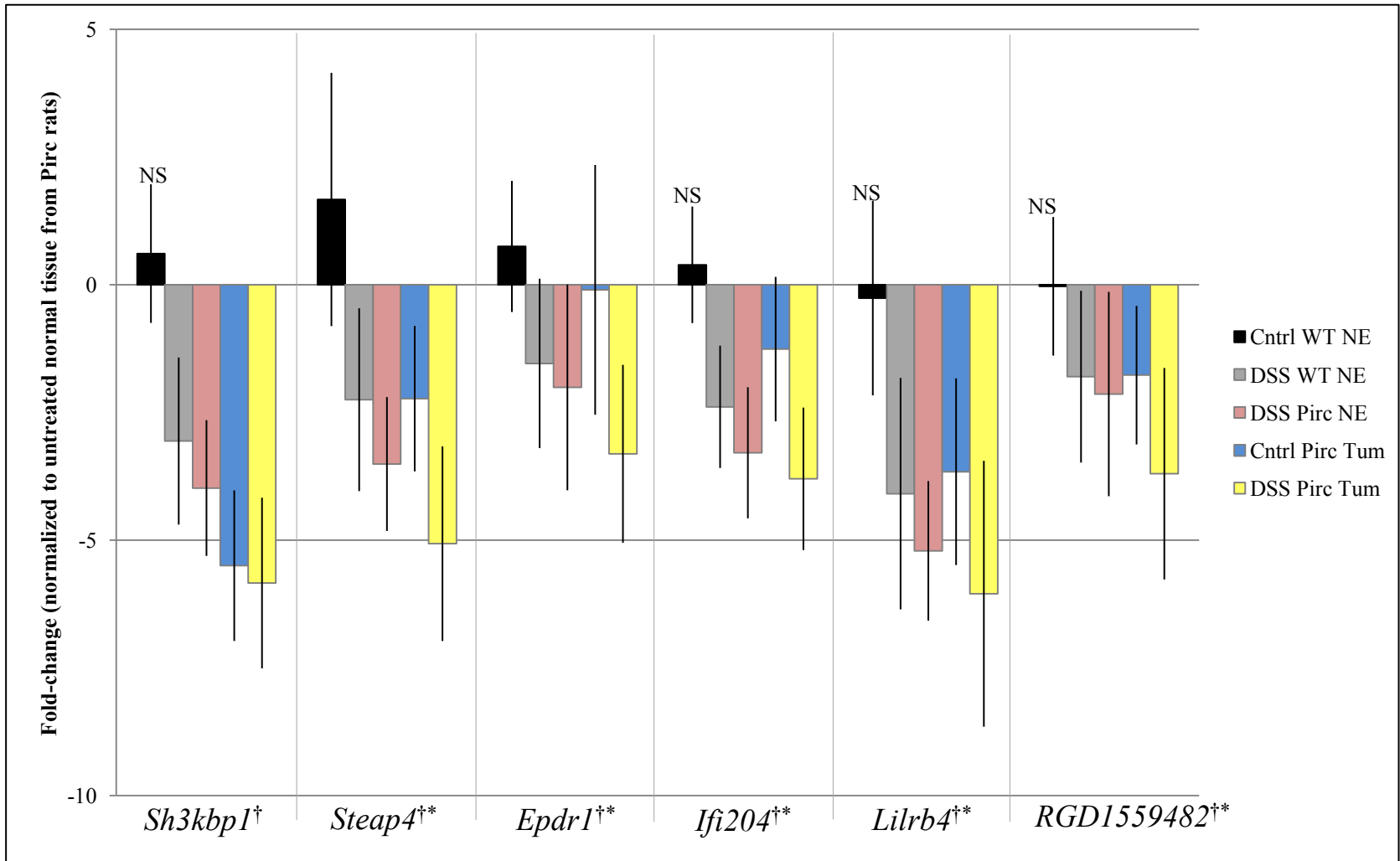
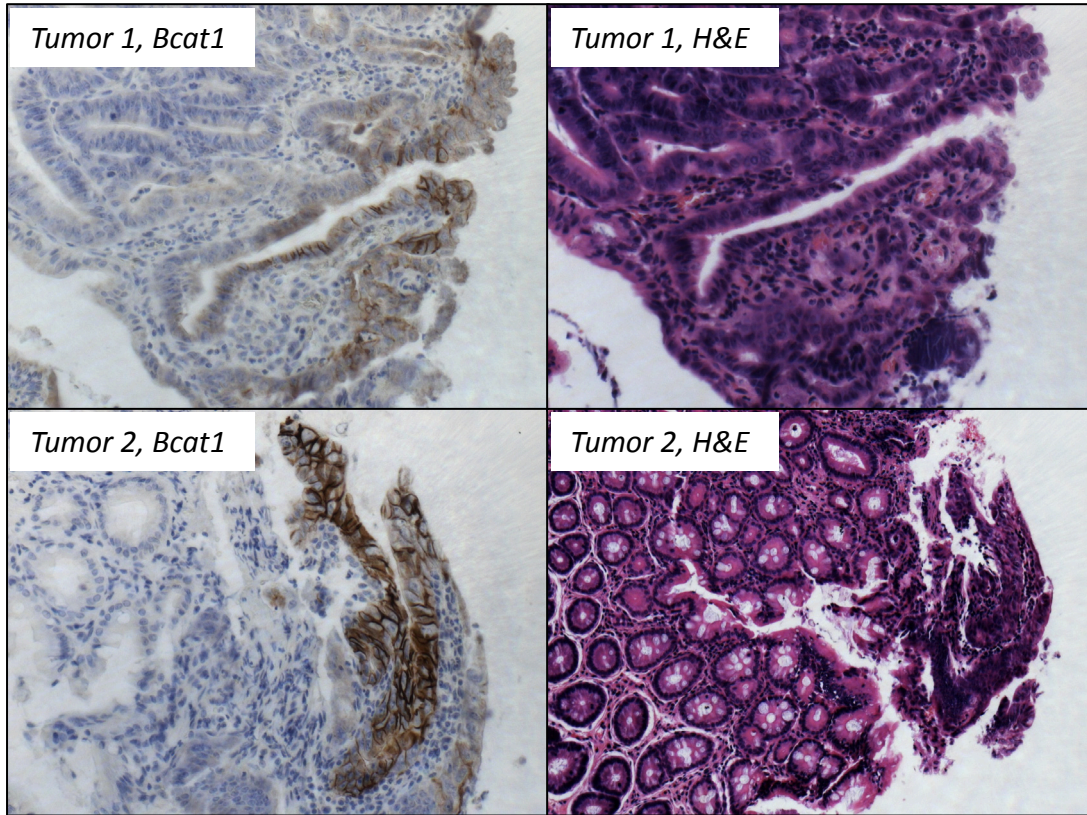


**Fig 2-7.** Immunohistochemical analysis of BCAT1 protein shows localization to the cell membrane and cytoplasm of tumors. Upon examination of the H&E slides corresponding to this staining, the cells appear less columnar in shape and more flattened and multilayered.



finger nuclease construct for subsequent *in vivo* analysis of causation. Preliminary, but reproducible results using an antibody to BCAT1 show that the protein is expressed at high levels in focal areas within tumors. As expected for BCAT1, which is cytoplasmic (in contrast to BCAT2 which is nuclear), the staining is mostly membranous with some cytoplasmic accumulation, but never nuclear (Fig 2-7). The cell morphology within these concentrated areas of BCAT1 staining appear less columnar and occasionally tend to become more flattened and multilayered. Further study is needed to assess whether BCAT1 protein levels or localization differs between untreated and DSS-treated normal mucosa and tumors.

## **Discussion**

In these studies we sought to discover gene candidates whose expression in apparently normal mucosa from DSS-treated rats might foreshadow tumor development. Although tumors in an inflammatory microenvironment do eventually become more invasive than those lacking this environment (see Chapter 1), we chose to examine tumors at a point before this divergence in stage occurs. Here, we consider the possibility that any differences detected early between tumors that will eventually follow different fates may give insight into the processes driving this divergence.

Investigation into the apparently normal mucosa surrounding a tumor, or comparisons with normal tissue from tumor-free individuals is not a new concept. Over six decades ago Slaughter first described a subset of patients in which multiple oral squamous cancers formed<sup>54</sup>. This occurred at a higher rate than would be expected in a random population. He termed this observation “field cancerization”. Since then, study into molecular changes surrounding a tumor

has continued. Recently, others have begun investigating changes that occur within “normal” tissue predisposed to cancer formation<sup>37</sup>. Combined with what is already known about the tumors themselves, these studies may lead to the discovery of some of the earliest molecular changes supportive of tumorigenesis.

This approach is being successfully utilized in patients with an inflammatory bowel disease predisposed to cancer. In several UC patients, carcinogenic mutations have been found in apparently normal colonic tissue years before the development of neoplasia<sup>32</sup>. While this is one approach to determine molecular alterations in apparently normal tissue, it is important to note that not all genes with differential expression in tumors are mutated<sup>60</sup>. These “altered” gene expression levels could instead be attributed to an increased or decreased presence of a certain cell type.

Pekow and colleagues found over 1000 genes that were differentially expressed between UC patients harboring a neoplasia and those without any neoplasia<sup>47</sup>. Nine of these genes were progressively and significantly upregulated from controls to nondysplastic tissue from UC patients to UC patients with neoplasia. Although this study did not examine the gene expression of these candidates within tumor samples, other studies have shown that three of these candidates, *Birc3*, *Thbd* and *S100a9*, are dysregulated in colonic cancers<sup>20,27,49,59</sup>. Interestingly, both *Thbd* and *S100a9* also made our list of candidates based on gene expression microarray in Pirc rats. Compared to untreated normal colonic tissue, *S100a9* is upregulated 15-fold in normal tissue from DSS-treated rats and 11-fold in tumors, while *Thbd* is upregulated 4-fold in normal tissue from DSS-treated rats and 6-fold in tumors. However, only *Thbd* was differentially expressed in a Pirc-independent manner in wild type rats.

Interestingly, nearly all of the candidates examined by real time PCR showed levels of transcript from untreated wild type rats opposite from all DSS-treated and tumor categories. For example, while transcript levels of *Steap4* in untreated normal tissue from Pirc rats is 2- to 5-fold higher than in DSS-treated normal tissue and tumors, transcript levels are about 2-fold lower than in untreated normal tissue from wild type rats (Fig 2-6). This may indicate that expression of these candidates or interacting molecules are affected by the single hit loss of expression from one allele of the *Apc* gene in Pirc rats. Alternatively, cell types may differ between wild type and Pirc rats in the normal colonic tissue. While obvious differences have not been previously observed, this has not been systematically examined.

The tissue selected for microarray analysis includes many different cell types, including epithelium, stroma and immune cells. Cells from any or all of these compartments may be contributing to differences in gene expression. Alternatively, differences in cell number rather than an actual change in expression may explain increases in detected expression. For example, macrophages surrounding an area of carcinoma intensely stain for APOE protein<sup>42</sup>, which could explain the detected increase in *ApoE* expression in our data. Candidates, or cell types expressing those molecules, whose expression does not change by microarray analysis are not necessarily unimportant in the process. Changes in cell localization, particularly that of immunocytes, could affect tumor development and progression. Therefore, immunohistochemical analysis of candidate proteins must be investigated to further understand where our candidate molecules are being expressed within the tissue. Although preliminary analysis of tumors indicates that BCAT1 protein expression is high in DSS-treated tumors, further study is needed to understand this unique focal staining pattern near the surface of lesions. The cells with intense BCAT1 staining appear less columnar in shape and more flattened and multilayered, similar to the appearance of squa-

mous cells. DSS has been previously shown to induce squamous metaplasia within the colon<sup>30</sup> and squamous cell metaplasia has also been reported rarely in humans<sup>46</sup>. In a review of over 5500 cases of colorectal adenomas, areas of squamous differentiation were found in about 0.5% of cases<sup>3</sup>. In this review, they also found that the areas of squamous metaplasia resembled discrete nests, which were located equally near the surface, middle and base of the adenoma. Some have proposed that chronic inflammation could be a predisposing factor to squamous metaplasia<sup>10</sup>, and others suggest that these areas of metaplasia may serve as precursor lesions to invasive carcinomas<sup>28,34</sup>.

Although samples were collected over a month after the final DSS treatment, there is some indication that metabolic pathways possibly activated by treatment could remain active long after DSS is removed from the system, particularly in Pirc rats. While transcript levels of 14 different cytochrome P450s were altered in normal tissue from DSS-treated Pirc rats, only 2 were differentially expressed in normal tissue from DSS-treated wild type rats at 97 days of age. One cytochrome of interest upregulated in normal tissue from DSS-treated Pirc rats, but not in DSS-treated wild type rats is Cyp1b1. It is known that Cyp1b1 plays a role in carcinogenic activation of certain compounds, particularly polycyclic aromatic hydrocarbons. The increase in tumor multiplicity and size upon carcinogen treatment of wild type mice is abolished in mice lacking Cyp1b1<sup>26</sup>. These enzymes may be induced during the metabolism of DSS and then be unable to return to normal levels, further potentiating tumor development.

A similar difference in expression after DSS treatment between wild type and Pirc rats in the number of defensins altered in normal tissue. Only two defensins were differentially expressed in normal tissue between untreated and DSS-treated wild type rats, but six defensins were differentially expressed in normal tissue between untreated and DSS-treated Pirc rats.

Defensins are host defense peptides that function to protect against bacteria, fungi and viruses. A previous study found that DSS causes the intestinal mucous layer to become permeable to bacteria<sup>31</sup>, which could in turn trigger the activation of defensins or the aggregation of cells that produce them, such as neutrophils. While the DSS-treated wild type rat appears to only have slight perturbations to the defensin system after DSS, the treated Pirc rat seems to maintain high activation of these systems. The KAD rat, a homozygously viable *Apc* mutant, also shows a similar resistance to recovery after inflammation induced by DSS compared to wild type rats<sup>64</sup>. The phenomena observed in the DSS-treated Pirc rat, which is heterozygous for a mutation in *Apc*, may indicate the affect of loss of only a single allele in recovery following inflammatory insult. The importance of the microbiome is beginning to be recognized in both normal development and pathological processes. While a link between the microbiome and inflammatory processes might be more obvious, a role for microbiota is emerging in intrinsic epithelial processes such as proliferation and differentiation<sup>41</sup>. This intrinsic processes could also play a role in aberrant development and induction of neoplasia.

Future studies will investigate the causative role for candidates of the “soil” and “priming” hypotheses. Gene knockout of select candidates in the Pirc rat may alter the phenotype of tumors- either in number, growth profile or pathological status. Two candidates that are particularly attractive are *Bcat1* (priming) and *ApoE* (soil). For each of these candidates proven zinc-finger nuclease constructs exist which could be injected directly into Pirc embryos. As demonstrated above, the levels of *Bcat1* expression are increased greatly in DSS-treated normal mucosa, further in sporadic tumors and even further in DSS-associated tumors. *ApoE* is at the center of many different protein-protein networks and could represent a crux, when which removed, may destroy the tumor scaffolding. This has been shown to be true for *Mmp7*, a candidate impli-



cated in inflammatory bowel disease and colon cancer. When *Apc*<sup>Min/+</sup> mice are made deficient in *Mmp7*, mean tumor multiplicity and average tumor diameter is significantly reduced<sup>63</sup>.

Importantly, the loss of any one of these candidates may not completely inhibit spontaneous or DSS-induced tumor formation. As with the loss of *Mmp7* expression cited above, tumor burden was reduced but not eliminated. Several different factors could account for this observation<sup>6</sup>. A homeostatic response to the loss of expression of any gene candidate may in turn be compensated for by an alteration in expression of gene family members. Alternatively, tumors may develop through multiple different pathways. Loss of a candidate gene may inhibit the formation of some tumors, but not others that developed along a different trajectory. Another redundancy mechanism by which the tumor may overcome loss of a specific gene candidate is through dependence upon multiple different avenues of growth. Removal of one avenue may simply drive the tumor down an alternate avenue. For example, if a candidate that decreased cellular apoptosis is lost, causing an increase in cell death, selection may result in the tumor increasing cell division to overcome this loss.

The candidates examined here represent only a first step into investigating changes occurring in inflamed normal tissue that may lead to the initiation or progression of colon cancers. Additional studies are needed to investigate whether a change in transcript leads to consequent changes in protein and where the encoded proteins are expressed. Feedback systems could detect proteins that are being pumped into the system at a rate different from normal conditions and thus compensate by altering the rate of protein degradation. Therefore, changes in transcript level do not guarantee changes in steady-state protein level. Then, if changes in protein level are observed, the causative role of each candidate in tumor formation and progression can be investigated by gene knockout in experimental animal models (see Appendix G). If tumor multiplicity

ty, growth rate, stage or other parameters are altered by loss of a particular gene function, in either the spontaneous or DSS-induced case, it may shed light on the earliest stages of the neoplastic process. These could then be strong candidates either for early detection efforts or targets for chemoprevention or treatment of colorectal cancer.

## References

1. **Amos-Landgraf JM, Kwong LN, Kendzierski CM, Reichelderfer M, Torrealba J, Weichert J, Haag JD, Chen K-S, Waller JL, Gould MN, et al.** 2007. A target-selected Apc-mutant rat kindred enhances the modeling of familial human colon cancer. *Proceedings of the National Academy of Sciences USA*. **104**:4036–41.
2. **STRING Protein Database.** Available from: <http://string-db.org/> (Accessed 11/14/13).
3. **Bansal M, Fenoglio C, Robboy S, West King D.** 1983. Are metaplasias in colorectal adenomas truly metaplasias? *American Journal of Pathology*. **115**:253–265.
4. **Bartlett RS, Heckman WW, Isenberg J, Susan L, Dailey SH.** 2012. Genetic characterization of vocal fold lesions: leukoplakia and carcinoma. *Laryngoscope*. **122**:336–342.
5. **Brazma A, Hingamp P, Quackenbush J, Sherlock G, Spellman P, Stoeckert C, Aach J, Ansorge W, Ball CA, Causton HC, et al.** 2001. Minimum information about a microarray experiment (MIAME)-toward standards for microarray data. *Nature Genetics*. **29**:365–71.
6. **Brenner S, Dove W, Herskowitz I, Thomas R.** 1990. Genes and development: molecular and logical themes. In: Crow J, Dove W, editors. *Perspectives on Genetics*. Madison, WI: The University of Wisconsin Press. pp. 182–89.
7. **Broussard EK, Kim R, Wiley JC, Marquez JP, Annis JE, Pritchard D, Disis ML.** 2013. Identification of putative immunologic targets for colon cancer prevention based on conserved gene upregulation from preinvasive to malignant lesions. *Cancer Prevention Research*. **7**:666-674.
8. **Bustin SA, Benes V, Garson JA, Hellemans J, Huggett J, Kubista M, Mueller R, Nolan T, Pfaffl MW, Shipley GL, et al.** 2009. The MIQE guidelines: minimum information for publication of quantitative real-time PCR experiments. *Clinical Chemistry*. **55**:611–22.
9. **Chai N, Zhang W, Wang Y, Zhou Z, Zhang Y, Liu H, Wan J, Qin J, Wang S, Wang Y, Pei X, Wu B, Linghu E.** 2013. Lgr5 and CD44 expressions in different types of intestinal polyps and colorectal cancer. *Journal of South Med University*. **7**:972-976.
10. **Chen K.** 1981. Colonic adenomatous polyp with focal squamous metaplasia. *Human Pathology*. **12**:848–9.

11. **Cho SH, Park YS, Kim HJ, Kim CH, Lim SW, Huh JW, Lee JH, Kim HR.** 2012. CD44 enhances the epithelial-mesenchymal transition in association with colon cancer invasion. *International Journal of Oncology*. **41**:211–8.
12. **Claessen MMH, Schipper MEI, Oldenburg B, Siersema PD, Offerhaus GJA, Vleggaar FP.** 2010. WNT-pathway activation in IBD-associated colorectal carcinogenesis: potential biomarkers for colonic surveillance. *Cellular Oncology*. **32**:303–10.
13. **Connelly TM, Koltun WA.** 2013. The Cancer “Fear” in IBD Patients: Is It Still REAL? *Journal of Gastrointestinal Surgery*. [Epub ahead of print].
14. **Debald M, Schildberg FA, Linke A, Walgenbach K, Kuhn W, Hartmann G, Walgenbach-Brünagel G.** 2013. Specific expression of k63-linked ubiquitination of calmodulin-like protein 5 in breast cancer of premenopausal patients. *Journal of Cancer Research and Clinical Oncology*. **12**:2125-32.
15. **Duan Z, Zheng H, Xu S, Jiang Y, Liu H, Li M, Hu D, Li W, Bode AM, Dong Z, et al.** 2013. Activation of the Ig Iα1 promoter by the transcription factor Ets-1 triggers Ig Iα1-Cα1 germline transcription in epithelial cancer cells. *Cellular & Molecular Immunology*. [Epub ahead of print].
16. **Durai R, Yang SY, Seifalian AM, Goldspink G, Winslet MC.** 2007. Role of insulin-like growth factor binding protein-4 in prevention of colon cancer. *World Journal of Surgical Oncology*. **5**:128.
17. **Durai R, Yang SY, Sales KM, Seifalian AM, Goldspink G, Winslet MC.** 2007. Insulin-like growth factor binding protein-4 gene therapy increases apoptosis by altering Bcl-2 and Bax proteins and decreases angiogenesis in colorectal cancer. *International Journal of Oncology*. **4**:883-888.
18. **Durand J, Lampron A, Mazzuco TL, Chapman A, Bourdeau I.** 2011. Characterization of differential gene expression in adrenocortical tumors harboring β-catenin (CTNNB1) mutations. *The Journal of Clinical Endocrinology and Metabolism*. **96**:E1206–11.
19. **Dyson JK, Rutter MD.** 2012. Colorectal cancer in inflammatory bowel disease: what is the real magnitude of the risk? *World Journal of Gastroenterology*. **18**:3839–48.
19. **Edgar R, Domrachev M, Lash AE.** 2002. Gene Expression Omnibus: NCBI gene expression and hybridization array data repository. *Nucleic Acids Research*. **30**:207-10.
20. **Endo T, Abe S, Seidler B, Nagoaka S, Takemura T, Utsuyama M, Kitagawa M, Hirokawa K.** 2004. Expression of IAP family proteins in colon cancers from patients with different age groups. *Cancer Immunol Immunother*. **53**:770–76.
21. **Fearnhead N, Britton M, Bodmer W.** 2001. The ABC of Apc. *Human Molecular Genetics*. **10**:721–733.

22. **Galamb O, Wichmann B, Sipos F, Spisak S, Krenacs T, Toth K, Leiszter K, Kalmar A, Tulassay Z, Molnar B.** 2012. Dysplasia-carcinoma transition specific transcripts in colonic biopsy samples. *PLoS One.* **11**:e48547.
23. **Gillen CD, Walmsley RS, Prior P, Andrews HA, Allan RN.** 1994. Ulcerative colitis and Crohn's disease: a comparison of the colorectal cancer risk in extensive colitis. *Gut.* **35**:1590–1592.
24. **Gomes IM, Maia CJ, Santos CR.** 2012. STEAP proteins: from structure to applications in cancer therapy. *Molecular Cancer Research.* **5**:573-587.
25. **Granlund AVB, Flatberg A, Ostvik AE, Drozdov I, Gustafsson BI, Kidd M, Beisvag V, Torp SH, Waldum HL, Martinsen TC, et al.** 2013. Whole genome gene expression meta-analysis of inflammatory bowel disease colon mucosa demonstrates lack of major differences between Crohn's disease and ulcerative colitis. *PloS One.* **8**:e56818.
26. **Halberg RB, Larsen MC, Elmergreen TL, Ko AY, Irving AA, Clipson L, Jefcoate CR.** 2008. Cyp1b1 exerts opposing effects on intestinal tumorigenesis via exogenous and endogenous substrates. *Cancer Research.* **1**:7394–7402.
27. **Hanly AM, Redmond M, Winter DC, Brophy S, Deasy JM, Bouchier-Hayes DJ, Kay EW.** 2006. Thrombomodulin expression in colorectal carcinoma is protective and correlates with survival. *British Journal of Cancer.* **9**:1320–1325.
28. **Hayashi I, Katsuda Y, Muto Y, Fujii Y, Morimatsu M.** 1984. Tubular adenoma with squamous metaplasia of the sigmoid colon: a case report. *Journal of Surgical Oncology.* **26**:130–4.
29. **Huang DW, Sherman BT, Lempicki RA.** 2009. Systematic and integrative analysis of large gene lists using DAVID bioinformatics resources. *Nature Protocols.* **4**:44–57.
30. **Ishioka T, Kuwabara N, Oohashi Y, Wakabayashi K.** 1987. Induction of colorectal tumors in rats by sulfated polysaccharides. *Critical Reviews in Toxicology.* **17**:215–44.
31. **Johansson ME V, Gustafsson JK, Holmén-Larsson J, Jabbar KS, Xia L, Xu H, Ghishan FK, Carvalho FA, Gewirtz AT, Sjövall H, et al.** 2013. Bacteria penetrate the normally impenetrable inner colon mucus layer in both murine colitis models and patients with ulcerative colitis. *Gut.* [Epub ahead of print].
32. **Kanaan Z, Rai SN, Eichenberger MR, Barnes C, Dworkin AM, Weller C, Cohen E, Roberts H, Keskey B, Petras RE, et al.** 2012. Differential microRNA expression tracks neoplastic progression in inflammatory bowel disease-associated colorectal cancer. *Human Mutation.* **33**:551–60.

33. **Kiran RP, Khoury W, Church JM, Lavery IC, Fazio VW, Remzi FH.** 2010. Similarities and differences between Crohn's and ulcerative colitis based on three decades of experience. *Annals of Surgery.* **2**:330-335.
34. **Kontozoglou T.** 1985. Squamous metaplasia in colonic adenomata: report of two cases. *Journal of Surgical Oncology.* **29**:31-4.
35. **Korkmaz CG, Korkmaz KS, Kurys P, Eldi C, Wang L, Klokk TL, Hammarstrom C, Troen G, Svindland A, Hager GL, Saatcioglu F.** 2005. Molecular cloning and characterization of STAMP2, an androgen-regulated six transmembrane protein that is overexpressed in prostate cancer. *Oncogene.* **31**:4934-4935.
36. **Koskensalo S, Louhimo J, Nordling S, Hagström J, Haglund C.** 2011. MMP-7 as a prognostic marker in colorectal cancer. *Tumour Biology.* **32**:259-64.
37. **Leclerc D, Lévesque N, Cao Y, Deng L, Wu Q, Powell J, Sapienza C, Rozen R.** 2013. Genes with aberrant expression in murine preneoplastic intestine show epigenetic and expression changes in normal mucosa of colon cancer patients. *Cancer Prevention Research.* **6**:1171-81.
38. **Liu G-H, Guan T, Datta K, Coppinger J, Yates J, Gerace L.** 2009. Regulation of myoblast differentiation by the nuclear envelope protein NET39. *Molecular and Cellular Biology.* **29**:5800-12.
39. **Mikami T, Yoshida T, Numata Y, Kikuchi M, Araki K, Nakada N.** 2011. Invasive behavior of ulcerative colitis-associated carcinoma is related to reduced expression of CD44 extracellular domain: comparison with sporadic colon carcinoma. *Diagnostic Pathology.* **6**:30.
40. **Miyake M, Lawton A, Goodison S, Urquidi V, Gomes-Giacoia E, Zhang G, Ross S, Kim J, Rosser CJ.** 2013. Chemokine (C-X-C) ligand 1 (CXCL1) protein expression is increased in aggressive bladder cancers. *BMC Cancer.* **13**:322.
41. **Neish AS.** 2011. The Microbiota and colonic neoplasia: An emerging link? *Journal of Gastroenterology.* **45**:571.
42. **Niemi M, Hakkinen T, Karttunen TJ, Eskelinen S, Kervinen K, Savolainen MJ, Lehtola J, Makela J, Yla-Herttuala S, Kesaniemi YA.** 2002. Apolipoprotein E and colon cancer. Expression in normal and malignant human intestine and effect on cultured human colonic adenocarcinoma cells. *European Journal of Internal Medicine.* **13**:37-43.
43. **Noble CL, Abbas a R, Cornelius J, Lees CW, Ho G-T, Toy K, Modrusan Z, Pal N, Zhong F, Chalasani S, et al.** 2008. Regional variation in gene expression in the healthy colon is dysregulated in ulcerative colitis. *Gut.* **57**:1398-405.

44. **Yoshikawa R, Yanagi H, Shen CS, Fujiwara Y, Noda M, Yagy T, Gega M, Oshima T, Yamamura T, Okamura H, Nakano Y, Morinaga T, Hasimoto-Tamaoki T.** 2006. ECA39 is a novel distant metastasis-related biomarker in colorectal cancer. *World Journal of Gastroenterology*. **36**:5884-5889.
45. **Österberg L, Levan K, Partheen K, Delle U, Olsson B, Sundfeldt K, Horvath G.** 2009. Potential predictive markers of chemotherapy resistance in stage III ovarian serous carcinomas. *BMC Cancer*. **9**:368.
46. **Pantanowitz L.** 2009. Colonic adenoma with squamous metaplasia. *International Journal of Surgical Pathology*. **17**:340–2.
47. **Pekow J, Dougherty U, Huang Y, Gometz E, Nathanson J, Cohen G, Levy S, Kocherginsky M, Venu N, Westerhoff M, et al.** 2013. Gene signature distinguishes patients with chronic ulcerative colitis harboring remote neoplastic lesions. *Inflammatory Bowel Diseases*. **3**:461-470.
48. **Persano L, Moserle L, Esposito G, Bronte V, Barbieri V, Iafrate M, Gardiman MP, Larghero P, Pfeffer U, Naschberger E, et al.** 2009. Interferon-alpha counteracts the angiogenic switch and reduces tumor cell proliferation in a spontaneous model of prostatic cancer. *Carcinogenesis*. **30**:851–60.
49. **Pucci S, Bonanno E, Sesti F, Mazzarelli P, Mauriello A, Ricci F, Zoccai GB, Rulli F, Galat G, Spagnoli LG.** 2009. Clusterin in stool: a new biomarker for colon cancer screening? *American Journal of Gastroenterology*. **11**:2807–2815.
50. **Rachadi SM, Qin T, Sun S, Zheng WJ, Li Z.** 2013. Molecular profiling of multiple human cancers defines an inflammatory cancer-associated molecular pattern and uncovers KPNA2 as a uniform poor prognostic marker. *PLoS One*. **3**:e57911.
51. **Sabour Alaoui S, Dessirier V, Araujo E de, Alexaki V-I, Pelekanou V, Lkhider M, Stathopoulos EN, Castanas E, Bagot M, Bensussan A, et al.** 2012. TWEAK affects keratinocyte G2/M growth arrest and induces apoptosis through the translocation of the AIF protein to the nucleus. *PloS One*. **7**:e33609.
52. **Shenoy AK, Fisher RC, Butterworth E a, Pi L, Chang L-J, Appelman HD, Chang M, Scott EW, Huang EH.** 2012. Transition from colitis to cancer: high Wnt activity sustains the tumor-initiating potential of colon cancer stem cell precursors. *Cancer Research*. **72**:5091–100.
53. **Slattery ML, Sweeney C, Murtaugh M, Ma KN, Potter JD, Levin TR, Samowitz W, Wolff R.** 2005. Associations between *apoE* genotype and colon and rectal cancer. *Carcinogenesis*. **8**:1422-1429.
54. **Slaughter D, Southwick H, Smejkal W.** 1953. “Field cancerization” in oral stratified squamous epithelium. *Cancer*. **5**:963-968.

55. **Soletti RC, Rodrigues NALV, Biasoli D, Luiz RR, Souza HSP de, Borges HL.** 2013. Immunohistochemical analysis of retinoblastoma and  $\beta$ -catenin as an assistant tool in the differential diagnosis between Crohn's disease and ulcerative colitis. *PloS One*. **8**:e70786.
56. **Suga T, Iwakawa M, Tsuji H, Ishikawa H, Oda E, Noda S, Otsuka Y, Ishikawa A, Ishikawa K-I, Shimazaki J, et al.** 2008. Influence of multiple genetic polymorphisms on genitourinary morbidity after carbon ion radiotherapy for prostate cancer. *International Journal of Radiation Oncology, Biology, Physics*. **72**:808–13.
57. **Tonjes M, Barbus S, Park YJ, Wang W, Scholtter M, Lindroth AM, Pleier SV, Bai AHC, Karra D, Piro RM, et al.** 2013. BCAT1 promotes cell proliferation through amino acid catabolism in gliomas carrying wild-type IDH1. *Nature Medicine*. **7**:901-908.
58. **Toyota M, Ho C, Ahuja N, Jair KW, Li Q, Ohe-Toyota M, Baylin SB, Issa JP.** 1999. Identification of differentially methylated sequences in colorectal cancer by methylated CpG island amplification. *Cancer Research*. **10**:2307-2312.
59. **Turovskaya O, Foell D, Sinha P, Newlin R, Nayak J, Nguyen M, Olsson A, Nawroth PP, Bierhaus A, Varki N, et al.** 2008. RAGE, carboxylated glycans and S100A8 / A9 play essential roles in colitis-associated carcinogenesis. *Carcinogenesis*. **29**:2035–2043.
60. **Vogelstein B, Papadopoulos N, Velculescu VE, Zhou S, Diaz LA, Kinzler KW.** 2013. Cancer genome landscapes. *Science*. **339**:1546–58.
61. **Washington MK, Powell AE, Sullivan R, Sundberg J, Wright N, Coffey RJ, Dove WF.** 2013. Pathology of rodent models of intestinal cancer: progress report and recommendations. *Gastroenterology*. **4**:705–17.
62. **Whitsett TG, Cheng E, Inge L, Asrani K, Jameson NM, Hostetter G, Weiss GJ, Kingsley CB, Loftus JC, Bremner R, et al.** 2012. Elevated expression of Fn14 in non-small cell lung cancer correlates with activated EGFR and promotes tumor cell migration and invasion. *American Journal of Pathology*. **1**:111–120.
63. **Wilson C, Heppner K, Labosky P, Hogan B, Matrisian L.** 1997. Intestinal tumorigenesis is suppressed in mice lacking the metalloproteinase matrilysin. *Proceedings of the National Academy of Sciences USA*. **94**:1402–1407.
64. **Yoshimi K, Tanaka T, Serikawa T, Kuramoto T.** 2013. Tumor suppressor APC protein is essential in mucosal repair from colonic inflammation through angiogenesis. *The American Journal of Pathology*. **4**:1263-1274.
65. **Yu R, Dhall D, Nissen NN, Zhou C, Ren SG.** 2011. Pancreatic neuroendocrine tumors in glucagon receptor-deficient mice. *PLoS One*. **8**:e23397.



66. **Zhou W, Feng X, Ren C, Jiang X, Liu W, Huang W, Liu Z, Zeng L, Wang L, et al.** 2013. Over-expression of BCAT1, a c-Myc target gene, induces cell proliferation, migration and invasion in nasopharyngeal carcinoma. *Molecular Cancer*. **12**:53.
67. **Zhour C, Dhall D, Nissen NN, Chen CR, Yu R.** 2009. Homozygous P86S mutation of the human glucagon receptor is associated with hyperglucagonemia, alpha cell hyperplasia, and islet cell tumor. *Pancreas*. **8**:941-946.

### Chapter 3

#### **Supplementation by vitamin D compounds does not affect colonic tumor development in vitamin D sufficient murine models**

Amy A. Irving performed the majority of the rat dissections and endoscopies (assisted by Kathleen J. Krentz), completed all of the data analysis for the rat studies and wrote the final manuscript. Richard B. Halberg and Dawn M. Albrecht performed all of the mouse studies and data analysis. Lori A. Plum directed the serum analysis and shared her expertise in vitamin D. Linda Clipson created and edited the figures. Norman Drinkwater gave statistical advice. James M. Amos-Landgraf initiated the design of the original experiments and offered both technical and intellectual support throughout the project. William F. Dove, an expert in Cancer Biology, and Hector F. DeLuca, an expert in Vitamin D Biochemistry, served as advisors.

*This chapter has been modified from its original publication in the Archives of Biochemistry and Biophysics. Permission to use this copyrighted material was obtained from Elsevier on 7/18/13.*

*Irving AA, Halberg RB, Albrecht DM, Plum LA, Krentz KJ, Clipson L, Drinkwater N, Amos-Landgraf JM, Dove WF, DeLuca HF. Supplementation by vitamin D compounds does not affect colonic tumor development in vitamin D sufficient murine models. Arch Biochem Biophys. 2011 Nov;515(1-2):64-71 doi: 10.1016/j.abb.2011.08.011.*

**Abstract**

Epidemiological studies indicate that sunlight exposure and serum 25-hydroxy-vitamin D<sub>3</sub> [25(OH)D<sub>3</sub>] levels are each associated with a lower risk of colon cancer. The few controlled supplementation trials testing vitamin D in humans reported to date show conflicting results. We have used two genetic models of familial colon cancer, the *Apc*<sup>Pirc/+</sup> (Pirc) rat and the *Apc*<sup>Min/+</sup> (Min) mouse, to investigate the effect of 25(OH)D<sub>3</sub> and two analogs of vitamin D hormone on colonic tumors. Longitudinal endoscopic monitoring allowed us to test the efficacy of these compounds in preventing newly arising colonic tumors and in affecting established colonic tumors. 25(OH)D<sub>3</sub> and two analogs of vitamin D hormone each failed to reduce tumor multiplicities or alter the growth patterns of colonic tumors in the Pirc rat or the Min mouse. Further studies with a wider range of doses and different vitamin D compounds on various stages of colon cancer are needed to assess whether vitamin D supplementation is effective against any point during tumorigenesis.

## **Introduction**

Colorectal cancer is the third leading cause of cancer-related death in men and women in the US<sup>1</sup>. Colon cancer risk and mortality vary greatly around the world, indicating an environmental component to its pathogenesis. Epidemiological studies have shown that vitamin D is associated with a reduced risk of colon cancer. In particular, individuals with lower exposure to sunlight, resulting in reduced 25(OH)D<sub>3</sub> serum levels, have increased rates of colon cancer<sup>7,21</sup>. However, supplementation studies in normal human populations show conflicting results regarding the efficacy of vitamin D<sup>49,51</sup>.

Three decades ago Garland and Garland recognized an association between lower exposure to sunlight and increased colon cancer mortality rates across the United States<sup>21</sup>. From this observation, they proposed a protective mechanism involving vitamin D. Five years later, Garland *et al* reported a 19-year prospective study in which increased vitamin D and calcium intake, as gathered from dietary histories, correlated with a decreased risk for developing colon cancer<sup>19</sup>. However, other studies based on dietary recall have failed to find a similar risk reduction<sup>25,27</sup>. Some association studies that measured serum 25(OH)D<sub>3</sub> levels and compared individuals in the lowest quartile with those in the highest quartile have shown a correlation with reduced colon cancer risk<sup>53</sup>. Similarly, the Nurse's Health Study, a nested case-control study where colorectal cancer incidence was the primary endpoint, identified 193 colorectal cancer cases diagnosed up to 11 years after a single blood collection<sup>16</sup>. Those findings indicated a significant association between high plasma 25(OH)D<sub>3</sub> levels and lower colorectal cancer incidence. Interestingly, the results were significant only among women older than 60 years of age, residing in areas with high levels of available sunlight, and for cancers of the distal colon and rectum. By contrast,

other studies have failed to find an association between serum 25(OH)D<sub>3</sub> levels and colon cancer. In the Japan Public Health Centre-based Prospective Study, a nested case-control study, no association was seen between serum 25(OH)D<sub>3</sub> levels and the risk for developing colon cancer<sup>37</sup>. Looking further, some studies have found associations only with certain patient subpopulations or tumor sites within the colon<sup>2,16</sup>.

Overall, epidemiological studies attempting to assess dietary and lifestyle factors for cancer susceptibility frequently encounter uncontrolled confounders. While many studies attempt to control for variables that may impact vitamin D status or colon cancer risk, other unappreciated confounding variables may exist. These variables, taken together, could lead to an apparent protective effect attributed to vitamin D status. In a prospective study, Freedman *et al* examined a list of lifestyle characteristics that varied by quantile of serum 25(OH)D<sub>3</sub> status<sup>18</sup>. They found an inverse association between colon cancer mortality and 25(OH)D<sub>3</sub> status, which was adjusted for sex, race/ethnicity and smoking status. However, trends are evident for reduced total body fat and increased level of physical activity in individuals with elevated 25(OH)D<sub>3</sub> status. A trend for lower body mass index and higher level of physical activity with higher circulating 25(OH)D<sub>3</sub> levels has also been observed in several other studies<sup>2,52</sup>. Plausibly, individuals with higher serum levels of vitamin D metabolites tend to be healthier overall and any combination of these lifestyle factors may play a role in protection from colon and other cancers. Thus, evidence for a *bona fide* link between circulating 25(OH)D<sub>3</sub> levels and colon cancer risk in human populations must take into account factors such as geographic location, diet, exercise, lifestyle and culture.

Although controlled prospective clinical trials are needed to assess causation, some reported studies have combined calcium with vitamin D supplementation, making it difficult to

evaluate the effect of vitamin D itself<sup>28,51</sup>. Some studies have reported an inverse association between dietary calcium intake or serum calcium levels and colon cancer risk<sup>25</sup>. Similar effects have also been seen in animal models. One such study found that supplemental calcium alone was able to decrease tumor multiplicity and size<sup>44</sup>. Interestingly, studies have also shown an interaction between serum 25(OH)D<sub>3</sub> and calcium levels. In the Health Professionals Follow-up Study, a nested case-control study, the inverse association between a decreased risk for colon cancer and increased serum 25(OH)D<sub>3</sub> levels was limited to patients who also had a high calcium intake<sup>53</sup>. Further, Jenab and colleagues showed that individuals with both low serum 25(OH)D<sub>3</sub> and low calcium levels had the highest risk for colon cancer (incidence rate ratio 1.33, 95% CI 1.14-1.54), while those with both high serum 25(OH)D<sub>3</sub> and high calcium levels had the lowest risk (IRR 0.72, 95% CI 0.57-0.91)<sup>25</sup>.

As a result of the conflicting reports for the association between vitamin D and colon cancer in humans, we tested three vitamin D compounds in two rodent models of colon cancer. Both the Pirc rat and the Min mouse are heterozygous for mutations in *Apc*, a tumor suppressor gene that is mutated in approximately 80% of human colorectal cancers<sup>3,15,45</sup>. The Pirc rat spontaneously develops a high incidence and multiplicity of colonic tumors. Treatment of Pirc rats with dextran sodium sulfate (DSS), a polymer that further increases the multiplicity of colonic tumors, allows us to study tumors with a potentially different etiology, and to test the effectiveness of vitamin D both in prevention of newly emergent tumors and treatment of existing tumors. Therefore, both untreated and DSS-treated Pirc rats have been utilized to test these compounds. By contrast, the C57BL/6J Min mouse, the most commonly used genetic model of intestinal cancer, develops few colonic tumors. Thus, studies with the Min mouse may lack the power to detect an effect of agents on colonic tumors<sup>9,39</sup>. This limitation has been overcome by treating Min

mice with DSS which increases the number of colonic tumors and by following the tumors longitudinally<sup>11</sup>. To complement terminal tumor counts, endoscopy was performed regularly to detect changes in colonic tumor emergence, growth rate, or regression<sup>14</sup>.

## **Materials and Methods**

**Animal Breeding and Maintenance.** Rats and mice were maintained under a protocol approved by the Animal Care and Use Committee of the University of Wisconsin School of Medicine and Public Health and in a facility in the McArdle Laboratory approved by the American Association of Laboratory Animal Care. Animals were housed in standard caging with free access to food and acidified water. F1 hybrid rats were generated by breeding ACI *Apc*<sup>+/+</sup> females (Harlan, Indianapolis, IN) to F344/NTac *Apc*<sup>Pirc/+</sup> males (developed in the laboratory of WFD and now commercially available through Taconic, Hudson, NY). The numbers of tumors in the small intestine versus the colon of Pirc rats is strain dependent in the F1 hybrids<sup>3</sup>. F1 generation rats were used in these studies to increase the number of colonic tumors and to shift the distribution of tumors even further in favor of the colon. F1 hybrid mice were generated by breeding SWR *Apc*<sup>+/+</sup> females (Jackson Laboratory, Bar Harbor, ME) to C57BL/6J *Apc*<sup>Min/+</sup> males (developed in the laboratory of WFD and now commercially available through Jackson Laboratory, Bar Harbor, ME). The distribution of tumors between the small intestine and colon also differs among the various inbred strains of Min mice<sup>34</sup>. F1 generation mice were used to decrease the number of tumors in the small intestine, thereby reducing blockage and increasing lifespan. In addition, using F1 generation animals creates the opportunity in future studies to examine allelic

ratios at any informative SNP sites for somatic changes in the genome or epigenome of tumors in response to these compounds.

**Chemicals.** Dextran sodium sulfate (500 kDa) was purchased from Fisher Scientific (Pittsburgh, PA). 25(OH)D<sub>3</sub> was purchased from Chemvon (Shanghai, China) and was determined to be 97% pure by HPLC<sup>13</sup>. The “high potency” vitamin D analog, 2 $\alpha$ -methyl-19-nor-(20S)-1 $\alpha$ ,25-dihydroxyvitamin D<sub>3</sub> (HP), and the relatively “non-calcemic” analog, 2-methylene-19-nor-(20S)-1 $\alpha$ -hydroxybishomopregnacalciferol (NC), were developed in the laboratory of HFD<sup>38,43</sup>. These two analogs possess different tissue selective actions with NC having specific activity in the skin<sup>36</sup> and HP in the bone<sup>43</sup>. Another known distinction between these two analogs is that the potency of HP is approximately one thousand-fold greater than that of NC. Both analogs efficiently suppress parathyroid hormone, suggesting a common pathway in the parathyroid gland<sup>38</sup> and unpublished work.

**Diets.** Control rats were fed either AIN-76A (Harlan, Madison, WI) or 5020 chow (Purina, St. Louis, MO); no difference between these diets was seen for tumor multiplicity, time to first tumor, or growth of tumors (data not shown). Therefore, control rat data from both diets were combined. Control mice were fed AIN-76A. All supplemented diets were formulated in the AIN-76A base diet. The vehicle used to incorporate the 25(OH)D<sub>3</sub> into the AIN-76A diet was 5% (w/w) Wesson soybean oil and 0.25% (v/w) ethanol (Pharmaco Aaper, Brookfield, CT). Daily doses of the test compounds were calculated based on a consumption rate of 20 grams of food per day for the rat and 4 grams of food per day for the mouse<sup>4,47,48,50</sup>.

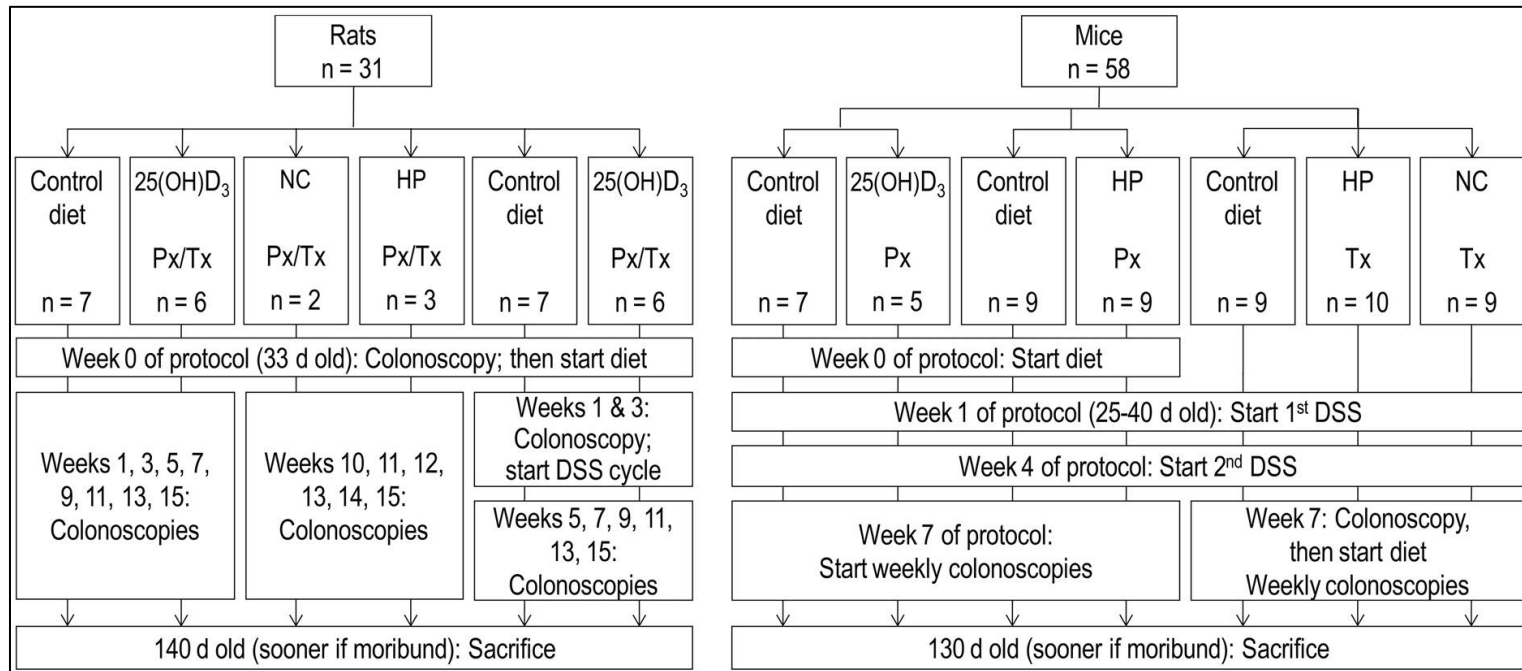


25(OH)D<sub>3</sub> was added to achieve a target dose of 1500 µg/kg body weight/day for the rat and 500 µg/kg body weight/day for the mouse. From pilot studies, these concentrations were sufficient to provide a 1-2 mg increase in calcium per 100 ml of serum, demonstrating that the 25(OH)D<sub>3</sub> was biologically effective. This increase in serum calcium did not affect the weight of the experimental animals at 140 days of age versus the controls (male rats 338.5 ± 19.8 vs 351.8 ± 15.1 grams; female rats 218.8 ± 13.2 vs 224.2 ± 14.0 grams; male mice 28.4 ± 3.1 vs 26.2 ± 2.4 grams; female mice 22.8 ± 1.5 vs 23 ± 1.7 grams) as measured at sacrifice. This indicates that the increase in serum calcium did not affect the overall health of the animals during the study.

The HP analog diet was made up to reach a target dose of 0.02 µg/kg body weight/day in the rat and mouse; while the NC analog diet was made up to reach a target dose of 1200 µg/kg body weight/day in the rat and 600 µg/kg body weight/day in the mouse. These maximum tolerated doses each resulted in a 1-2 mg increase in calcium per 100 ml serum.

**Rat Experimental Design.** At 33 days of age, male and female (ACI x F344/NTac)F1 *Apc<sup>Pirc/+</sup>* rats were assigned to either 25(OH)D<sub>3</sub>-supplemented diet or vehicle diet. Assignments to protocols were random, except that sexes and littermates were evenly distributed (Fig 3-1). Then, at 40 days of age half of each of the sexes were given 4% (w/v) DSS in the drinking water to study the effect of 25(OH)D<sub>3</sub> on DSS-induced tumors (chemoprevention). The rat dosing regimen consisted of two rounds of DSS, each lasting seven days and separated by a seven-day period without DSS. The dose and molecular weight of DSS used in these experiments maintained normal crypt architecture, minimized inflammatory infiltrates, and did not affect body weight until the tumor burden became high (data not shown). Batches of DSS used in this study were consistent in the resultant multiplicity of rat colonic tumors and therefore one control group

**Fig 3-1.** Experimental design. Protocol time points are given in weeks; ages of animals are given in days. In the rats, tumors observed during the colonoscopy at week 0 were used to assess the efficacy of treatment; chemoprevention was evaluated by observing whether additional tumors arose in subsequent colonoscopies. In the mice, chemoprevention (Px) was assessed in the protocols in which the supplemented diet was started before the first cycle of DSS. Treatment (Tx) of DSS-induced tumors was tested in the protocols where the DSS cycles were completed before transfer to the supplemented diet.



was used for all test diets. Another small number of male Pirc rats not treated with DSS were randomized to one of two analog diets: NC analog or HP analog. Animals underwent colonoscopy every other week starting before diet supplementation until sacrifice at 140 days of age or when they became moribund. Weights were measured during each colonoscopy procedure and at sacrifice. Tumors identified before supplementation, as well as those arising during supplementation, were used to test the effects of these compounds on existing tumors (treatment). Tumors that arose during supplementation provided a test of the effects of these compounds to prevent newly arising tumors (chemoprevention). At sacrifice, the small intestine and colon were opened longitudinally, laid flat, washed with PBS and fixed with formalin; the small intestine was divided into four equal sections before fixation. Blood was obtained at sacrifice by cardiac puncture.

**Mouse Experimental Design.** Starting at 25-40 days of age, all male and female (SWR x B6J)F1 *Apc*<sup>Min/+</sup> mice were given 4% (w/v) DSS in the drinking water to increase the number of colonic tumors (Fig 3-1). The mouse dosing regimen consisted of two rounds of DSS, each lasting four days and separated by a 17-day period without DSS. As in the rat experiments, the dose and molecular weight of DSS used in these studies did not cause severe damage to the colonic epithelium (data not shown). In the chemoprevention mode (prior to the first DSS exposure) mice in one group were assigned to one of three diets: 25(OH)D<sub>3</sub>, HP analog or vehicle alone. In the treatment mode (following completion of the last DSS exposure) mice in a second group were assigned to one of three diets: NC analog, HP analog, or vehicle alone. Assignments to protocols distributed sexes and littermates evenly across protocols, but were otherwise random. Batches of DSS used in this study differed in the resultant multiplicity of mouse colonic tumors, so each test diet in the mouse was analyzed with its own set of contemporaneous controls. Ani-

mals underwent colonoscopy every week until sacrifice at 130 days of age or when they became moribund. At sacrifice, the small intestine and colon were treated as described above. Blood was obtained at sacrifice by laceration of the abdominal aorta.

**Endoscopy and Terminal Tumor Counts.** Endoscopy was performed on rats and mice at pre-determined intervals until sacrifice (Fig 3-1). Briefly, the animal was anesthetized with isoflurane and placed on a sterile surgical field, ventral side down. The colon was flushed with warm PBS to remove any fecal material and to provide lubrication. A 2.7 mm x 18 cm Hopkins Optik 30° endoscope (7219BA, Karl Storz, Tuttlingen, Germany) for the rat or a 1.9 mm x 10 cm Hopkins II 0° endoscope (R1232AA, Karl Storz) for the mouse was placed within a sheath (67065C, Karl Storz) and inserted to the proximal colonic flexure. Illuminated by the Xenon Nova 175 (201315, Karl Storz), still and video images were captured at each visit using the Image 1 hub (22200, Karl Storz) and AidaVet software (692040, Karl Storz). The anatomy of the rat allows the distal two-thirds of the colon to be visualized with endoscopy, while the anatomy of the mouse allows the distal half of the colon to be visualized. Video and still images of colonic tumors were obtained and analyzed after each colonoscopy visit.

For the Pirr rats, endoscopy began before dietary supplementation, which allowed the effects of the compounds to be examined both on existing tumors (treatment) and in preventing newly arising tumors (chemoprevention). For the Min mice, endoscopy began after the second DSS treatment, because young mice were too small for insertion of the endoscope into the anus.

The longitudinal fate of tumors was determined by three observers blinded to the diet of the animal. Tumors were examined during each endoscopy visit and any tumor that appeared at least twice during the study was given one of four scores: growing, static, regressing or

unscorable; those judged to be unscorable were excluded from the longitudinal analysis. A score was generated based on agreement between at least two of the three blinded observers. After sacrifice, formalin-fixed tumors were counted on a dissecting microscope. Total tumor counts were obtained for each of the four sections of the small intestine and for the entire colon.

**Biochemical Assays.** Serum 25(OH)D<sub>3</sub> levels were measured using a <sup>125</sup>I-radioimmunological assay following manufacturer's instructions (DiaSorin; Stillwater, MN)<sup>6</sup>. Serum calcium was measured by atomic absorption spectrometry on the ABX Pentra clinical chemistry analyzer (Horiba ABX, Montpellier, France)<sup>6</sup>.

**Statistical Methods.** For the biochemical assays, a two-sided Wilcoxon rank sum test was used to compare the experimental to the control population; a p-value  $\leq 0.05$  was considered significant. Longitudinal analysis of endoscopic images utilized a chi-square test of growing versus non-growing tumors; no significant sex-specific differences in this ratio of tumor fates were observed for either the rat or the mouse, therefore sexes were combined for analysis. The means and standard deviations of tumor multiplicity data from Pirc rats and Min mice are not normally distributed, leading us to test our hypotheses using nonparametric statistics<sup>3,35</sup>. Tumor multiplicities in the Pirc rat show significant sex differences, as described previously<sup>3</sup>. Therefore, terminal multiplicity data of the Pirc rat were blocked by sex based on Lehmann's extension to the Wilcoxon rank sum test<sup>30</sup> and both sexes were tested jointly for effects of the test diets. Since multiplicities of colonic tumors in the Min mouse show no sex-specific differences, the data were combined to analyze the terminal multiplicity data in the mouse experiments, and a two-sided Wilcoxon rank sum test was employed.

To correct for multiple testing in both the rat and the mouse studies, the Dunn-Sidak correction was utilized. For the purpose of the Dunn-Sidak correction, experiments with and without DSS in the Pirc rat were considered to be two separate studies, as were the chemoprevention and treatment experiments in the Min mouse. Therefore, for the terminal multiplicity data in the rat, three comparisons were made without DSS and one comparison was made with DSS. A p-value  $\leq 0.0167$  for studies without DSS and a p-value  $\leq 0.05$  for studies with DSS was considered significant. For the terminal multiplicity data for the mouse, there were two comparisons in the prevention mode and two comparisons in the treatment mode. A p-value  $\leq 0.025$  was considered significant for each of these modes.

## **Results**

### **25(OH)D<sub>3</sub> did not reduce the multiplicity of colonic tumors in Pirc rats or Min mice.**

Groups of Pirc rats underwent endoscopy to identify existing tumors and were then placed on the 25(OH)D<sub>3</sub>-supplemented diet. Although serum 25(OH)D<sub>3</sub> levels were significantly increased (Table 3-1A), there was no reduction in the multiplicity of tumors in the small intestine or colon (Fig 3-2A, Table 3-2A).

In an experiment specifically designed to test chemopreventive action against newly arising tumors, additional groups of Pirc rats underwent endoscopy to identify and exclude any existing tumors from analysis. They were then placed on the 25(OH)D<sub>3</sub>-supplemented diet in advance of DSS treatment. Although serum 25(OH)D<sub>3</sub> levels were significantly increased (Table 3-1A), there was no reduction in the multiplicity of tumors in the small intestine or colon (Fig 3-2A, Table 3-2A).

Cohorts of Min mice were treated with DSS to increase the multiplicity of colonic tumors. To test chemopreventive action, they were placed on the 25(OH)D<sub>3</sub>-supplemented diet in advance of DSS treatment. Again, although serum 25(OH)D<sub>3</sub> and calcium levels were significantly increased (Table 3-1B), there was no effect on the multiplicity of tumors in the small intestine or colon (Fig 3-2B, Table 3-2B).

**Table 3-1.** Serum measurements for (A) Pirc rats and (B) Min mice. Rat serum data combines male and female, as well as untreated and DSS-treated Pirc rats. Mouse serum data combines both male and female DSS-treated Min mice. P-values were determined using the Wilcoxon rank sum test for significance; a p-value  $\leq 0.05$  is considered significant for the biochemical assays.

Species	Test Diet	Serum component measured	Level in serum, mean $\pm$ SD (n of animals)		P-value
			Control diet	Test diet	
A. Rat	25(OH)D <sub>3</sub>	25(OH)D <sub>3</sub> (ng/ml)	28.0 $\pm$ 17.9 (12)	550 $\pm$ 169 (26)	< 0.00001
		Calcium (mg/dl)	11.8 $\pm$ 0.7 (14)	14.0 $\pm$ 1.1 (26)	< 0.00001
B. Mouse	25(OH)D <sub>3</sub>	25(OH)D <sub>3</sub> (ng/ml)	26.2 $\pm$ 8.4 (7)	290 $\pm$ 11 (5)	0.004
		Calcium (mg/dl)	11.3 $\pm$ 1.1 (8)	13.2 $\pm$ 1.0 (5)	0.02
	HP analog	Calcium (mg/dl)	9.2 $\pm$ 0.3 (5)	10.4 $\pm$ 0.6 (16)	< 0.002
	NC analog	Calcium (mg/dl)	9.2 $\pm$ 0.3 (5)	11.7 $\pm$ 0.8 (9)	< 0.003

**Two analogs of vitamin D did not reduce the multiplicity of colonic tumors in Pirc rats or Min mice.** To explore compounds related to vitamin D with different pharmacokinetic properties, we analyzed the effects of two vitamin D analogs on tumors of the small intestine and colon (Fig 3-1). Maximum tolerated dosages, even of the “non-calcemic” analog, were established on the basis of elevation of serum calcium compared to controls (Table 3-1B). The HP and NC analogs were tested in a small number of male Pirc rats not treated with DSS and no significant change in tumor multiplicity was seen (Fig 3-1B, Table 3-2B).





**Table 3-2.** Terminal small intestinal and colonic tumor counts for Pirc rats and Min mice. (A) Rat *p*-values compare each test result to controls of the same DSS status with male and female values blocked and jointly tested. (B) Male and female data have been combined for the mice and corresponding controls are shown in the same row as test results. Unadjusted *p*-values are reported; a *p*-value  $\leq 0.0167$  is considered significant for rat studies without DSS, a *p*-value  $\leq 0.05$  is considered significant for rat studies involving DSS, and a *p*-value  $\leq 0.025$  is considered significant for all mouse studies (see Materials and Methods). Px, prevention; Tx, treatment; ND, not done.

Species	Treated with DSS	Diet	Supplementation mode	Small Intestinal Tumors			Colonic Tumors		
				Count, mean $\pm$ SD		p-value	Count, mean $\pm$ SD		p-value
				Female	Male		Female	Male	
A. Rat	No	Control		2 $\pm$ 2	6 $\pm$ 3		4 $\pm$ 2	23 $\pm$ 7	
		25(OH)D <sub>3</sub>	Px/Tx	1 $\pm$ 1	9 $\pm$ 3	0.29	17 $\pm$ 3	42 $\pm$ 12	0.003
		NC	Px/Tx	ND	12 $\pm$ 5	0.08	ND	34 $\pm$ 9	0.18
	Yes	HP	Px/Tx	ND	5 $\pm$ 1	0.77	ND	39 $\pm$ 4	0.08
		Control		0.3 $\pm$ 0.6	10 $\pm$ 5		45 $\pm$ 11	58 $\pm$ 3	
		25(OH)D <sub>3</sub>	Px/Tx	0 $\pm$ 0	4 $\pm$ 2	0.06	79 $\pm$ 11	80 $\pm$ 24	0.02
B. Mouse	Yes	25(OH)D <sub>3</sub>	Control	12 $\pm$ 4	17 $\pm$ 6	0.12	16 $\pm$ 8	16 $\pm$ 5	0.74
			Test Diet	17 $\pm$ 9	23 $\pm$ 9	0.20	8 $\pm$ 5	9 $\pm$ 5	0.48
			Control	23 $\pm$ 8	30 $\pm$ 10	0.12	2 $\pm$ 2	3 $\pm$ 3	0.56
			Test Diet	23 $\pm$ 8	19 $\pm$ 7	0.25	2 $\pm$ 2	2 $\pm$ 2	0.24
		NC	Tx						

To test the chemopreventive action of the HP analog, a group of mice was placed on diet containing HP analog and then treated with DSS. To test the analogs in a treatment modality, other groups of mice were placed on diet containing HP analog or NC analog following the completion of the DSS administration. There was no effect of the HP analog (chemoprevention or treatment) or NC analog (treatment) on the multiplicity of tumors in the small intestine or colon in the mice (Fig 3-2B, Table 3-2B).

**Supplementation with 25(OH)D<sub>3</sub> or either of two vitamin D hormone analogs did not cause tumor regression in Pirr rats or Min mice.** Both rats and mice routinely underwent endoscopy throughout the study. Thus, any substantial change in existing tumors or emergence of newly formed tumors in the distal colon would have been detected. Most of the colonic tumors were newly emerging during this study in both the rats and the mice. Supplementation of Pirr rats or Min mice with 25(OH)D<sub>3</sub> or either analog of vitamin D hormone did not appear to inhibit the emergence of these newly arising colonic tumors (Fig 3-3 and data not shown).

In the rat, only 1 of 101 scorable tumors appeared to regress; this tumor occurred in the control group. The tumor growth patterns were not significantly different in rats given the 25(OH)D<sub>3</sub>-supplemented diet versus those in the control group (Table 3-3A).

In the mouse, only 1 of 111 scorable tumors appeared to regress; this tumor occurred in the HP prevention group. The growth patterns of tumors from the various control sets were indistinguishable and therefore were combined (data not shown). The tumor growth patterns were not significantly different in mice given either the HP analog diet or the NC analog diet versus those in the control group (Table 3-3B).

All rats not treated with DSS survived until the termination of the study (data not shown). However, about half of the DSS-treated rats had to be sacrificed before the scheduled 140 day time point, owing to the weight loss caused by their high tumor burden (data not shown). By contrast, no such weight loss or shortened time to morbidity was seen in any of the Min mice.

**Fig 3-3.** Longitudinal endoscopic tracking of colonic tumors in the Pirc rat. The top row represents a single animal from the vehicle diet; the bottom row represents a single animal from the 25(OH)D<sub>3</sub>-supplemented diet. Each column represents one time point when a still image of the tumor(s) was acquired. The 25(OH)D<sub>3</sub>-supplemented diet did not prevent further growth of existing tumors (white arrow) or emergence of new tumors (black arrow). Qualitatively similar results were found for colonic tumors in the Min mice.

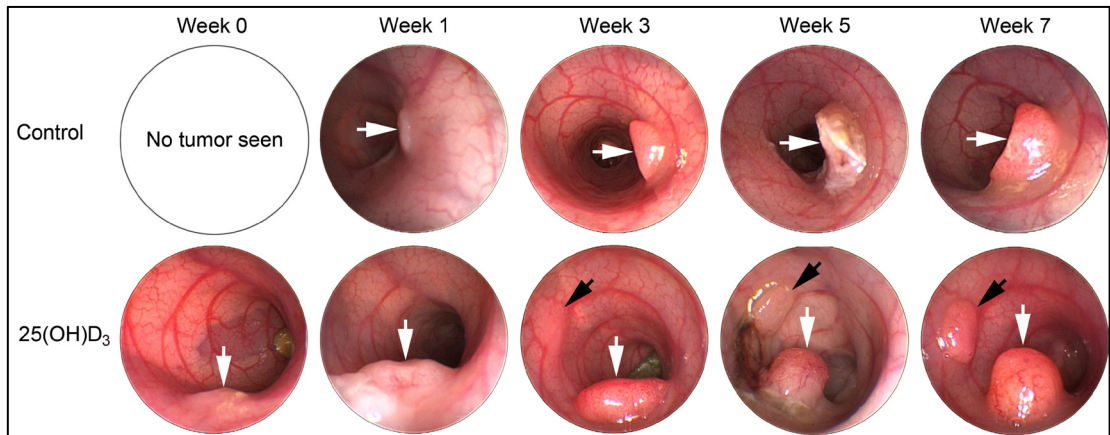


**Table 3-3.** Longitudinal assessments of tumor growth for Pirc rats and Min mice. No test diet in either the Pirc rats or the Min mice decreased the number of growing tumors as compared to control animals. “Grew” includes existing or newly arising tumors that increased in size; “Static” includes tumors that showed no net change in size; “Regressed” includes tumors that decreased in size or disappeared during the study. NS, not scorable: individual tumors could not be reliably followed longitudinally owing to growth of existing tumors and abundance of emerging tumors. Px, chemoprevention; Tx, treatment.

Species	Treated with DSS	Diet	Supplementation mode	Colonic tumors, % (n/total)		
				Grew	Static	Regressed
A. Rat	No	Control	None	71% (25/35)	26% (9/35)	3% (1/35)
		25(OH)D <sub>3</sub>	Px/Tx	85% (56/66)	15% (10/66)	0%
	Yes	Control	None	NS	NS	NS
		25(OH)D <sub>3</sub>	Px/Tx	NS	NS	NS
B. Mouse	Yes	Control	None	97% (35/36)	3% (1/36)	0%
		25(OH)D <sub>3</sub>	Px	NS	NS	NS
		HP Analog	Px	94% (32/34)	3% (1/34)	3% (1/34)
		HP Analog	Tx	95% (19/20)	5% (1/20)	0%
		NC Analog	Tx	90% (19/21)	10% (2/21)	0%

## Discussion

These studies were designed to test the effects of 25(OH)D<sub>3</sub> and two analogs of vitamin D hormone both on existing tumors (treatment) and to prevent newly arising tumors (chemoprevention) in two rodent models. Our studies are unique in two respects. First, to avoid issues of species-specificity in animal modeling of human disease, we used models for colon cancer in two distinct mammalian genera, the Pirc rat (*Rattus norvegicus*) and the Min mouse (*Mus musculus*). Second, to assess action by these agents in both chemopreventive and treatment modes, we have utilized longitudinal monitoring by endoscopy and tumor induction with DSS.

Longitudinal monitoring provides the further advantages of detecting concurrent emergence and disappearance of tumors as well as changes in tumor size over time; such information would be lost with terminal tumor counting alone. Overall, these studies constitute a comprehensive investigation of whether supplementation by 25(OH)D<sub>3</sub> or analogs of vitamin D hormone provides any protective effect against colon tumors in animal models.

We have found that 25(OH)D<sub>3</sub> and two analogs of vitamin D hormone each failed to reduce colonic tumor multiplicity in Pirc rats or Min mice. Further, we have also shown that these agents neither reduced the number of newly emerging tumors, nor changed the growth rate nor caused regression of existing tumors. Vitamin D supplementation should be evaluated carefully before routinely implemented in human populations<sup>10</sup>.

Colon cancer is a disease with a long latency period<sup>26</sup>. Therefore, chemopreventive agents may need to be in place for a decade or more to show an effect in humans<sup>26</sup>. Thus, owing to their relatively short lifespan, rodent models may not provide an appropriate test of chemopreventive agents that require a long treatment period to exert a significant effect<sup>12</sup>. In our study, supplemented diets were given for a significant portion of the animal's natural lifespan, which is approximately two years for laboratory rats and mice. Some agents have recently been shown to be chemopreventive in humans over a short period of time<sup>23,24</sup>. The negative results from our current study gain significance in contrast to positive results with other chemopreventive agents. A 40-day treatment with celecoxib was shown to significantly reduce tumor multiplicity in Pirc rats<sup>3</sup>. Additionally, 25-50 day studies of the combination of d,l- $\alpha$ -difluoromethylornithine (DFMO) and piroxicam in the Min mouse seeded the human trials of DFMO and sulindac<sup>22,33</sup>. Thus, rodent models can offer an important platform for short-term

studies of chemoprevention. Clearly, short-term supplementation studies are the highest priority to explore, particularly for the individuals at risk of recurrent adenoma formation.

25(OH)D<sub>3</sub> may act at the initial stage of adenomagenesis and may need to be given for a long period, as speculated by Levine and Ahnen for aspirin<sup>31</sup>. Studies examining the efficacy of aspirin in humans as a colorectal chemopreventive agent have shown that significant effects can be observed only after five years of supplementation with follow-up performed at least ten years after starting the regimen<sup>17</sup>. This lag may represent a differential response to early stages of colon cancer to vitamin D compounds.

Reduced expression of the vitamin D receptor (VDR) may also explain the lack of response to supplementation in this study. Many colon cancers lose VDR expression as they progress, possibly rendering useless any increase in vitamin D status at that time. We have shown that VDR gene expression decreases over time in Pirc rat tumors (data not shown). However, the test diet in this study was introduced before most of the tumors were visible by endoscopy and certainly before progression. It seems likely that VDR expression was intact in these early tumors. Using endoscopy, we demonstrated that 25(OH)D<sub>3</sub> and two analogs of vitamin D hormone each failed to prevent new tumor formation in two rodent models of familial colon cancer.

Prospective clinical supplementation trials of vitamin D are limited. In a randomized double-blind placebo-controlled trial of men and women between 65 and 85 years of age, Trivedi *et al* showed no significant change in colorectal cancer incidence after 5 years of vitamin D supplementation and follow-up<sup>49</sup>, where development of cancer or cause of mortality were secondary endpoints. In addition, a double-blinded trial by the Women's Health Initiative, where participants were randomized to receive either placebo or 500 mg calcium plus 200 IU vitamin D twice daily, also showed no effect on colorectal cancer incidence after seven years<sup>51</sup>. Important-

ly, some studies have demonstrated that calcium supplementation alone appears to reduce colon adenoma occurrence<sup>8</sup>. Therefore, studies examining the combination of calcium and vitamin D make causation difficult to assess. Patients who have had a polyp removed are at enhanced risk of developing subsequent colonic tumors. Therefore, these individuals represent a focused group in which to study chemopreventive agents. To our knowledge, no clinical trials examining the efficacy of vitamin D supplementation on adenoma recurrence have been conducted in patients who have a history of colonic adenomas or cancer.

Evidence is accumulating to indicate that tumors develop through more than one pathway<sup>41</sup> and may respond differentially to various chemopreventive agents. In studies that do show an association between higher vitamin D levels and lower rates of colon cancer, the effect tends to be stronger on tumors in the distal colon and rectum than for those in the proximal region<sup>16,29,37</sup>. Similarly, Rothwell and colleagues have shown that aspirin protects against cancers of the proximal colon and rectum but not those in the distal colon<sup>40</sup>. Thus, the colon may not be uniform in response to chemopreventive agents across cancer sites. Accordingly, combination chemoprevention may be necessary to have an impact on all colon cancer risk. The combination of aspirin and 25(OH)D<sub>3</sub> may result in synergistic effects by complementary action between promotion of apoptosis by aspirin and of terminal differentiation by vitamin D. To test this hypothesis, a pilot study involving cohorts of Pirc rats (with and without DSS) and Min mice (with DSS) were given a combination diet consisting of both 25(OH)D<sub>3</sub> and aspirin and followed longitudinally as in the above studies. We found no difference in small intestinal or colonic tumor multiplicities or in colonic tumor growth patterns (data not shown).

Current recommended daily intakes for vitamin D range from 400-800 IU, depending on age and gender<sup>10</sup>. Serum 25(OH)D<sub>3</sub> levels of at least 20 ng/ml are considered adequate for over-

all health in humans, and levels greater than 50 ng/ml are linked to potential adverse effects<sup>10</sup>. However, studies in humans have shown that doses of vitamin D much higher than recommended can be tolerated in some individuals<sup>20</sup>. Similarly, one study in rats has shown that serum 25(OH)D<sub>3</sub> levels up to 436 ng/ml were well tolerated; only when serum levels reached 688 ng/ml was severe hypercalcemia and weight loss observed<sup>42</sup>. The serum 25(OH)D<sub>3</sub> levels achieved in our studies were 552 ± 152 ng/ml in rats and 290 ± 11 ng/ml in mice. However, it remains unclear whether super-supplementation of vitamins above sufficiency is beneficial. Bashir and colleagues have reported that Min mice given a diet either low or high in multi-vitamin content had increased intestinal tumor multiplicities in both cases<sup>5</sup>. Future studies are needed to address whether a U-shaped curve exists for vitamin D in the area of cancer therapy, as for vitamin D protection against vascular calcification<sup>32</sup>.

Several specific issues were not explored in our studies. The duration of treatment with the vitamin D compounds was between 11 and 16 weeks in our various studies. It is possible that in animal models with increased longevity, prolonged treatment may result in a different outcome. Our use of endoscopic methods allowed us to track tumors only in the distal portion of the colon, and thus limited our overall detection.

Finally, the important issue whether 25(OH)D<sub>3</sub> deficiency would cause an increase in tumor formation remains to be addressed. Poor vitamin D status may be correlated with increased cancer risk, whereas supplementation above sufficiency may not. In a mouse xenograft model of colon cancer, mice with undetectable levels of serum 25(OH)D had 40% larger tumors than mice with sufficient serum levels<sup>46</sup>. This has also been shown to be true in carcinogen-induced rodent models of colon cancer. DMH-treated rats that were fed a high calcium and low



vitamin D diet developed significantly larger colonic tumors than DMH-treated rats that were fed a high calcium diet<sup>44</sup>.

We have found that 25(OH)D<sub>3</sub> supplementation above normal levels failed to reduce tumor multiplicities in the small intestine or colon in both the Pirc rat and the Min mouse models. Longitudinal monitoring by endoscopy showed no change in the number of newly arising tumors or the growth patterns of existing tumors in rats and mice given the 25(OH)D<sub>3</sub> diet. Our study highlights the need for further investigation of these specific issues, and of the issue with which we began this report, the association between high sunlight exposure and low colon cancer incidence. In sufficient individuals, are there effects of sunlight beyond changes in serum vitamin D levels? A recent publication by Becklund *et al* showed that ultraviolet radiation exposure was able to suppress an experimental mouse model of autoimmune disease, independent of increases in serum 25(OH)D<sub>3</sub><sup>6</sup>.

## References

1. **Cancer Facts & Figures 2010**. 2010. Atlanta, GA, American Cancer Society.
2. **Adams SV, Newcomb PA, Burnett-Hartman AN, White E, Mandelson MT, Potter JD**. 2011. Circulating 25-hydroxyvitamin-D and risk of colorectal adenomas and hyperplastic polyps. *Nutr Cancer* **63**:319-326.
3. **Amos-Landgraf JM, Kwong LN, Kendziorski CM, Reichelderfer M, Torrealba J, Weichert J, Haag JD, Chen KS, Waller JL, Gould MN, Dove WF**. 2007. A target-selected *Apc*-mutant rat kindred enhances the modeling of familial human colon cancer. *Proc Natl Acad Sci U S A* **104**:4036-4041.
4. **Bachmanov AA, Reed DR, Beauchamp GK, Tordoff MG**. 2002. Food intake, water intake, and drinking spout side preference of 28 mouse strains. *Behav Genet* **32**:435-443.
5. **Bashir O, FitzGerald AJ, Goodlad RA**. 2004. Both suboptimal and elevated vitamin intake increase intestinal neoplasia and alter crypt fission in the *Apc*<sup>Min/+</sup> mouse. *Carcinogenesis* **25**:1507-1515.
6. **Becklund BR, Severson KS, Vang SV, DeLuca HF**. 2010. UV radiation suppresses experimental autoimmune encephalomyelitis independent of vitamin D production. *Proc Natl Acad Sci U S A* **107**:6418-6423.
7. **Boscoe FP, Schymura MJ**. 2006. Solar ultraviolet-B exposure and cancer incidence and mortality in the United States, 1993-2002. *BMC Cancer* **6**:264.
8. **Carroll C, Cooper K, Papaioannou D, Hind D, Pilgrim H, Tappenden P**. 2010. Supplemental calcium in the chemoprevention of colorectal cancer: a systematic review and meta-analysis. *Clin Ther* **32**:789-803.
9. **Chiu CH, McEntee MF, Whelan J**. 2000. Discordant effect of aspirin and indomethacin on intestinal tumor burden in *Apc*<sup>Min/+</sup> mice. *Prostaglandins Leukot Essent Fatty Acids* **62**:269-275.
10. **Committee to Review Dietary Reference Intakes for Vitamin D and Calcium**. Dietary Reference Intakes for Calcium and Vitamin D. Institute of Medicine. <http://www.nap.edu/catalog/13050.html> (Accessed 11/3/13).
11. **Cooper HS, Everley L, Chang WC, Pfeiffer G, Lee B, Murthy S, Clapper ML**. 2001. The role of mutant *Apc* in the development of dysplasia and cancer in the mouse model of dextran sulfate sodium-induced colitis. *Gastroenterology* **121**:1407-1416.
12. **Corpet DE, Pierre F**. 2005. How good are rodent models of carcinogenesis in predicting efficacy in humans? A systematic review and meta-analysis of colon chemoprevention in rats, mice and men. *Eur J Cancer* **41**:1911-1922.

13. **DeLuca HF, Prahl JM, Plum LA.** 2010. 1,25-Dihydroxyvitamin D is not responsible for toxicity caused by vitamin D or 25-hydroxyvitamin D. *Arch Biochem Biophys* **505**:226-230.
14. **Durkee BY, Shinki K, Newton MA, Iverson C, Weichert J, Dove WF, Halberg RB.** 2009. Longitudinal assessment of colonic tumor fate in mice by computed tomography and optical colonoscopy. *Academic Radiology* **16**:1475-1482.
15. **Fearnhead NS, Britton MP, Bodmer WF.** 2001. The ABC of APC. *Hum Mol Genet* **10**:721-733.
16. **Feskanich D, Ma J, Fuchs CS, Kirkner GJ, Hankinson SE, Hollis BW, Giovannucci EL.** 2004. Plasma vitamin D metabolites and risk of colorectal cancer in women. *Cancer Epidemiol Biomarkers Prev* **13**:1502-1508.
17. **Flossmann E, Rothwell PM.** 2007. Effect of aspirin on long-term risk of colorectal cancer: consistent evidence from randomised and observational studies. *Lancet* **369**:1603-1613.
18. **Fredman DM, Looker AC, Chang SC, Graubard BI.** 2007. Prospective study of serum vitamin D and cancer mortality in the United States. *J Natl Cancer Inst* **99**:1594-1602.
19. **Garland C, Shekelle RB, Barrett-Connor E, Criqui MH, Rossof AH, Paul O.** 1985. Dietary vitamin D and calcium and risk of colorectal cancer: a 19-year prospective study in men. *Lancet* **1**:307-309.
20. **Garland CF, French CB, Baggerly LL, Heaney RP.** 2011. Vitamin D supplement doses and serum 25-hydroxyvitamin D in the range associated with cancer prevention. *Anticancer Res* **31**:607-611.
21. **Garland CF, Garland FC.** 1980. Do sunlight and vitamin D reduce the likelihood of colon cancer? *Int J Epidemiol* **9**:227-231.
22. **Halberg RB, Katzung DS, Hoff PD, Moser AR, Cole CE, Lubet RA, Donehower LA, Jacoby RF, Dove WF.** 2000. Tumorigenesis in the multiple intestinal neoplasia mouse: redundancy of negative regulators and specificity of modifiers. *Proc Natl Acad Sci U S A* **97**:3461-3466.
23. **Hosono K, Endo H, Takahashi H, Sugiyama M, Sakai E, Uchiyama T, Suzuki K, Iida H, Sakamoto Y, Yoneda K, Koide T, et al.** 2010. Metformin suppresses colorectal aberrant crypt foci in a short-term clinical trial. *Cancer Prev Res (Phila)* **3**:1077-1083.
24. **Hosono K, Endo H, Takahashi H, Sugiyama M, Uchiyama T, Suzuki K, Nozaki Y, Yoneda K, Fujita K, Yoneda M, et al.** 2010. Metformin suppresses azoxymethane-induced colorectal aberrant crypt foci by activating AMP-activated protein kinase. *Mol Carcinog* **49**:662-671.

25. **Jenab M, Bueno-de-Mesquita HB, Ferrari P, van Duijnhoven FJ, Norat T, Pischon T, Jansen EH, Slimani N, Byrnes G, Rinaldi S, et al.** 2010. Association between pre-diagnostic circulating vitamin D concentration and risk of colorectal cancer in European populations: a nested case-control study. *BMJ* **340**:b5500.
26. **Jones S, Chen WD, Parmigiani G, Diehl F, Beerenwinkel N, Antal T, Traulsen A, Nowak MA, Siegel C, Velculescu VE, Kinzler KW, Vogelstein B, Willis J, Markowitz SD.** 2008. Comparative lesion sequencing provides insights into tumor evolution. *Proc Natl Acad Sci U S A* **105**:4283-4288.
27. **Kampman E, Giovannucci E, van 't V, Rimm E, Stampfer MJ, Colditz GA, Kok FJ, Willett WC.** 1994. Calcium, vitamin D, dairy foods, and the occurrence of colorectal adenomas among men and women in two prospective studies. *Am J Epidemiol* **139**:16-29.
28. **Lappe JM, Travers-Gustafson D, Davies KM, Recker RR, Heaney RP.** 2007. Vitamin D and calcium supplementation reduces cancer risk: results of a randomized trial. *Am J Clin Nutr* **85**:1586-1591.
29. **Lee JE, Li H, Chan AT, Hollis BW, Lee IM, Stampfer MJ, Wu K, Giovannucci E, Ma J.** 2011. Circulating Levels of Vitamin D and Colon and Rectal Cancer: The Physicians' Health Study and a Meta-analysis of Prospective Studies. *Cancer Prev Res (Phila)* **4**:735-743.
30. **Lehmann EL.** 1998. *Nonparametrics: Statistical Methods Based on Ranks*. Upper Saddle River, New Jersey: Prentice Hall.
31. **Levine JS, Ahnen DJ.** 2006. Clinical practice. Adenomatous polyps of the colon. *N Engl J Med* **355**:2551-2557.
32. **Mathew S, Lund RJ, Chaudhary LR, Geurs T, Hruska KA.** 2008. Vitamin D receptor activators can protect against vascular calcification. *J Am Soc Nephrol* **19**:1509-1519.
33. **Meyskens FL, McLaren CE, Pelot D, Fujikawa-Brooks S, Carpenter PM, Hawk E, Kelloff G, Lawson MJ, Kidao J, McCracken J, et al.** 2008. Difluoromethylornithine Plus Sulindac for the Prevention of Sporadic Colorectal Adenomas: A Randomized Placebo-Controlled, Double-Blind Trial. *Cancer Prev Res (Phila Pa)* **1**:9-11.
34. **Moser AR, Luongo C, Gould KA, McNeley MK, Shoemaker AR, Dove WF.** 1995. ApcMin: a mouse model for intestinal and mammary tumorigenesis. *Eur J Cancer* **31A**:1061-1064.
35. **Moser AR, Pitot HC, Dove WF.** 1990. A dominant mutation that predisposes to multiple intestinal neoplasia in the mouse. *Science* **247**:322-324.
36. **Nieves NJ, Ahrens JM, Plum LA, DeLuca HF, Clagett-Dame M.** 2010. Identification of a unique subset of 2-methylene-19-nor analogs of vitamin D with comedolytic activity in the rhino mouse. *J Invest Dermatol* **130**:2359-2367.

37. **Otani T, Iwasaki M, Sasazuki S, Inoue M, Tsugane S.** 2007. Plasma vitamin D and risk of colorectal cancer: the Japan Public Health Center-Based Prospective Study. *Br J Cancer* **97**:446-451.
38. **Plum LA, PrahJ JM, Ma X, Sicinski RR, Gowlugari S, Clagett-Dame M, DeLuca HF.** 2004. Biologically active noncalcemic analogs of 1alpha,25-dihydroxyvitamin D with an abbreviated side chain containing no hydroxyl. *Proc Natl Acad Sci U S A* **101**:6900-6904.
39. **Reuter BK, Zhang XJ, Miller MJ.** 2002. Therapeutic utility of aspirin in the *Apc<sup>Min/+</sup>* murine model of colon carcinogenesis. *BMC Cancer* **2**:19.
40. **Rothwell PM, Wilson M, Elwin CE, Norrving B, Algra A, Warlow CP, Meade TW.** 2010. Long-term effect of aspirin on colorectal cancer incidence and mortality: 20-year follow-up of five randomised trials. *Lancet* **376**:1741-1750.
41. **Shen L, Toyota M, Kondo Y, Lin E, Zhang L, Guo Y, Hernandez NS, Chen X, Ahmed S, Konishi K, Hamilton SR, Issa JP.** 2007. Integrated genetic and epigenetic analysis identifies three different subclasses of colon cancer. *Proc Natl Acad Sci U S A* **104**:18654-18659.
42. **Shephard RM, DeLuca HF.** 1980. Plasma concentrations of vitamin D3 and its metabolites in the rat as influenced by vitamin D3 or 25-hydroxyvitamin D3 intakes. *Arch Biochem Biophys* **202**:43-53.
43. **Sicinski RR, PrahJ JM, Smith CM, DeLuca HF.** 1998. New 1alpha,25-dihydroxy-19-norvitamin D3 compounds of high biological activity: synthesis and biological evaluation of 2-hydroxymethyl, 2-methyl, and 2-methylene analogues. *J Med Chem* **41**:4662-4674.
44. **Sitrin MD, Halline AG, Abrahams C, Brasitus TA.** 1991. Dietary calcium and vitamin D modulate 1,2-dimethylhydrazine-induced colonic carcinogenesis in the rat. *Cancer Res* **51**:5608-5613.
45. **Su LK, Kinzler KW, Vogelstein B, Preisinger AC, Moser AR, Luongo C, Gould KA, Dove WF.** 1992. Multiple intestinal neoplasia caused by a mutation in the murine homolog of the APC gene. *Science* **256**:668-670.
46. **Tangpricha V, Spina C, Yao M, Chen TC, Wolfe MM, Holick MF.** 2005. Vitamin D deficiency enhances the growth of MC-26 colon cancer xenografts in Balb/c mice. *J Nutr* **135**:2350-2354.
47. **Biomethodology of the mouse.** The University of Iowa Institutional Animal Care and Use Committee. <http://research.uiowa.edu/animal/?get=mouse>. (Accessed June 2011).
48. **Biomethodology of the rat.** The University of Iowa Institutional Animal Care and Use Committee. <http://research.uiowa.edu/animal/?get=rat>. (Accessed June 2011).

49. **Trivedi DP, Doll R, Khaw KT.** 2003. Effect of four monthly oral vitamin D<sub>3</sub> (cholecalciferol) supplementation on fractures and mortality in men and women living in the community: randomised double blind controlled trial. *BMJ* **326**:469.
50. **Vento PJ, Swartz ME, Martin LB, Daniels D.** 2008. Food intake in laboratory rats provided standard and fenbendazole-supplemented diets. *J Am Assoc Lab Anim Sci* **47**:46-50.
51. **Wactawski-Wende J, Kotchen JM, Anderson GL, Assaf AR, Brunner RL, O'Sullivan MJ, Margolis KL, Ockene JK, Phillips L, Pottern L, et al.** 2006. Calcium plus vitamin D supplementation and the risk of colorectal cancer. *N Engl J Med* **354**:684-696.
52. **Weinstein SJ, Yu K, Horst RL, Ashby J, Virtamo J, Albanes D.** 2011. Serum 25-hydroxyvitamin D and risks of colon and rectal cancer in Finnish men. *Am J Epidemiol* **173**:499-508.
53. **Wu K, Feskanich D, Fuchs CS, Willett WC, Hollis BW, Giovannucci EL.** 2007. A nested case control study of plasma 25-hydroxyvitamin D concentrations and risk of colorectal cancer. *J Natl Cancer Inst* **99**:1120-1129.

## Chapter 4

### **Dietary hyper-supplementation with 25(OH)D<sub>3</sub> affects tumor multiplicity, size and net growth rate in the Pirc rat**

Amy A. Irving designed the study in collaboration with Lori A. Plum, performed the endoscopies, collected the blood samples, performed the majority of the rat dissections, completed all of the data analysis and wrote the final manuscript. Lori A. Plum directed the serum analysis and designed the study diets. William Wardle created the study diets and analyzed the serum calcium levels. Chao Weng analyzed the serum 25(OH)D<sub>3</sub> levels. Linda Clipson created and edited the figures. William F. Dove, an expert in cancer biology, and Hector F. DeLuca, an expert in vitamin D biochemistry, served as advisors.

## **Abstract**

Epidemiological studies in humans have shown an inverse association between serum 25(OH)D<sub>3</sub> levels and rates of colon cancer. However, results from vitamin D supplementation trials in either vitamin D deficient or sufficient individuals are much less conclusive. We have previously shown that 25(OH)D<sub>3</sub> supplementation failed to reduce tumor multiplicity or alter tumor growth patterns in the *Apc*<sup>Pirc/+</sup> rat. To the contrary, we found initial evidence for an increase in the number of colonic tumors after 25(OH)D<sub>3</sub> supplementation.

Here, we extend our previous study to test five different dose levels of 25(OH)D<sub>3</sub> in the Pirc rat. Two dose-dependent phenomena emerged from this study. First, similar to our previous observation, colonic tumor multiplicity increased with increasing 25(OH)D<sub>3</sub> dose. Second, we discovered that colonic tumor size decreased with increasing 25(OH)D<sub>3</sub> dose.

Mechanistic studies investigating the effect of vitamin D compounds on colorectal cancer cells often use *in vitro* methods. Through several decades of research, these studies have shown that vitamin D can inhibit proliferation and induce differentiation and apoptosis of colorectal cancer cells *in vitro*. Utilizing the Pirc rat model we observed a phenomenon that would not have been discovered by *in vitro* studies alone - increasing doses of 25(OH)D<sub>3</sub> increases the number of colonic tumors. Further, vitamin D compounds may act differently during different states of progression or on different aspects of the tumor. This study emphasizes the need for modeling of disease *in vivo* and provides further evidence to support investigation of the effects of supplementation by 25(OH)D<sub>3</sub> or other vitamin D compounds in humans, especially caution regarding higher doses and in individuals who already have sufficient serum 25(OH)D<sub>3</sub> levels.



## **Introduction**

Colorectal cancer is the third leading cause of cancer-related death in men and women in the United States<sup>2</sup>. Generally a disease associated with aging, colon cancer tends to affect individuals 50 and older<sup>2</sup>. However, the full development of cancer in the colon can take a decade or longer<sup>16</sup>. Thus, effective chemopreventives that can be incorporated into a healthy diet far in advance of early tumor development could reduce long-term disease burden. A chemopreventive for use in the general population must, however, pass very stringent criteria for detrimental effects. For those at-risk for recurrent cancer, the criteria are less but still significant.

One such dietary component that has received a great deal of attention for its potential to reduce colorectal cancer risk is vitamin D. Observations made over three decades ago by Garland and Garland suggested that sunlight exposure was inversely related to colon cancer risk<sup>11</sup>. They subsequently hypothesized that vitamin D was the active agent responsible for the role of sunlight in reducing cancer risk. Since then, numerous studies have indeed shown an association between serum 25(OH)D<sub>3</sub> levels and risk for developing colon cancer, especially when particular cancer sub-sites are considered<sup>12,26,30</sup>.

Further, *in vitro* studies corroborate this finding. Treatment of cells with various vitamin D compounds has been shown to inhibit proliferation and induce differentiation and apoptosis of colorectal cancer cells *in vitro*<sup>7,9,18,24</sup>. Based on the human association data and mechanistic *in vitro* data, vitamin D appears to be a strong candidate dietary compound for preventing or even treating colorectal cancer.

Although the data showing an association between higher serum 25(OH)D<sub>3</sub> levels and reduced cancer risk is strong, and plausible mechanisms for the action of vitamin D against colo-

rectal cancer cells have been demonstrated, the ultimate test is to determine whether increasing an individual's serum 25(OH)D<sub>3</sub> level by supplementation decreases their future risk for colon cancer. The results from such supplementation trials are limited and much less conclusive than the association studies. Men and woman over the age of 65 supplemented with a bolus dose of 100,000 IU cholecalciferol every four months for five years showed no significant difference in the rate of colon cancer development in a randomized double blind placebo-controlled trial<sup>27</sup>. Daily supplementation trials have also shown no effect. Postmenopausal women given 400 IU vitamin D plus 1000 mg calcium daily for seven years with follow-up during the same interval also found no effect on the incidence of colon cancer<sup>28</sup>.

Assessment of the effect of supplements in human populations can encounter many life-style and dietary confounders. Using rodent models of the disease in a controlled setting can overcome many of these factors. Recently, we found that supplementation with 25(OH)D<sub>3</sub> did not reduce the multiplicity of small intestinal or colonic tumors or alter the growth patterns of colonic tumors in either Min mice or Pirc rats<sup>15</sup>. Surprisingly, both male and female Pirc rats supplemented with 1500 µg 25(OH)D<sub>3</sub>/kg body weight/day showed a significant increase in colonic tumor multiplicity over control Pirc rats. A similar phenomenon has been observed for small intestinal tumor multiplicity in Min mice given a diet either low or high in multi-vitamin content<sup>4</sup>. This suggests that a moderate balance of vitamins may result in the lowest risk for cancer development, and deviation above or below that balance can each increase risk.

Human data also support the idea that both hypo- and hypervitaminosis D each result in an increased risk for cancer. Examination of plasma 25(OH)D<sub>3</sub> levels and eventual development of colon cancer in individuals enrolled in the Health Professionals Followup Study (HPFS) showed that individuals in quintile two with a median plasma 25(OH)D concentration of 25.0

ng/mL (OR 0.97, 95% CI 0.55-1.70), quintile three with a median plasma 25(OH)D concentration of 29.1 ng/mL (OR 0.66, 95% CI 0.35-1.24) and quintile four with a median plasma 25(OH)D concentration of 33.3 ng/mL (OR 0.51, 95% CI 0.27-0.97) had a lower risk for developing colon cancer than individuals in quintile one with a median plasma 25(OH)D concentration of 18.4 ng/mL (OR 1.00, referent)<sup>30</sup>. However, individuals in quintile five with a median plasma 25(OH)D concentration of 39.4 ng/mL actually appear to have an increased risk compared to quintiles three and four (OR 0.83, 95% CI 0.45-1.52). Further support comes from a recent study where vitamin D levels were measured and esophageal cancer risk was subsequently determined<sup>21</sup>. An increased risk (OR 1.99, 95% CI 1.03-3.86) for esophageal adenocarcinoma risk was found in individuals with the highest vitamin D intake (>3.0 µg/day) compared to individuals with the lowest intake (<2.05 µg/day).

To more rigorously test the phenomenon observed in our previous study with 25(OH)D<sub>3</sub>-supplemented Pirc rats, and to test the observations seen in some human studies, we examined 25(OH)D<sub>3</sub>-supplementation over a range of five doses from 60-4500 µg 25(OH)D<sub>3</sub>/kg body weight/day. Rats were followed longitudinally by colonoscopy every other week to assess tumor growth patterns during supplementation, and terminal tumor counts for the small intestine and colon, as well as serum for calcium and 25(OH)D<sub>3</sub> measurements, were obtained at sacrifice.

## **Materials and Methods**

**Animal Breeding and Maintenance.** Rats were maintained under a protocol approved by the Animal Care and Use Committee of the University of Wisconsin School of Medicine and Public Health and in a facility in the McArdle Laboratory approved by the American Association of

Laboratory Animal Care. Rats were individually housed in standard caging with free access to food and acidified water. F<sub>1</sub> generation rats were generated by breeding female ACI *Apc*<sup>+/+</sup> rats (Harlan, Indianapolis, IN) to male Fisher344 (F344) *Apc*<sup>Pirc/+</sup> rats (developed in the laboratory of WFD and now commercially available through Taconic, Hudson, NY)<sup>3</sup>. Pirc rats on the F344 background get roughly an equal number of small intestinal and colonic tumors; this distribution is shifted towards the colon in ACI Pirc rats. F<sub>1</sub> generation rats were used in this study to shift the distribution of tumors in favor of colonic tumors, while avoiding the rapid emergence of a large number of colonic tumors typically seen in the parental ACI Pirc strain<sup>29</sup>.

**Chemicals.** 25(OH)D<sub>3</sub> was purchased from Chemvon (Shanghai, China) and was determined to be 97% pure by straight-phase HPLC<sup>5</sup>.

**Diets.** Control rats were fed either Lab Diet 5020 chow (St. Louis, MO) or a vehicle diet of AIN-76A (Harlan, Madison, WI) plus 5% (w/w) Wesson soybean oil and 0.25% (v/w) ethanol (Pharmaco Aaper, Brookfield, CT). The soybean oil and ethanol were necessary to incorporate the 25(OH)D<sub>3</sub> into the AIN-76A diet, and were therefore also added to the vehicle diet. A consumption rate of 20 grams of food per day per rat was used to estimate the daily dose levels of 25(OH)D<sub>3</sub>. In this study we chose to supplement with 25(OH)D<sub>3</sub>, as this is the compound that is measured in the serum and with which cancer risk has been associated. 25(OH)D<sub>3</sub> was added to the diet to achieve target doses of 60, 170, 500, 1500, and 4500 µg/kg body weight/day. These concentrations were determined from data from a previous study<sup>15</sup> and pilot studies showing that the 1500 µg/kg body weight/day dose would provide a 1-2 mg increase in calcium per 100 ml of serum, demonstrating that the 25(OH)D<sub>3</sub> was biologically effective.

**Experimental Design.** At 33 days of age, male and female (ACI x F344/NTac) $F_1$  *Apc*<sup>Pirc/+</sup> rats were randomized to either vehicle diet or one of six 25(OH) $D_3$ -supplemented diets: 60, 170, 500, 1500, and 4500  $\mu\text{g}/\text{kg}$  body weight/day. Animals underwent colonoscopy every other week starting before diet supplementation until sacrifice at 140 days of age or when they became moribund. Weights were measured at each colonoscopy visit and at sacrifice.

**Endoscopy.** Beginning at 33 days of age, endoscopy was performed every other week until sacrifice. This allowed us to examine the effect of 25(OH) $D_3$  on both existing tumors (by measuring growth rate and tumor size) and against newly arising tumors (by assessing tumor multiplicity). Briefly, the animal was anesthetized with 3% isoflurane and placed on a sterile surgical field, ventral side down. The colon was flushed with warm saline to remove any fecal material and to provide lubrication. A 2.7 mm x 18 cm Hopkins Optik 30° endoscope (7219BA, Karl Storz, Tuttlingen, Germany) within a sheath (67065C, Karl Storz) was inserted to the proximal colonic flexure. Illuminated by the Xenon Nova 175 (201315, Karl Storz), still and video images were captured at each visit using the Image 1 hub (22200, Karl Storz) and AidaVet software (692040, Karl Storz). The anatomy of the rat allows the distal two-thirds of the colon to be visualized by endoscopy.

Three observers blinded to the diet of the animal determined the longitudinal fate of each tumor. Tumors were examined at all visits and any tumor that appeared at least twice during the study was given one of four scores: growing, static, regressing or unscorable; those judged to be unscorable were excluded from analyses. A score was generated based on agreement between at least two of the three observers.

**Terminal Tumor Sizing and Counts.** At sacrifice, the small intestine and colon were opened longitudinally, laid flat, washed with PBS and fixed with formalin; the small intestine was divided into four equal sections before fixation. Formalin-fixed tumors from dissected intestines were counted and sized on a dissecting microscope. Tumor counts were obtained for each of the four small intestinal sections and for the entire colon. Following fixation, each tumor was measured to the nearest tenth millimeter using an eyepiece reticule at 10x magnification on a dissecting microscope. Two measurements were taken for each tumor. The longest dimension parallel to the epithelium was measured first, followed by a second measurement, also parallel to the epithelium, but perpendicular to the first measurement.

**Biochemical Assays.** Blood was obtained from the retro-orbital sinus after the animals had been on diet for 21-days and by cardiac puncture at sacrifice. Serum 25(OH)D<sub>3</sub> levels were measured using HPLC. Serum calcium was measured by atomic absorption spectrometry on the ABX Pentra clinical chemistry analyzer (Horiba ABX, France)<sup>22</sup>.

**Statistical Methods.** Significant sex differences were observed in the multiplicities of small intestinal and colonic tumors, as described previously for the Pirc rat<sup>3</sup>. Therefore, data from male and female rats were analyzed separately. A 2-sided Jonckheere-Terpstra test was employed to test for a trend in tumor multiplicity, tumor size, or serum values across the 25(OH)D<sub>3</sub> dose series. A 2-sided Wilcoxon rank sum test with Bonferonni correction was used to test for a difference between each of the serum measurements. A 2-sided Kendall's rank correlation test was used to test for an association between tumor multiplicity and each of the serum measurements. Longitudinal analysis of endoscopic images utilized a chi-square test of growing versus non-growing tumors. For each of the tests, a p-value  $\leq 0.05$  was considered significant.

## **Results**

**Serum Calcium and 25(OH)D<sub>3</sub> Levels in 25(OH)D<sub>3</sub>-Supplemented Pirc Rats.** Between 8 and 10 serum samples were analyzed for blood calcium levels per 25(OH)D<sub>3</sub> dietary dose (six total groups, including the vehicle diet group). Serum calcium levels did not differ between females and males; therefore these values were combined for both sexes within each dose group. Serum calcium was increased in a dose-dependent manner in animals supplemented with any one of the 25(OH)D<sub>3</sub> diets compared to controls ( $p < 0.00001$ , Table 4-1). A 2 mg increase in serum calcium is considered hypercalcemic, and only the highest dose group exceeded this level. This increase in serum calcium may explain why female and male rats given the highest dose of 25(OH)D<sub>3</sub> gained significantly less weight than animals in the other treatment groups (Fig 4-1). However, we found no direct correlation between serum calcium and tumor multiplicity, indicating that the change in tumor multiplicity was not directly caused by the change in serum calcium (Kendall's rank correlation test, females  $p = 0.1361$ , males  $p = 0.6725$ ).

A total of four serum samples were analyzed for blood 25(OH)D<sub>3</sub> levels per 25(OH)D<sub>3</sub> dietary dose. Surprisingly, although serum calcium showed a correlation with 25(OH)D<sub>3</sub> dose, 25(OH)D<sub>3</sub> serum measures did not. Although rats given doses of 25(OH)D<sub>3</sub> between 60  $\mu\text{g}$  and 1500  $\mu\text{g}$  had serum 25(OH)D<sub>3</sub> levels about 4-6 times higher than rats given vehicle diet, none of these 25(OH)D<sub>3</sub>-supplemented diets significantly differed from one another. However, rats given the highest 25(OH)D<sub>3</sub> dose had serum 25(OH)D<sub>3</sub> levels about 10 times that of rats given vehicle diet. This lack of a dose-dependent response in serum 25(OH)D<sub>3</sub> measures may indicate that other components in the vitamin D metabolic pathway, particularly enzymes involved in detoxification and clearance, may be altered upon supplementation with 25(OH)D<sub>3</sub>.

**Table 4-1.** Terminal serum calcium and 25(OH)D<sub>3</sub> measurements. A 2-sided Wilcoxon rank sum test was employed to test for a difference between each of the test diets and the vehicle only group. P-values shown are Bonferonni-corrected; a p-value ≤ 0.05 was considered significant. To test for a dose-response relationship, the Jonckheere-Terpstra test was used. A P<sub>Trend</sub> ≤ 0.05 was considered significant.

Serum Component	25(OH)D <sub>3</sub> diet (µg/kg body weight/day)	N of animals	Serum level (mean ± SD)	P-value (vs. Vehicle)	P <sub>Trend</sub>
A. Calcium	0 µg (Vehicle)	9	11.5 ± 0.1		
	60 µg	10	12.2 ± 0.1	0.003	
	170 µg	10	12.7 ± 0.1	0.0005	
	500 µg	8	13.0 ± 0.3	0.0016	
	1500 µg	8	13.1 ± 0.2	0.0012	
	4500 µg	9	13.8 ± 0.3	0.0004	<0.000001
B. 25(OH)D <sub>3</sub>	0 µg (Vehicle)	8	36.5 ± 17.4		
	60 µg	4	114.8 ± 11.1	0.0110	
	170 µg	4	105.9 ± 11.8	0.0110	
	500 µg	4	119.2 ± 14.9	0.0110	
	1500 µg	4	88.1 ± 10.3	0.0110	
	4500 µg	4	239.9 ± 45.2	0.0222	0.00015

**Small Intestinal Tumor Multiplicity in 25(OH)D<sub>3</sub>-Supplemented Pirc Rats.** Control rats were fed either breeder chow or vehicle diet; no difference in small intestinal tumor multiplicity was seen in male (p=0.27) or female (p=0.11) animals between these two diets. Therefore, the two diets were combined for all analysis involving tumor multiplicity in the small intestine. A reduction in the number of tumors in the small intestine was seen for both female (P<sub>Trend</sub> < 0.007) and male (P<sub>Trend</sub> < 0.045) Pirc rats with increasing doses of 25(OH)D<sub>3</sub> (Fig 4-2, Table 4-2). On average, rats on vehicle diet had three- to four-fold more small intestinal tumors compared with rats given the highest dose of 25(OH)D<sub>3</sub>. However, female and male rats given the highest dose of 25(OH)D<sub>3</sub> were considered hypercalcemic during the study (Table 4-1). When the highest dose group is excluded, there is no longer a statistically significant trend for reduced small intestinal tumor multiplicity with 25(OH)D<sub>3</sub> dose (P<sub>Trend</sub> = 0.77 for females and 0.40 for males).

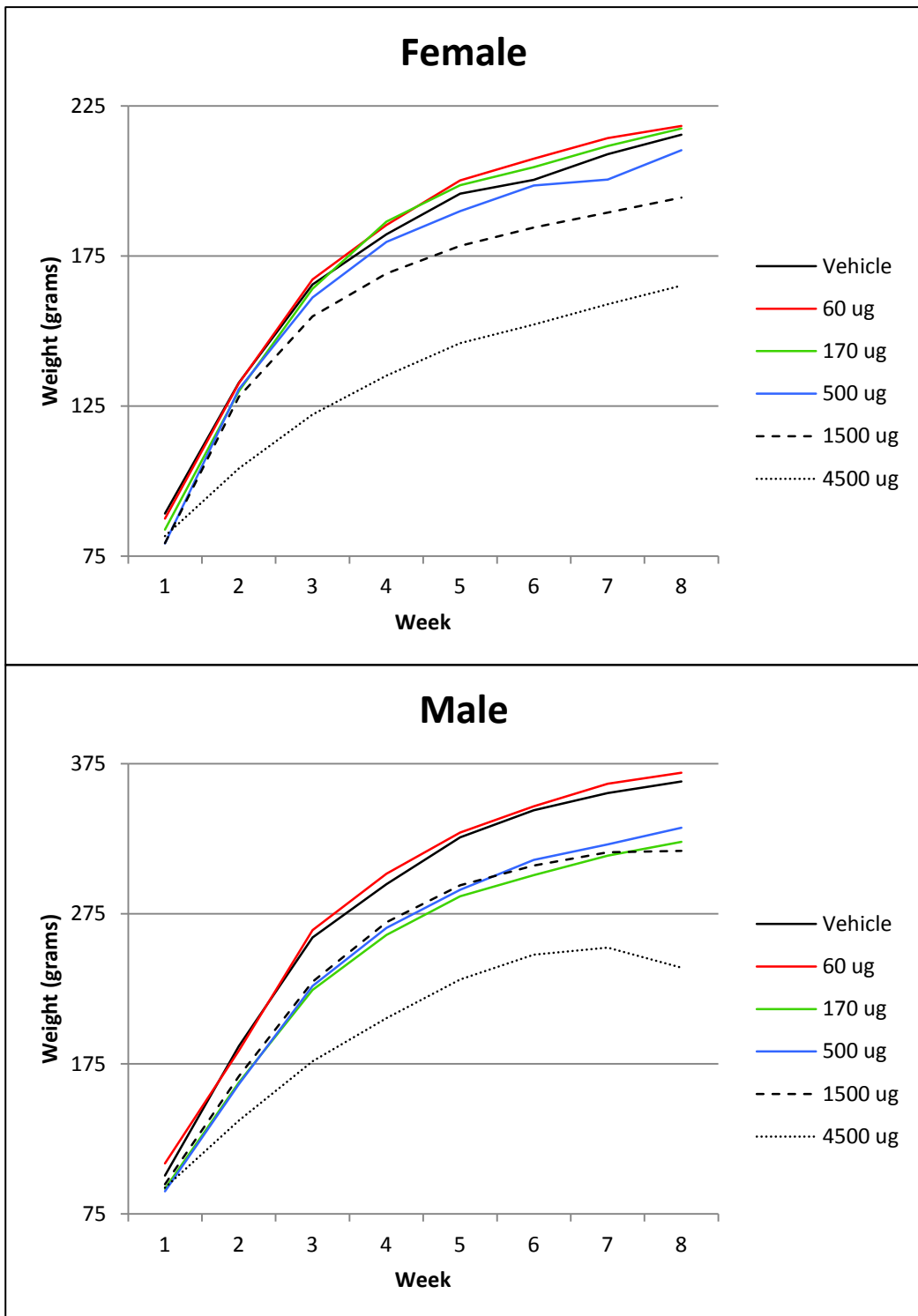


Though for both females and males, on average every 25(OH)D<sub>3</sub> -supplemented group had fewer small intestinal tumors than control rats.

**Colonic Tumor Multiplicity in 25(OH)D<sub>3</sub>-Supplemented Pirc Rats.** Control rats were fed either breeder chow or vehicle diet; no difference in colonic tumor multiplicity was seen in male ( $p=0.83$ ) or female ( $p=0.30$ ) animals between these two diets. Therefore, the two diets were combined for all analysis involving tumor multiplicity in the colon as well. An increase in the number of colonic tumors with increasing doses of 25(OH)D<sub>3</sub> was seen for both female ( $P_{\text{Trend}} < 0.0005$ ) and male ( $P_{\text{Trend}} < 0.009$ ) Pirc rats (Fig 4-2, Table 4-2). On average, rats given the highest dose of 25(OH)D<sub>3</sub> had up to three-fold more colonic tumors compared with rats on vehicle diet. However, female and male rats given the highest dose of 25(OH)D<sub>3</sub> were considered hypercalcemic during the study (Table 4-1). When the highest dose group is excluded, the dose-dependent enhancement of colonic tumor multiplicity by 25(OH)D<sub>3</sub> remained significant in both female ( $P_{\text{Trend}} < 0.032$ ) and male ( $P_{\text{Trend}} < 0.009$ ) rats. The only supplemented group that had, on average, fewer colonic tumors than vehicle-treated animals were the male rats given the lowest dose (60  $\mu\text{g}$ ) of 25(OH)D<sub>3</sub>, but this was not statistically significant ( $p < 0.66$ , 2-sided Wilcoxon rank sum test).

**Growth Profile Analysis of Colonic Tumors in 25(OH)D<sub>3</sub>-Supplemented Pirc Rats.** Rats underwent endoscopy every other week starting before diet randomization until sacrifice. Tumors were judged to have grown, become static, or regressed during the study based on review of archived endoscopy videos and still images. Only tumors from female rats were evaluated for

**Fig 4-1.** Longitudinal Weights. Weights were obtained at each colonoscopy visit. Both male and female rats given the highest dose (4500  $\mu\text{g}$ ) of 25(OH) $\text{D}_3$  gained significantly less weight over the course of the study. Plausibly, this was caused by their hypercalcemic status (see Table 4-1).



longitudinal growth patterns; male rats develop a large number of tumors that become difficult to annotate accurately between endoscopic visits.

Of a total 221 scorable tumors, 172 grew, 42 were static, and 7 regressed (Fig 4-3). Based on scoring by three blinded observers, no difference in the number of growing versus non-growing tumors was found between animals given breeder chow and those given vehicle diet ( $p=0.85$ ); therefore, these groups were combined into one control group for further analysis against the supplemented groups.

Female rats in the 60  $\mu\text{g}$  and 170  $\mu\text{g}$  25(OH) $\text{D}_3$  dose groups showed a significantly different number of growing tumors compared to control animals; however these differences were in opposite directions. Female rats in the 60  $\mu\text{g}$  25(OH) $\text{D}_3$  dose group showed a decrease in the number of growing tumors compared to controls ( $p=0.01$ ), while those in the 170  $\mu\text{g}$  25(OH) $\text{D}_3$  dose group showed a highly significant increase in the number of growing tumors ( $p<0.0001$ ). All other doses were not significantly different from controls.

**Sizing of Colonic Tumors in 25(OH) $\text{D}_3$ -Supplemented Pirc Rats.** Following formalin fixation, two perpendicular measurements were obtained for each colonic tumor. Although tumor multiplicity did not differ between Pirc rats given breeder chow and those given the vehicle diet, tumor size was significantly greater in male ( $p=0.05$ ) and female ( $p=0.028$ ) rats given breeder chow (2-sided Wilcoxon rank sum test). Therefore, only rats fed the vehicle diet were included for further analysis regarding tumor size. Multiplying the two perpendicular measurements, we found that there was a statistically significant association between increased 25(OH) $\text{D}_3$  dose and

**Fig 4-2.** A dose-response relationship was found between a statistically-significant decrease in small intestinal tumor multiplicity with increasing 25(OH)D<sub>3</sub> dose (top boxes). By contrast, colonic tumors significantly increased with increasing 25(OH)D<sub>3</sub> dose (bottom boxes). This was true for both female (left boxes) and male (right boxes) Pirc rats.

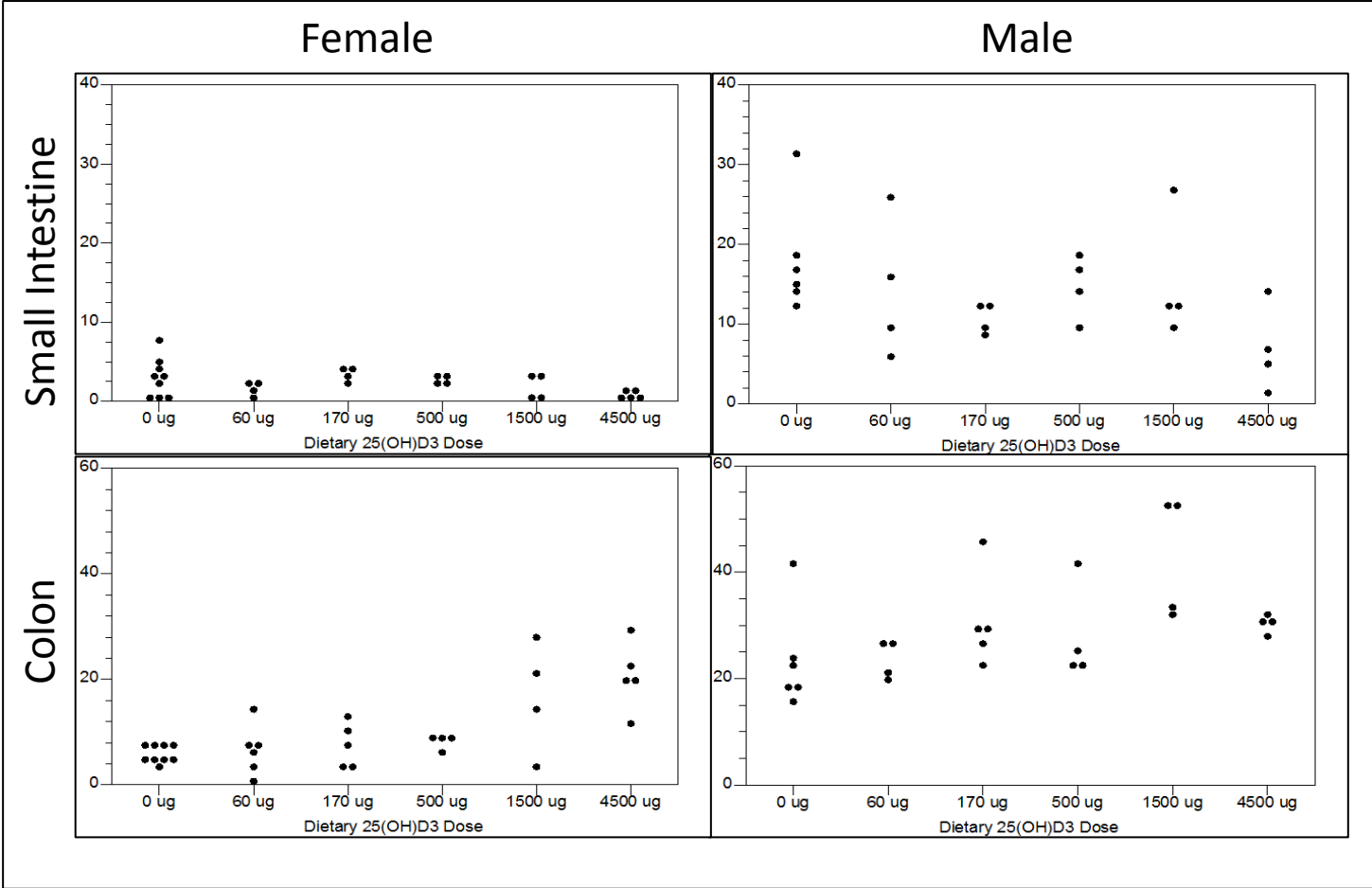
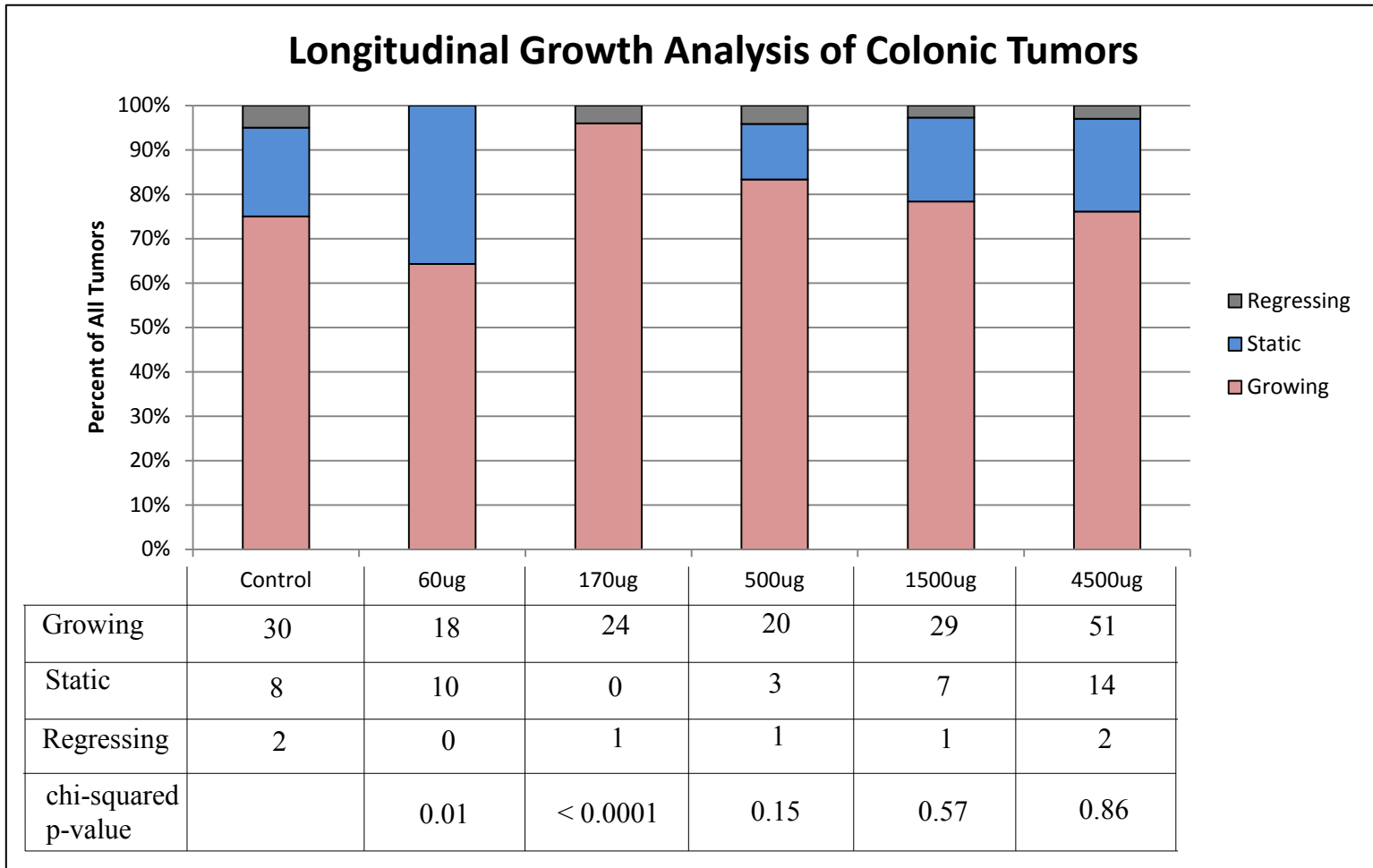


**Fig 4-3.** Tumors were classified as growing, static or regressing over the study period as judged by longitudinal endoscopy. The number of tumors in each category for each dose is shown below in the table. A chi-squared test of growing versus non-growing (static + regressing) tumors between the respective dose and controls was employed. A p-value  $\leq 0.05$  was considered significant.



decreased tumor size in male ( $p_{\text{Trend}} < 0.029$ ) but not female Pirr rats ( $p_{\text{Trend}} = 0.144$ ). However, when the highest dose of 25(OH)D<sub>3</sub> was discounted, any association between 25(OH)D<sub>3</sub> dose and tumor size disappears. The same trends were apparent when only the maximum tumor diameter was used.

**Table 4-2.** Tumor multiplicity in the small intestine and colon. Both male and female rats show a statistically significant trend for a decrease in small intestinal tumor multiplicity and an increase in colonic tumor multiplicity with increasing 25(OH)D<sub>3</sub> dose.

25(OH)D <sub>3</sub> diet (µg/kg body weight/day)	n (females, males)	Tumor multiplicity (mean ± SD)			
		Small intestine		Colon	
		Female	Male	Female	Male
Vehicle	9, 6	4.2 ± 2.4	20.3 ± 7.5	6.2 ± 1.1	25.5 ± 10.5
60	6, 4	1.3 ± 1.0	14.5 ± 8.7	6.7 ± 4.5	23.4 ± 3.8
170	5, 5	3.3 ± 1.0	10.8 ± 1.5	7.6 ± 4.2	30.8 ± 8.9
500	4, 4	2.5 ± 0.6	15.0 ± 3.9	8.3 ± 1.5	28.0 ± 9.4
1500	4, 4	1.5 ± 1.7	15.3 ± 7.9	16.5 ± 10.7	42.5 ± 11.0
4500	5, 4	0.4 ± 0.5	6.8 ± 5.4	20.6 ± 6.1	30.5 ± 1.7
<b>P<sub>Trend</sub></b>		<b>0.006234</b>	<b>0.04497</b>	<b>0.000429</b>	<b>0.008851</b>

## Discussion

Utilizing a vitamin D-sufficient rat model of familial colon cancer, this study was specifically designed to test the effects of 25(OH)D<sub>3</sub>-supplementation on three different measures of tumor development: multiplicity, size, and growth rate. In each of the 25(OH)D<sub>3</sub> doses tested, the colonic tumor multiplicity was higher than for control animals, in both male and female Pirr rats. No suppression of tumor emergence was detected. Instead, a significant trend for increased tumor multiplicity with increasing 25(OH)D<sub>3</sub> dose was found. By contrast, small intestinal tumor multiplicity did decrease with increasing doses of 25(OH)D<sub>3</sub> in both male and female Pirr

rats. This finding may explain experimental data showing the effectiveness of vitamin D against tumors arising in mouse models, where the majority of the tumor burden occurs in the small intestine. Our study highlights the important difference between tumors of the small intestine and those of the colon, and emphasizes the care that must be taken when applying findings in the small intestine to the colon.

Effects of vitamin D on tumor initiation, often detected as multiplicity, and tumor size or growth may be independent. Though in our study tumor multiplicity increased with increasing 25(OH)D<sub>3</sub> dose, the size of tumors in the colon decreased with increasing 25(OH)D<sub>3</sub> dose. However, this was mostly attributable to the highest dose group. Similarly, when *Apc*<sup>Min/+</sup>*VDR*<sup>-/-</sup> mice were studied over a period up to 7 months, there was no effect of loss of the vitamin D receptor on tumor multiplicity, but tumor size increased significantly<sup>32</sup>. It should not be assumed that tumor multiplicity and size are always proportional. As individual indicators of tumor status, they each give insight into different stages of tumor development.

The longitudinal growth profile of a tumor may offer further insights into the effects of vitamin D at various steps during tumor development and progression. Although we found that tumor size decreased with increasing 25(OH)D<sub>3</sub> dose, only the 170 µg 25(OH)D<sub>3</sub> dose showed a significant increase in the percent of growing tumors compared with control animals. After correcting for testing of multiple dose groups, none of the 25(OH)D<sub>3</sub> groups had significantly altered tumor growth potential. Further research using quantitative measures of tumor size are needed to better understand the role of 25(OH)D<sub>3</sub> during each stage of the tumor development process.

Emerging evidence in human patients shows that the majority of early adenomas in the colon do not grow, and a subset even spontaneously regress<sup>23</sup>. It is possible that tumors in pa-

tients with higher serum vitamin D levels encounter greater growth inhibition. Indeed, combination therapy using a traditional chemotherapeutic in conjunction with vitamin D has been shown to be more effective than the therapeutic compound alone<sup>19,20</sup>. This growth inhibition could in turn lead to a greater likelihood that these tumors can be overcome by traditional chemotherapeutics or the patient's own natural defense systems. In human association studies relying on end-point endoscopy, an impact on tumor growth may not be detected. Importantly, more research is warranted to determine whether vitamin D is a viable treatment option for patients with advanced cancer, or whether it may exacerbate the disease.

As the role of vitamin D may differ depending on tumor stage, it may also play different roles depending on the dose. High doses of 25(OH)D<sub>3</sub> may alter the expression of various enzymes and receptors in the vitamin D pathway that low doses may not affect. In turn, these changes could affect the development and progression of tumors. Indeed, vitamin D receptor (VDR) expression has been shown to spontaneously decrease over time in both human and rat colonic tumors. Effects of high dose supplementation on components of this pathway may also occur in normal intestinal tissue. When colorectal adenoma patients were treated with vitamin D<sub>3</sub>, the ratio of APC protein to  $\beta$ -catenin protein increased 31% in the upper 40% of crypts<sup>1</sup>. While an increase in APC and decrease in  $\beta$ -catenin activity in normal mucosa appears to occur with standard doses of vitamin D supplementation, higher doses of vitamin D may have a different effect. *Apc*<sup>Min/+</sup> mice lacking the vitamin D receptor have higher levels of  $\beta$ -catenin in normal intestinal tissues than *Apc*<sup>Min/+</sup> mice expressing VDR<sup>32</sup>. However, in an AOM/DSS mouse model, increasing doses of vitamin D<sub>3</sub>, a compound upstream of 25(OH)D<sub>3</sub>, did not appear to alter VDR levels<sup>13</sup>. To our knowledge, it is not known what effect 25(OH)D<sub>3</sub> supplementation



may have on components of the Wnt pathway in normal or tumor tissue of the colon, or whether differences exist between low dose and high dose supplementation on these measurements.

In humans, an individual is considered vitamin D deficient when their serum 25(OH)D<sub>3</sub> level drops below 20 ng/ml. A study of the National Health and Nutrition Examination Survey (NHANES) found that about 1 in 4 individuals is deficient for vitamin D<sup>31</sup>. However, they also showed that although multi-vitamin supplementation use has increased in adults, it has not translated to an overall increase in serum 25(OH)D concentrations<sup>31</sup>. Recently, there has been a call by some groups to increase the recommended daily allowance (RDA) of vitamin D both because of the high proportion of individuals defined as deficient and the evidence supporting associations between vitamin D and various disease states. In 2010 the Institute of Medicine (IOM) conducted an exhaustive review of the literature to determine whether an increase in the RDA was warranted. The IOM decided against increasing the RDA, citing data showing that average blood levels of vitamin D are indeed above 20 ng/ml and emerging evidence suggesting that too much vitamin D may be harmful<sup>14</sup>.

Any role for vitamin D on colon cancer risk is likely to be highly complex, depending on a multitude of factors, both within the tumor and surrounding normal colonic tissue, the vitamin D compound used, and the dose and timing at which it is given. Just as human studies are not always in agreement, various rodent models show conflicting evidence regarding vitamin D. However, the etiology of the tumors being studied in these models should not be discounted. The Pirc rat is a model for familial colon cancer, where one allele of the *Apc* gene is mutated and not expressed. However, the Pirc rat is also a model for sporadic colon cancer as over 80% of the tumors in humans also possess mutations in *Apc*<sup>10</sup>. Other studies have used environmentally induced cancer models, by Western diet or carcinogens such as AOM. While results from these

studies may appear to conflict with those utilizing models of genetically induced cancer, there may be a resolution to this apparent discordance. In genetically induced models, supplemental vitamin D may decrease the expression of enzymes in the vitamin D pathway. In particular, it is known that VDR can bind  $\beta$ -catenin, and thus loss of VDR can allow  $\beta$ -catenin levels to increase<sup>25</sup>. This could exacerbate the tumor phenotype in *Apc* models of colon cancer. By contrast, in environmentally induced models, vitamin D may be acting to increase apoptosis, thereby eliminating cells that may have otherwise become cancerous.

Differences in metabolism and the effect on cancer initiation and progression may also exist between 25(OH)D<sub>3</sub> and vitamin D<sub>3</sub>. Vitamin D<sub>3</sub> is biologically inactive and must be converted first by CYP27A1 to the 25-hydroxy form and then by CYP27B1 to the active 1,25-dihydroxy hormone<sup>8</sup>. It is known that this final activation step can take place in almost any tissue in the body, including the colon. Therefore, it is not necessarily required that vitamin D<sub>3</sub> be metabolized elsewhere after being absorbed from the diet into the gut. These two compounds may act differently to affect processes in the vitamin D pathway. In an animal model of breast cancer, Krishnan *et al.* recently showed that vitamin D<sub>3</sub> possesses the same anticancer benefit as the active hormone 1,25(OH)<sub>2</sub>D<sub>3</sub>, but 1,25(OH)<sub>2</sub>D<sub>3</sub> caused the animals to become hypercalcemic while vitamin D<sub>3</sub> did not<sup>17</sup>. Further, they demonstrated that CYP27B1 expression within the tumors changed only with vitamin D<sub>3</sub> but not 1,25(OH)<sub>2</sub>D<sub>3</sub> supplementation. They also suggest that vitamin D metabolism could be different in tumor-free versus tumor-bearing individuals. This is a potential confounder that can be addressed by studies of the effects of vitamin D for preventing polyp formation in the general population versus recurrence or treatment of patients with existing tumors.

Human supplements generally contain vitamin D<sub>3</sub>, but the level of 25(OH)D<sub>3</sub> in serum is regarded as an excellent biomarker to assess an individual's vitamin D status. It is plausible that differences in metabolism of these two compounds could explain why many association studies examining serum 25(OH)D<sub>3</sub> levels find a correlation with tumor development, while supplementation trials with vitamin D<sub>3</sub> often fail to show the same effects. Clearly, much more research is needed to understand how each of these compounds affects both normal colonic tissue and tumors, and the vitamin D pathway and its associated enzymes in both tumor-free and tumor-bearing individuals.

Clear benefits of supplementation exist for those deficient in essential nutrients or unable to metabolize these nutrients on their own. By contrast, two crucial points should be considered when determining whether healthy individuals should take supplements to potentially reduce the risk of some diseases. First, when an association is first found between the incidence of a particular disease and some dietary factor, it is generally just that: a diet or lifestyle that reduces risk. For example, the Mediterranean Diet, where the consumption of fish is high, has led to the widespread use of fish oil supplements to prevent disease. However, we must also consider the other macro- and micronutrients that come with eating whole fish, and how those could add to or even act synergistically with the fish oil supplement. Second, we must consider dose. Being deficient in a particular nutrient may be deleterious, and taking a supplement to become "sufficient" may be beneficial, but this does not imply that taking higher doses is even better. To the contrary, there is emerging evidence for many supplements that either show a detriment at higher doses or a susceptibility to particular disease states. Omega-3 fatty acids represent one recent example. Some studies suggest that omega-3 fatty acids may protect against heart disease and rheumatoid

arthritis, but Brasky and colleagues have now shown that high blood concentrations of plasma phospholipid omega-3s are associated with an increased risk for prostate cancer<sup>6</sup>.

It is clear that our understanding of the interactions between vitamin D compounds and normal and tumor tissue of the colon is in its infancy. The original observation that increased UV exposure was associated with decreased rates of colon cancer and mortality of colon cancer should be revisited. While association studies show that higher serum vitamin D levels do translate to lower risk for cancer development, this may not be the entire story. Distilled down to a single element, vitamin D supplementation may not offer the same benefits provided by a lifestyle with higher vitamin D exposure, both through sunlight and diet. Crucially, a better understanding is necessary for which compound to supplement with, at what dose, and during what stage. In going forward, the results from our study offer a basis for further investigation of 25(OH)D<sub>3</sub> and vitamin D<sub>3</sub> on each of the components in the pathway to tumorigenesis.

## References

1. **Ahearn TU, McCullough ML, Flanders WD, Long Q, Sidelnikov E, Fedirko V, Daniel CR, Rutherford RE, Shaukat A, Bostick RM.** 2011. A randomized clinical trial of the effects of supplemental calcium and vitamin D3 on markers of their metabolism in normal mucosa of colorectal adenoma patients. *Cancer Research*. **71**:413–23.
2. **American Cancer Society.** 2013. Colorectal Cancer Facts & Figures 2011-2013.
3. **Amos-Landgraf JM, Kwong LN, Kendzierski CM, Reichelderfer M, Torrealba J, Weichert J, Haag JD, Chen K-S, Waller JL, Gould MN, et al.** 2007. A target-selected Apc-mutant rat kindred enhances the modeling of familial human colon cancer. *Proceedings of the National Academy of Sciences USA*. **104**:4036–41.
4. **Bashir O, FitzGerald AJ, Goodlad RA.** 2004. Both suboptimal and elevated vitamin intake increase intestinal neoplasia and alter crypt fission in the ApcMin/+ mouse. *Carcinogenesis*. **25**:1507–15.
5. **Becklund BR, Severson KS, Vang SV, DeLuca HF.** 2010. UV radiation suppresses experimental autoimmune encephalomyelitis independent of vitamin D production. *Proceedings of the National Academy of Sciences USA*. **107**:6418–23.
6. **Brasky TM, Darke AK, Song X, Tangen CM, Goodman PJ, Thompson IM, Meyskens FL, Goodman GE, Minasian LM, Parnes HL, et al.** 2013. Plasma phospholipid fatty acids and prostate cancer risk in the SELECT trial. *Journal of the National Cancer Institute*. **105**:1132–41.
7. **Brehier A, Thomasset M.** 1988. Human colon cell line HT-29: Characterisation of 1,25-dihydroxyvitamin D3 receptor and induction of differentiation by the hormone. *Journal of Steroid Biochemistry*. **29**:265–270.
8. **DeLuca HF.** 2008. Evolution of our understanding of vitamin D. *Nutrition Reviews*. **66**:S73–87.
9. **Díaz GD, Paraskeva C, Thomas MG, Binderup L, Hague A.** 2000. Apoptosis is induced by the active metabolite of vitamin D3 and its analogue EB1089 in colorectal adenoma and carcinoma cells: possible implications for prevention and therapy. *Cancer Research*. **60**: 2304-12.
10. **Fearnhead N, Britton M, Bodmer W.** 2001. The ABC of Apc. *Human Molecular Genetics*. **10**:721–733.
11. **Garland CF, Garland FC.** 1980. Do sunlight and vitamin D reduce the likelihood of colon cancer? *International Journal of Epidemiology*. **9**:227–231.

12. **Hong SN, Kim JH, Choe WH, Lee S-Y, Seol DC, Moon H-W, Hur M, Yun Y-M, Sung IK, Park HS, et al.** 2012. Circulating vitamin D and colorectal adenoma in asymptomatic average-risk individuals who underwent first screening colonoscopy: a case-control study. *Digestive Diseases and Sciences*. **57**:753–63.
13. **Hummel DM, Thiem U, Höbaus J, Mesteri I, Gober L, Stremnitzer C, Grac J, Obermayer-pietsch B, Kallay E.** 2012. Prevention of preneoplastic lesions by dietary vitamin D in a mouse model of colorectal carcinogenesis. *Journal of Steroid Biochemistry and Molecular Biology*. **136**:284-88.
14. **Institute of Medicine.** 2010. Dietary Reference Intakes for Calcium and Vitamin D.
15. **Irving AA, Halberg RB, Albrecht DM, Plum LA, Krentz KJ, Clipson L, Drinkwater N, Amos-Landgraf JM, Dove WF, DeLuca HF.** 2011. Supplementation by vitamin D compounds does not affect colonic tumor development in vitamin D sufficient murine models. *Archives of Biochemistry and Biophysics*. **515**:64–71.
16. **Jones S, Chen W-D, Parmigiani G, Diehl F, Beerenwinkel N, Antal T, Traulsen A, Nowak M a, Siegel C, Velculescu VE, et al.** 2008. Comparative lesion sequencing provides insights into tumor evolution. *Proceedings of the National Academy of Sciences USA*. **105**:4283–8.
17. **Krishnan A V, Swami S, Feldman D.** 2013. Equivalent anticancer activities of dietary vitamin D and calcitriol in an animal model of breast cancer: Important of mammary CYP27B1 for treatment and prevention. *Journal of Steroid Biochemistry and Molecular Biology*. **136**: 289-95.
18. **Lointier P, Wargovich M, Saez S, Levin B, Wildrick D, Boman B.** 1987. The role of vitamin D3 in the proliferation of a human colon cancer cell line in vitro. *Anticancer Research*. **7**:817–22.
19. **Milczarek M, Psurski M, Kutner A, Wietrzyk J.** 2013. Vitamin D analogs enhance the anticancer activity of 5-fluorouracil in an in vivo mouse colon cancer model. *BMC Cancer*. **13**:294.
20. **Milczarek M, Rosinska S, Psurski M, Maciejewska M, Kutner A, Wietrzyk J.** 2013. Combined colonic cancer treatment with vitamin D analogs and irinotecan or oxaliplatin. *Anticancer research*. **33**:433–44.
21. **Mulholland HG, Murray LJ, Anderson LA, Cantwell MM.** 2011. Vitamin D, calcium and dairy intake, and risk of oesophageal adenocarcinoma and its precursor conditions. *The British Journal of Nutrition*. **106**:732–41.
22. **Nieves NJ, Ahrens JM, Plum L a, DeLuca HF, Clagett-Dame M.** 2010. Identification of a unique subset of 2-methylene-19-nor analogs of vitamin D with comedolytic activity in the rhino mouse. *The Journal of Investigative Dermatology*. **130**:2359–67.

23. **Pickhardt PJ, Kim DH, Pooler BD, Hinshaw JL, Barlow D, Jensen D, Reichelderfer M, Cash BD.** 2013. Assessment of volumetric growth rates of small colorectal polyps with CT colonography: a longitudinal study of natural history. *The Lancet Oncology*. **14**:711–20.
24. **Shabahang M, Buras RR, Davoodi F, Schumaker LM, Nauta RJ, Evans SRT.** 1993. 1,25-dihydroxyvitamin D<sub>3</sub> receptor as a marker of human colon carcinoma cell line differentiation and growth inhibition. *Cancer Research*. **53**:3712–3718.
25. **Shah S, Islam MN, Dakshanamurthy S, Rizvi I, Rao M, Herrell R, Zinser G, Valrance M, Aranda A, Moras D, et al.** 2006. The molecular basis of vitamin D receptor and beta-catenin crossregulation. *Molecular Cell*. **21**:799–809.
26. **Takahashi R, Mizoue T, Otake T, Fukumoto J, Tajima O, Tabata S, Abe H, Ohnaka K, Kono S.** 2010. Circulating vitamin D and colorectal adenomas in Japanese men. *Cancer Science*. **101**:1695–1700.
27. **Trivedi DP, Doll R, Khaw KT.** 2003. Effect of four monthly oral vitamin D<sub>3</sub> supplementation on fractures and mortality in men and women living in the community: randomised double blind controlled trial. *British Medical Journal*. **326**:1–6.
28. **Wactawski-Wende J, Ph D, Kotchen JM, Anderson GL, Assaf AR, Brunner RL, Sullivan MJO, Margolis KL, Ockene JK, Phillips L, et al.** 2006. Calcium plus vitamin D supplementation and the risk of colorectal cancer. *New England Journal of Medicine*. **7**:684-96.
29. **Washington MK, Powell AE, Sullivan R, Sundberg J, Wright N, Coffey RJ, Dove WF.** 2013. Pathology of rodent models of intestinal cancer: progress report and recommendations. *Gastroenterology*. **4**:705-17.
30. **Wu K, Feskanich D, Fuchs CS, Willett WC, Hollis BW, Giovannucci EL.** 2007. A nested case – control study of plasma 25-hydroxyvitamin D concentrations and risk of colorectal cancer. *Cancer*. **14**:1120-29.
31. **Yetley EA.** 2008. Assessing the vitamin D status of the US population. *The American Journal of Clinical Nutrition*. **88**:558S–564S.
32. **Zheng W, Wong K, Zhang Z, Dougherty U, Mustafi R, Kong J, Deb D, Zheng H, Bissonnette M, Li Y.** 2013. Inactivation of the vitamin D receptor in *ApcMin/+* mice reveals a critical role for the vitamin D receptor in intestinal tumor growth. *International Journal of Cancer*. **130**:10–19.

## Chapter 5

### **A simple, quantitative method to determine rat colonic tumor volume *in vivo* using alginate gel**

Amy A. Irving supervised and performed the majority of the experiments, completed all of the data analysis and wrote the final manuscript. Lindsay B. Young, Madeline R. Ford and James M. Amos-Landgraf each assisted with portions of the rat experiments. Jennifer K. Pleiman and Lindsay B. Young performed all of the mouse experiments. As part of the Biomedical Engineering Design Curriculum, Michael J. Konrath, Blake Marzella, Michael Nonte, and Justin Cacciatore, under the advisement of Amit Nimunkar, designed the original alginate molding and dental stone casting methods, and created the pegs to perform the control experiments. Linda Clipson created and edited the figures. Norman Drinkwater gave statistical advice. Alexandra Shedlovsky and Kevin Eliceiri provided critical reading of the manuscript. James M. Amos-Landgraf offered technical and intellectual support throughout the project. William F. Dove served as an advisor.

*This chapter has been modified from its original publication in Comparative Medicine. Permission to use this copyrighted material was obtained from AALAS on 1/6/14.*

*Irving AA, Young LB, Pleiman JK, Konrath MJ, Marzella B, Nonte M, Cacciatore J, Ford MR, Clipson L, Amos-Landgraf JM, Dove WF. A simple, quantitative method to determine rat colonic tumor volume in vivo using alginate gel. Comparative Medicine. In Press.*



## **Abstract**

Many studies of the response of colonic tumors to therapeutics use tumor multiplicity as the endpoint to determine effectiveness of the agent. These studies can be greatly enhanced by accurate tumor volume measurements. Existing methods for measuring the size of colonic tumors often require the animal to be given antiperistaltic agents and be anesthetized for extensive periods. Additionally, costly equipment and complex analytical software often require shared resources, where pathogen status may limit the transfer of animals between facilities.

In this report, we present a quantitative method to easily and accurately determine colonic tumor volume. This approach utilizes a biocompatible alginate to create a negative mold of a tumor-bearing colon, followed by making dental stone positive casts that replicate the shape of each original tumor. The weight of dental stone casts correlate to a high degree with the weight of the dissected tumors ( $R^2= 0.93$ ). After refinement of the technique, overall tumor volume error was  $16.9\% \pm 7.9\%$ , which includes error from both the alginate and dental stone methods. Tumor volumes ranging in size from  $4\text{mm}^3$  to  $196\text{mm}^3$  have been successfully determined with this method.

Alginate molding combined with dental stone casting is a facile method to determine tumor volume *in vivo* without the need of costly equipment or knowledge of analytic software. This broadly accessible method also creates the opportunity to objectively study colonic tumors over time in the living animal in conjunction with other experiments being performed, without transferring the animals from the facility where they are maintained.

## **Introduction**

Colon cancer is the third leading cause of cancer in men and women, with over 100,000 new cases diagnosed each year in the US alone. This disease is not limited to humans – cancers of the colon and rectum also affect companion species, such as dogs, albeit less frequently than in humans<sup>17</sup>. The high rate of survival of cancers detected early demonstrates the need to better understand tumor growth dynamics in models of the disease.

Sizing of tumors creates an additional dimension beyond studies examining tumor multiplicity alone. Terminal sizing of tumors uses an eyepiece reticule under a dissection microscope to measure the maximum diameter of each tumor. However, this method likely misrepresents tumor volume for several reasons. First, tumors are often not symmetrically shaped, limiting interpretation of even multiple linear measurements. Where volume calculations rely on the use of a standard formula, the irregular shape of solid tumors may require the testing of many different formulas to find the optimal one for that particular measurement and model<sup>8</sup>. Second, if tumor sizing occurs post-fixation, the original shape of the tumor may be distorted. If instead tumor sizing occurs before fixation, the added time to size the tumors may result in degradation of the intestinal tissue, limiting further analysis. An alternate method of tumor sizing involves using the surrogate of tumor weight, the current ‘gold standard’ for terminal studies. Tumor weight does correlate closely with tumor size, though the density of tumors may not all be the same and this technique is limited to use at the terminal time point only. Methods that determine true tumor volume are powerful; those that can be applied *in vivo* to study the tumor longitudinally are even more compelling.

It has been recently recognized that not all early colonic tumors grow; some remain static for years while a few spontaneously regress<sup>20</sup>. Importantly, it appears that the early growth profile of a tumor may correlate with its eventual fate<sup>20</sup>. This aspect of tumor biology is a newly emerging area that deserves deeper study. The current ‘gold standard’ for determining longitudinal tumor volume is computed tomography (CT), as tumor weight is available only in terminal experiments. In the mouse, microCT colonography can be used to detect a 16% change in tumor volume in the living animal with 95% confidence<sup>5</sup>. However, the cost of CT equipment limits this technology to shared facilities and the pathogen status of these facilities may allow only for one-way transfer of animals, limiting longitudinal study. Importantly, many institutions do not have access to microCT technology, and even if available, 3D renderings must be recreated to determine tumor volume, a process requiring specialized software and detailed computing knowledge. Further, CT exposes the animal to radiation, which may interfere with the tumor biology. Magnetic resonance imaging (MRI) can also accurately determine tumor volume and does not use radiation, but specialized scanners and software are still required, and enemas or intravenous treatments are needed to accurately visualize tumors<sup>23</sup>.

Another imaging modality utilizes the surface area of proteins expressing a fluorescent marker, such as red fluorescent protein, as a surrogate for tumor volume<sup>15</sup>. However, tumor volume measured by fluorescent surface area<sup>11</sup> may not accurately represent tumor volume in irregularly-shaped tumors. In addition, this method necessitates a surgical procedure to orthotopically transplant fluorophore-expressing cells, raising questions of immune interactions between the recipient animal and the donor cells, or of the surgery itself. If nude or immunocompromised animals are used in the procedure, the ability to study the immune aspect of tumor biology is reduced or eliminated.

Alternatively, tumor volume can be estimated from endoscopic images. The study of tumors by colonoscopy has become routine for both mouse<sup>6,10</sup> and rat<sup>1,13</sup> models of the disease. By contrast to terminal assessments, colonoscopy allows tumors to be visualized *in vivo* over time, capturing the dynamics of tumor growth. Documentation of this aspect of tumor biology can greatly enrich studies evaluating chemopreventive or therapeutic agents<sup>6,13</sup>. Quantitative methods to determine tumor volume take this a step further, allowing investigation of the effects of background strain, therapeutic agents, environmental factors or other modifiers of tumor growth pattern. One method to estimate tumor size uses the fraction of luminal cross-section occluded by the tumor<sup>2</sup>. However, the colonic lumen expands as the animal grows and its size often increases to accommodate the growing tumor to prevent intestinal blockage. Optical methods to extrapolate tumor sizes from 2D images obtained *in vivo* during colonoscopy are achieved by inserting a flexible metal rod of known dimensions into the endoscope working channel<sup>10</sup>. However, since colonic tumors can differ in shape (some are flat while others are pedunculated), area measurements may not accurately translate to tumor volume.

To overcome these limitations and add another tool to the growing cancer research toolbox, we have developed a method using a biologically inert alginate to create negative molds of colonic tumors. These molds are filled with dental stone to achieve a positive cast of each tumor. A conversion factor is then used to calculate original tumor volume from the dry weight of the dental stone cast. This procedure, which requires no specialized or expensive equipment and no complicated analytical methods, can be performed within the facility where the animals are housed, and takes less than 15 minutes, including the time during which the alginate sets. Thus, it opens up possibilities to study the dynamics of tumor growth by researchers in virtually any animal facility, regardless of health status or existing equipment.

## **Materials and Methods**

**Animal Breeding and Maintenance.** The *Apc*<sup>Pirc/+</sup> rat model for familial intestinal cancer (developed in the laboratory of WFD and now commercially available through Taconic, Hudson, NY), was utilized in this study<sup>1</sup>. As reported previously, tumor multiplicity and intestinal distribution differs between Pirc strains and between male and female Pirc rats<sup>1,21</sup>. Therefore, both male and female F344 and (F344 x ACI)F<sub>1</sub> rats were used in the study. Rats over a range of ages were utilized in order to mold and cast a broad spectrum of tumor sizes. Age was controlled for in experiments where it could be a confounder, as both the multiplicity and size of tumors increase with age. Rats were specific-pathogen free and purpose-bred in-house for research only. The pathogen status of the facility is monitored by a sentinel program. Rats were housed in sex-specific groups of 2-3 in standard shoebox caging containing corncob bedding. Rats were allowed free access to a commercial diet (Harlan 5020 chow, Madison, WI) and acidified water (hydrochloric acid to pH 2.5) delivered via an automatic watering system. Rats were maintained in a facility in the McArdle Laboratory approved by the American Association of Laboratory Animal Care (AALAC). Rat room temperature was maintained at an average 71.5° F, and humidity was maintained between 30% and 70%. An automated timer system was used to maintain a 12:12 hour light:dark cycle. All protocols were approved by the Animal Care and Use Committee of the University of Wisconsin School of Medicine and Public Health and were consistent with the *Guide for the Care and Use of Laboratory Animals*.

**Endoscopy.** Rats were anesthetized with 3% isoflurane and placed ventral side down on a sterile surgical field above a heating pad to maintain a consistent body temperature during the proce-

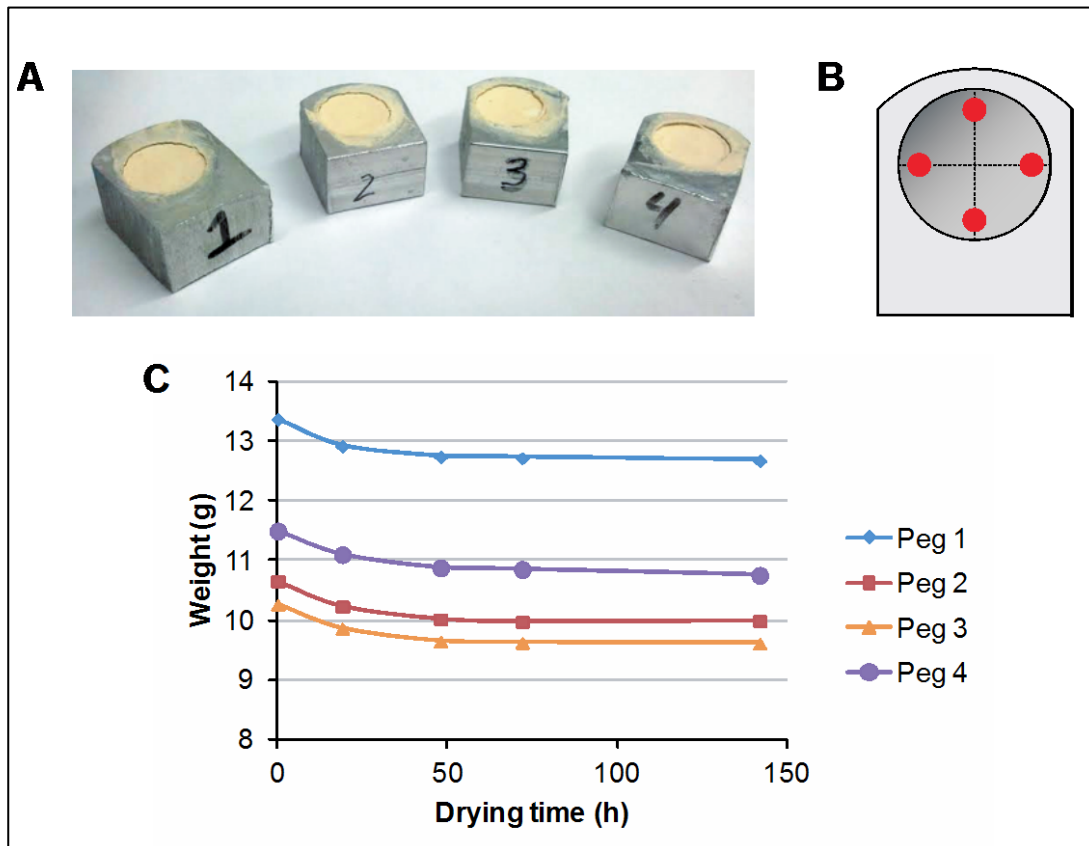
dure. The colon was flushed with 37°C Dulbecco's phosphate buffered saline (DPBS, Invitrogen, Grand Island, NY) to remove any fecal material and to provide lubrication. A 2.7 mm x 18 cm Hopkins Optik 30° endoscope (7219BA, Karl Storz, Tuttlingen, Germany) within a sheath (67065C, Karl Storz) was inserted to the proximal colonic flexure. Illuminated by the Xenon Nova 175 (201315, Karl Storz), still and video images were captured at each visit using the Image 1 hub (22200, Karl Storz) and AidaVet software (692040, Karl Storz). The anatomy of the rat allows the distal two-thirds of the colon to be visualized by endoscopy.

**Alginate Negative Molds.** A detailed protocol and photographs of the procedure can be found on pages 246-250. Briefly, the anesthetized rat was prepared by inserting a 5.5 French (1.83 mm) Fogarty catheter (Edwards Lifesciences, Irvine, CA, #12TLW405F35) about 10-12 cm into the colon and inflating. A 13.5 cm long silicone filling tube (Fisher Scientific, Waltham, MA, #14-176-332B) with a stainless steel Luer lock adapter (Vita Needle, Needham, MA, #VN530) was lubricated with mineral oil (noting that the mineral oil must not contact any of the colonoscopy equipment) and gently inserted into the rectum up to the inflated Fogarty balloon. 1.5 grams of GenesisV alginate (Accu-cast, Bend, OR) was mixed with 6 ml of room temperature deionized water in a 20 ml Luer-Lok™ Tip syringe (BD, Franklin Lakes, NJ, #309661). The alginate was then pushed through the filling tube into the colon while the filling tube was slowly removed from the colon. The alginate was left in place to solidify, about 8-12 minutes, depending on ambient temperature and humidity. After the alginate mold was gently extruded from the colon, it was rinsed of fecal material and stored in a conical tube until dental stone casts could be made (within 1 week). To determine the reproducibility of the alginate process, two to three alginate molds were made for each of a subset of rats on the same day.

**Dental Stone Positive Casts.** A detailed protocol can be found on pages 251-253. Briefly, the alginate molds were removed from storage and the tumor impressions gently dried using a KimWipe (Kimberly-Clark, Irving, TX). 2.5 grams of yellow dental stone (The Plaster Guys, Glenside, PA) was added to a small beaker containing 1.0 ml of deionized water, and mixed completely. A small scoopula was used to fill the impressions in the alginate mold, with care to avoid bubbles and completely fill the impression. The dental stone was left to set for 15-20 minutes at room temperature before it was gently removed from the mold. Casts were then put into labeled multi-well cell culture plates and placed uncovered into a 90°C hybridization oven for 48 hours before being weighed. From each alginate tumor mold, three individual stone casts were made to determine the reproducibility of the dental stone casting process. Dental stone casts can be stored indefinitely in sealed tubes at room temperature.

**Tumor volume calculations.** Four aluminum pegs each containing a cylindrical hole were machined and their initial empty weights determined (Fig 5-1A). The volume of each cylindrical hole was determined using the formula for the volume of a cylinder ( $\pi \times \text{radius}^2 \times \text{height}$ ) where the radius was determined by averaging two diameter measurements perpendicular to one another and dividing by 2, and the height determined by averaging four depth measurements for each hole (Fig 5-1B). The holes were then filled completely with dental stone and dried in a 90°C hybridization oven. Filled pegs were then reweighed at 0, 19, 48, 72 and 142 hours of drying and the empty peg weight subtracted to yield the cast weight (Fig 5-1C). A conversion factor was then determined from the initial volume of a peg hole and weight of its dry cast. The average

**Fig 5-1.** Determination of dental stone conversion factor and drying time. (A) Four pegs each containing a cylindrical hole were filled with dental stone and dried for various periods of time. (B) Peg volume was calculated by averaging two measurements for diameter (dashed lines) and four measurements for depth (red dots). (C) After 48 hours of drying at 90°C, the weight of the dental stone changed very little. The volume of the pegs and dry weight of the dental stone was used to determine the conversion factor (1.3236 gm/cm<sup>3</sup>).





conversion factor was then applied to tumor dental stone casts to allow the individual tumor volume to be calculated from the weight of each dry dental stone cast.

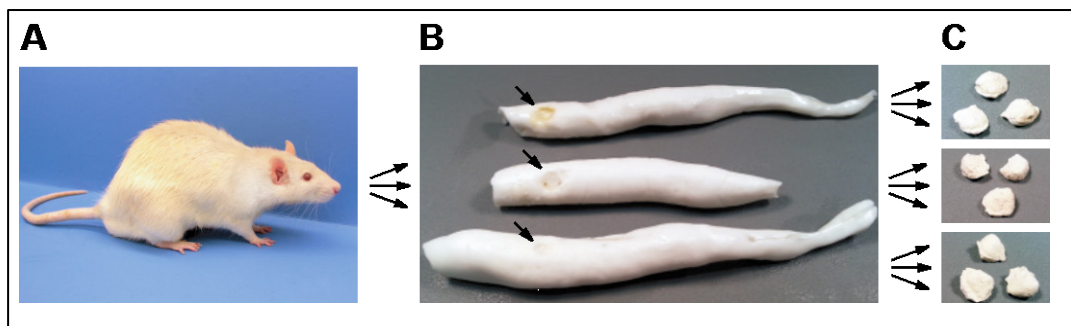
**Terminal tumor wet and dry weight.** Rats were sacrificed by CO<sub>2</sub> asphyxiation. The colon was removed, flushed with PBS, opened longitudinally and laid flat. Tumors that underwent the alginate molding procedure were cut at the base of the stalk and weighed before fixation to determine 'wet' weight. Tumors were then transferred to 10% neutral buffered formalin for 24 hours. The tumors were removed from formalin, allowed to air dry for 10 minutes and reweighed to determine 'dry' weight.

**Statistical Methods.** All statistical test were performed using the freely available software MSTAT (version 5.5.7). To test for a correlation between error rate and experience level of the experimenter performing the procedure, the Jonckheere-Terpstra test was employed. To test for a difference between two groups, a 2-sided Wilcoxon rank sum test was utilized. To test for a correlation between two variables, such as error rate and tumor size, a two-sided Kendall rank correlation test was used. For each of these tests a p-value  $\leq 0.05$  was considered significant. Regression analysis was used to determine how closely the weight of the dental stone casts correlated with the weight of the dissected tumors.

## **Results**

To determine the time required to dry casts to a constant weight, four pegs each containing a cylindrical hole with volumes ranging from 1224.6 - 1259.6 mm<sup>3</sup> were filled with wet den

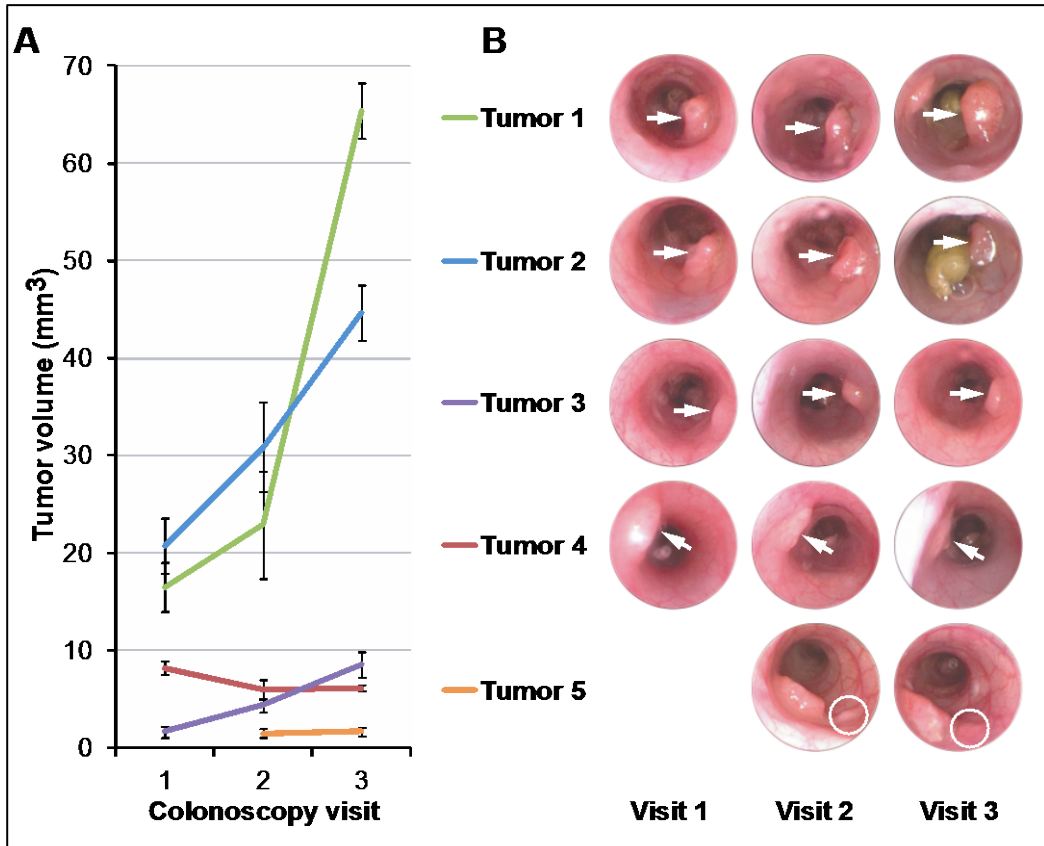
**Fig 5-2.** Experimental procedure to determine the error rate of alginate molding and dental stone casting. (A) 21 rats underwent the alginate molding procedure, with several rats examined at multiple time points (see Fig 5-3). (B) One to three alginate molds were made per visit for each rat; multiple alginate molds made on the same day of the same rat were used to test the reproducibility of the molding procedure. The negative impression left by the tumor in each alginate mold is indicated with an arrow. (C) From each alginate mold one to three dental stone casts were made; multiple dental stone casts of each tumor were used to test the reproducibility of the casting procedure.



tal stone and heated to 90°C to speed drying (Fig 5-2 A-B). On average, the weight of the dental stone decreased by  $3.7\% \pm 0.3\%$  between 0 and 19 hours, by  $1.9\% \pm 0.3\%$  between 19 and 48 hours, but only by  $0.3\% \pm 0.4\%$  or less after 48 hours (Fig 5-2C). Thus, we determined that drying for 48 hours was sufficient to obtain a stable dry dental stone weight. Then, based on the known volume of each peg hole and the weight of the corresponding dry dental stone in a series of three experiments, we found the conversion factor to be  $0.001324 \pm 0.000310 \text{ gm/mm}^3$ . To determine the initial tumor volume in  $\text{mm}^3$ , the weight in grams of the dry dental stone cast was divided by 0.001324.

Multiple alginate molds and dental stone casts were made from 21 rats, each containing 1 to 5 colonic tumors (Fig 5-3). A total of 66 tumors, 133 molds and over 300 casts were created. The overall average errors were  $17.9\% \pm 11.6\%$  for the molding procedure and  $20.9\% \pm 18.9\%$  for the casting procedure, which resulted in an overall tumor volume error of  $22.7\% \pm 16.7\%$ . The errors from both procedures significantly decreased over time as the skill level and experience of the experimenter increased (Jonckheere-Terpstra test  $p < 0.0001$ ). The mean error of the alginate molding procedure was not statistically significant by a 2-sided Wilcoxon rank sum test in the first compared with the second half of the study ( $p = 0.42$ ). However, the standard deviation from the mean was greater in the first half of the study ( $17.2\% \pm 14.5\%$ ) compared with the second half ( $18.4\% \pm 8.8\%$ ). Similarly, the average dental stone cast error was significantly greater in the experiments run in the first half of the study ( $30.1\% \pm 21.6\%$ ) compared with the second half ( $11.5\% \pm 7.8\%$ , 2-sided Wilcoxon rank sum test  $p < 0.0001$ ). Thus, the overall calculated tumor volume error after refinement of the technique was  $16.5\% \pm 7.9\%$ .

**Fig 5-3.** Longitudinal tumor volume measurements. Five representative tumors from three rats followed longitudinally are shown. Over a period of five weeks, Tumors 1 (green), 2 (blue) and 3 (purple) grew, Tumor 5 (orange) was static, and Tumor 4 (red) regressed. Error bars represent cumulative error from both the alginate molding and dental stone casting procedures.

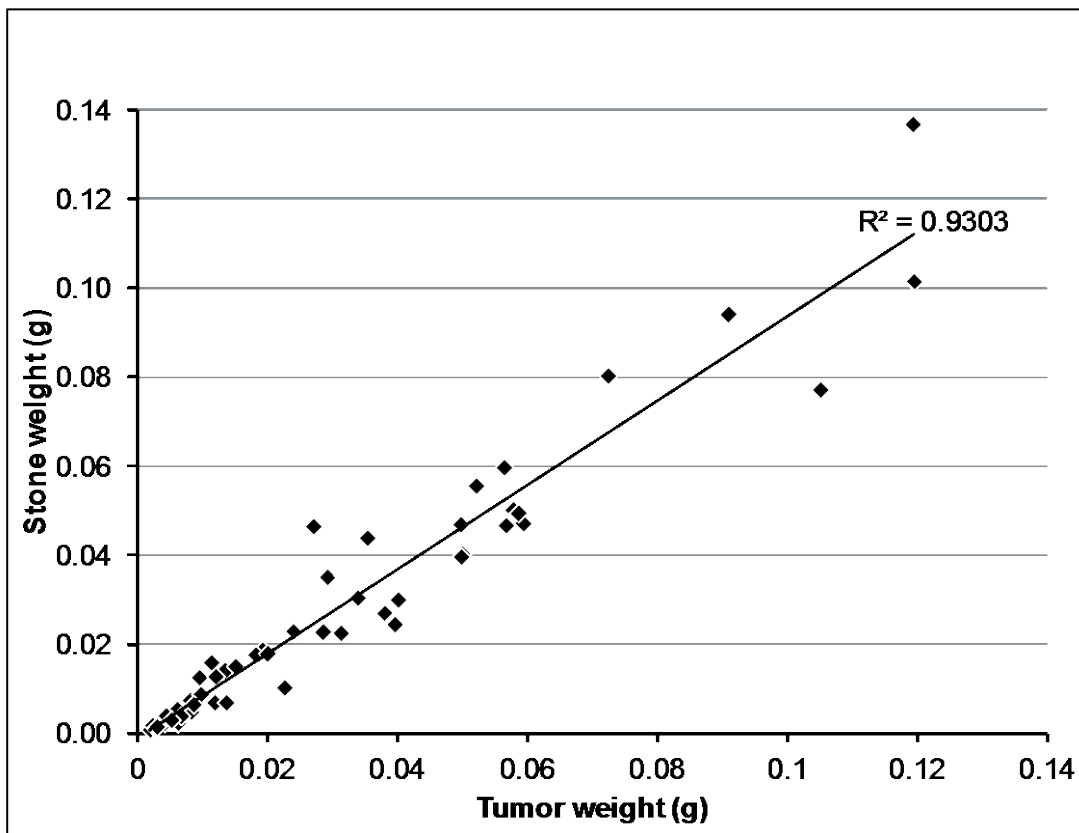


Tumors as small as 4 mm<sup>3</sup> (about 2 x 2 x 1 mm) and as large as 196 mm<sup>3</sup> (about 7 x 7 x 4 mm) have been successfully molded using this technique (Fig 5-4). Alginate molding error did not correlate with tumor size, indicating that this procedure works as well for small tumors as for larger tumors (two-sided Kendall rank correlation test  $p=0.87$ ). However, the dental stone cast error did increase with tumor size, presumably a result of incomplete filling of large deep holes in the alginate mold with dental stone (two-sided Kendall rank correlation test,  $p<0.00001$ ). Each stone must be examined when removed from the mold to ensure that no bubbles are present and that it accurately represents the impression within the alginate mold.

To determine whether tumor volume derived from the alginate method correlated with actual tumor weight, a cohort of rats underwent alginate molding as a terminal procedure and were subsequently dissected to harvest individual tumors. From 16 rats, a total of 50 tumors were both cast and directly weighed, 40 of which had both wet and dry weights determined. The correlation between tumor wet weight and dry weight was very high ( $R^2 = 0.999$ ). In this experiment, tumor weights ranged from 0.008 grams to 0.137 grams (corresponding to tumor volumes of about 6 mm<sup>3</sup> to about 104 mm<sup>3</sup>) and the correlation between dental stone cast weight and tumor weight was high ( $R^2 = 0.93$ , Fig 5-4). These data were based on a single dental stone cast from a single alginate mold. This correlation between tumor volume derived from dental stone weight and terminal tumor weight is similar to that reported between microCT and terminal tumor weight ( $R^2 = 0.87$ )<sup>5</sup>.

While this technique is useful for determining terminal tumor volume, it is even more powerful when applied longitudinally. To test this method longitudinally, alginate molds were made every 1-2 weeks over a period of 4-5 weeks in six rats. Throughout the study all animals appeared healthy, active, and recovered following the procedure similarly to those who under

**Fig 5-4.** Dry dental stone weight correlates closely with tumor weight. From 16 rats, a total of 50 tumors were both molded/cast and directly weighed. Tumor weights ranged from 0.008 grams to 0.137 grams and were highly correlated with dry dental stone weight ( $R^2=0.9303$ ), the surrogate for tumor size.



went colonoscopy alone. Of ten tumors, eight grew, one remained static and one regressed during the study; Figure 5-3 shows (A) the longitudinal growth profiles and (B) the images obtained during colonoscopy for five representative tumors.

This method has proven highly successful to determine *in vivo* tumor volume. However, it was essential to explore whether the procedure had any overt effect on tumor growth or multiplicity in longitudinal studies. Indeed, alginates are able to bind iron and high iron levels have been associated with increased rates of colorectal cancer<sup>19</sup>. To determine whether alginate had any effect on tumor multiplicity, six rats were followed longitudinally for five weeks: three underwent both colonoscopy and alginate molding on weeks 0, 3 and 5 while another group of three rats underwent colonoscopy only. Although the number of animals examined was small, tumor multiplicity did not differ markedly and the means for each were within one standard deviation. At dissection, those undergoing colonoscopy had  $2.0 \pm 1.7$  tumors while those undergoing both colonoscopy and repeat alginate exposure had  $2.7 \pm 0.6$  tumors (2-sided Wilcoxon rank sum test  $p=0.5$ ). To determine whether there was a significant effect on tumor size, eight control rats underwent alginate molding as a terminal procedure only. Tumor sizes of these rats were then compared to those of six rats that had undergone three alginate moldings at least one week apart over a period of 4-5 weeks. No significant difference was observed ( $22.8 \text{ mm}^3 \pm 23.9 \text{ mm}^3$  in animals undergoing only terminal alginate molding versus  $16.0 \text{ mm}^3 \pm 18.4 \text{ mm}^3$  in animals undergoing longitudinal alginate molding, 2-sided Wilcoxon rank sum test  $p=0.27$ ).

## **Discussion**

We have developed a method to monitor the growth of colonic tumors *in vivo* using alginate molding coupled with dental stone casting. This method has successfully measured the vol-

ume of a wide range of tumor sizes, from 4 mm<sup>3</sup> to 196 mm<sup>3</sup>. Dental stone casts made from tumors correlate to a high degree with the weight of the dissected tumor ( $R^2=0.93$ ). Beyond single time point measurements, this method has been applied longitudinally to follow the growth trajectory of tumors in a quantitative manner.

Biocompatible alginate, or alginic acid, is an anionic polysaccharide found in the cell walls of brown algae<sup>4</sup>. When treated with Ca<sup>2+</sup> ions and D-glucono-d-lactone, a homogenous, strong gel can be prepared with gelation rates proportional to the concentration of Ca<sup>2+</sup> ions<sup>16</sup>. This material is not absorbed or fermented in the gastrointestinal tract, is approved for human consumption, and is often used to encapsulate pharmaceutical compounds<sup>3</sup>. When solidified, alginate is strong yet flexible, making it easy to extrude from the colon without undue stress to the animal. It is these properties that make alginate a good candidate material to mold tumors of the colon. The gel setting time depends on the ratio of water to alginate powder, as well as water temperature, ambient temperature and humidity. In this procedure we were able to create a mixture that would flow freely into the colon, yet had an *in situ* set time of about 10 minutes, allowing the animals to be under anesthesia for only a short period of time. This is in contrast to CT procedures, which can take 30 minutes or more to obtain images while the animal is anesthetized with a colon insufflated with air.

An added benefit of performing longitudinal studies is the ability to reduce significantly the number of animals needed for a study. When individual tumors can be followed over time, the “sample” for statistical analysis becomes each tumor rather than each animal.

As the method is developed in our laboratory and others, more detailed analyses are required to assess any effects on normal colonic tissue and tumors. Though we have not detected any adverse effects on the growth of colonic tumors, any method to measure colonic tumor vol-



ume interferes with the biological system. Only by further use of this method can investigators at large detect any unanticipated biological perturbation. The proportion of growing, static and regressing tumors observed using the alginate method was similar to those previously observed based on subjective scoring of images by blinded observers<sup>13</sup>. Thus, it appears that alginate does not have an overt effect on tumor growth profiles. Similarly, we observed no significant difference in tumor multiplicity or size between animals undergoing colonoscopy alone and those also exposed to several alginate molding procedures. However, the potential for effects at the molecular or cellular level should be investigated further.

We note that tumor volume determination by alginate molding does have limitations. Tumors that cluster closely together may not be resolved individually, and large tumors that occlude the lumen may prove difficult to cast as the alginate may not flow freely around the entire tumor. Further, completely flat lesions would not be detected with this technique; however, these tumors can be visualized by other methods, such as endoscopy. Although alginate can mold the entire colon, the rigid endoscope is limited to visualization of only the distal two-thirds of the rat colon, to the point where the colon turns to meet the cecum. Therefore, impressions made at the anterior end of the mold may not connect to endoscopic images. However, the use of endoscopy equipment is not essential to utilize the alginate molding technique. Although endoscopic visualization of tumors gives added confidence, making several replicate molds from the same animal can yield a similar level of confidence. The reproducibility of this method has proven to be good, but room for improvement remains. The current level of error for an individual tumor may not correspond to regulatory stringency as an approved method for determining tumor volume in translational rodent studies. Further work is needed to improve upon the precision of the technique and to compare this method directly with CT.

Attempts were made to adapt this procedure to the mouse, using the *Apc*<sup>Min/+</sup> model. Various ratios of alginate to water were used to find a mixture that would flow through the narrow filling tube required by the small diameter of the mouse colon, yet solidify in a reasonable amount of time; set times of over 20 minutes were tested without success. Attempts to fill the colon without a filling tube resulted in the alginate molding only the distal portion of the colon. Further, the mouse colonic wall is much more fragile than that of the rat and is easily pierced. Nonetheless, with further procedural refinement, alginate molding may hold potential for determining accurate tumor volume measurements in the colon of the mouse.

Although the deep understanding of mouse genetics and the ability to manipulate the mouse genome has historically made it a model of choice, the rat has recently made dramatic strides in this area. For biological reasons the rat is an increasingly preferred choice to model some human diseases, in cases where the rat recapitulates the human disease more closely than the mouse<sup>7,12,14</sup>. Azoxymethane and dextran sodium sulfate models of rat colonic carcinogenesis have been utilized for several decades and are still used to research environmentally induced colon cancers. In the last several years, two rat models of familial colon cancer have been developed: the *Apc*<sup>Pirc/+</sup> rat, used here, and the KAD rat, a homozygously viable *Apc*-mutant model<sup>22</sup>. Tumors form preferentially in the colon in both of these models, similar to the human disease and distinct from genetic mouse models that develop tumors primarily in the small intestine. Recently, the ability to readily manipulate the rat genome through the use of zinc-finger nucleases, transcription activator-like effector nucleases (TALENs) or other methods have all rapidly accelerated the study and use of genetically modified rat models<sup>9,18</sup>. The growing prominence of the rat makes this method essential for the study of colonic neoplasia in experimental animals.

In summary, we have shown that alginate molding combined with dental stone casting is a facile and reliable method to determine tumor volume *in vivo* without the need for expensive equipment and software. MicroCT measurements can cost several hundred dollars per animal for each scan and the data analysis can be time consuming and require detailed command of the software. By contrast, the methods discussed within this report cost only a few cents per alginate mold and even less for the dental stone casts. Only an accurate balance and calculator are required to determine tumor volume from dental stone weight. Importantly, this method can also be done directly in the animal facility or laboratory in conjunction with other experiments. Such a simple method opens up possibilities for researchers around the globe to study tumor dynamics. Further, we have shown that the *Apc*<sup>Pirc/+</sup> rat, readily available to researchers worldwide, is an appropriate model in which to carry out longitudinal studies of the dynamics of colonic tumorigenesis.

## References

1. **Amos-Landgraf JM, Kwong LN, Kendzioriski CM, Reichelderfer M, Torrealba J, Weichert J, Haag JD, Chen KS, Waller JL, Gould MN, Dove WF.** 2007. A target-selected Apc-mutant rat kindred enhances the modeling of familial human colon cancer. *Proc Natl Acad Sci USA* **104**:4036-4041.
2. **Becker C, Fantini MC, Neurath MF.** 2006. High resolution colonoscopy in live mice. *Nature Protocols* **1**:2900-2904.
3. **Bodmeier R, Chen HG, Paeratakul O.** 1989. A novel approach to the oral delivery of micro- or nanoparticles. *Pharm Res* **6**:413-417.
4. **Draget KI, Smidsrod O, Skjak-Braek G.** 2005. Alginates from Algae. In: *Biopolymers Online*.
5. **Durkee BY, Mudd SR, Roen CN, Clipson L, Newton MA, Weichert JP, Pickhardt PJ, Halberg RB.** 2008. Reproducibility of tumor volume measurement at microCT colonography in living mice. *Academic Radiology* **15**:334-341.
6. **Durkee BY, Shinki K, Newton MA, Iverson C, Weichert J, Dove WF, Halberg RB.** 2009. Longitudinal assessment of colonic tumor fate in mice by computed tomography and optical colonoscopy. *Academic Radiology* **16**:1475-1482.
7. **Dwinell MR, Lazar J, Geurts AM.** 2011. The emerging role for rat models in gene discovery. *Mamm Genome* **22**:466-475.
8. **Faustino-Rocha A, Oliveira PA, Pinho-Oliveira J, Teixeira-Guedes C, Soares-Maia R, da Costa RG, Colaco B, Pires MJ, Colaco J, Ferreira R, Ginja M.** 2013. Estimation of rat mammary tumor volume using caliper and ultrasonography measurements. *Lab Anim (NY)* **42**:217-224.
9. **Geurts AM, Cost GJ, Freyvert Y, Zeitler B, Miller JC, Choi VM, Jenkins SS, Wood A, Cui X, Meng X, Vincent A, Lam S, Michalkiewicz M, Schilling R, Foeckler J, Kalloway S, Weiler H, Menoret S, Anegon I, Davis GD, Zhang L, Rebar EJ, Gregory PD, Urnov FD, Jacob HJ, Buelow R.** 2009. Knockout rats via embryo microinjection of zinc-finger nucleases. *Science* **325**:433.
10. **Hensley HH, Merkel CE, Chang WC, Devarajan K, Cooper HS, Clapper ML.** 2009. Endoscopic imaging and size estimation of colorectal adenomas in the multiple intestinal neoplasia mouse. *Gastrointest Endosc* **69**:742-749.
11. **Hoffman RM.** 2005. The multiple uses of fluorescent proteins to visualize cancer in vivo. *Nat Rev Cancer* **5**:796-806.
12. **Iannaccone PM, Jacob HJ.** 2009. Rats! *Dis Model Mech* **2**:206-210.

13. **Irving AA, Halberg RB, Albrecht DM, Plum LA, Krentz KJ, Clipson L, Drinkwater N, Amos-Landgraf JM, Dove WF, Deluca HF.** 2011. Supplementation by vitamin D compounds does not affect colonic tumor development in vitamin D sufficient murine models. *Arch Biochem Biophys* **515**:64-71.
14. **Jacob HJ.** 2010. The rat: a model used in biomedical research. *Methods Mol Biol* **597**:1-11.
15. **Katz MH, Takimoto S, Spivack D, Moossa AR, Hoffman RM, Bouvet M.** 2003. A novel red fluorescent protein orthotopic pancreatic cancer model for the preclinical evaluation of chemotherapeutics. *J Surg Res* **113**:151-160.
16. **Kuo CK, Ma PX.** 2001. Ionically crosslinked alginate hydrogels as scaffolds for tissue engineering: part 1. Structure, gelation rate and mechanical properties. *Biomaterials* **22**:511-521.
17. **Lingeman CH, Garner FM.** 1972. Comparative study of intestinal adenocarcinomas of animals and man. *J Natl Cancer Inst* **48**:325-346.
18. **Mashimo T, Kaneko T, Sakuma T, Kobayashi J, Kunihiro Y, Voigt B, Yamamoto T, Serikawa T.** 2013. Efficient gene targeting by TAL effector nucleases coinjected with exonucleases in zygotes. *Sci Rep* **3**:1253.
19. **Nelson RL.** 2001. Iron and colorectal cancer risk: human studies. *Nutr Rev* **59**:140-148.
20. **Pickhardt PJ, Kim DH, Pooler BD, Hinshaw JL, Barlow D, Jensen D, Reichelderfer M, Cash BD.** 2013. Assessment of volumetric growth rates of small colorectal polyps with CT colonography: a longitudinal study of natural history. *Lancet Oncol* **14**:711-720.
21. **Washington MK, Powell AE, Sullivan R, Sundberg J, Wright N, Coffey RJ, Dove WF.** 2013. Pathology of Rodent Models of Intestinal Cancer: Progress Report and Recommendations. *Gastroenterology* **144**:705-717.
22. **Yoshimi K, Tanaka T, Takizawa A, Kato M, Hirabayashi M, Mashimo T, Serikawa T, Kuramoto T.** 2009. Enhanced colitis-associated colon carcinogenesis in a novel Apc mutant rat. *Cancer Sci* **11**:2022-2027.
23. **Young MR, Ileva LV, Bernardo M, Riffle LA, Jones YL, Kim YS, Colburn NH, Choyke PL.** 2009. Monitoring of tumor promotion and progression in a mouse model of inflammation-induced colon cancer with magnetic resonance colonography. *Neoplasia* **11**:237-46.

## Conclusions & Prospectus

### I. The Power of Modeling Human Colon Cancer in the Rat

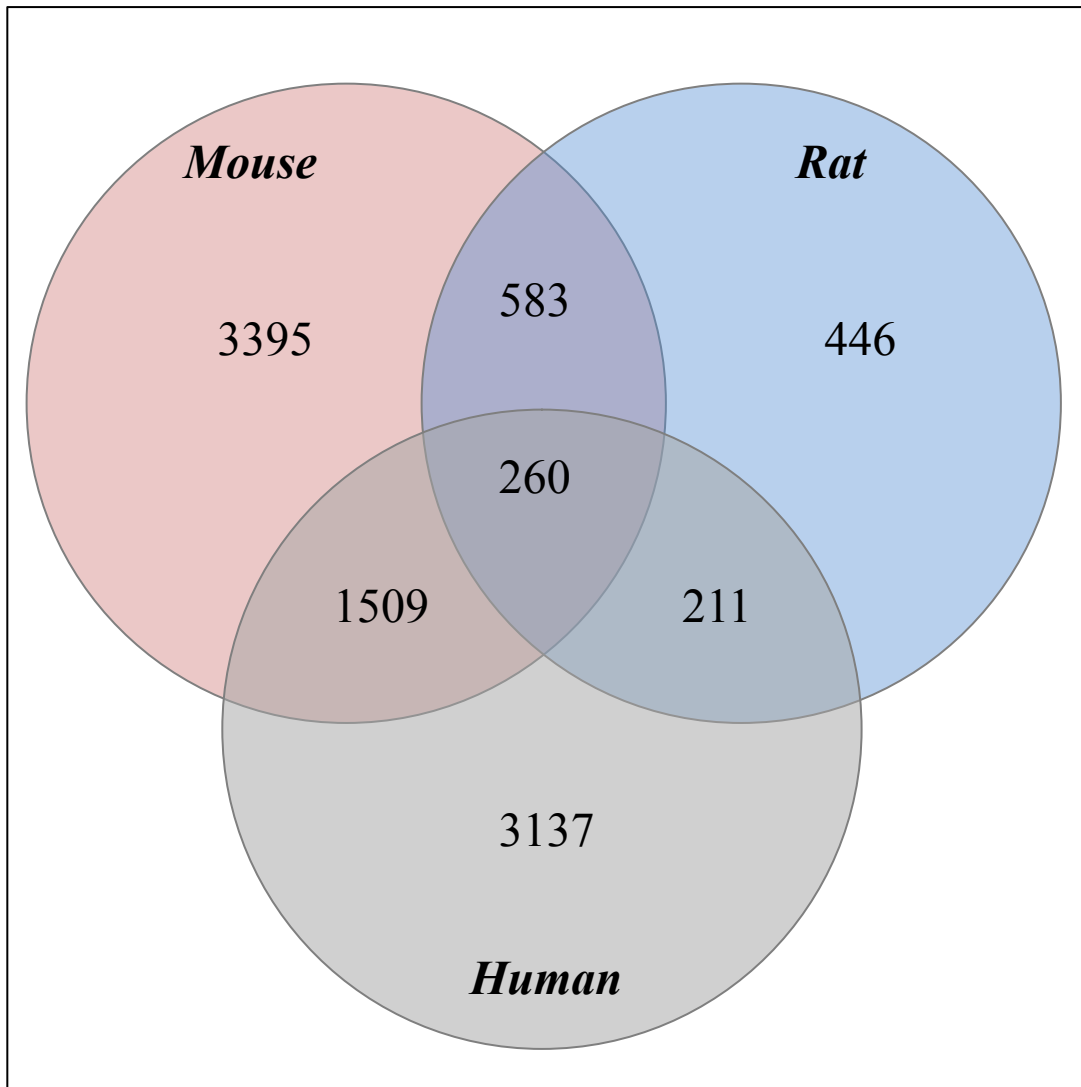
**Three genera.** The mouse has been a mainstay in research laboratories for decades, owing to the detailed understanding of and ability to manipulate their genome. However, use of the rat is making great strides in these areas, with full genome sequencing of multiple laboratory rat strains and new technologies to functionally alter that genome. In certain cases, the rat may more closely model the human disease. Moreover, the study of disease in both the rat and the mouse increases the likelihood for overlap with important aspects of the human disease.

The laboratory mouse, *mus musculus*, and rat, *rattus norvegicus*, are of two separate genera. It is estimated that mice and rats diverged 20-25 million years ago, while the most recent common ancestor between the mouse, rat and human diverged over 90 million years ago<sup>16</sup>. The mouse and rat are about 93% identical in nucleotide and amino acid sequence<sup>38</sup>. However, one study of large-scale genomic rearrangement differences between mouse, rat and human suggests that the structure of the rat genome may be more similar to that of the human<sup>39</sup>. Further, while chromosomes in the mouse are telocentric<sup>35</sup>, those in the rat and human are both metacentric<sup>18</sup>. These structural similarities help to make the rat more useful for studying the effects of chromosome loss or rearrangement in disease processes<sup>2,3</sup>.

The mouse and rat each offer unique overlap with the human; therefore, models in both genera are essential to understand disease to the furthest extent possible in model organisms. A study investigating the physiology of the long-lived naked mole rat, which is in a separate family

(Bathyergidae) from the laboratory mouse and rat (Muridae), found that *mus musculus* and *homo sapiens* share 9033 gene families, while *rattus norvegicus* and *homo sapiens* share 8803 gene families<sup>16</sup>. However, when both *mus musculus* and *rattus norvegicus* are compared to *homo sapiens*, 9178 gene families are shared between human and at least one of the rodent models, a greater overlap than either model alone. Similarly, in our lab we have further demonstrated this multi-model benefit. Using whole genome microarray, when comparing differential expression between normal colonic tissue and tumor tissue, the mouse shows an overlap with human of 1769 Entrez IDs, and the rat shows an overlap with human of 471 Entrez IDs (Fig CP-1). When both rodent models are compared against the human, 1980 Entrez IDs overlap between human and at least one of the rodent models, with 1509 Entrez IDs unique to mouse and human and 211 Entrez IDs unique to rat and human. This enhanced overlap between the disease models and humans illustrates the importance of examining disease processes in more than one model. We note the much smaller overlap apparent between rat and human compared with mouse and human. However, this is likely an artifact of the annotation of the rat genome available at the time of analysis, and the overlap between rat and human may grow as the annotation becomes more complete. We don't dismiss the 3173 Entrez IDs that are shown to be altered in human tumors but not in either rodent model. The human case must always be revisited to determine whether changes seen in the rodent models accurately reflect the human disease. Further, associations between altered gene expression and disease found in human tissues can be tested for causation in rodent models. Neither association studies in humans nor causation studies in rodent models can stand alone.

**Fig CP-1.** Overlap of Entrez IDs differentially expressed between normal tissue and colonic tumors in mouse, rat and human. Rat data is derived from the experiments in the Pirc rat discussed in Chapter 2. Owing to the available annotation of the rat genome, fewer rat probe IDs mapped to Entrez IDs, resulting in a smaller dataset overall. Mouse data is a comparison of four biological replicates each of normal tissue and tumors from Min mice (unpublished results from Jennifer Pleiman). Human data is gathered from the published GEO dataset GDS2947 where normal tissue and tumor samples were collected from 32 patients. Each comparison between normal tissue and tumor was made at a stringency of at least a 2-fold change in expression and a false discovery rate no greater than 5%.





**Manipulating the rat genome.** Variability in phenotype is essential to finding the underlying cause for that observed difference. To date, 26 rat strains have been sequenced by four independent institutions<sup>23</sup>. Different inbred strains can vary greatly in their phenotypic representation of and susceptibility to disease and each of these strains offers benefits for the study of particular diseases. This concept has been illustrated by the susceptibility to spontaneous and DSS-induced tumorigenesis in the Pirc rat. While the coisogenic F344-Pirc rat develops many spontaneous tumors, which is further enhanced by DSS treatment, the congenic BN-Pirc rat develops none or few spontaneous tumors, and is unaffected by DSS treatment. Both strains can help us to better understand spontaneous and inflammation-associated colon cancer. What critical genetic, epigenetic, cellular or molecular factors differ between F344 and BN to allow the former to be susceptible to both spontaneous and inflammation-associated cancer, while creating strong resistance to disease in the latter? Are these factors related to susceptibility in humans?

Since many strains are utilized to study disease, technologies that readily allow the genome to be manipulated in any strain are key. Further, technologies that can be utilized in transgenics or lines carrying other mutations make the study of combinatorial effects of genomic alterations more efficient. Only a few years ago, zinc-finger nuclease (ZFN) technology was the most efficient process for knocking out a gene of interest in the rat. In the first published study using ZFNs in the rat, of 295 founder animals, over 10% harbored targeted mutations<sup>10</sup>. Since then, transcription activator-like effector nucleases (TALENs) are becoming more widely used in the rat<sup>22</sup>. TALENs can be designed easily by researchers without the proprietary restrictions or costs associated with ZFNs. Very recently, gene targeting in the rat has been described using the clustered regulatory interspaced short palindromic repeat (CRISPR)-Cas system. The efficiency of the CRISPR-Cas system in the rat has been shown to be greater than 70%<sup>19</sup>, although a high-

frequency of off-target mutations has been shown in human cells using this method<sup>8</sup>. These techniques are each highly versatile and can be customized to recognize virtually any sequence. It should be noted that these technologies work not only in the rat or in mammalian systems, but in any organism with DNA repair mechanisms, and are poised to transform through genetic manipulation biological study from insects to plants, rodents to humans.

These techniques can be utilized in different ways to test for causation of particular genotypes or expression patterns associated with disease phenotypes. We are beginning to explore the complete germ line loss of *Bcat1* expression, induced by ZFN technology, and its effects on tumor initiation and progression in both the spontaneous and inflammation-associated case.

Occasionally, total loss of expression of a particular gene is not tolerated owing to an essential function of that gene for viability. Although global gene loss is a simplified starting point to determine whether there are effects on the phenotype of interest, conditional or tissue-specific modifications can more directly address questions of mechanism. For example, *Bcat1* is over-expressed in inflamed normal tissue and in tumors. Therefore, we hypothesize that global loss of *Bcat1* expression will reduce the number, growth or size of spontaneous tumors and will make animals more resistant to the enhancing effects of DSS. If this turns out to be true, we can further assess when and where *Bcat1* expression assists tumorigenesis. By eliminating *Bcat1* in one particular cell population at a time, we can determine what cells expressing *Bcat1* may be contributing to tumorigenesis. It is also possible that *Bcat1* is necessary for the repair process following DSS exposure, and complete elimination of its expression could instead enhance DSS-induced tumorigenesis. Here, conditional expression of *Bcat1* would be useful. *Bcat1* expression could be shut down before, during or after DSS treatment and before or after a tumor has become invasive to determine when its effects are exerted the most.

As technologies to manipulate the genome become more accessible, cost-effective and efficient, modeling of human disease will become even more powerful. Understanding the effects of genetic alterations and the causative role of these alterations in disease phenotypes in animal models will contribute significantly to how diseases are detected and treated.

**Rat resources.** A concerted effort by those using rodent models of disease is needed to make the knowledge garnered from these resources useful to researchers at large. The Knockout Mouse Project (KOMP) Repository<sup>37</sup> at the University of California-Davis accomplishes this for mouse models. Similarly, the Rat Genome Database (RGD)<sup>24</sup> at the Medical College of Wisconsin, the Rat Resource and Research Center (RRRC)<sup>30</sup> at the University of Missouri and the National BioResource Project for the Rat (NBRP)<sup>26</sup> in Japan compile data from laboratories that are utilizing rat models around the globe. Both the RRRC and NBRP are repositories and distributors of embryos, sperm and live rats. These institutions allow resources created by one investigator to be shared with others, without the cost or expertise needed to freeze and store stock from their strains. Currently, about 250 rat strains are available from the RRRC, and over 600 are available from the NBRP. The RGD, RRRC and NBRP each offer resources for creating genetically-modified rat strains by various technologies. The RGD has nearly 90 different knockout models generated in-house available for distribution, and is the source of our *Bcat1*<sup>-/-</sup> model. The ever-growing list of open-source resources offered by the RGD, RRRC and NBRP illustrates the desire of those in the rat “community” to share their data and bring the rat to prominence in research. By combining genomic resources with phenotyping data in one location, information is more accessible to those using rat models to study disease and to those just beginning to work with the rat.

## II. MANAGING HUMAN COLON CANCER

**Early detection.** The greatest impact on colon cancer can come through two modes: early detection and chemoprevention. Early detection allows polyps to be detected and removed before they become cancerous. Endoscopy is currently the gold standard method to detect colonic polyps. While the rate of eligible individuals who have undergone screening is increasing, about 1 in 3 individuals age 50 to 75 has not had the procedure<sup>5</sup>. This could be due to economic hurdles, limited access to the procedure, or unwillingness to comply with the uncomfortable preparations and invasive procedure. Colonoscopy is not perfect: especially in those patients with poor colonic preparation, adenomas can be missed. On average, the overall miss rate of polyp detection by colonoscopy is roughly 20%<sup>31</sup>, with the rate being highest for smaller polyps<sup>11</sup>. The procedure can also be risky in some individuals. More than 3 million colonoscopies are performed each year in the United States alone. Complication rates are low, but can be serious. The rate of perforations in asymptomatic patients is less than 1 in 1000, but increases to 1 in 500 when considering those patients with conditions, such as severe colitis<sup>34</sup>. Of those perforations, about 5% are estimated to be fatal. There is also a risk of bleeding following polypectomy, which may be greater than 10% for polyps larger than 2 cm. In spite of these risks, colonoscopy has the power to greatly reduce risk. Returning to our local Dane County cohort with which this dissertation began, if 1 in 3 individuals of the 25,000 who will develop colon cancer within their lifetime never underwent colonoscopy, 8250 lives could be lost simply because the cancer would go undetected until it was too late.

On the flip-side of this argument, if all 500,000 individuals in our Dane County cohort undergo colonoscopy once during their lifetime, 475,000 unnecessary colonoscopies will be performed because these individuals will never develop cancer. Although about 30-50% of individuals over the age of 50 have colonic polyps<sup>6</sup>, most never progress to cancer. Though these statistics may be complicated by the routine removal of polyps, which would prohibit their progression to frank cancer, a recent publication following patients longitudinally supports this argument of over-diagnosis. In over 300 6-9mm polyps followed by CT for an average of 2.3 years, only 22% progressed, while 50% were stable and 28% regressed spontaneously<sup>29</sup>. Further, growing lesions were indicative of advanced neoplasia. A total polyp volume of 180mm<sup>3</sup> or greater could detect 92% of advanced neoplasias with a specificity of 94%. Therefore, we can conclude that even of the 475,000 patients undergoing potentially unnecessary colonoscopy, a significant portion will have polyps removed that may never progress. This exposes a huge number of people to an unpleasant and potentially risky procedure unnecessarily. Importantly, those most at risk of developing advanced neoplasia, including individuals with a previously diagnosed advanced neoplasia, are generally underrepresented in screening groups<sup>33,34</sup>.

A better understanding of the growth profiles of tumors can be achieved using the Pirc rat. While the B6-Min mouse develops too few spontaneous colonic tumors to detect a difference in growth profiles, the Pirc rat shows a distribution of colonic tumor fates similar to the human (Chapter 1). Further, the growth profiles of these tumors can be altered in Pirc rats given DSS, enhancing the number of growing tumors and reducing the number of static and regressing tumors. Pirc rats where the spontaneous fate of the tumors has been determined could subsequently be treated with DSS to determine how inflammation shifts the fate of specific tumors, and to determine how the cellular and molecular profiles differ in the same tumor before and af-

ter DSS treatment. These candidates could then become targets for specifically detecting tumors fated to grow and progress or for treating early polyps to prevent their growth and progression. This information, if obtainable, would help reduce the number of unnecessary polypectomies that occur in patients.

In order to increase the rate of adenoma detection and decrease the rate of unnecessary colonoscopy and polyp removal, new screening techniques must be developed. While CT colonography may be a less invasive procedure than traditional colonoscopy, it still requires bowel preparation, and if a growing lesion is detected the patient must then proceed to traditional colonoscopy. A new method to detect methylated DNA in stool requires no bowel preparation and can detect 95% of advanced cancers with 90% specificity<sup>20</sup>. However, only 57% of advanced pre-cancers greater than 1 cm in size were detected, and 73% of those greater than 2 cm in size, which are specifically likely to progress. Furthermore, generally patients must collect and submit their stool samples from home, which could discourage some patients from complying.

Alternatively, a simple, accurate method incorporated as part of routine care could greatly enhance screening coverage of the general population. Primary care physicians have contact with a vast majority of the population that is generally affected by colorectal cancer. 85% or more of all individuals 45 years and older, and over 93% of individuals 65 years and older, visited a health care professional at least once during 2011<sup>32</sup>. While primary care physicians routinely recommend colonoscopy screening and may even offer the service within their practice, long average wait times before the procedure can be scheduled are often cited as reasons for noncompliance<sup>7,36</sup>. However, a test that could be run at the clinic as a part of a routine visit would greatly reduce this problem. Only those with a positive test would be sent for follow-up endoscopy.

Several groups are beginning to investigate different blood-based tests, which have the potential to get patients screened easily and rapidly. Crucially, the test would also address diagnosis of early adenomas in developing regions where the rates of colon cancer are increasing, but where trained endoscopists or equipped facilities may not exist<sup>1</sup>. ELISA methods are one way in which researchers are attempting to detect altered proteins in serum and plasma<sup>17,21</sup>. However, these methods rely on the availability of an antibody specific to their target of interest. By contrast, quantitative proteomics by mass spectrometry does not require an antibody and allows for multiplexing of many peptides within a single assay. Recently, this technique was used in the Min mouse model of intestinal cancer, and 40 proteins were discovered to be differentially expressed in serum from animals bearing early stage cancers compared to wild type animals<sup>14</sup>. While this technique appears promising, more research is needed to determine whether the signals detected are specific to the presence of tumors or to the genotype of the animal, and to determine how sensitive the test is. Here, the Pirc rat model may offer a unique resource to help address these questions. In the male (F344xBN)F<sub>1</sub>-Pirc rat at 90 days of age, half of the animals develop 1-2 colonic tumors while the other half bear no colonic tumors (Appendix E). First, by comparing serum or plasma from tumor bearing Pirc rats to serum from tumor free Pirc rats, we can specifically test whether the presence of a tumor alters the serum proteome. Second, since these rats develop only a few tumors compared with the hundreds throughout the gastrointestinal tract of the B6-Min mouse, we can determine the threshold for detection.

While transcripts altered within the colonic tumor do not fully correlate with protein changes observed in the serum<sup>14</sup>, these candidates should be investigated as targets both for early detection and early intervention. Furthermore, transcripts that are altered in apparently normal mucosa either in tumor bearing individuals (Appendix E) or in individuals predisposed to cancer

or invasion (Chapters 2 and 3) may offer an even earlier glimpse into events initiating tumorigenesis. One particular candidate highlighted here, *Bcat1*, shows increased expression in normal tissue previously exposed to an inflammatory environment compared to uninflamed normal tissue, even further increased in expression in spontaneous tumors, and expression even higher yet in tumors associated with inflammation, which will eventually become more invasive than their spontaneous counterparts. While it is unknown whether BCAT1 protein is present in serum from patients bearing tumors at levels different than that in serum from patients without tumors, it may be a target for detection at the tissue level or in other biological fluids, or for chemoprevention. In 2012, a patent application was filed for a Bcat1 inhibitor, specifically for the treatment of cancer and inflammatory diseases<sup>27</sup>. Our studies in the Pirc-Bcat1 knockout rat (Appendix G) may give important insight into the role of *Bcat1* in early tumorigenesis, especially that associated with inflammation.

**Chemoprevention.** The companion to early detection in decreasing the morbidity and mortality from colon cancer is chemoprevention. Polyps that can be prevented by changes in lifestyle or diet will reduce the proportion that eventually develop into cancer. Often, potential chemopreventive agents are first recognized through epidemiological studies. While these observational studies are valuable, confounding variables often make it difficult to tease apart factors with an active role in altering disease susceptibility versus other factors. For example, individuals who eat a healthy diet may be more likely to also exercise, undergo routine preventative care, and take vitamin supplements. Controlled supplementation trials in humans can also be difficult to achieve for the same reasons, as well as for regulatory reasons. Therefore, experi-



mental models play a crucial role in helping to understand what factors can impact disease risk most.

Here, we have explored two highly debated potential chemopreventives: vitamin D (Chapters 3 and 4) and aspirin (Appendix B). While these studies form a basis for further investigation, more study is needed to determine if and when these agents play a role in preventing polyp formation or their transition to cancer. Moreover, it is essential to determine which subsets of patients would specifically benefit most in the face of any potential adverse effects.

In humans, the strongest data for vitamin D currently is that of an association between increased serum vitamin D levels and decreased risk for developing colon cancer. Although much is known about potential vitamin D mechanisms as related to cancer *in vitro*, this is understood to a lesser extent *in vivo*. Owing to the complex regulation of vitamin D within the body, it is likely that some *in vivo* effects will not be recapitulated *in vitro*. Testing of this association in animal models is crucial to determine the best compound, dose and timing for supplementation before introduction to the general human population or specific patient subsets for the prevention or treatment of colon cancer.

Long-term aspirin use is also associated with a decreased risk for colon cancer. Aspirin may exert its effects early, by preventing growth of adenomas. In two randomized, double-blind trials involving FAP patients, this was indeed shown to be the case: 100 mg aspirin per day for 6-10 months<sup>13</sup> or 600 mg aspirin per day for greater than two years<sup>4</sup>, significantly reduced mean polyp size compared with the placebo groups. While this growth inhibition has also been shown *in vitro*<sup>28</sup>, we are unaware of any published study of the effects of aspirin supplementation on polyp size in humans without a predisposing disease. It is possible that when aspirin is removed from the system this growth repression may disappear allowing escape of the adenomas towards

cancer. Future study should investigate this in more detail, specifically focusing on adenoma growth before, during and after interval supplementation by aspirin.

Although the alginate molding method for determining tumor volume (Chapter 5) was developed after the completion of the studies described here, it has the potential to greatly enhance future studies. In the rat, both absolute tumor volume and change in volume between visits can be measured before, during and after supplementation by various potential chemopreventive agents, including vitamin D and aspirin. Even if a compound does not affect terminal tumor multiplicity, it may impact tumor growth. This aspect of tumor biology is important to understand, as chemopreventives that can inhibit tumor growth could reduce the rate of colon cancer. Further, by understanding at what stage during development the tumor is affected- initiation, growth or progression- we can learn a great deal more about the biology of the tumor at each of those stages.

Animal modeling is not a perfect answer to cancer in the uncontrolled human population. Colon cancer is a disease with a long latency<sup>15</sup>, and may take decades to develop. If chemopreventive agents need to be in place long before initiation of a lesion, this may not be possible in the relatively short-lived animal models. Genetic models of intestinal cancer may also not reflect the initiating mechanism by which the majority of human colon cancers develop, and therefore chemopreventive agents may not work in a similar manner. Nonetheless, rodent models currently offer the best platform in which to manipulate the diet, environment and genome to test the role of these factors in colonic tumorigenesis. Crucially, any chemopreventive that would be recommended routinely to prevent colon cancer would need to demonstrate benefits that clearly outweigh any associated risks. Both vitamin D and aspirin, in our model<sup>12</sup> and in

human studies<sup>9,13,25</sup>, have shown adverse effects depending on the dose or the population studied. These aspects can be more safely modeled in the rat prior to testing in humans.

### **III. SUMMARY**

The Pirc rat has proven to be a valuable asset in the study of colorectal cancer. Specifically, the range of tumor fates and stages observed has allowed us to examine early events that may indicate future tumor phenotypes. We have demonstrated that DSS treatment of the Pirc rat enhances tumor multiplicity, growth and invasion, similar to that seen in ulcerative colitis patients with cancer. Gene signatures in normal colonic tissue from DSS-treated rats that foreshadow the development of the tumor have been discussed and the function of one candidate, *Bcat1*, is being explored further in a knockout rat model. We have also assessed the effects of two potential chemopreventive agents, vitamin D and aspirin, on tumor multiplicity and size. These preliminary studies lay the foundation for further study of when, where and at what dose these compounds may be effective. The results from each of these studies in the Pirc rat will help us to better understand the detection and treatment of the disease in human populations. Finally, our new method for quantitatively determining tumor volume *in vivo* will expand the parameters of the tumor that investigators at large can study. Taken together, studies in the human and rat will each help to increase early detection and prevention of polyps to reduce the toll from colorectal cancer.

## **References**

1. **Ahmed F.** 2013. Barriers to colorectal cancer screening in the developing world: The view from Pakistan. *World Journal of Gastrointestinal Pharmacology and Therapeutics*. **4**:83–5.
2. **Amos-landgraf JM, Clipson L, Newton MA, Dove WF.** 2012. The many ways to open the gate to colon cancer. *Cell Cycle*. **11**:1261–1262.
3. **Amos-Landgraf JM, Irving AA, Hartman C, Hunter A, Laube B, Chen X, Clipson L, Newton MA, Dove WF.** 2011. Monoallelic silencing and haploinsufficiency in early murine intestinal neoplasms. *Proceedings of the National Academy of Sciences USA*. **109**:2060–2065.
4. **Burn J, Bishop DT, Chapman PD, Elliott F, Bertario L, Dunlop MG, Eccles D, Ellis A, Evans DG, Fodde R, et al.** 2011. A randomized placebo-controlled prevention trial of aspirin and/or resistant starch in young people with familial adenomatous polyposis. *Cancer Prevention Research*. **4**:655–65.
5. **Centers for Disease Control.** 2013. Colorectal cancer screening rates remain low. <http://www.cdc.gov/media/releases/2013/p1105-colorectal-cancer-screening.html> (Accessed 11/20/13).
6. **Charette A, Fletcher R.** 2013. Colon polyps (beyond the basics). UpToDate. <http://www.uptodate.com/contents/colon-polyps-beyond-the-basics> (Accessed 11/20/13).
7. **Denberg TD, Melhado T V, Coombes JM, Beaty BL, Berman K, Byers TE, Marcus AC, Steiner JF, Ahnen DJ.** 2005. Predictors of Nonadherence to Screening Colonoscopy. *Journal of Internal Medicine*. **11**:989–995.
8. **Fu Y, Foden JA, Khayter C, Maeder ML, Reyon D, Joung JK, Sander JD.** 2013. High-frequency off-target mutagenesis induced by CRISPR-Cas nucleases in human cells. *Nature Biotechnology*. **31**:;822–6.
9. **Gallicchio L, Helzlsouer KJ, Chow W-H, Freedman DM, Hankinson SE, Hartge P, Hartmuller V, Harvey C, Hayes RB, Horst RL, et al.** 2010. Circulating 25-hydroxyvitamin D and the risk of rarer cancers: design and methods of the Cohort Consortium Vitamin D Pooling Project of Rarer Cancers. *American Journal of Epidemiology*. **172**:10–20.
10. **Geurts AM, Cost GJ, Freyvert Y, Zeitler B, Miller JC, Choi VM, Jenkins SS, Wood A, Cui X, Meng X, et al.** 2009. Knockout rats via embryo microinjection of zinc-finger nucleases. *Science*. **325**:433.

11. **Heresbach D, Barrioz T, Lapalus MG, Coumaros D, Bauret P, Potier P, Sautereau D, Grimaud JC, Serraj I, Branger B, et al.** 2008. Miss rate for colorectal neoplastic polyps: a prospective multicenter study of back-to-back video colonoscopies. *Endoscopy*. **4**:284–290.
12. **Irving AA, Halberg RB, Albrecht DM, Plum LA, Krentz KJ, Clipson L, Drinkwater N, Amos-Landgraf JM, Dove WF, DeLuca HF.** 2011. Supplementation by vitamin D compounds does not affect colonic tumor development in vitamin D sufficient murine models. *Archives of Biochemistry and Biophysics*. **515**:64–71.
13. **Ishikawa H, Wakabayashi K, Suzuki S, Mutoh M, Hirata K, Nakamura T, Takeyama I, Kawano A, Gondo N, Abe T, et al.** 2013. Preventive effects of low-dose aspirin on colorectal adenoma growth in patients with familial adenomatous polyposis: double-blind, randomized clinical trial. *Cancer Medicine*. **2**:50–56.
14. **Ivancic MM, Huttlin EL, Chen X, Pleiman JK, Irving A a, Hegeman AD, Dove WF, Sussman MR.** 2013. Candidate serum biomarkers for early intestinal cancer using  $^{15}\text{N}$  metabolic labeling and quantitative proteomics in the  $\text{Apc}^{\text{Min/+}}$  mouse. *Journal of Proteome Research*. **12**:4152–66.
15. **Jones S, Chen W-D, Parmigiani G, Diehl F, Beerenwinkel N, Antal T, Traulsen A, Nowak M a, Siegel C, Velculescu VE, et al.** 2008. Comparative lesion sequencing provides insights into tumor evolution. *Proceedings of the National Academy of Sciences USA*. **105**:4283–8.
16. **Kim EB, Fang X, Fushan AA, Huang Z, Lobanov A V, Han L, Marino SM, Sun X, Turanov AA, Yang P, et al.** 2011. Genome sequencing reveals insights into physiology and longevity of the naked mole rat. *Nature*. **479**:223-227.
17. **Ladd J, Buson TB, Johnson M.** 2012. Increased plasma levels of the APC-interacting protein MAPRE1, LRG1 and IGFBP2 preceding a diagnosis of colorectal cancer in women. *Cancer Prevention Research*. **4**:655-664.
18. **Larsson M, Asp E, Johansson, Lü XC, Röhme D, Levan G.** 1998. Sublocalizing the centromeric region in linkage groups from three metacentric rat chromosomes by FISH. *Mammalian Genome*. **9**:479–81.
19. **Li D, Qiu Z, Shao Y, Chen Y, Guan Y, Liu M, Li Y, Gao N, Wang L, Lu X, et al.** 2013. Heritable gene targeting in the mouse and rat using a CRISPR-Cas system. *Nature Biotechnology*. **31**:681–3.
20. **Lidgard GP, Domanico MJ, Bruinsma JJ, Light J, Gagrat ZD, Oldham-Haltom RL, Fourrier KD, Allawi H, Yab TC, Taylor WR, et al.** 2013. Clinical performance of an automated stool DNA assay for detection of colorectal neoplasia. *Clinical Gastroenterology and Hepatology*. **11**:1313–8.

21. **Lin D, Alborn WA, Slebos RJC, Liebler DC.** 2013. Comparison of protein immunoprecipitation-multiple reaction monitoring with ELISA for assay of biomarker candidates in plasma. *Journal of Proteome Research*. [Epub ahead of print].
22. **Mashimo T, Kaneko T, Sakuma T, Kobayashi J, Kunihiro Y, Voigt B, Yamamoto T, Serikawa T.** 2013. Efficient gene targeting by TAL effector nucleases coinjected with exonucleases in zygotes. *Scientific Reports*. **3**:1253.
23. **Medical College of Wisconsin Bioinformatics Program.** Rat Genome Database: Variant Visualizer. <http://rgd.mcw.edu/rgdweb/front/select.html>. (Accessed 11/20/13).
24. **Medical College of Wisconsin Bioinformatics Program.** Rat Genome Database. <http://www.rgd.mcw.edu>. (Accessed 11/20/13).
25. **Mulholland HG, Murray LJ, Anderson L a, Cantwell MM.** 2011. Vitamin D, calcium and dairy intake, and risk of oesophageal adenocarcinoma and its precursor conditions. *The British Journal of Nutrition*. **106**:732–41.
26. **National BioResource Project for the Rat in Japan.** <http://www.anim.med.kyoto-u.ac.jp/nbr/>. (Accessed 11/20/13).
27. **Papathanassiou A.** 2012. Patent Application: Methods of treatment using a bcat1 inhibitor.
28. **Pathi S, Jutooru I, Chadalapaka G, Nair V, Lee S-O, Safe S.** 2012. Aspirin inhibits colon cancer cell and tumor growth and downregulates specificity protein (Sp) transcription factors. *PloS One*. **7**:e48208.
29. **Pickhardt PJ, Kim DH, Pooler BD, Hinshaw JL, Barlow D, Jensen D, Reichelderfer M, Cash BD.** 2013. Assessment of volumetric growth rates of small colorectal polyps with CT colonography: a longitudinal study of natural history. *The Lancet Oncology*. **14**:711–20.
30. **Rat Resource and Research Center.** <http://www.rrrc.us>. (Accessed 11/20/13).
31. **Rijn JC van, Reitsma JB, Stoker J, Bossuyt PM, Deventer SJ van, Dekker E.** 2006. Polyp miss rate determined by tandem colonoscopy: a systematic review. *The American Journal of Gastroenterology*. **101**:343–50.
32. **Schiller JS, Lucas JW, Ward BW, Peregoy JA.** 2012. Summary health statistics for U.S. adults: National Health Interview Survey, 2010. *Vital and Health Statistics*. **10**:1–207.
33. **Schoen RE, Pinsky PF, Weissfeld JL, Lance A, Reding DJ, Hayes RB, Church T, Yurgalevich S, Doria-rose VP, Hickey T, et al.** 2010. Utilization of surveillance colonoscopy in community practice. *Gastroenterology*. **138**:73–81.

34. **Schoenfeld P, Cohen J.** 2013. Quality indicators for colorectal screening colonoscopy. *Tech Gastrointest Endosc.* **15**:59–68.
35. **Silver L.** 1995. Karyotypes, chromosomes, and translocations. In: *Mouse genetics: concepts and applications.* Oxford University Press. pp. 83–92.
36. **Singh H, Coster C De, Shu E, Fradette K, Latosinsky S, Pitz M, Cheang M, Turner D.** 2010. Wait times from presentation to treatment for colorectal cancer: a population-based study. *Canadian Journal of Gastroenterology.* **24**:33–9.
37. **University of California Davis.** Knockout Mouse Project Repository. <http://www.komp.org>. (Accessed 11/20/13).
38. **Wolfe K, Sharp P.** 1993. Mammalian gene evolution: nucleotide sequence divergence between mouse and rat. *Journal of Molecular Evolution.* **37**:441–456.
39. **Zhao S, Shetty J, Hou L, Delcher A, Zhu B, Osoegawa K, Jong P De, Nierman WC, Strausberg RL, Fraser CM.** 2004. Human, mouse, and rat genome large-scale rearrangements: stability versus speciation. *Genome Research.* **10A**:1851–1860.

## Appendix A

### **Reciprocal F<sub>1</sub> crosses to investigate the influence of maternal and paternal strain on tumor number and time to emergence**

Amy A. Irving designed this project (in collaboration with James M. Amos-Landgraf), directed the experiments, analyzed the data and wrote the Appendix. Madeline R. Ford performed the endoscopies, dissections and terminal tumor counts and managed the data. William F. Dove served as an advisor.



The human population shows great variability in susceptibility to disease, and colon cancer risk is no exception. To better understand what genes might be responsible for some of this variation, rodent models with an array of genetic backgrounds can be utilized. The Pirc rat shows differences in phenotype depending on the rat strain on which the mutation is carried. Brown Norway (BN) Pirc rats are highly resistant to developing colonic tumors, often surviving greater than one year without forming tumors. By contrast, ACI-Pirc rats are quite susceptible to colonic tumor formation, becoming moribund due to high tumor burden around 180 days of age. F344-Pirc rats show an intermediate phenotype between BN and ACI.

As part of an experiment to find a cross that would yield only a few tumors in a reasonable amount of time (see Appendix E), Pirc rats of susceptible strains (F344 and ACI) were crossed to BN, which are resistant to forming intestinal tumors. Four crosses were examined, with the first strain representing the maternal strain and the second representing the paternal strain: (F344-Pirc x BN) $F_1$ , (BN x F344-Pirc) $F_1$ , (ACI-Pirc x BN) $F_1$ , and (BN x ACI-Pirc) $F_1$ . The Pirc allele was always brought in through either the ACI or the F344 strain (never from BN), as designated by a hyphen in the nomenclature (e.g. F344-Pirc).

Rats underwent endoscopy monthly between 30 and 150 days of age for a total of five visits. This allowed us to determine the latency to tumor formation in each of the crosses. Upon dissection and following formalin-fixation, tumors of the small intestine and colon were counted. (BN x ACI-Pirc) $F_1$  male rats developed tumors in the distal colon more rapidly compared to the reciprocal cross of (ACI-Pirc x BN) $F_1$  males (Fig A-1, top panels). Crosses involving the ACI strain were dissected at 180 days (Fig A-2). Female (ACI-Pirc x BN) $F_1$  and (BN x ACI-Pirc) $F_1$  rats did not differ in terminal colonic tumor number (2-sided Wilcoxon rank sum  $p=0.85$ ). However, male (BN x ACI-Pirc) $F_1$  rats showed a statistically

**Fig A-1.** Latency to colonic tumor emergence. Male rats underwent endoscopy monthly between 30 and 150 days of age. The number of rats with 0 tumors (blue bars), 1-2 tumors (red bars) and 3-5 tumors (gray bars) are shown for each of the four reciprocal crosses at each time point. (BN x ACI-Pirc) $F_1$  rats tended to get their first tumor about a month earlier than (ACI-Pirc x BN) $F_1$  rats. (F344-Pirc x BN) $F_1$  males also appeared to develop colonic tumors more rapidly than (BN x F344-Pirc) $F_1$  males, though data are limited. ND, not done.

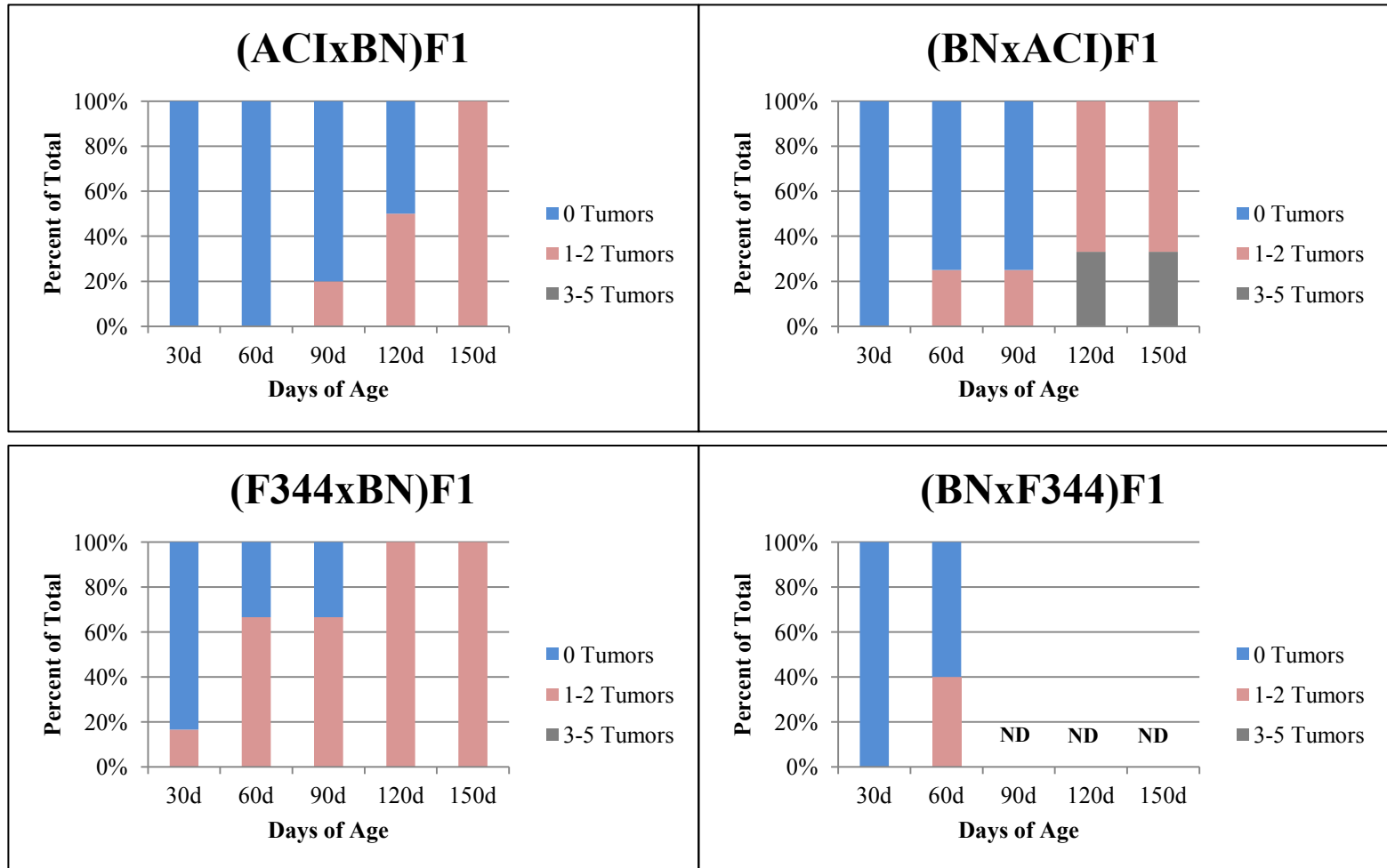
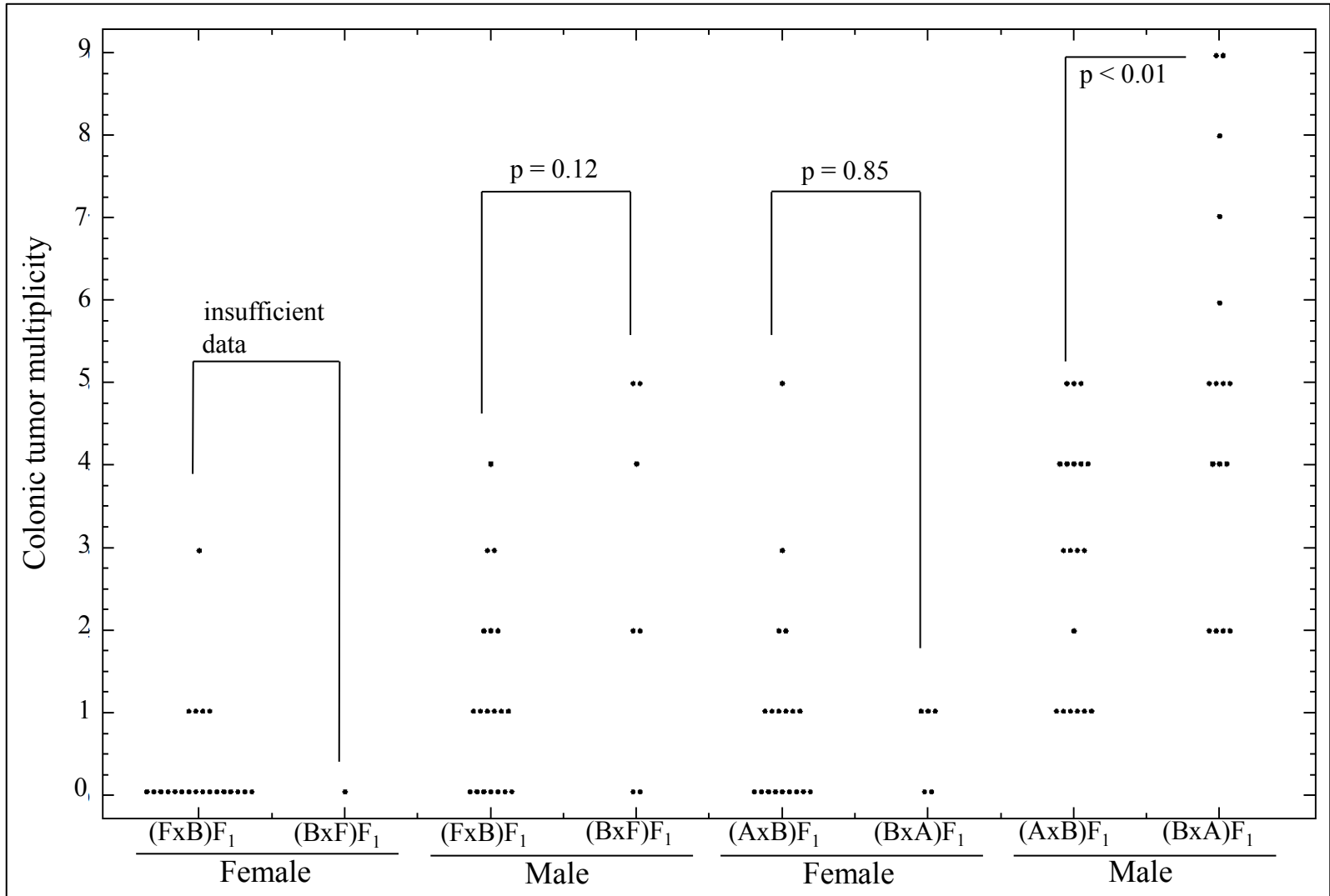


**Fig A-2.** Terminal counting of colonic tumors revealed that only the male (ACI-Pirc x BN) $F_1$  and (BN x ACI-Pirc) $F_1$  cross had significantly different terminal colonic tumor multiplicities from one another; the other reciprocal crosses were each not statistically different or had insufficient data to make a judgment.



significant increase in terminal total tumor number ( $p=0.05$ ) and colonic tumor number ( $p<0.01$ ) over male (ACI-Pirc x BN) $F_1$  rats.

The F344 by BN crosses showed an even more dramatic difference in tumor latency between the two reciprocal matings. (F344-Pirc x BN) $F_1$  male rats developed distal tumors much more rapidly than their (BN x F344-Pirc) $F_1$  counterparts (Fig A-1, bottom panels). Crosses involving the F344 strain were dissected at 210 days (Fig A-2). Insufficient numbers of female (BN x F344-Pirc) $F_1$  rats were generated during the study to determine with statistical significance whether they differed from female (F344-Pirc x BN) $F_1$  rats. Despite the apparent difference in tumor latency, no statistically significant difference was found between terminal colonic tumor counts in (F344-Pirc x BN) $F_1$  versus (BN x F344-Pirc) $F_1$  male ( $p=0.12$ ) rats.

One caveat to endoscopy is that it allows visualization of only the distal two-thirds of the rat colon. Therefore, differences between observations made by endoscopy and those made by terminal dissection could be explained by this bias in data acquisition.

In this small study, there appears to be an indication that parental strain of origin may affect tumor multiplicity in offspring. Genomic imprinting, an epigenetic process depending on parent of origin, may be one cause for this observation. Imprinted alleles may silence a gene so that expression comes only from the allele derived from one of the two parental types. A second possibility is that the strain of the mother and her resultant milk production and care of her offspring may affect tumor multiplicity, which can be tested by foster studies. The amount of grooming that a pup receives early in life helps to determine portions of the pups epigenome<sup>1</sup>. These epigenetic patterns persist into adulthood. One well-known candidate that has been studied in relation to this phenomenon is the GR gene. When GR is more greatly methylated, as occurs in less frequently groomed pups, these pups

become anxious. Different rat strains care for their pups to varying degrees and increased pup stress could plausibly lead to greater colonic tumors later in life.

Alternatively, there is equal likelihood that we were testing the effect of maternal versus paternal input of the Pirc allele rather than parental strain, since the Pirc allele was always brought in through ACI or F344, regardless of the sex of the animal. Further study, including crosses where the Pirc allele was brought in through BN, would be required to tease apart this possible interaction.

### **References**

1. **University of Utah Genetic Science Learning Center.** “Lick your rats.” 2009. Available from: <http://learn.genetics.utah.edu/content/epigenetics/rats/> (Accessed 11/3/13).

## Appendix B

### **Aspirin does not protect against colonic tumor formation in the Pirc rat in the presence or absence of inflammation induced by dextran sodium sulfate**

Amy A. Irving designed this project in collaboration with James M. Amos-Landgraf, performed the majority of the rat dissections and endoscopies (assisted by Kathleen J. Krentz), completed all of the data analysis and wrote the Appendix. Linda Clipson created and edited the figures. Norman Drinkwater gave statistical advice. James M. Amos-Landgraf initiated the design of the original experiments and offered both technical and intellectual support throughout the project. William Blaser generated the test diets, and Jennifer Pleiman and Sarah Hamilton analyzed longitudinal tumor data. William F. Dove served as an advisor.

**Abstract**

Epidemiological studies indicate that aspirin is associated with a lower risk of colon cancer. We have used a genetic model of familial colon cancer, the  $Apc^{Pirc/+}$  (Pirc) rat, to investigate the effect of aspirin on sporadic colonic tumors. In addition, by treating Pirc rats with dextran sodium sulfate (DSS) we tested aspirin on inflammation-associated colonic tumors. Longitudinal endoscopic monitoring allowed us to test the efficacy of aspirin in preventing newly arising colonic tumors and against established colonic tumors. Aspirin failed to reduce sporadic or inflammation-associated tumor multiplicities or to alter tumor growth profiles in the Pirc rat.

## **Introduction**

Colorectal cancer is the third leading cause of cancer-related death in men and women in the US<sup>1</sup>. Epidemiological studies have shown that aspirin is associated with a reduced risk of colon cancer. Though conflicting reports exist, epidemiological observations have shown that individuals who take aspirin regularly have a reduced risk of developing colon cancer.

Aspirin has been suspected as a potential chemopreventive agent in part because of its ability to inhibit prostaglandin synthesis. Prostaglandins and cyclooxygenase enzymes are associated with polyp development and blocking these pathways may in turn prevent colorectal cancer<sup>16</sup>. Randomized trials have shown that aspirin reduces short-term risk of recurrent adenomas in patients following polypectomy<sup>19</sup>. However, a short-term trial in patients with hereditary nonpolyposis colorectal cancer (HNPCC) found that treatment with aspirin for up to four years had no effect on the incidence of colorectal adenomas or cancer<sup>5</sup>.

Whether aspirin can prevent spontaneous adenomas in individuals without a history of colon cancer has also proven difficult to establish. A randomized placebo-controlled study involving nearly 40,000 individuals without a previous history of cancer enrolled in the Women's Health Study showed no effect of 100 mg of aspirin administered every other day after a follow-up of ten years<sup>6</sup>. By contrast, a meta-analysis of two randomized trials- the British Doctors Aspirin Trial and the UK-TIA trial- showed aspirin to be effective as a primary chemopreventive agent after a follow-up of ten years<sup>10</sup>. Recently, a case-control study by Din *et al* showed that aspirin was associated with a reduced risk of colorectal cancer when taken daily for only five years at the lowest dose (75 mg/day)<sup>8</sup>. An extensive meta-analysis by Rothwell and colleagues of four randomized trials, in which prevention of vascular events was the primary endpoint, has



demonstrated that the chemopreventive effects of aspirin for colon cancer become increasingly apparent the longer an individual took aspirin<sup>18</sup>. This long-term administration scenario in humans is more difficult to model in animals; our study focuses specifically on short-term intervention.

In this report, we have utilized a model for familial colon cancer, the *Apc*<sup>Pirc/+</sup> rat, to test aspirin as a chemopreventive and therapeutic<sup>2</sup>. The Pirc rat is a suitable model to study human colon cancer as it is heterozygous for a mutation in *Apc*, and this tumor suppressor gene is mutated in approximately 80% of human colorectal cancers<sup>9</sup>. The Pirc rat spontaneously develops a high incidence and multiplicity of tumors in the colon rather than those in the small intestine, in contrast to most mouse models. Further, tumors in the Pirc rat have been previously shown to be responsive to celecoxib, similar to the human<sup>9</sup>. Treatment of Pirc rats with dextran sodium sulfate (DSS), a polymer that increases the multiplicity and level of invasion of colonic tumors, allows us to study tumors with potentially different etiologies. Therefore, both untreated and DSS-treated Pirc rats have been utilized to test the effect of aspirin. To complement terminal tumor counts, rats underwent routine endoscopy to detect any changes in colonic tumor emergence, growth rate, or regression.

## **Materials and Methods**

**Animal Breeding and Maintenance.** Rats were maintained under a university-approved protocol in a facility in the McArdle Laboratory approved by the American Association of Laboratory Animal Care. Rats were housed in standard caging with free access to food and acidified water. F1 rats were generated by breeding ACI *Apc*<sup>+/+</sup> females (Harlan, Indianapolis, IN) to F344

*Apc*<sup>Pirc/+</sup> N10-N12 males (developed in this laboratory and now commercially available through Taconic, Hudson, NY). The number of small intestinal versus colonic tumors differs between the various inbred strains of Pirc rats<sup>2</sup>. F1 generation rats were used in these studies to shift the distribution of the tumors even further in favor of colonic tumors.

**Chemicals.** Dextran sodium sulfate (500 kDa) was purchased from Fisher Scientific (Pittsburgh, PA). Acetylsalicylic acid was purchased from Sigma Life Science (St. Louis, MO).

**Diets.** Control rats were fed either AIN-76A (vehicle) or 5020 chow (Purina, St. Louis, MO); no difference between these diets was seen for tumor multiplicity, time to first tumor, or growth of tumor. Therefore, control rat data from both diets were combined. The aspirin-supplemented diet was formulated in the AIN-76A base diet using 5% (w/w) Wesson soybean oil and 0.25% (v/w) ethanol (Pharmaco Aaper, Brookfield, CT) as a vehicle; Wesson oil and ethanol were also added to the AIN-76A base diet for control animals.

Aspirin was added to the diet to provide 25 mg acetylsalicylate /kg body weight/day. The daily dose of aspirin was calculated based on a consumption rate of 20 grams of food per rat per day. These aspirin levels were based on human studies reporting that 300 mg aspirin per day was effective to decrease the incidence of colonic tumors<sup>10</sup>. From these studies, we extrapolated the effective dose in animals by using the body surface area conversion between the human and the rat<sup>21</sup>.

**Rat Experimental Design.** At 33 days of age, male and female (ACI x F344)F1 *Apc*<sup>Pirc/+</sup> rats were assigned to one of two diets: vehicle or aspirin. At 40 days of age half of the animals were given 4% (w/v) DSS in the drinking water to study DSS-induced tumors. The DSS dosing regi-

men consisted of two rounds of DSS, each lasting seven days and separated by a seven-day period without DSS. The dose and molecular weight of DSS used in these experiments did not cause severe damage to the colonic epithelium. Treated animals had normal crypt architecture, inflammatory infiltrates were minimal, and body weight was not affected until the tumor burden became high (see Chapter 1). Protocol assignment was random, except that sexes and littermates were evenly distributed (Fig B-1). Animals underwent colonoscopy every other week starting before diet supplementation until sacrifice at 140 days of age or when they became moribund. Weights were measured at each colonoscopy visit and at sacrifice. At sacrifice, the small intestine and colon were opened longitudinally, laid flat, washed with PBS and formalin-fixed; the small intestine was divided into four equal sections before fixation. Blood was obtained at sacrifice by cardiac puncture.

**Endoscopy, Terminal Tumor Counts, and Salicylate Assay.** Endoscopy was performed on rats at predetermined intervals until sacrifice (Fig B-1). Briefly, the animal was anesthetized with isoflurane and placed on a sterile surgical field. The colon was flushed with warm saline to remove any fecal material and to lubricate the colon. The anatomy of the rat allows the distal two-thirds of the colon to be visualized by the endoscope. Video and still images of colonic tumors were obtained and analyzed after each colonoscopy visit. Endoscopy began before dietary supplementation, which allowed us to examine the effects of the compounds both on existing tumors (treatment) and to prevent newly arising tumors (chemoprevention). The longitudinal fate of tumors from Pirc rats not given DSS was determined by three observers blinded to the diet of the animal; in the DSS-treated Pirc rat, tumor multiplicity increased too rapidly to accurately correlate tumors between visits. Tumors were examined at all visits and any tumor that appeared at least twice during the study was given one of four scores: growing, static, regressing

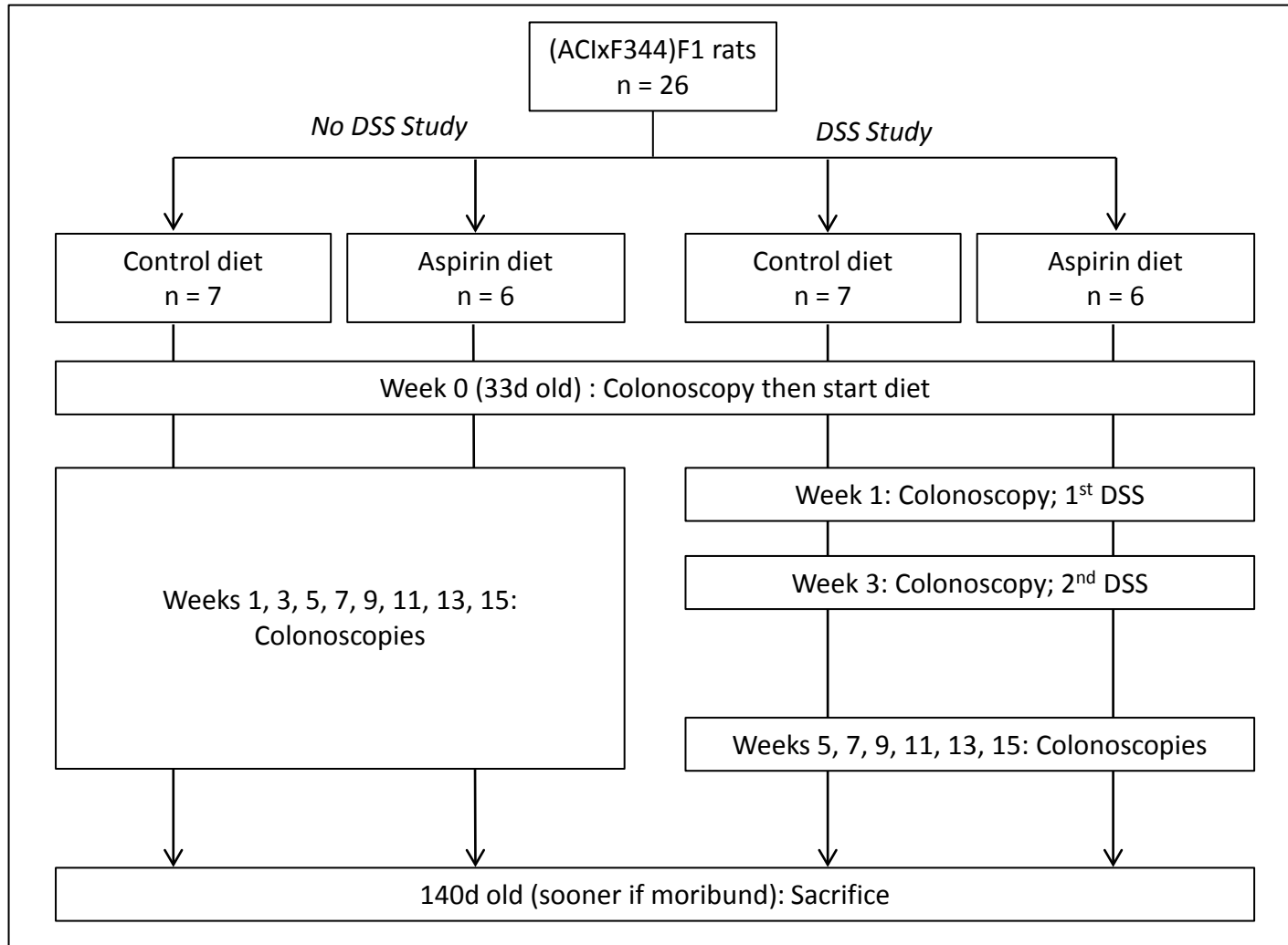
or unscorable; those judged to be unscorable were excluded from longitudinal analysis. A score was generated based on agreement between at least two of the three blinded observers. After sacrifice, formalin-fixed tumors were counted on a dissecting microscope. Total tumor counts were obtained for each of the four small intestinal sections and for the entire colon. Serum salicylate assays were run by the University of Wisconsin-Madison Clinical Laboratory.

**Statistical Methods.** For terminal tumor counts and the serum salicylate assay, a two-sided Wilcoxon rank sum test was used to test whether the experimental group differed from the control group; a p-value  $\leq 0.05$  was considered significant. Tumor multiplicities in the Pirc rat show significant sex differences, as described previously<sup>2</sup>. Therefore, terminal multiplicity data of the Pirc rat were blocked by sex based on Lehmann's extension to the Wilcoxon rank sum test<sup>14</sup> and both sexes were tested jointly for an effect of aspirin. Longitudinal analysis of endoscopic images utilized a chi-square test of growing versus non-growing tumors; no significant sex-specific differences in this ratio of tumor fates were observed, therefore sexes were combined for analysis.

## **Results**

**Aspirin did not reduce the multiplicity of colonic tumors in Pirc rats.** Groups of Pirc rats underwent endoscopy to identify existing tumors and were then placed on diet supplemented with aspirin. Although serum salicylate levels were significantly increased in these Pirc rats, the multiplicity of tumors in neither the small intestine nor colon were reduced (Fig B-2, Table B-1).

**Fig B-1.** Experimental design. Protocol time points are given in weeks; ages of animals are given in days. In the DSS study, rats were given 4% DSS in the drinking water following colonoscopy at weeks 1 and 3. Each DSS treatment lasted for one week; during week 2 these rats were given regular drinking water.



Additional Pirc rats underwent endoscopy to identify and exclude from analysis any existing tumors and were then placed on diet supplemented with aspirin prior to their first DSS treatment. Again, serum salicylate levels were significantly increased without affecting the multiplicity of tumors in the small intestine or colon (Fig B-2, Table B-1).

**Supplementation with aspirin did not cause tumor regression in Pirc rats.** Rats routinely underwent endoscopy throughout the study. Thus, any substantial change in existing tumors or emergence of newly formed tumors in the distal colon would have been detected. Most of the colonic tumors were newly emerging during this study. Supplementation of Pirc rats with aspirin did not appear to inhibit the appearance of these newly emerging colonic tumors (Fig B-3). Only 3 of 200 scorable tumors appeared to regress; these regressing tumors occurred in the control group (Fig B-4). Instead, aspirin significantly enhanced the proportion of growing versus non-growing tumors (chi-squared  $p = 0.003$ ).

All rats not treated with DSS survived until the termination of the study. However, about half of the DSS-treated rats also given aspirin had to be sacrificed before the scheduled 140 day time point, owing to weight loss likely due to the high tumor burden.

**Table B-1.** Terminal small intestinal and colonic tumor counts. Note: Tumor multiplicities in the Pirc rat show significant sex differences, as previously described. Therefore, terminal multiplicity data of the Pirc rat were blocked by sex based on Lehmann's extension to the Wilcoxon rank sum test and both sexes were tested jointly for an effect of aspirin. A  $p$ -value  $\leq 0.05$  was considered significant.

DSS?	Diet	n (female, male)	Small Intestine			Colon		
			Count, mean $\pm$ SD		p-value	Count, mean $\pm$ SD		p-value
			Female	Male		Female	Male	
No	Control	4, 3	2 $\pm$ 2	6 $\pm$ 3	0.17	4 $\pm$ 2	23 $\pm$ 7	0.38
	Aspirin	3, 3	1 $\pm$ 1	14 $\pm$ 5		8 $\pm$ 3	19 $\pm$ 7	
Yes	Control	3, 4	0.3 $\pm$ 0.6	10 $\pm$ 5	0.85	45 $\pm$ 11	58 $\pm$ 3	0.006
	Aspirin	3, 3	1 $\pm$ 0	8 $\pm$ 4		56 $\pm$ 1	66 $\pm$ 4	

**Fig B-2.** Terminal total intestinal tumor counts. Supplementation with aspirin failed to reduce the multiplicity of intestinal tumors in male (filled circles) or female (open circles) Pirr rats, with (right panel) or without (left panel) DSS treatment.

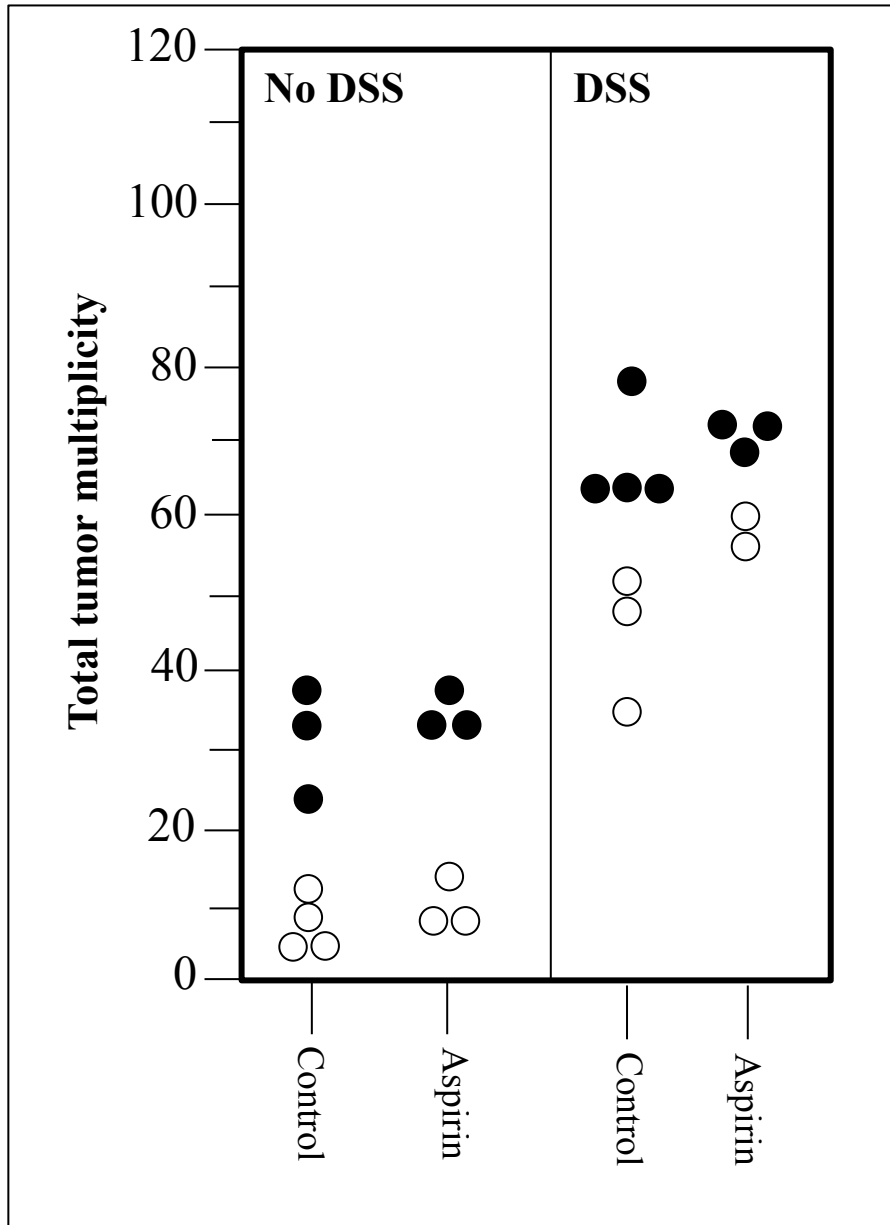


**Fig B-3.** Longitudinal endoscopic tracking of colonic tumors in the Pirr rat. Each row represents a single animal from either the control (top), or aspirin (bottom) supplemented diets. Each column represents one time point when a still image of the tumor(s) was acquired. Aspirin did not prevent further growth of existing tumors (white arrows) or appearance of new tumors (black arrows).

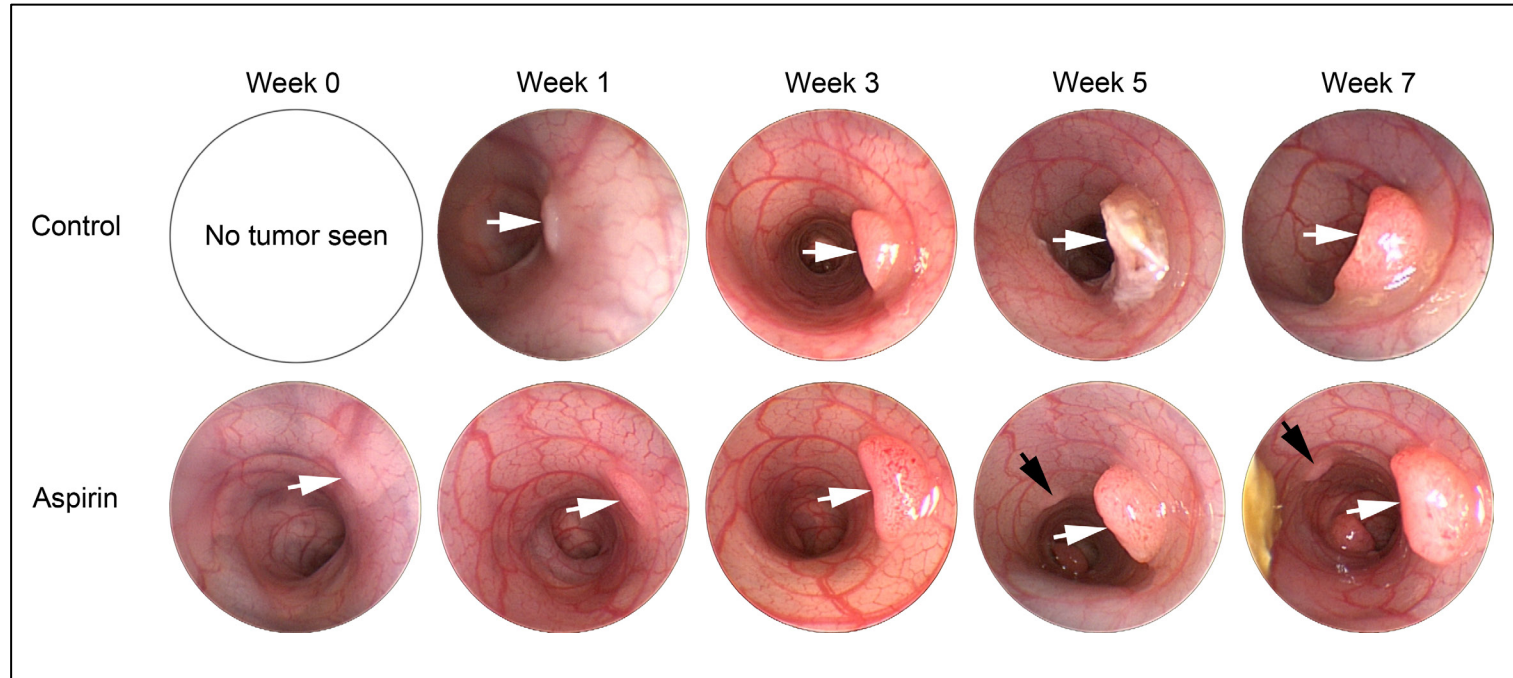
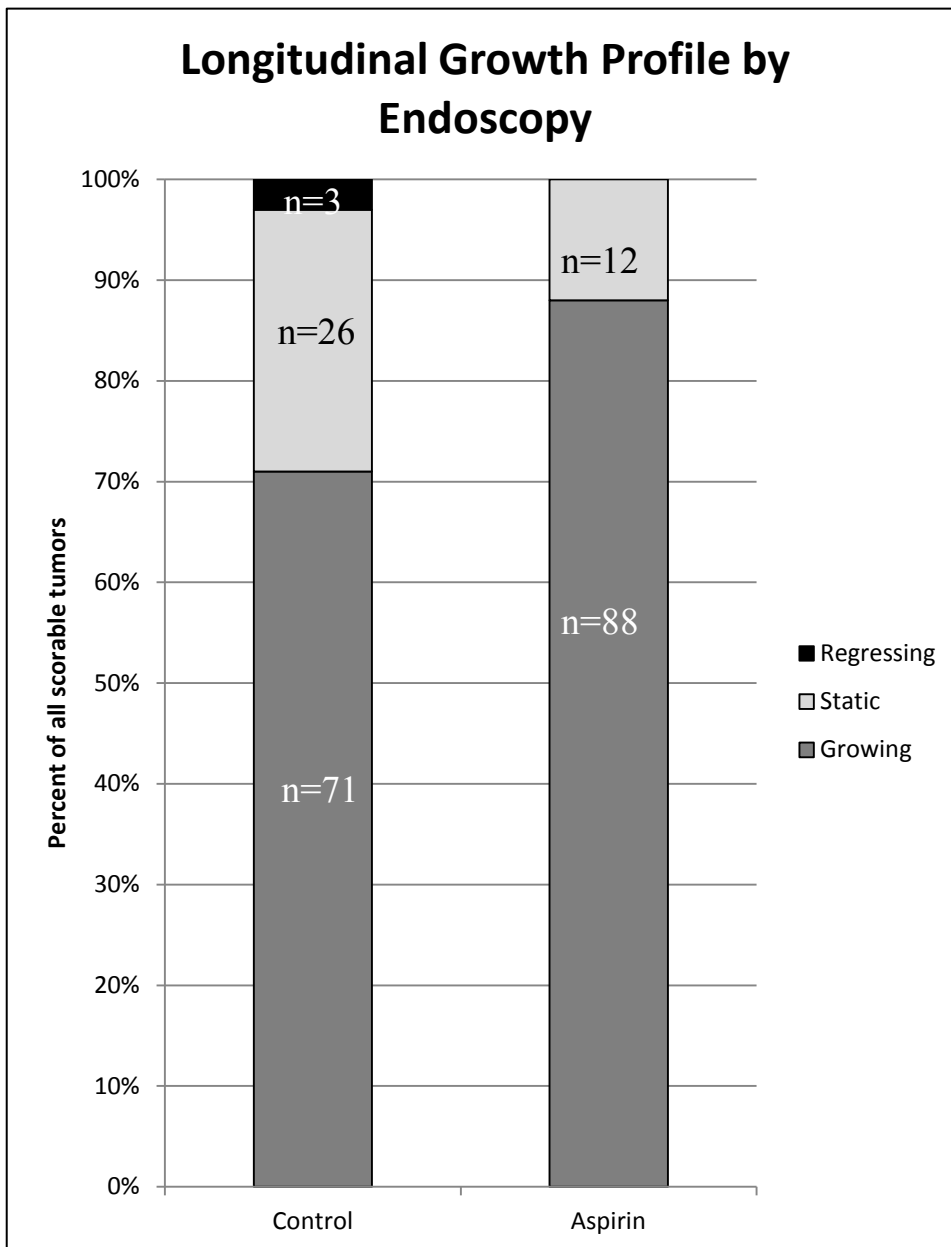




**Fig B-4.** Assessment of longitudinal tumor growth profile. In a total of 200 tumors, only 3 appeared to regress and these tumors occurred in the control group. Aspirin significantly enhanced the proportion of growing colonic tumors in the Pirc rat (chi-squared  $p = 0.003$ ).



## **Discussion**

These studies were designed to test the effects of aspirin both on existing tumors and in preventing newly arising tumors during short-term administration in a sporadic (Pirc) and inflammation-associated (DSS-treated Pirc) rat model. This study is unique because we were able to assess action by aspirin in both chemopreventive and treatment modes, by utilizing longitudinal endoscopic monitoring to visualize the emergence of new tumors. The use of longitudinal monitoring provided the further advantages of detecting concurrent appearance and disappearance of tumors and changes in tumor size over time; such information would be lost with terminal tumor counting alone.

Overall, these studies constitute a comprehensive investigation of whether supplementation by aspirin provides any protective effect against colon tumors in an animal model. We have shown that within the constraints of this study design, aspirin failed to reduce colonic tumor multiplicity in Pirc rats. Further, we have also shown that aspirin failed to reduce the number of newly emerging tumors, and actually enhanced the proportion of growing colonic tumors.

Colon cancer is a disease with a long latency period<sup>13</sup>. Therefore, chemopreventive agents may need to be in place for a decade or more to show an effect in humans<sup>13</sup>. In our study, supplemented diets were given for a significant portion of the natural lifespan of the laboratory rat, which is approximately two years. Owing to their relatively short lifespan compared to humans, rodent models may not provide an appropriate test of chemopreventive agents, such as aspirin, that may require a long treatment period to exert a significant effect<sup>7</sup>. Nonetheless, some agents have recently been shown to be chemopreventive in humans over a short period of time<sup>12</sup>.

The negative results published herein gain significance in contrast to positive results with other chemopreventive agents. A 40-day treatment with celecoxib was shown to significantly reduce tumor multiplicity in Pirc rats<sup>2</sup>. Additionally, 25-50 day studies of the combination of d,l- $\alpha$ -difluoromethylornithine (DFMO) and piroxicam in the Min mouse seeded the human trials of DFMO and sulindac<sup>11,20</sup>. Thus, in some cases rodent models can offer an important platform for short-term studies of chemoprevention.

These cases of short-term supplementation are a high priority to understand, particularly for the individuals at risk of recurrent adenoma formation. Patients who have had a polyp removed are at enhanced risk of developing subsequent colonic tumors. Therefore, these individuals represent a focused group in which to study chemopreventive agents. Randomized trials examining patients with a history of adenomas or cancer have shown that short-term aspirin use reduces the risk of recurrent adenomas of the colorectum. Sandler *et al* randomized 635 patients with a personal history of colon cancer to either placebo or 325 mg of aspirin daily<sup>19</sup>. Within thirteen months of randomization, only 17% (43/259) of those patients in the aspirin group had at least one adenoma compared to 27% (70/258) of those patients in the placebo group. Furthermore, among those taking aspirin, significantly fewer recurrent adenomas per patient were found, at significantly later times than in the placebo group. In a similar study, Baron *et al* randomized 1121 patients with a personal history of adenomas to either placebo, 81 mg of aspirin daily, or 325 mg of aspirin daily<sup>3</sup>. At follow-up colonoscopy performed at least one year following randomization, only the 81 mg daily aspirin dose was protective against development of new lesions. In this group there was a 19% reduction in the risk of adenomas and a 40% reduction in the risk of advanced lesions. These data, taken together, may indicate that aspirin has greater effects against advanced lesions than early lesions.

In contrast, patients with HNPCC randomized to either placebo or 600 mg of aspirin daily for two years had no difference in incidence of colorectal adenomas or carcinomas compared with patients given placebo<sup>5</sup>. Evidence is accumulating to suggest that tumors develop through different pathways<sup>23</sup> and may not respond in the same manner to chemoprevention with certain compounds. In this context, Rothwell and colleagues have shown that aspirin is protective only against cancers of the proximal colon and rectum but not against those in the distal colon<sup>18</sup>. This may represent a differential response to specific cancer sites. This further supports our study of tumors specifically in the colon and not solely small intestinal tumors, the target of many previous chemopreventive studies in Min mice.

In our study, aspirin did not reduce the multiplicity of tumors in the small intestine or colon, despite increases in serum salicylate to about 3-6 mg/dl ( $p < 0.03$  compared to vehicle controls). Single oral doses of 1000 mg in the human produce serum levels of 3.1-11.4 mg/dl two hours after ingestion, which fall to about 2.6 mg/dl ten hours after ingestion<sup>4</sup>.

Different rodent models testing the effect of aspirin on intestinal tumor formation show contradictory results. An important difference may exist between genetic and chemical models of colorectal neoplasia, or between colonic ACFs and tumors. Similarly to our study, Reuter *et al* saw no effect on the number or size of small intestinal or colonic tumors in Min mice treated with aspirin<sup>17</sup>. In contrast, wild type rats injected with the chemical carcinogen azoxymethane followed by treatment with aspirin show a reduction in the formation of aberrant crypt foci (ACFs), a controversial surrogate for colonic tumors<sup>22</sup>.

One explanation for this paradox comes from the Multiple Pathway Hypothesis cited above<sup>23</sup>. The study of patients with HNPCC by Burn *et al* would indicate that different pathways respond to chemoprevention differently<sup>5</sup>. Although the evidence for aspirin against sporadic

cancers appears strong, no effect of aspirin was found in patients with HNPCC after four years of use.

Another resolution to this apparent paradox is that aspirin may act at the initial stage of adenomagenesis, as speculated by Levine and Ahnen<sup>15</sup>. Studies examining the efficacy of aspirin as a chemopreventive agent for colorectal cancer in general human populations have shown that significant effects can be observed only after five years of supplementation with follow-up performed at least ten years after starting the aspirin regimen<sup>10</sup>. This lag may represent a differential response to early stages of colon cancer.

By contrast, human studies by Sandler *et al* and Baron *et al* have suggested that aspirin may be more effective against advanced lesions<sup>3,19</sup>. If this is true, relatively short-lived animal models may not fully recapitulate colon cancer in humans, as a majority of the tumors in these animal models are early or locally invasive adenomas and not frank cancers.

In this study we have shown that aspirin failed to prevent the formation of both sporadic colon tumors in the Pirc rat and inflammation-associated tumors in the DSS-treated Pirc rat. Longitudinal endoscopy enabled us to detect changes in tumor growth patterns over time; however, no change was observed upon aspirin supplementation in either the sporadic or inflammatory model of colon cancer.

Further study in appropriate rodent models under controlled dietary conditions are needed to investigate whether there is a dose of aspirin that prevents the emergence of new colonic tumors or slows the growth of either sporadic or inflammatory tumors. Once an effective dose is established, further work can delve deeper into an important question: does aspirin work early in tumor emergence or later during tumor development and progression?

## References

1. **American Cancer Society.** 2008. Colorectal Cancer Facts & Figures 2011-2013.
2. **Amos-Landgraf JM, Kwong LN, Kendzierski CM, Reichelderfer M, Torrealba J, Weichert J, Haag JD, Chen K-S, Waller JL, Gould MN, et al.** 2007. A target-selected Apc-mutant rat kindred enhances the modeling of familial human colon cancer. *Proceedings of the National Academy of Sciences USA.* **104**:4036–41.
3. **Baron JA, Cole BF, Sandler RS, Haile RW, Ahnen D, Bresalier R, McKeown-Eyssen G, Summers RW, Rothstein R, Burke CA, et al.** 2003. A randomized trial of aspirin to prevent colorectal adenomas. *The New England Journal of Medicine.* **348**:891–9.
4. **Baselt R.** 2002. Acetylsalicylic Acid. In: *Disposition of Toxic Drugs & Chemicals in Man.* 6th Editio. Biomedical Publications.
5. **Burn J, Bishop DT, Mecklin J-P, Macrae F, Moslein G, Olschwang S, Bisgaard M-L, Ramesar R, Eccles D, Maher E, et al.** 2009. Effect of aspirin or resistant starch on colorectal neoplasia in the Lynch syndrome. *The New England Journal of Medicine.* **360**:1462-1463.
6. **Cook NR, Lee I-M, Gaziano JM, Gordon D, Ridker PM, Manson JE, Hennekens CH, Buring JE.** 2005. Low-dose aspirin in the primary prevention of cancer: the Women's Health Study: a randomized controlled trial. *The Journal of the American Medical Association.* **294**:47–55.
7. **Corpet DE, Pierre F.** 2005. How good are rodent models of carcinogenesis in predicting efficacy in humans? A systematic review and meta-analysis of colon chemoprevention in rats, mice and men. *European Journal of Cancer.* **41**:1911–22.
8. **Din FVN, Theodoratou E, Farrington SM, Tenesa A, Barnetson R a, Cetnarskyj R, Stark L, Porteous ME, Campbell H, Dunlop MG.** 2010. Effect of aspirin and NSAIDs on risk and survival from colorectal cancer. *Gut.* **59**:1670–9.
9. **Fearnhead N, Britton M, Bodmer W.** 2001. The ABC of Apc. *Human Molecular Genetics.* **10**:721–733.
10. **Flossmann E, Rothwell PM.** 2007. Effect of aspirin on long-term risk of colorectal cancer: consistent evidence from randomised and observational studies. *Lancet.* **369**:1603–13.
11. **Halberg RB, Katzung DS, Hoff PD, Moser AR, Cole CE, Lubet RA, Donehower LA, Jacoby RF, Dove WF.** 2000. Tumorigenesis in the multiple intestinal neoplasia mouse: redundancy of negative regulators and specificity of modifiers. *Proceedings of the National Academy of Sciences USA.* **97**:3461–6.

12. **Hosono K, Endo H, Takahashi H, Sugiyama M, Sakai E, Uchiyama T, Suzuki K, Iida H, Sakamoto Y, Yoneda K, et al.** 2010. Metformin suppresses colorectal aberrant crypt foci in a short-term clinical trial. *Cancer Prevention Research*. **3**:1077–83.
13. **Jones S, Chen W-D, Parmigiani G, Diehl F, Beerenwinkel N, Antal T, Traulsen A, Nowak M a, Siegel C, Velculescu VE, et al.** 2008. Comparative lesion sequencing provides insights into tumor evolution. *Proceedings of the National Academy of Sciences USA*. **105**:4283–8.
14. **Lehmann E.** 1998. *Nonparametrics: Statistical Methods Based on Ranks*. Revised Fifth Ed. Prentice Hall (Upper Saddle River, NJ).
15. **Levine JS, Ahnen DJ, New T, Journal E, Dec B.** 2006. Adenomatous Polyps of the Colon. *New England Journal of Medicine*. **355**:1–9.
16. **Nelson C.** 1995. Aspirin prevention update: new data on lung and colon cancers. *Journal of the National Cancer Institute*. **87**:567–569.
17. **Reuter BK, Zhang X, Miller MJS.** 2002. Therapeutic utility of aspirin in the *Apc*<sup>Min/+</sup> murine model of colon carcinogenesis. *BMC Cancer*. **2**:19.
18. **Rothwell PM, Wilson M, Elwin C, Norrving B, Algra A, Warlow CP, Meade TW.** 2010. Long-term effect of aspirin on colorectal cancer incidence and mortality: 20-year follow-up of five randomised trials. **9754**:1741-1750.
19. **Sandler RS, Halabi S, Baron JA, Budinger S, Paskett E, Keresztes R, Petrelli N, Pipas JM, Karp DD, Loprinzi CL, et al.** 2003. A randomized trial of aspirin to prevent colorectal adenomas in patients with previous colorectal cancer. *New England Journal of Medicine*. **348**:883–90.
20. **Meyskens FL Jr, McLaren CE, Pelot D, Fujikawa-Brooks S, Carpenter PM, Hawk E, Kelloff G, Lawson MJ, Kidao J, et al.** 2008. Difluoromethylornithine plus sulindac for the prevention of sporadic colorectal adenomas: a randomized placebo-controlled, double-blind trial. *Cancer Prevention Research*. **1**:32–38.
21. **US Food and Drug Administration.** 2010. Oncology Tools: Dose Calculator. Available from: <http://www.accessdata.fda.gov/scripts/cder/onctools/animalquery.cfm> (Accessed 4/2009).
22. **Wargovich MJ, Jimenez A, McKee K, Steele V, Velasco M, Woods J, Price R, Gray K, Kelloff G.** 2000. Efficacy of potential chemopreventive agents on rat colon aberrant crypt formation and progression. *Carcinogenesis*. **21**:1149–1155.
23. **Wood LD, Parsons DW, Jones S, Lin J, Sjöblom T, Leary RJ, Shen D, Boca SM, Barber T, Ptak J, et al.** 2007. The genomic landscapes of human breast and colorectal cancers. *Science*. **318**:1108–13.

## Appendix C

### **Dextran Sodium Sulfate does not induce colonic tumorigenesis in the TGF- $\beta$ R2 mutant rat**

Amy A. Irving designed this project (in collaboration with James M. Amos-Landgraf), performed the endoscopies and dissections, completed the data analysis, and wrote the Appendix.



Transforming growth factor, beta receptor II (TGF- $\beta$ R2) is a transmembrane protein that inhibits cell growth and division<sup>1</sup>. Somatic TGF- $\beta$ R2 mutations have been linked to an increased risk of some cancers, and about 30% of malignant colon tumors contain TGF- $\beta$ R2 mutations<sup>2</sup>.

To test whether an inflammatory stimulus would initiate colonic tumorigenesis in a rat model with a mutated TGF- $\beta$ R2 gene, we treated rats heterozygous and homozygous for the TGF- $\beta$ R2 mutation with dextran sodium sulfate (DSS). Eight total rats (4 TGF- $\beta$ R2 heterozygous mutants and 4 TGF- $\beta$ R2 homozygous mutants) were given 4% DSS (500 kDa MW) from 40-47 and 54-61 days of age and were dissected at 210 days of age. None of the DSS-treated TGF- $\beta$ R2 heterozygous mutants developed any tumors, but one of the TGF- $\beta$ R2 homozygous mutants treated with DSS developed a single tumor.

Since this study did not include untreated TGF- $\beta$ R2 mutants or DSS-treated wild type animals it is impossible to tell whether the TGF- $\beta$ R2 mutation or the DSS-treatment is responsible for the development of a single tumor. We have observed colonic tumor development in DSS-treated wild type animals, albeit at a very low frequency (see Chapter 1). This small study would indicate that mutations in TGF- $\beta$ R2 might make the intestine more susceptible to inflammatory insult, resulting in the development of colonic tumors. However, a larger study including the above-mentioned controls is needed to determine the effect of added inflammation in the TGF- $\beta$ R2 mutant rat.

## References

1. **TGF-BR2 Genecards**. <http://www.ncbi.nlm.nih.gov/gene/7048>. (Accessed 11/15/2013)
2. **Bellam N, Pasche B**. 2010. Tgf-beta signaling alterations and colon cancer. *Cancer Treatment Research*. **155**:85–103.

## **Appendix D**

### **Dextran sodium sulfate does not induce colonic tumorigenesis in a p53 knockout rat**

Amy A. Irving designed this project (in collaboration with James M. Amos-Landgraf), performed the endoscopies and dissections (assisted by Madeline R. Ford), completed the data analysis, created the figures and wrote the Appendix.

Mutations in p53 are common in colon cancer, especially in more advanced cases<sup>1</sup> and those associated with inflammation<sup>2,3</sup>. In a small pilot study we wanted to determine if *Apc*<sup>+/+</sup> rats lacking p53 (CrI:WI(UL)-*Tp53*<sup>m1/Hubr</sup>, Charles River) would be more susceptible to tumorigenesis induced by the inflammatory agent dextran sodium sulfate (DSS). A total of 13 Wistar rats wild type for *Apc* (3 p53<sup>+/+</sup>, 8 p53<sup>+/-</sup>, and 2 p53<sup>-/-</sup>) were given two rounds of 4% DSS (500 kDa) each lasting one week and separated by a one week period of regular drinking water. Rats were allowed to age as old as 380 days; however, no intestinal tumors were discovered in any of the rats (Table D-1, top panel).

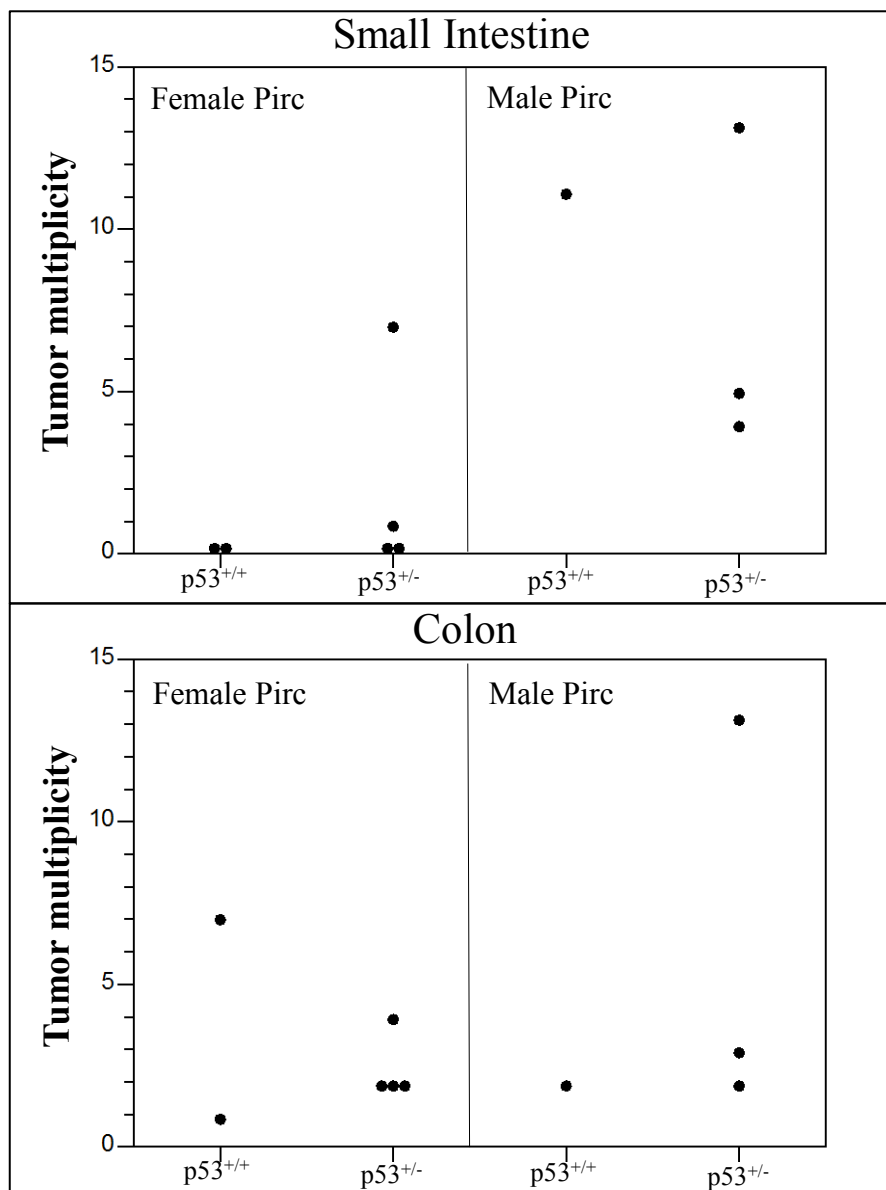
The p53 null rats were then crossed to two parental Pirc lines (ACI and F344) to determine whether p53 in heterozygous form would alter the Pirc phenotype. The loss of one allele of p53 did not appear to significantly alter tumor multiplicities in either of the parental Pirc lines (Table D-1, bottom two panels). The number of animals was limited to 1-4 per cross. The greatest number of animals occurred in the (ACI x Wistar)F<sub>1</sub> cross. Here, there was no difference in the number of tumors in the small intestine or the colon (Fig D-1).

We did not further pursue this project to determine what effect complete loss of p53 would have on the Pirc phenotype. It is likely that p53 expression needs to be completely lost in order to see a difference in tumor phenotype. However, even though we did not see differences in tumor multiplicity in p53<sup>+/-</sup> Pirc rats, there may have been a difference in tumor stage. These samples were not studied histologically so this is currently unknown. Deeper phenotyping may be needed to see any differences in Pirc tumors that have also lost p53 expression.

**Table D-1.** Based on a limited number of samples, DSS did not induce tumorigenesis in Wistar  $p53^{+/+}$ ,  $p53^{+/-}$  or  $p53^{-/-}$  rats (top panel). When the  $p53$  knockout rat was crossed to two *Pirc* parental lines (ACI and F344) in a very limited number of samples, there did not appear to be differences in small intestinal or colonic tumor multiplicity in male or female *Pirc* rats, regardless of whether they had both alleles or only one allele of  $p53$  (bottom two panels).

Strain/Cross	Sex	Apc genotype	P53 genotype	DSS tx?	N of animals	Tumor Multiplicity	
						Small Intestine	Colon
Wistar	F	+/+	+/+	Y	2	0	0
		+/+	+/-	Y	3	0	0
		+/+	-/-	Y	2	0	0
	M	+/+	+/+	Y	1	0	0
		+/+	+/-	Y	5	0	0
(ACIxWistar)F1	F	<i>Pirc</i> /+	+/+	N	2	0	4 ± 4.2
		<i>Pirc</i> /+	+/-	N	4	2 ± 3.4	2.5 ± 1
	M	<i>Pirc</i> /+	+/+	N	1	11	2 ± 0
		<i>Pirc</i> /+	+/-	N	3	7.3 ± 4.9	6 ± 6.1
(F344xWistar) F1	F	<i>Pirc</i> /+	+/+	N	1	1	1
		<i>Pirc</i> /+	+/-	N	-	-	-
	M	<i>Pirc</i> /+	+/+	N	3	12.7 ± 3.1	3 ± 2.6
		<i>Pirc</i> /+	+/-	N	-	-	-

**Fig D-1.** Small intestinal and colonic tumor multiplicities in male and female (ACI $\times$ Wistar) $F_1$  Pirc rats either wild type or heterozygous for p53. Based on a limited number of samples, there did not appear to be differences in tumor multiplicity in the small intestine (top) or colon (bottom) in male or female Pirc rats, regardless of whether they had one or both alleles of the p53 gene.



## References

1. **Berg FM van den, Tigges AJ, Schipper ME, Hartog-Jager FC den, Kroes WG, Walboomers JM.** 1989. Expression of the nuclear oncogene p53 in colon tumours. *The J of Path.* **157**:193–9.
2. **Risques RA, Rabinovitch PS, Brentnall TA.** 2006. Cancer surveillance in inflammatory bowel disease: new molecular approaches. *Current Opin in Gastro.* **22**:382–90.
3. **Vogelstein B, Fearon E, Hamilton S, Kern S, Preisinger A, Leppert M, Nakamura Y, White R, Smits A, Bos J.** 1988. Genetic alterations during colorectal-tumor development. *New England J of Med.* **319**:525–32.

## **Appendix E**

### **Whole genome analysis of Field Cancerization in the Pirr rat**

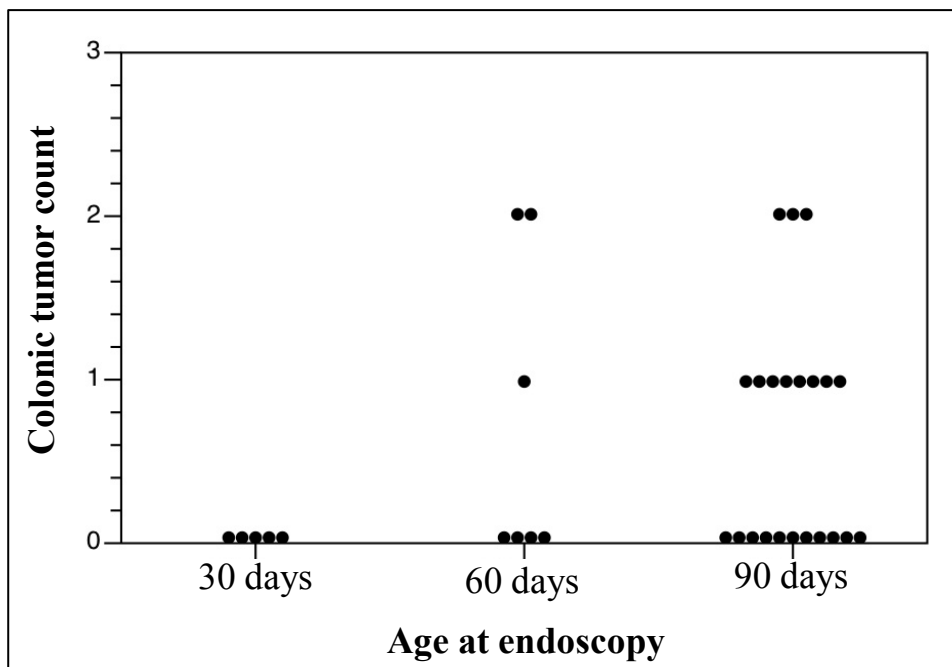
Amy A. Irving designed this project (in collaboration with James M. Amos-Landgraf and Jennifer Pleiman), created the figures and wrote the Appendix. Madeline R. Ford performed the endoscopies and dissections, managed the data, isolated and prepared the RNA samples for microarray analysis, and completed the data analysis. Microarrays were run by the McArdle Shared Services Microarray Facility. William F. Dove served as an advisor.

The term “field cancerization” was first coined by Danely P. Slaughter in 1953 when he observed that a subset of patients formed multiple oral squamous cancers at a higher rate than would be predicted in a random population<sup>3</sup>. He suggested that this phenomenon may be caused by changes that occur in the normal tissue that predispose it to forming tumors. These changes may either be causative and occur before formation of the first tumor or else they may be a symptom of tumor formation. Experiments investigating the field cancerization hypothesis in the intestine have been conducted in the *Apc*<sup>Min/+</sup> (Min) mouse in our laboratory, which resulted in the discovery of two genes that were differentially expressed in normal colonic epithelium between tumor-bearing mice and tumor-free mice: *Irg1* and *Pde4b*. In the rat, we sought to perform a similar experiment to ask whether we could find differentially expressed genes in a rodent model of another genus. Second, we sought to determine whether any of the gene candidates found in the rat showed overlap with those that had been previously observed in the Min Mouse Field Effect study, or in rat, mouse or human adenomas of the colon.

We found that crossing F344 to BN-Pirc to generate (F344xBN)F<sub>1</sub>-Pirc offspring resulted in the development of an optimal number of tumors (0-2 per animal) in a reasonable time frame (90 days of age) ideal for this experiment (Fig E-1). This low tumor multiplicity allowed us to harvest the normal colonic epithelium from a subset of Pirc rats that had not formed tumors and from tumor-bearing Pirc rats with a reduced likelihood that we were harvesting a nascent tumor. At 90 days of age Pirc rats underwent colonoscopy to pair a tumor-free rat with a tumor-bearing rat for dissection. The paired rats were then dissected side-by-side so that normal colonic epithelium could be harvested from the same area of the colon in both rats, determined by the location of the tumor in the tumor-bearing rat. Tissue was preserved in RLTplus buffer and the remainder of the intestine was formalin-fixed.



**Fig E-1.** Longitudinal colonic tumor counts by endoscopy. (F344xBN)F<sub>1</sub>-Pirc male rats underwent endoscopy at 30, 60 and 90 days to determine the optimal time point for dissection. Our goal was to find a time point when roughly half of the rats had no visible colonic tumors and the other half had 1-2 colonic tumors. We found that this distribution occurred around 90 days of age.

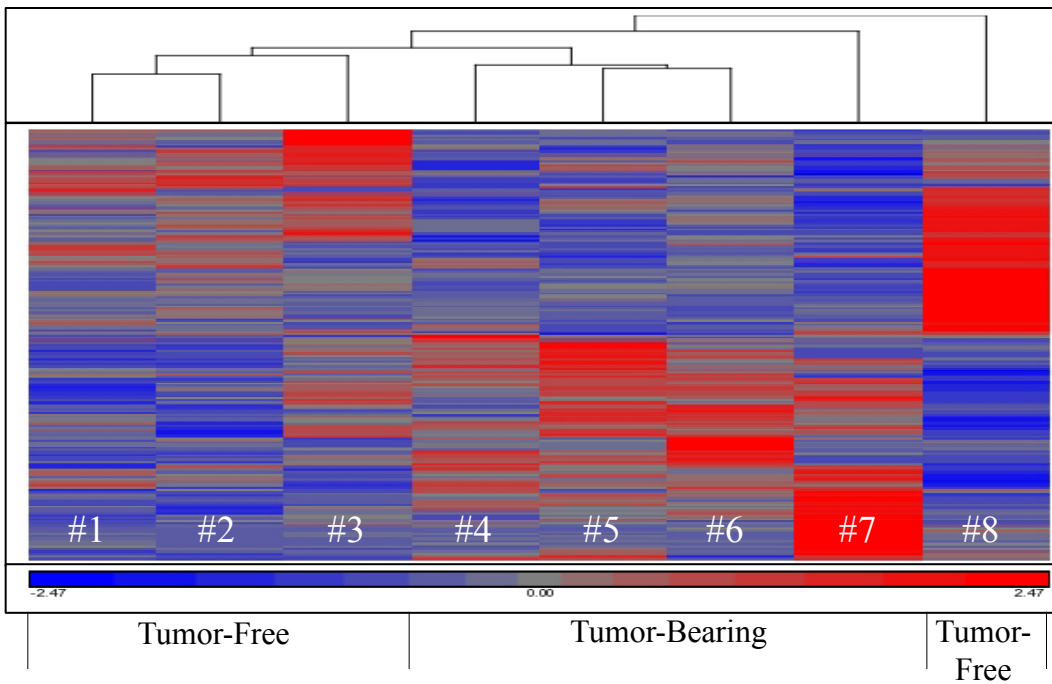


RNA was isolated from the harvested normal epithelium, checked for integrity using a NanoDrop and BioAnalyzer and made into cDNA for microarray analysis. One microarray with four normal epithelium samples from tumor-free rats and four normal epithelium samples from tumor-bearing rats was run to generate preliminary data. Upon analysis using Partek Genomics Suite, we found that the differences between the two sample types were small. 235 genes were differentially expressed at a threshold of 2-fold or greater, while only 18 of the genes were differentially expressed at a threshold of 3-fold or greater (Supplementary Table S-8). Through hierarchical clustering of the samples based on the list of 235 genes, one sample (#8) stands out as a clear outlier (Fig E-2). Sample #7 also appears to differ from the remaining samples. However, it is evident from this heat map that, for this set of genes, those represented in the top portion of the map seem to be expressed at a higher level in tumor-free Pirc rats compared to tumor-bearing Pirc rats, whereas genes represented in the bottom portion of the map seem to be expressed at a higher level in tumor-bearing rats compared to tumor-free Pirc rats.

The list of genes generated in the Pirc Rat Field Effect study was compared with those from the Min Mouse Field Effect study to determine if there was any overlap; none was found. However, when the list of candidates from the Pirc Rat Field Effect study were compared with candidates from early adenomas in the Min mouse (our lab and online databases), Pirc rat (our lab) or humans (GEO dataset GDS2947) several gene families were in common between multiple genera. The serpin, interleukin (IL), transforming growth factor  $\beta$  (TGF- $\beta$ ), suppressor of cytokine signaling (SOCS) and KCN gene families showed overlap between the rat and human, and the solute carrier (SLC) gene family showed overlap between all three genera.

The serpins function as serine protease inhibitors. Despite poor sequence homology, a highly conserved core structure is shared among family members. Therefore, serpins discovered

**Fig E-2.** Hierarchical clustering of differentially expressed genes. Microarray samples underwent analysis by Partek Genomics Software. A 2-fold cut-off threshold was used to generate a heat map with hierarchical clustering. The four normal epithelial samples from tumor-bearing rats appear more similar in their gene expression profile than do the four normal epithelial samples from tumor-free rats.



to be altered in a disease state in one species may be related to serpins discovered in the same disease state in another species. *Serpin-f1* was down-regulated 2.5-fold in normal colonic epithelium in tumor-free rats in our field effect study. *Serpin-i1* and *Serpin-e1* have each been shown to be differentially expressed between normal colonic tissue and colonic adenomas in human patients<sup>1,2</sup>.

The interleukins are a type of cytokine that regulate immune response and promote the development and differentiation of T and B cells. Interleukin-1 alpha (*Il-1a*) is altered in human adenomas, functions in the inflammatory response and binds to the interleukin-1 receptor (*Il-1r*). *Il-10ra* and *Il-28ra*, both interleukin receptors, are slightly differentially expressed in normal epithelium from tumor-free versus tumor-bearing rats in our field effect study.

TGF- $\beta$ , another class of cytokine, controls proliferation and cellular differentiation in many cells. *TGF- $\beta$ 1* is differentially expressed between normal colonic tissue and colonic adenomas in human patients, and polymorphisms in this gene show an association with colon cancer risk<sup>5</sup>. TGF- $\beta$  receptor 2 is differentially expressed between normal epithelium from tumor-free versus tumor-bearing rats in our field effect study. Mutation of the *TGF- $\beta$ r2* gene has not appeared to affect the Pirc phenotype (see Appendix C), including the rate or multiplicity at which animals develop colonic tumors, but more animals are clearly needed.

The Socs family of genes suppressing cytokine signaling by inhibiting the JAK-STAT pathway. *Socsb* expression was 2.1-fold higher in normal epithelium from tumor-bearing Pirc rats compared to normal epithelium from tumor-free Pirc rats, while *Socs2* expression is altered in human adenoma.

KCN genes encode for potassium channels, which are critical for cell signaling. *Kcnd3* was differentially expressed in the rat field effect study while another family member, *Kcnmb4*,

is differentially expressed in human adenomas. Recently, another potassium channel gene, *Kcnq1*, was shown to be differentially expressed in mouse and human gastrointestinal cancers. Further, this gene was shown to affect cancer phenotype in *Apc*<sup>Min/+</sup> mice, as Min mice lacking *Kcnq1* had significantly more intestinal tumors than Min mice with functional *Kcnq1*<sup>4</sup>.

The SLC superfamily of genes encode for solute carrier proteins. In the Pirc rat Field Effect study, SLC members in the 6, 8, 25, and 38 families were each differentially expressed between normal epithelium from tumor-free versus tumor-bearing rats. In both mouse and human adenomas *Slc2a5* is differentially expressed when compared to normal colonic tissue. In human adenomas SLC members in the 12 and 16 families were also differentially expressed. It is not known to what degree these members could overlap in their functions in cancer between the three genera.

The scope of this study was limited by the small sample size. We expect that differences in normal epithelium between tumor-free and tumor-bearing rats would be subtle at best. Therefore a greater number of highly controlled samples would be needed to detect any potential significant differences. Confirmation of these gene candidates on an individual basis has not yet been pursued.

## **References**

1. **Barderas R, Mendes M, Torres S, Bartolomé RA, López-Lucendo M, Villar-Vázquez R, Peláez-García A, Fuente E, Bonilla F, Casal JI.** 2013. In-depth characterization of the secretome of colorectal cancer metastatic cells identifies key proteins in cell adhesion, migration, and invasion. *Molecular & Cellular Proteomics*. **12**:1602–20.
2. **Mazzoccoli G, Paziienza V, Panza A, Valvano MR, Benegiamo G, Vinciguerra M, Andriulli A, Piepoli A.** 2012. ARNTL2 and SERPINE1: potential biomarkers for tumor aggressiveness in colorectal cancer. *Journal of Cancer Research and Clinical Oncology*. **138**:501–11.

3. **Slaughter D, Southwick H, Smejkal W.** 1953. “Field cancerization” in oral stratified squamous epithelium. *Cancer*. **6**:963-68.
4. **Than BL, Goos JA, Sarver AL, O’Sullivan MG, Rod A, Starr TK, Fijneman RJ, Meijer GA, Zhao L, Zhang Y, et al.** 2013. The role of KCNQ1 in mouse and human gastrointestinal cancers. *Oncogene*. [epub ahead of print].
5. **Wang Y, Yang H, Li L, Xia X.** 2013. An updated meta-analysis on the association of TGF-B1 gene promoter -509C/T polymorphism with colorectal cancer risk. *Oncogene*. **61**:181–187.

## Appendix F

### **N<sub>2</sub> backcrosses to investigate kinky tail phenotype in an (ACIxF344)F<sub>1</sub> female and tumor multiplicity in the N<sub>2</sub> generations of ACI and F344**

Amy A. Irving designed this project (in collaboration with James M. Amos-Landgraf), performed the dissections, completed the data analysis, created the figures and wrote the Appendix. Lindsay B. Young counted the tumors. Norman Drinkwater gave statistical advice. William F. Dove served as an advisor.

A female (ACIxF344)F<sub>1</sub>-Pirc/+ female was observed to have a kinky tail. The “kinky tail” phenotype, due to undulations in the vertebrae, is present in some rodent mutants<sup>2</sup>. We sought to investigate the possibility that a spontaneous mutation arose in one of our strains that would cause this phenotype. To investigate whether the kinky tail was linked to a recessive mutation, we backcrossed the kinky tail female to both ACI and F344 males to generate N<sub>2</sub> litters. Ideally, this female would have been mated back to her father or his siblings, but they were deceased at the time the phenotype was discovered. We were also unable to cross to any siblings of the mother, as she was a purchased breeder from Harlan. We were unable to identify another rat with a kinky tail phenotype in a total of 116 offspring from the original kinky tail female. One possibility is that she suffered a broken tail that misaligned during healing, which could present similar to the kinky tail phenotype.

Despite not finding another rat with a kinky tail, this experiment afforded us the opportunity to determine the tumor multiplicities of the small intestine and colon in the ACI and F344 N<sub>2</sub> populations. After correcting for multiple comparisons, only four comparisons were statistically different from one another: F344-N<sub>2</sub> female rats had significantly more small intestinal tumors than ACI female rats, and male F344, F344-N<sub>2</sub> and (ACIxF344)F<sub>1</sub> rats each had significantly more small intestinal tumors than ACI rats (Fig F-1, Table F-1). These data confirm a previous observation that F344 male rats have a roughly equal distribution of tumors between the small intestine and colon (ratio of  $0.85 \pm 0.47$ ), while ACI male rats have a much lower propensity for developing tumors in the small intestine than the colon (ratio of  $0.18 \pm 0.14$ ).

Dietrich et al has shown that dominant effects can be detected by estimating the number of loci using backcrosses<sup>1</sup>. With additional backcrosses and increased numbers of animals it

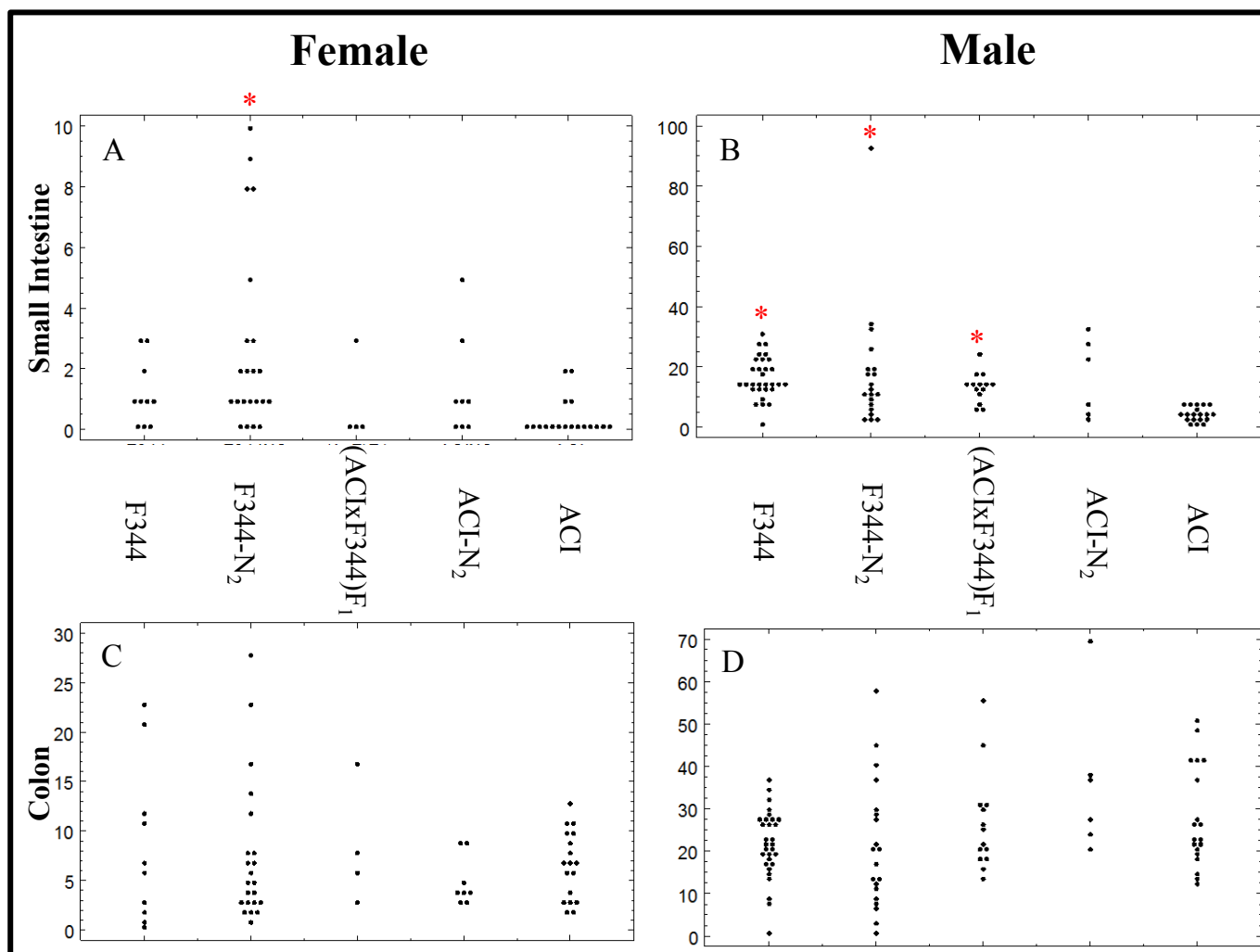


might be possible to determine how many loci exist between F344 and ACI and how they may effect tumor multiplicity. From these data it does appear that the suppressing effect of ACI on small intestinal tumors may be semi-dominant, but this does not appear to be the case for colonic tumors. Though the data is preliminary, the observation that the tumorigenic process and genes controlling tumorigenic potential may differ between the small intestine and colon is highly intriguing.

**Table F-1.** Terminal small intestinal and colonic tumor counts. ACI and ACI-N<sub>2</sub> rats were dissected at 180 days of age, (ACIxF344)F<sub>1</sub> rats were dissected between 180 and 210 days of age, and F344 and F344-N<sub>2</sub> rats were dissected at 210 days of age.

Strain/Cross	Small Intestine (mean ± SD)		Colon (mean ± SD)	
	Female	Male	Female	Male
F344	1.2 ± 1.1	16.6 ± 6.9	8.6 ± 8.1	21.7 ± 8.0
F344-N <sub>2</sub>	2.8 ± 3.1	17.9 ± 19.8	7.6 ± 7.1	21.2 ± 15.1
(ACIxF344)F <sub>1</sub>	0.8 ± 1.5	13.5 ± 5.0	8.5 ± 6.0	26.6 ± 11.8
ACI-N <sub>2</sub>	1.4 ± 1.8	16.5 ± 13.1	5.1 ± 2.5	36.2 ± 18.0
ACI	0.3 ± 0.7	4.3 ± 2.6	6.8 ± 3.4	27.7 ± 11.8

**Figure F-1:** Distribution of small intestinal and colonic tumors in female and male Pirr rats of the F344 and ACI strains, their F1 derivative and their respective N<sub>2</sub> generation backcrosses. (A) Only the F344-N<sub>2</sub> differs significantly from ACI in number of small intestinal tumors in female Pirr rats. (B) F344, F344-N<sub>2</sub> and (ACIxF344)F<sub>1</sub> each have significantly more small intestinal tumors than ACI in male Pirr rats. Colonic tumor multiplicities in neither the female (C) or male (D) Pirr rats are significantly different between any of the five strains/crosses. Note: Significance is denoted by a red asterisk (\*) above and indicates a difference between the designated strain and ACI in the respective tumor location and sex. Significance was determined using Pair-wise two-sided Wilcoxon rank sum tests with a Bonferonni correction for multiple comparisons.



**References**

1. **Dietrich W, Katz H, Lincoln SE, Shin HS, Friedman J, Dracopoli NC, Lander ES.** 1992. A genetic map of the mouse suitable for typing intraspecific crosses. *Genetics*. **131**:423–47.
2. **Schrick JJ, Dickinson ME, Hogan BL, Selby PB, Woychik RP.** 1995. Molecular and phenotypic characterization of a new mouse insertional mutation that causes a defect in the distal vertebrae of the spine. *Genetics*. **140**:1061–7.

## Appendix G

### **Generation of *Apc*<sup>Pirc/+</sup>*Bcat1*<sup>-/-</sup> rats to investigate the Priming Effect Hypothesis**

Amy A. Irving designed this project (in collaboration with James M. Amos-Landgraf), created the figures and wrote the Appendix. With assistance from Jennifer Pleiman, Lindsay Young and Madeline R. Ford, Pirc embryos were collected for pro-nuclear injection of *Bcat1* zinc-finger nuclease mRNA by Kathleen Krentz. *Bcat1* mRNA was supplied by our collaborator Dr. Aron Geurts at the Medical College of Wisconsin (Milwaukee, WI). Under the guidance of Dr. Geurts, Michael Grzybowski performed the cloning and sequencing of the resultant animals from the injected embryos. William F. Dove served as an advisor.

Inflammatory diseases of the colon significantly raise the risk of developing colon cancer. An inflammatory microenvironment in the colon may alter gene expression in the normal epithelium to make it more likely to support tumorigenesis. To determine whether gene candidates exist to support this hypothesis, whole genome microarray was used to compare normal colonic epithelium and tumors from untreated Pirc rats to normal colonic epithelium and tumors from DSS-treated Pirc rats. DSS treatment of Pirc rats mimics an inflammatory response and increases both the multiplicity, growth rate and stage of tumors compared to untreated Pirc rats. Refer to Chapter 2 regarding the DSS model and Chapter 3 for a detailed explanation of the microarray studies.

One gene candidate that emerged to support our hypothesis was branched-chain amino-acid transaminase 1, cytosolic, or *Bcat1*. In untreated Pirc rats, colonic tumors have 150-fold greater expression of *Bcat1* than normal colonic epithelium. Tumors from DSS-treated Pirc rats have an even greater expression difference than tumors from untreated Pirc rats, showing over 250-fold greater expression compared with untreated Pirc normal colonic epithelium. (see Chapter 2, Fig 2-4). In support of our hypothesis, *Bcat1* expression in normal colonic epithelium is 50-fold higher in DSS-treated Pirc rats compared to untreated Pirc rats.

*Bcat1* is also a promising candidate in human cancers. *Bcat1* protein is overexpressed in human colon cancers<sup>10</sup> and has recently been shown to be over-expressed in other cancers as well, including glioblastoma<sup>8,9</sup>, chemoresistant epithelial ovarian cancer<sup>6</sup> and nasopharyngeal carcinoma<sup>11</sup>. In colorectal cancer patients, the presence of *Bcat1* protein in tumors is associated with a significant decrease in disease-free survival, and is a reliable predictor of distant metastasis<sup>10</sup>. Similarly, in ovarian cancer patients, *Bcat1* gene expression was 5.3-fold higher in chemoresistant cancers compared to chemosensitive cancers<sup>6</sup>. Also supportive of our hypothesis

that *Bcat1* upregulation is an early event in predisposed tissues, even low-to-moderate grade atypical hyperplastic nasopharyngeal tissue shows a significant increase in Bcat1 immunostaining compared to normal tissue<sup>11</sup>.

*Bcat1* is a direct target of *c-Myc* which controls the G<sub>1</sub>/S transition during mitosis to promote cell proliferation<sup>3</sup>. In the rat, the mitochondrial form, *Bcat2*, is the predominant isoenzyme and is found in almost all tissues of the body<sup>4</sup>. The cytosolic form, *Bcat1*, has been shown by RNAseq to be expressed at moderately high levels in the colon, but negligible levels in the small intestine<sup>1</sup>. RNA levels of *Bcat1* are moderately high in many immune cell classes, but particularly so in B lymphoblasts<sup>1</sup>. BCAT activity has also been shown in fibroblasts<sup>4</sup>.

To determine whether loss of *Bcat1* would affected the tumor phenotype in Pirc rats, we knocked out the *Bcat1* gene in Pirc embryos. We hypothesized that by eliminating *Bcat1* expression, tumors in untreated Pirc rats might be smaller and less frequent, and the increase in tumor multiplicity and growth rate seen in DSS-treated Pirc tumors (see Chapter 1) might be suppressed. *C-myc* has numerous biological effects, including driving cell proliferation, and regulating apoptosis and differentiation. As a target of *C-myc*, *Bcat1* may be responsible for some of the actions attributed to a *C-myc* response. By knocking out *Bcat1* cell proliferation may be reduced or apoptosis increased, which could result in smaller or fewer tumors forming.

A zinc-finger nuclease (ZFN) construct for *Bcat1* was available through a collaboration with Dr. Aron Geurts at the Medical College of Wisconsin (Milwaukee, WI). ZFNs are a class of engineered DNA-binding proteins that create a double-strand break in the DNA at a location specified by the sequence. During genome editing, homologous recombination and Non-Homologous End Joining (NHEJ) work to repair the double strand break. The fidelity of these processes in repairing double-strand breaks is low enough to generate targeted gene deletions at

the site of NHEJ-attempted repair. This results in loss of at least one allele of the targeted gene in up to 40% of the offspring born<sup>5</sup>. Insertions have also been documented to occur using ZFN technology<sup>2,7</sup>, which may appear as band shift to a larger product, versus a deletion which would appear as a band shift to a smaller product. All offspring should undergo sequencing of the gene of interest to determine whether an insertion or a deletion has occurred.

ZFN technology allows the target gene to be knocked out in any chosen rat strain using the same targeting vector if the sequence is conserved. mRNA or plasmid DNA can be delivered by pronuclear (PNI) or intracytoplasmic injection (ICI). We chose to inject mRNA into the pronucleus because it yields very high rates of mutant offspring while technically easier to accomplish than ICI. To increase the chance of obtaining *Bcat1* mutants that already possessed the Pirc allele, we injected Bcat1 mRNA directly into Pirc rat embryos. Alternatively, mutants that do not carry the heterozygous Pirc allele can then be bred to F344 *Apc*<sup>Pirc/+</sup> rats to generate F344*Apc*<sup>Pirc/+</sup>*Bcat1*<sup>-/-</sup> rats.

In the rat, *Bcat1* is located on the q arm of chromosome 4. The Bcat1 ZFN sequence, CAGTCTGTACATCCGCCCCacattCATCGGGATTGAGGTA, targets a region in exon 5. The two knockout strains that have been created by this ZFN construct at the Medical College of Wisconsin each carry a 15-bp deletion created by the targeting vector. However, our resultant deletion may be slightly smaller or larger, depending on the specific repair process that occurs during NHEJ.

Two rounds of embryo harvest and injection were performed (Table G-1). Between the two groups, a total of 83 embryos were injected, 63 of which were transferred into pseudopregnant recipient mothers. Of these, 21 pups were born, but only 12 of these survived into adulthood.

**Table G-1.** *Bcat1* ZFN mRNA injection outcomes. Of a total 83 embryos that were injected with *Bcat1* ZFN, 63 (76%) of these were of suitable quality following injection to implant into a pseudopregnant female. Of the total 63 embryos that were implanted, 33% resulted in pups, but only a total 19% survived. This resulted in an overall 8% rate of pups born with a *Bcat1* event occurring in at least one allele of the gene.

<b>Injection Date</b>	<b>Embryos Injected</b>	<b>[mRNA] ng/ul</b>	<b>Embryos Transferred (% injected)</b>	<b>Pups Born (% implanted)</b>	<b>Pups Alive (%born)</b>	<b><i>Bcat1</i> Events</b>
4/11/13	22	1.5	18 (82%)	5 (28%)	3 (60%)	1 (dead, both alleles altered)
5/14/13	61	1.75	45 (74%)	16 (36%)	9 (56%)	4 (1 dead; 6 other pups died before DNA harvested)

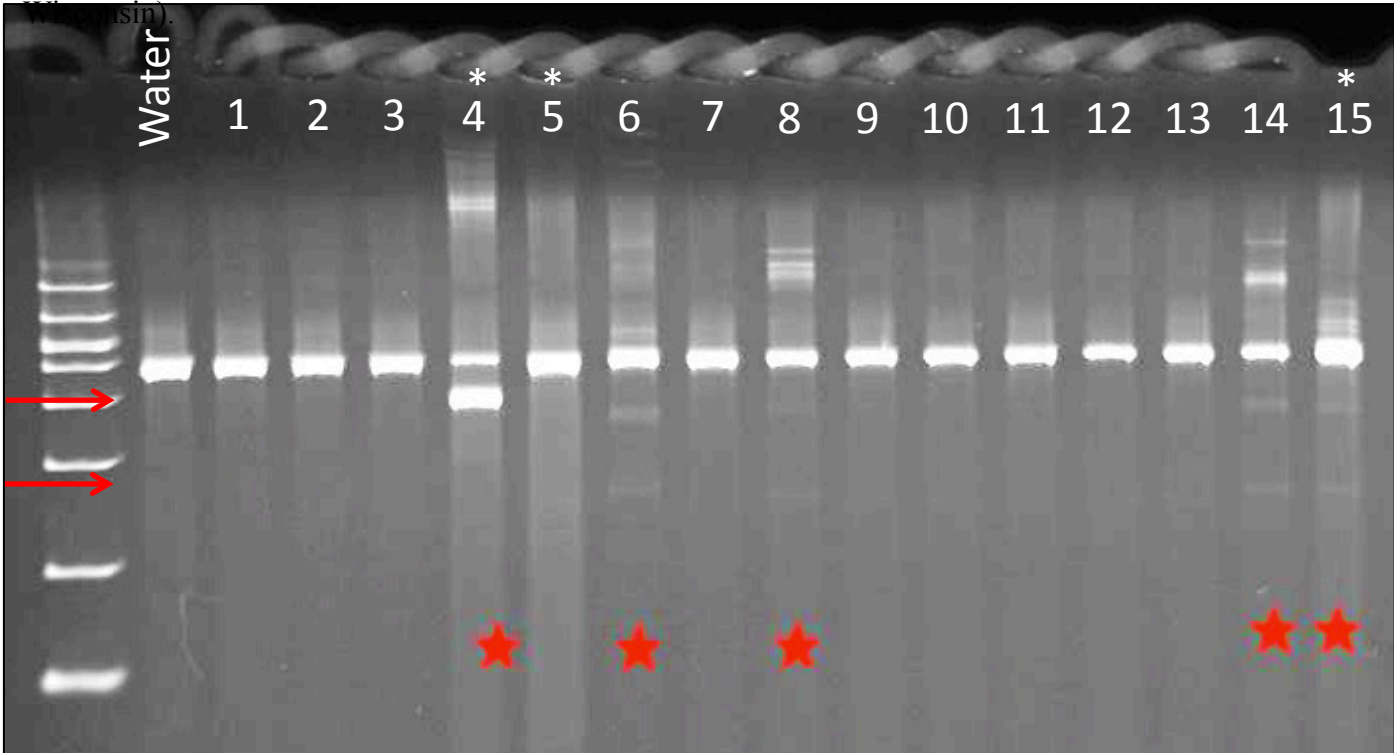
All DNA that could be preserved from live and dead pups first underwent standard PCR for *Bcat1* to determine the success rate of the pronuclear injections. Of a total 15 pups with DNA collected, 5 pups showed some event in the *Bcat1* gene as a result of the ZFN injection (Fig G-1). The Cel-I Surveyor Nuclease Mutation Detection assay (Transgenomic, Omaha, NE) is a more specific way to detect even small base pair deletions that may not be detected by standard PCR. The same 5 pups suspected of carrying *Bcat1* deletions based on standard PCR were confirmed by the Surveyor assay (Fig G-2).

To determine the specific genetic sequences lost in the presumed *Bcat1* mutants, DNA from these 5 rats were cloned using the TOPO TA Cloning Kit (Invitrogen, Carlsbad, CA) and underwent Sanger Sequencing. One rat was found to have only wild type sequence, but the poor reads for this sample may have obscured any potential mutant sequences. Six different mutant sequences were found in the remaining 4 rats (Table G-2). Rat #4 had two different deletion sequences, both of which occurred at the intron/exon boundary. Rats #6, 14 and 15 have





**Fig G-2.** Using the Cel-I assay, samples with a mutated *Bcat1* allele and mismatched base pairs are cleaved by the Surveyor nuclease to create one or both smaller bands (red arrows). The Surveyor nuclease mutation detection assay confirmed mutations in the five rats suspected by traditional PCR (indicated by a red star). However, three of these rats did not survive into adulthood, indicated by an asterisk (\*) above the Rat ID number. (Data from Aron Guertz and Michael Grzybowski at the Medical College of



deletions within exon 5. Wild type sequence was also found for rats #4, 6 and 14. When more than one sequence is found it can be attributed either to two different mutations on each allele of the diploid *Bcat1* locus or to mosaicism within the animal. Depending on when the mRNA incorporated into the dividing embryo, multiple cells may have been present and targeted individually. Only rats #6, 8 and 14 are still alive.

**Table G-2.** Sanger sequencing of *Bcat1* in ZFN-injected embryos. Two different deletion lengths represent either two different mutations on each allele of the diploid *Bcat1* locus or mosaicism. bp, basepairs.

Rat ID	Sex	Deletion	Sequence	Wild type sequence?	Status
4	Unknown	115 bp, 97 bp	Intron/Exon boundary	Yes	Dead at birth
6	Male	1 bp	within Exon 5	Yes	Alive
8	Male	-	-	Yes	Alive
14	Female	6 bp	within Exon 5	Yes	Alive
15	Unknown	5 bp, 6 bp	Both within Exon 5	No	Dead at birth

The next step to create a Pirc rat that is also a *Bcat1* knockout is to separate the different *Bcat1* mutations by breeding each of the founder rats to F344 Pirc rats wild type for *Bcat1*. Each resultant pup will carry at most one deletion sequence, and some will also carry the Pirc mutation. DNA from these pups will then be subjected to Sanger sequencing to select the knockout founder breeders. By crossing male and female rats heterozygous for the same *Bcat1* mutation (one of which should also carry the Pirc mutation), we will generate  $Apc^{Pirc/+} Bcat1^{-/-}$  rats. This process is currently underway.

Once a population of  $Apc^{+/+} Bcat1^{-/-}$  and  $Apc^{Pirc/+} Bcat1^{-/-}$  rats is established, we will determine whether the loss of expression of *Bcat1* affects the tumor phenotype. If *Bcat1* expression plays a role in tumor initiation, we hypothesize that fewer tumors will form in null

rats. If instead *Bcat1* expression is necessary for tumor growth or progression, we hypothesize that null rats will have smaller or less invasive tumors. A subset of the rats will be treated with DSS to determine whether the role of *Bcat1* in tumors associated with inflammation is similar to that in spontaneous tumors. If *Bcat1* plays a role in the ability of DSS to increase tumor stage in DSS-treated rats, we expect that null animals will have less invasive tumors following DSS treatment.

## References

1. **Genecards:** Bcat1. PubMed (Accessed 11/3/13).
2. **Ansai S, Ochiai H, Kanie Y, Kamei Y, Gou Y, Kitano T, Yamamoto T, Kinoshita M.** 2012. Targeted disruption of exogenous EGFP gene in medaka using zinc-finger nucleases. *Development, Growth & Differentiation*. **54**:546–56.
3. **Ben-Yosef T, Yanuka O, Benvenisty N.** 1996. ECA39 is regulated by c-Myc in human and by a Jun/Fos homolog, Gcn4, in yeast. *Oncogene*. **13**:1859–66.
4. **Bledsoe R, Dawson P, Hutson S.** 1997. Cloning of the rat and human mitochondrial branched chain aminotransferases (BCATm). *Biochimica et Biophysica Acta*. **1339**:9–13.
5. **Geurts AM, Cost GJ, Rémy S, Cui X, Tesson L, Usal C, Ménoret S, Jacob HJ, Anegon I, Buelow R.** 2009. Generation of gene-specific mutated rats using zinc-finger nucleases. *Rat Genomics: Methods and Protocols*. **597**:211–225.
6. **Ju W, Yoo B, Kim I-J, Kim J, Kim S, Lee H.** 2009. Identification of genes with differential expression in chemoresistant epithelial ovarian cancer using high-density oligonucleotide microarrays. *Oncology Research*. **18**:47–56.
7. **Mashimo T, Kaneko T, Sakuma T, Kobayashi J, Kunihiro Y, Voigt B, Yamamoto T, Serikawa T.** 2013. Efficient gene targeting by TAL effector nucleases coinjected with exonucleases in zygotes. *Scientific reports*. **3**:1253.
8. **Mayers JR, Heiden MG Vander.** 2013. BCAT1 defines gliomas by IDH status. *Nature Medicine*. **19**:816–7.
9. **Tönjes M, Barbus S, Park YJ, Wang W, Schlotter M, Lindroth AM, Pleier S V, Bai AHC, Karra D, Piro RM, et al.** 2013. BCAT1 promotes cell proliferation through amino acid catabolism in gliomas carrying wild-type IDH1. *Nature Medicine*. **19**:901–8.
10. **Yoshikawa R, Yanagi H, Shen C-S, Fujiwara Y, Noda M, Yagyu T, Gega M, Oshima T, Yamamura T, Okamura H, et al.** 2006. ECA39 is a novel distant metastasis-related biomarker in colorectal cancer. *World Journal of Gastroenterology*. **12**:5884–9.
11. **Zhou W, Feng X, Ren C, Jiang X, Liu W, Huang W, Liu Z, Li Z, Zeng L, Wang L, et al.** 2013. Over-expression of BCAT1, a c-Myc target gene, induces cell proliferation, migration and invasion in nasopharyngeal carcinoma. *Molecular Cancer*. **12**:53.

## **Alginate Molding of Colonic Tumors in Rodent Models**

### **Reagents**

Mineral oil, GenesisV alginate (Accu-cast, Bend, OR), deionized water.

### **Equipment**

Microwave heating pad, 5.5 French (1.83mm) Fogarty catheter (Edwards Lifesciences, Irvine, CA, #12TLW405F35), 13.5 cm silicone tubing (Fisher Scientific, Waltham, MA, #14-176-332B), stainless steel Luer lock adapter (Vita Needle, Needham, MA, #VN530), 15 or 50 ml conical tubes, 20 ml Luer-Lok™ Tip syringe (BD, Franklin Lakes, NJ, #309661).

### **Procedure**

1. Place an anesthetized animal on a heating pad and flush the colon with warmed PBS to eliminate any fecal pellets. This can be achieved by filling a syringe with warmed PBS and attaching to a gavage needle. The gavage needle is then inserted into the rectum of the rat and the opening of the rectum pinched closed around the needle. Rinse the colon with 1-4 ml of warmed PBS depending on the size of the animal. Fecal pellets should easily rinse out but if they do not, they can be guided from the animal by placing one hand underneath the ventral side of the animal and palpating the pellets. The pellets can then be squeezed out by placing pressure above the point of where the pellet is and sliding the hand down towards the rectum. With practice this is a highly effective method for removing pellets and retrieving the alginate mold (see step #7).

2. Insert the Fogarty catheter into the proximal colon (approximately 10 to 12 cm in an adult rat); use medical tape to secure the catheter wire to the tail. Inflate the Fogarty balloon and secure the top of the plunger of a 20 ml Luer-Lok™ Tip syringe with tape to keep the plunger down and the Fogarty balloon inflated (Fig S1A, B). This allows the Fogarty portion to function “hands-free” during the procedure.

*\* HINT: Measure 10-12 cm on the Fogarty wire and mark the point with a permanent marker to easily identify how far the wire will be inserted into the colon.*

*\* HINT: To ensure that the balloon is inflated to the correct size, the syringe attached to the Fogarty should be set at about 0.5 cc. This volume should be adjusted according to the animal size. Over time, the syringe volume may change. Therefore, it is important to check the level regularly in order to prevent incomplete inflation which would allow alginate to go past the balloon and too far into the colon.*

3. Lubricate the silicone filling tube attached to the metal Luer lock adapter with a small amount of mineral oil; gently insert into the colon using small back and forth turning motions (Fig S1B).

**➔ ATTENTION:** *The mineral oil must not come in contact with any of the colonoscopy equipment.*

*\* HINT: Before beginning, weigh the alginate and measure the water needed for each mold so that it can be rapidly poured into the syringe. The alginate begins setting when mixed with water so it is important to move quickly to ensure that the alginate is able to freely flow through the filling tube and completely surround each tumor.*

4. Mix the alginate in a 1 gram to 4 ml ratio with room temperature water. We recommend 1.5 grams of alginate to 6 ml of water for smaller animals and 2 of grams alginate to 8 ml of water for larger animals. To ensure the best mixing, place a gloved finger over the Luer lock opening of the syringe and pour in about half of the water, followed by all of the alginate, and then the

remaining water (Fig S1C, D). Replace the plunger into the syringe. *Before mixing* invert the syringe, allowing the water and powder to fall against the plunger (Fig S1E). The finger covering the hole of the syringe can then be released to allow excess air to escape. Push the plunger down about half way, cover the Luer lock hole with a gloved finger and vigorously shake the syringe for 10-15 seconds. Shake the alginate down towards the plunger and push out all excess air (Fig S1F).

5. Attach the alginate-filled syringe to the Luer lock adapter of the filling tube already in the animal. As alginate is pushed into the animal, slowly pull the filling tube out of the colon (Fig S1G, H). The rate at which alginate is injected into the colon should be roughly proportional to the speed at which the filling tube is removed from the colon. Thus, most of the alginate should be ejected from the tube by the time the tube is completely removed from the colon.

6. When the filling tube has been completely removed from the colon, immediately hold a paper towel over the rectum of the animal to keep alginate from leaking out until it has begun to solidify, about 5 minutes. The alginate takes 8-12 minutes to fully set, depending on ambient temperature and humidity. If the alginate is removed too soon the mold may break or not be completely set.

**→ ATTENTION:** *Immediately following injection of the alginate, the filling tube and syringe should be cleaned before the alginate begins to set. Squeeze any remaining alginate from the filling tube on to a paper towel. Disassemble the syringe and rinse the syringe, plunger and filling tube with water. Do not allow pieces of solidified alginate to go down the drain.*

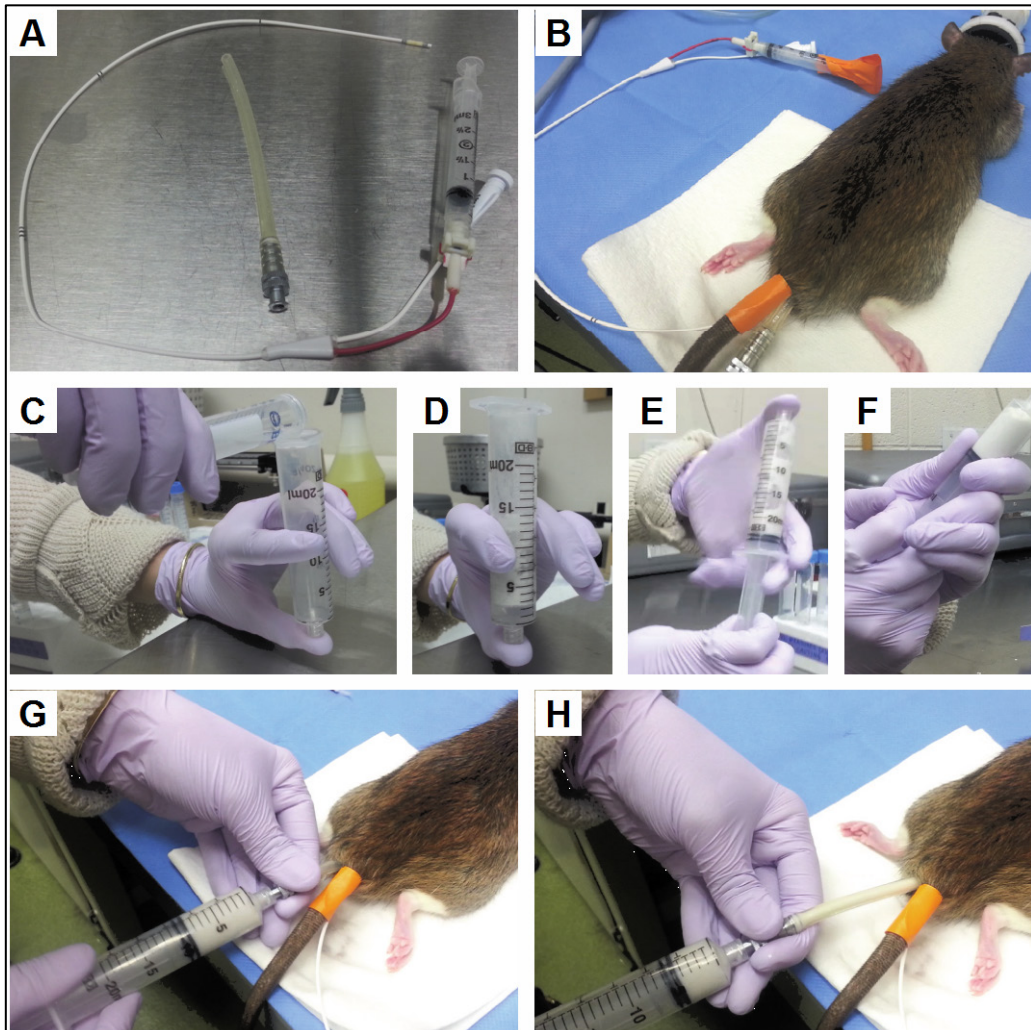


7. Carefully remove the alginate mold. The preferred method is outlined in step #1 above, where a hand on the underside of the animal is used to guide the alginate out. An alternate method involves gently pulling on the inflated Fogarty until part of the alginate mold is visible to grasp. Once the mold is exposed enough to grip by hand or to be seen protruding from the colon, the Fogarty should be deflated and gently removed from the mold. Be careful when grabbing the alginate directly lest it break.

8. Rinse the alginate mold with PBS to remove any fecal material and store in a conical tube until dental stone casts are made (within 1 week). If the alginate molds are stored for more than a few weeks microbial growth may occur.

9. Using the endoscope, check to make sure that no alginate material was left in the animal. If multiple alginate molds are to be made from the same animal, return to step 2 and repeat the procedure.

**Fig P-1.** Alginate molding procedure. A) Equipment needed for the procedure includes a Fogarty catheter and flexible silicone filling tube attached to a Luer lock adapter. B) After the rat is anesthetized, a Fogarty catheter is placed inside the colon, secured to the tail with tape, and the balloon inflated and secured by taping down the syringe plunger. C) Half of the water is poured into the back of the syringe while a finger closes the Luer lock hole. D) The alginate is added to the back of the syringe followed by the other half of the water. E) The plunger is placed into the back of the syringe and the syringe is carefully inverted to allow air to escape. The plunger is pushed in part way and the alginate mix is vigorously shaken. F) The plunger is carefully pushed into the syringe to remove any remaining air. G) The syringe is attached to the Luer lock adapter on the filling tube inside the rat. H) As the alginate is pushed through the filling tube into the colon, the tube is slowly removed from the colon. A paper towel is held at the anus for several minutes to make sure the alginate does not leak out. The alginate is left to set for 8-12 minutes before removing.



## **Dental Stone Casting of Colonic Tumor impressions in Alginate Molds**

### **Reagents**

Yellow dental stone (The Plaster Guys, Glenside, PA), deionized water.

### **Equipment**

KimWipes, multi-well culture plates, scoopula, forceps, hybridization oven, scale, 1.5 ml tubes.

### **Procedure**

1. Remove alginate molds from conical tube storage and gently dry within the negative tumor impressions using a KimWipe.
2. If multiple tumors were cast from an animal, draw a picture of the alginate cast and label the impressions so that they correspond to the tumor numbers from endoscopy. Label a multi-well cell culture plate so that each dental stone cast for each tumor from each alginate mold has its own well. Mark both the lid and the corresponding plate with an identifier if multiple plates will be used to avoid mix-ups when the lids are removed during the drying process.
3. Mix 2.5 grams of yellow dental stone to 1.0 ml of room temperature water. Generally, this is enough to fill 10-20 tumor impressions, depending on size. If multiple dental stone castings will be made from the same alginate mold a new batch of dental stone should be made each time.

4. Use a small scoopula to fill the negative impressions in the alginate, checking that no bubbles are left and that the impression is completely filled to the level of alginate corresponding to the surface of the colon. To reduce the possibility of introducing bubbles into the dental stone cast, fill the tumor impression along the cavity side wall so that air can escape as the dental stone fills in the impression. Filling the stone so that it is flush with the outside of the alginate mold is crucial. If a “divot” is left where the stone is made the volume will be underrepresented; if a “mound” is left where the stone is made the volume will be overrepresented. Filling beyond the negative impression can be corrected without disturbing the tumor cast by gently chipping away the excess stone using forceps prior to drying in the hybridization oven.

5. Leave the dental stone in place for 15-20 minutes at room temperature to solidify. Longer dental stone set times will improve ease of removal from the alginate.

6. Once set, gently remove the dental stone castings using the point of the forceps if necessary and transfer them into their respective wells in a cell culture plate. If excess dental stone surrounds the tumor cast it can now be gently chipped away without disturbing the tumor cast. Place the uncovered plates into a 90°C hybridization oven for 48 hours to speed drying.

7. After 48 hours in the hybridization oven, remove the culture plates containing the dental stones from the hybridization oven and weigh each dental stone.

8. Determine original tumor volume in  $\text{mm}^3$  by dividing the weight of the dry dental stone cast in grams by 0.0013236 (see Chapter 5 for details on how this number was calculated).

**Supplementary Table S-1. Genes differentially expressed between untreated normal colonic tissue and all colonic tumors**

Probe ID	Gene Symbol	p-value	Fold Change	Direction of Change
A_44_P276538	Gp49b	0.00141295	729.5	All Tumors up
A_44_P869362	LOC688150	6.78E-09	311.0	All Tumors up
A_44_P241070	RGD1565786_predicted	0.00188092	166.5	All Tumors up
A_43_P11672	Il1rl1	0.000146771	102.3	All Tumors up
A_44_P734459	DV718231	6.50E-08	89.8	All Tumors up
A_44_P256301	Grem1	1.29E-05	83.5	All Tumors up
A_44_P404861	Mmp10	0.000169404	82.9	All Tumors up
A_44_P1029697	Chl1	1.30E-07	71.4	All Tumors up
A_44_P670185	TC622294	0.000192172	69.8	All Tumors up
A_43_P11804	Ptn	7.88E-06	68.6	All Tumors up
A_43_P14796	LOC682861	3.51E-07	67.4	All Tumors up
A_44_P623856	Dkk4_predicted	2.07E-07	55.8	All Tumors up
A_43_P11590	Mmp7	2.14E-10	52.4	All Tumors up
A_44_P925373	AA997357	1.34E-07	49.9	All Tumors up
A_44_P1004886	Slc26a3	1.95E-05	47.5	Control Normal Tissue up
A_42_P839593	AW921479	9.02E-06	46.4	Control Normal Tissue up
A_44_P1023977	Spink1	1.83E-05	43.9	Control Normal Tissue up
A_44_P447373	MGC72614	3.03E-05	42.8	All Tumors up
A_44_P1036943	AW142999	1.05E-05	42.2	All Tumors up
A_44_P672002	Cmah	3.61E-11	40.1	Control Normal Tissue up
A_43_P11881	Sh3kbp1	1.86E-07	39.7	All Tumors up
A_43_P11684	Ass	1.25E-06	37.9	All Tumors up
A_44_P999845	AA900293	1.87E-07	37.6	All Tumors up
A_42_P660129	TC606854	1.77E-07	35.4	All Tumors up
A_44_P684180	Bcat1	5.37E-09	35.3	All Tumors up
A_42_P663722	Alpl	0.000107536	34.9	All Tumors up
A_42_P693316	Sh3kbp1	9.80E-09	34.0	All Tumors up
A_42_P803673	Casp12	1.14E-06	32.9	All Tumors up
A_43_P11621	Lrrn1	8.03E-06	32.7	All Tumors up
A_44_P1034926	Slc30a2	9.09E-08	32.1	All Tumors up
A_44_P476915	Cfi	4.68E-05	31.0	All Tumors up
A_44_P975889	LOC360228	7.59E-05	31.0	All Tumors up
A_44_P837709	Cd44	2.63E-09	30.1	All Tumors up
A_44_P1017035	BF281925	2.06E-07	28.2	All Tumors up
A_43_P10156	Pdyn	9.47E-05	27.7	All Tumors up
A_43_P17795	TC585827	1.39E-07	27.6	All Tumors up
A_43_P15819	CF112941	3.45E-06	27.4	All Tumors up
A_43_P15247	Slc26a4	1.00E-05	27.1	All Tumors up
A_44_P1053321	AW143833	0.000390527	27.0	All Tumors up
A_44_P450124	ENSRNOT00000021832	6.78E-05	26.6	Control Normal Tissue up
A_43_P15961	RGD1559565_predicted	2.90E-07	26.6	All Tumors up
A_44_P161470	Fmo2	0.000661106	26.4	Control Normal Tissue up
A_42_P646213	Prss22_predicted	8.11E-09	26.2	All Tumors up
A_44_P257893	Tac1	1.68E-05	26.2	All Tumors up
A_44_P975868	Gbp2	3.96E-07	25.9	All Tumors up
A_44_P687400	Spetex-2F	0.00695218	25.6	All Tumors up
A_44_P1004790	Rbclca2	0.000117824	25.5	All Tumors up
A_44_P245835	Defa6	3.22E-07	25.3	All Tumors up
A_43_P12200	ENSRNOT00000030609	0.000115157	25.1	All Tumors up
A_44_P518414	Gbp4_predicted	0.000134446	24.7	All Tumors up
A_43_P10201	TC575730	1.12E-09	24.6	All Tumors up
A_44_P330584	TC609088	6.72E-05	24.5	All Tumors up
A_44_P115142	Pck1	9.49E-06	23.8	Control Normal Tissue up
A_44_P251228	Slc30a2	9.86E-08	23.6	All Tumors up
A_42_P647599	RGD1310110_predicted	2.68E-06	23.6	All Tumors up
A_44_P288287	Slc26a1	4.32E-05	23.5	All Tumors up
A_44_P283464	LOC685312	0.000697032	23.5	All Tumors up
A_42_P556829	BG665180	7.10E-07	22.9	All Tumors up
A_44_P491796	Lix1_predicted	1.75E-05	22.8	All Tumors up

Probe ID	Gene Symbol	p-value	Fold Change	Direction of Change
A_44_P945840	Mycn	5.04E-06	22.6	All Tumors up
A_44_P377432	Cyp1b1	0.00567291	22.5	All Tumors up
A_44_P332744	Dcn	2.78E-06	22.2	All Tumors up
A_42_P773945	RGD1307724_predicted	0.00037678	22.0	All Tumors up
A_42_P484738	Gnat3	9.74E-06	22.0	Control Normal Tissue up
A_44_P421405	AF217587	0.00312789	22.0	All Tumors up
A_44_P1007347	Wif1	2.01E-06	21.9	All Tumors up
A_44_P160841	Spp1	1.31E-05	21.8	All Tumors up
A_44_P362981	Neto2_predicted	3.77E-05	21.7	All Tumors up
A_42_P588944	RGD1562101_predicted	2.00E-06	21.6	All Tumors up
A_44_P928163	Oas1b	0.00829371	21.5	All Tumors up
A_42_P626895	B4galt1_predicted	6.87E-10	21.2	All Tumors up
A_44_P547771	Klks3	0.000114655	21.2	Control Normal Tissue up
A_44_P749637	Ctgf	8.11E-06	20.9	All Tumors up
A_43_P13127	Sh3kbp1	1.64E-07	20.7	All Tumors up
A_43_P15638	Slco2b1	7.05E-06	20.4	Control Normal Tissue up
A_44_P151391	A_44_P659416	0.000134341	20.3	Control Normal Tissue up
A_42_P758222	Tgm2	1.62E-05	20.3	All Tumors up
A_44_P588315	Cla3_predicted	0.00034361	20.2	Control Normal Tissue up
A_44_P506817	Calcb	4.10E-06	20.0	All Tumors up
A_44_P879764	Fabp5	6.05E-06	19.4	All Tumors up
A_44_P358703	Mgp	5.81E-06	19.4	All Tumors up
A_44_P297818	DY472205	3.49E-06	18.7	All Tumors up
A_44_P104140	Klk7	0.000114396	18.7	Control Normal Tissue up
A_44_P579071	LOC689256	0.000153663	18.6	All Tumors up
A_44_P311126	Cited1	3.96E-06	18.6	All Tumors up
A_44_P463425	Ch11	4.86E-05	18.6	All Tumors up
A_42_P457756	Slc38a4	0.000159904	18.4	All Tumors up
A_44_P166068	Ton	7.39E-05	18.3	Control Normal Tissue up
A_43_P11152	Tnc	3.54E-07	18.3	All Tumors up
A_44_P108588	TC603520	6.34E-05	18.3	Control Normal Tissue up
A_44_P214846	Al179025	0.000377641	18.2	All Tumors up
A_43_P14162	Arg1	1.11E-06	18.0	All Tumors up
A_44_P157314	Xlkd1_predicted	3.97E-06	17.9	All Tumors up
A_44_P536676	BF287204	0.000814959	17.8	All Tumors up
A_44_P992908	Fabp6	2.57E-06	17.7	Control Normal Tissue up
A_44_P835675	B4galt1_predicted	2.35E-08	17.7	All Tumors up
A_44_P471294	Spetex-2D	8.02E-07	17.6	All Tumors up
A_44_P592221	XM_234745	0.00168043	17.6	All Tumors up
A_42_P573412	LOC679949	0.000112193	17.5	All Tumors up
A_44_P916210	TC614795	1.60E-05	17.5	All Tumors up
A_44_P730004	RGD1310935_predicted	8.26E-05	17.5	Control Normal Tissue up
A_44_P941248	Clu	4.47E-07	17.4	All Tumors up
A_42_P501233	Klk6_predicted	0.000230601	17.3	Control Normal Tissue up
A_44_P282443	AW917764	4.63E-05	17.2	All Tumors up
A_44_P123093	Sgk	2.38E-05	17.0	Control Normal Tissue up
A_42_P695401	Pkib	2.10E-06	16.9	All Tumors up
A_44_P518127	Spetex-2D	0.00024154	16.9	All Tumors up
A_44_P1022458	RGD1561831_predicted	6.31E-05	16.8	Control Normal Tissue up
A_44_P807861	Casr	0.000131122	16.7	Control Normal Tissue up
A_43_P14911	Nov	0.000207237	16.6	Control Normal Tissue up
A_44_P242397	Aldh1a1	3.52E-05	16.5	Control Normal Tissue up
A_44_P297777	Tm4sf1_predicted	3.22E-05	16.4	All Tumors up
A_44_P654924	Fbp1	8.99E-06	16.2	Control Normal Tissue up
A_44_P494662	TC598890	0.00012723	16.1	Control Normal Tissue up
A_43_P22577	Fst	0.000315584	16.1	All Tumors up
A_42_P637189	CB544899	0.00202387	16.1	Control Normal Tissue up
A_44_P918566	Mx2	0.000107666	16.1	All Tumors up
A_42_P473398	A2m	0.000164563	15.9	All Tumors up
A_43_P14249	ENSRNOT00000056464	0.000181129	15.9	Control Normal Tissue up
A_42_P828757	BF558825	0.000299939	15.9	All Tumors up
A_44_P294675	TC600025	0.000265322	15.8	Control Normal Tissue up
A_44_P914382	B3galt3	0.000109564	15.8	All Tumors up
A_42_P753675	Hspb1	9.35E-06	15.7	All Tumors up
A_44_P555072	CF110937	2.64E-07	15.7	All Tumors up

Probe ID	Gene Symbol	p-value	Fold Change	Direction of Change
A_44_P745269	Fhl1	3.01E-05	15.6	Control Normal Tissue up
A_44_P185015	TC615685	2.37E-05	15.5	Control Normal Tissue up
A_44_P303009	A_44_P471294	5.33E-05	15.5	All Tumors up
A_44_P237664	Gcgr	2.18E-06	15.4	Control Normal Tissue up
A_43_P11558	TC598512	2.12E-05	15.2	All Tumors up
A_44_P438863	Slc22a3	2.40E-07	15.1	Control Normal Tissue up
A_42_P466362	RGD1307150_predicted	5.29E-06	14.9	All Tumors up
A_44_P315562	TC629545	2.45E-05	14.9	All Tumors up
A_44_P274976	TC596605	1.78E-06	14.9	All Tumors up
A_44_P885679	BF286677	1.28E-07	14.8	All Tumors up
A_44_P745749	Ngfg	0.000151672	14.8	Control Normal Tissue up
A_44_P543641	Adra1d	5.71E-05	14.7	All Tumors up
A_44_P234550	AW920715	2.57E-05	14.7	All Tumors up
A_44_P161841	Fmo3	0.000216275	14.6	Control Normal Tissue up
A_42_P607026	TC601688	0.000173003	14.5	Control Normal Tissue up
A_42_P571433	Mep1a	3.69E-05	14.3	Control Normal Tissue up
A_42_P585695	AW914230	2.36E-07	14.3	All Tumors up
A_44_P200042	Ccl2	0.000136017	14.2	All Tumors up
A_44_P496643	ENSRNOT00000056448	0.00020242	14.2	Control Normal Tissue up
A_43_P12786	MGC116096	2.40E-10	14.2	All Tumors up
A_44_P1051894	Tubb6	9.15E-10	14.2	All Tumors up
A_44_P109684	Scnn1g	0.00124102	14.1	Control Normal Tissue up
A_43_P21655	Gk11	7.56E-05	14.1	Control Normal Tissue up
A_43_P15497	ENSRNOT00000056448	3.28E-05	14.0	Control Normal Tissue up
A_44_P125273	TC591769	0.009692	14.0	All Tumors up
A_44_P1018957	Aadac	3.26E-06	13.9	Control Normal Tissue up
A_44_P294838	Fhl1	5.59E-05	13.9	Control Normal Tissue up
A_44_P219598	I11b	5.94E-05	13.8	All Tumors up
A_44_P175912	Ppp2r2b	4.94E-06	13.8	All Tumors up
A_44_P326133	Flna_predicted	9.80E-06	13.3	All Tumors up
A_44_P393551	TC603750	5.69E-05	13.3	Control Normal Tissue up
A_44_P729428	Ces3	4.53E-05	13.3	Control Normal Tissue up
A_44_P536476	TC599445	1.89E-05	13.2	All Tumors up
A_43_P11464	RGD1560851_predicted	3.23E-06	13.2	All Tumors up
A_43_P12162	BF398472	2.74E-07	13.0	Control Normal Tissue up
A_44_P502678	RGD1563091_predicted	0.000391725	13.0	All Tumors up
A_42_P475885	Apln	0.000112491	12.9	All Tumors up
A_44_P209519	TC593044	0.00470413	12.8	All Tumors up
A_44_P961280	Cxcl1	1.32E-08	12.8	All Tumors up
A_44_P487269	CF110190	2.91E-07	12.8	All Tumors up
A_42_P541872	LOC498335	4.37E-05	12.8	Control Normal Tissue up
A_44_P450075	Rptn_predicted	0.00696854	12.8	Control Normal Tissue up
A_44_P353618	TC600845	7.25E-06	12.7	Control Normal Tissue up
A_44_P1047441	AW916070	0.000386332	12.7	Control Normal Tissue up
A_42_P799208	Tm4sf4	8.94E-06	12.7	All Tumors up
A_42_P602570	RGD1565378_predicted	0.0001225	12.5	Control Normal Tissue up
A_43_P14751	Fhl1	5.07E-05	12.5	Control Normal Tissue up
A_43_P11465	Slfn3	0.000484537	12.5	All Tumors up
A_43_P22696	Irx2	0.0019137	12.5	Control Normal Tissue up
A_44_P264240	RGD1559432_predicted	9.10E-09	12.5	All Tumors up
A_44_P397085	Arhgdig_predicted	1.00E-07	12.5	All Tumors up
A_44_P561395	MGC94782	9.47E-06	12.3	All Tumors up
A_44_P1055780	Ak311	0.000194438	12.3	All Tumors up
A_44_P346832	Spetex-2B	8.29E-07	12.3	All Tumors up
A_44_P730817	ENSRNOT00000029294	1.31E-05	12.3	Control Normal Tissue up
A_44_P475448	CB605594	9.66E-06	12.3	All Tumors up
A_44_P458627	TC597010	7.10E-05	12.2	Control Normal Tissue up
A_44_P411743	AW141875	2.64E-06	12.1	All Tumors up
A_44_P171220	Apod	4.41E-06	12.1	All Tumors up
A_44_P590984	Serpine2	3.54E-05	12.1	All Tumors up
A_44_P522195	Adecy8	8.51E-05	12.1	All Tumors up
A_44_P621522	Cald1	1.94E-06	12.0	All Tumors up
A_44_P500056	DV717216	2.66E-05	11.9	All Tumors up
A_44_P175495	Bnc1_predicted	9.99E-05	11.9	All Tumors up
A_44_P202318	A_44_P745749	2.95E-06	11.9	All Tumors up

Probe ID	Gene Symbol	p-value	Fold Change	Direction of Change
A_44_P435618	ENSRNOT00000012525	2.98E-06	11.8	All Tumors up
A_44_P545654	XM_340745	3.56E-05	11.7	All Tumors up
A_44_P421322	Alox12_predicted	1.04E-06	11.6	All Tumors up
A_44_P578061	Ptprn2	5.98E-06	11.6	Control Normal Tissue up
A_42_P638166	Lysmd2_predicted	5.59E-09	11.5	All Tumors up
A_44_P515197	Msx1	2.69E-05	11.5	All Tumors up
A_44_P1013006	Clecsf2_predicted	0.000700929	11.5	Control Normal Tissue up
A_44_P329239	Lox	0.000137232	11.5	All Tumors up
A_44_P515825	Twist1	0.000254807	11.5	All Tumors up
A_44_P950925	LOC503340	5.91E-06	11.5	All Tumors up
A_44_P203401	RGD1306105_predicted	0.000119108	11.4	Control Normal Tissue up
A_42_P806859	Fabp4	0.000122395	11.4	All Tumors up
A_44_P288291	LOC363915	8.75E-06	11.4	All Tumors up
A_42_P604033	AF220555	0.00328134	11.4	All Tumors up
A_44_P491308	Papss2_predicted	0.000176763	11.4	Control Normal Tissue up
A_44_P199447	LOC294762	1.88E-05	11.3	All Tumors up
A_43_P12356	BF547360	4.74E-05	11.3	Control Normal Tissue up
A_43_P13048	Msx2	0.000968223	11.3	All Tumors up
A_44_P433935	AA858448	0.0012473	11.3	All Tumors up
A_44_P1040642	Hsd11b1	5.95E-06	11.3	All Tumors up
A_42_P598365	Il1a	3.00E-08	11.2	All Tumors up
A_44_P288401	Unc5c	0.000182124	11.2	All Tumors up
A_44_P269055	RGD1309838_predicted	0.000782454	11.2	All Tumors up
A_44_P953483	Slc30a3	0.00337036	11.2	Control Normal Tissue up
A_44_P132325	TC613633	1.90E-06	11.2	Control Normal Tissue up
A_44_P547191	LOC296723	2.35E-06	11.1	All Tumors up
A_44_P793670	CK475991	0.000490552	11.1	Control Normal Tissue up
A_43_P14604	Gja1	0.000129706	11.0	All Tumors up
A_44_P868581	A_44_P729428	7.71E-07	11.0	All Tumors up
A_44_P405302	Hpgd	4.24E-06	11.0	Control Normal Tissue up
A_44_P638176	ENSRNOT00000005972	3.36E-06	11.0	All Tumors up
A_44_P1037456	Rragd_predicted	1.56E-07	11.0	Control Normal Tissue up
A_44_P454137	TC601834	7.33E-05	10.9	Control Normal Tissue up
A_43_P23209	Fgg	0.000101111	10.9	All Tumors up
A_42_P693096	Ppp2r2b	1.93E-05	10.9	All Tumors up
A_44_P173960	TC613577	5.49E-07	10.9	Control Normal Tissue up
A_44_P695547	AA875008	0.00354066	10.8	All Tumors up
A_44_P540511	Ptprz1	1.20E-05	10.8	All Tumors up
A_44_P220455	Chst4_predicted	0.00224084	10.8	Control Normal Tissue up
A_44_P980916	AW917496	0.00123335	10.8	All Tumors up
A_44_P1014619	TC601928	9.97E-05	10.8	All Tumors up
A_42_P655047	RGD1359539	5.43E-05	10.8	All Tumors up
A_44_P506273	B3galt3	0.000148686	10.8	All Tumors up
A_44_P426345	Ifit1_predicted	0.000271135	10.8	All Tumors up
A_44_P391296	S100a9	5.73E-06	10.7	All Tumors up
A_44_P1052046	TC606783	1.16E-05	10.7	Control Normal Tissue up
A_44_P273468	Rgs7	0.000123038	10.6	Control Normal Tissue up
A_44_P714397	Slc27a6_predicted	0.000194221	10.6	Control Normal Tissue up
A_44_P309913	Lrp2	0.000306723	10.5	All Tumors up
A_44_P317912	Scin	2.98E-06	10.5	Control Normal Tissue up
A_42_P686078	Cox8h	5.39E-05	10.5	Control Normal Tissue up
A_44_P1044658	DV726678	1.04E-06	10.5	All Tumors up
A_44_P359040	Bex1	1.73E-05	10.4	All Tumors up
A_44_P775722	Aqp9	0.00418665	10.4	All Tumors up
A_44_P699523	Fst	0.000552714	10.4	All Tumors up
A_44_P473663	A_43_P22696	1.20E-05	10.4	All Tumors up
A_44_P438295	Igfbp5	4.67E-05	10.3	All Tumors up
A_42_P611397	S100g	3.69E-05	10.3	Control Normal Tissue up
A_44_P674708	Fxyd5	0.0015832	10.3	All Tumors up
A_42_P606126	LOC683263	5.59E-05	10.3	All Tumors up
A_44_P199096	ENSRNOT00000057120	2.85E-05	10.3	Control Normal Tissue up
A_44_P533794	S100a8	5.81E-05	10.3	All Tumors up
A_42_P750683	CN382817	2.68E-05	10.2	Control Normal Tissue up
A_44_P290539	RGD1566317_predicted	7.89E-06	10.2	All Tumors up
A_44_P309596	Adora2b	0.000175818	10.1	Control Normal Tissue up



Probe ID	Gene Symbol	p-value	Fold Change	Direction of Change
A_43_P15980	TC603905	6.84E-06	10.1	All Tumors up
A_44_P792166	Sult1a1	8.56E-06	10.1	Control Normal Tissue up
A_44_P1048789	X60291	0.00478085	10.1	All Tumors up
A_44_P451244	Atp12a	0.00014148	10.1	Control Normal Tissue up
A_44_P158798	Lum	9.90E-05	10.1	All Tumors up
A_44_P820062	Gpx2	6.86E-05	10.0	All Tumors up
A_44_P1038028	Rps6kl1_predicted	8.80E-05	10.0	All Tumors up
A_44_P1040532	ENSRNOT00000042464	9.57E-05	10.0	All Tumors up
A_44_P838313	AI071307	0.00401558	10.0	All Tumors up
A_44_P256188	Abat	7.54E-05	9.9	Control Normal Tissue up
A_44_P175299	AI103119	0.000368679	9.9	Control Normal Tissue up
A_42_P521210	AA800429	9.95E-05	9.9	Control Normal Tissue up
A_44_P414544	Vsig2_predicted	0.000342774	9.9	Control Normal Tissue up
A_44_P173610	ENSRNOT00000041360	0.00600829	9.9	Control Normal Tissue up
A_42_P685287	A_44_P621522	0.00313563	9.8	All Tumors up
A_44_P295680	RGD1566243_predicted	2.89E-05	9.8	Control Normal Tissue up
A_44_P668373	Gpx2	6.68E-06	9.8	All Tumors up
A_44_P932042	Papss2_predicted	5.40E-05	9.8	Control Normal Tissue up
A_44_P371635	Cxcl11	1.10E-05	9.8	All Tumors up
A_43_P12462	AW917204	1.04E-05	9.7	All Tumors up
A_42_P736573	TC584998	6.33E-06	9.7	Control Normal Tissue up
A_44_P378514	Ednrb	4.63E-06	9.6	All Tumors up
A_44_P791638	Mt1a	2.21E-05	9.6	Control Normal Tissue up
A_44_P241616	Ppy	2.83E-07	9.6	Control Normal Tissue up
A_44_P239306	Slc1a2	0.000785393	9.6	All Tumors up
A_44_P194278	Nox1	2.28E-05	9.6	All Tumors up
A_44_P375102	TC639482	1.29E-05	9.5	All Tumors up
A_44_P787524	RGD1560368_predicted	0.00391676	9.5	All Tumors up
A_42_P468712	Cxcl2	2.61E-05	9.5	All Tumors up
A_44_P1017144	Steap1_predicted	6.82E-05	9.4	All Tumors up
A_43_P13307	AA858471	0.00103238	9.4	All Tumors up
A_44_P332422	RGD1562705_predicted	0.00023181	9.4	All Tumors up
A_44_P922150	TC632060	0.000170027	9.4	Control Normal Tissue up
A_44_P824935	TC639313	5.59E-06	9.4	Control Normal Tissue up
A_44_P212985	A_44_P950925	0.000899363	9.4	All Tumors up
A_44_P932768	RatNP-3b	4.52E-07	9.3	All Tumors up
A_44_P104418	AI229721	8.81E-06	9.3	All Tumors up
A_44_P298049	Akr1cl1_predicted	0.000173088	9.3	Control Normal Tissue up
A_42_P465601	Phlda3	1.23E-06	9.2	All Tumors up
A_43_P12718	Eaf2	0.000482963	9.2	All Tumors up
A_44_P192336	Cd44	0.00037312	9.2	All Tumors up
A_44_P501162	Elk3_predicted	2.18E-06	9.2	All Tumors up
A_44_P429298	Tmeff1	5.14E-06	9.2	All Tumors up
A_44_P543643	Tnfsf11	0.00384472	9.2	All Tumors up
A_44_P426107	TC624697	0.000132348	9.1	Control Normal Tissue up
A_44_P392849	LOC688864	1.52E-06	9.1	Control Normal Tissue up
A_44_P117389	St6galnac1	0.000109821	9.0	Control Normal Tissue up
A_44_P562483	Selenbp1	1.13E-05	9.0	Control Normal Tissue up
A_44_P855435	Plac1	0.000647287	9.0	All Tumors up
A_44_P508162	Mafb	2.76E-05	8.9	All Tumors up
A_43_P16767	Colec12	6.26E-05	8.9	All Tumors up
A_44_P290022	RGD1559887_predicted	0.00115812	8.9	All Tumors up
A_43_P16967	Ly6b	4.74E-05	8.9	All Tumors up
A_44_P242580	TC637089	3.45E-06	8.9	All Tumors up
A_44_P669066	AW531866	0.000522458	8.8	All Tumors up
A_44_P395918	BG378227	0.00929444	8.8	All Tumors up
A_44_P193945	TC603202	3.89E-05	8.8	All Tumors up
A_44_P1023538	Pck1	2.79E-06	8.8	Control Normal Tissue up
A_44_P975250	AW143134	0.0010054	8.8	All Tumors up
A_44_P392846	RGD1307443_predicted	1.23E-05	8.7	Control Normal Tissue up
A_44_P1016884	RGD1562095_predicted	0.0113603	8.7	All Tumors up
A_43_P22972	Cpxm2_predicted	3.98E-05	8.7	All Tumors up
A_44_P992535	Apob	1.56E-06	8.7	Control Normal Tissue up
A_42_P518855	LOC500152	0.000129105	8.7	All Tumors up
A_44_P1005051	Col22a1_predicted	0.00050712	8.7	All Tumors up

Probe ID	Gene Symbol	p-value	Fold Change	Direction of Change
A_44_P625272	Gpr37	7.55E-05	8.7	Control Normal Tissue up
A_44_P217744	Dync1i1	0.000806606	8.6	Control Normal Tissue up
A_44_P380839	Capn9	6.76E-05	8.6	Control Normal Tissue up
A_43_P19265	AA891826	0.00676967	8.6	All Tumors up
A_42_P473425	TC606539	1.75E-05	8.6	Control Normal Tissue up
A_44_P1048687	Dync2li1	7.52E-05	8.6	All Tumors up
A_44_P392845	AI454457	1.22E-05	8.6	All Tumors up
A_44_P454927	AW921140	0.000425436	8.5	Control Normal Tissue up
A_44_P532297	Muc2	0.00229583	8.5	Control Normal Tissue up
A_43_P10020	S68944	0.00412874	8.5	All Tumors up
A_44_P602122	XM_218590	0.0036668	8.5	Control Normal Tissue up
A_43_P10689	Gzmc	5.63E-05	8.5	Control Normal Tissue up
A_42_P733209	U39609	0.0011352	8.5	All Tumors up
A_44_P1004840	Pkib	6.23E-06	8.5	All Tumors up
A_44_P894727	Csf3r_predicted	0.00240105	8.5	All Tumors up
A_44_P239300	Kirrel3_predicted	2.07E-06	8.5	All Tumors up
A_44_P116539	Katnal1	0.00034008	8.5	All Tumors up
A_42_P688802	BM422817	6.04E-06	8.5	Control Normal Tissue up
A_44_P267024	Vmd2l1_predicted	1.36E-05	8.5	Control Normal Tissue up
A_44_P391982	Prrx2_predicted	2.78E-06	8.4	All Tumors up
A_44_P123818	Mlze_predicted	5.47E-05	8.4	Control Normal Tissue up
A_44_P931389	Neil3_predicted	0.00544615	8.4	All Tumors up
A_44_P508566	Hsd11b1	1.30E-05	8.4	All Tumors up
A_44_P635639	Cyp2d10	6.96E-06	8.4	Control Normal Tissue up
A_42_P787160	Ccl7	0.000393001	8.4	All Tumors up
A_44_P501112	Bmp3	0.000238841	8.4	Control Normal Tissue up
A_44_P1008867	TC607281	1.85E-05	8.4	Control Normal Tissue up
A_44_P243534	RGD1562717_predicted	5.69E-05	8.4	All Tumors up
A_44_P949804	Slc25a4	7.61E-07	8.3	All Tumors up
A_44_P515627	M12981	0.000960679	8.3	All Tumors up
A_43_P11589	CB547989	4.23E-05	8.3	All Tumors up
A_44_P288858	Tpsg1	1.72E-05	8.3	Control Normal Tissue up
A_44_P976406	RGD1564865_predicted	0.00251543	8.3	Control Normal Tissue up
A_44_P389590	Aldh1a2	3.66E-05	8.3	All Tumors up
A_44_P437956	AW143067	4.41E-06	8.3	All Tumors up
A_44_P563447	CX569326	6.20E-06	8.2	Control Normal Tissue up
A_43_P11448	AW251647	0.00324842	8.2	All Tumors up
A_44_P161917	TC618013	8.57E-06	8.2	Control Normal Tissue up
A_44_P450786	RGD1309051	1.06E-07	8.2	All Tumors up
A_44_P538616	ENSRNOT00000043097	0.000545107	8.2	All Tumors up
A_44_P481160	TC587634	5.83E-05	8.2	All Tumors up
A_44_P1007841	A_44_P473663	0.000406186	8.2	All Tumors up
A_44_P210568	T_predicted	0.0078359	8.2	All Tumors up
A_44_P741757	RGD1308544_predicted	0.000116236	8.1	Control Normal Tissue up
A_42_P507566	TC585018	6.57E-06	8.1	Control Normal Tissue up
A_44_P437721	AW143880	1.10E-07	8.1	Control Normal Tissue up
A_44_P423651	Cyp3a18	0.000386153	8.0	Control Normal Tissue up
A_44_P240867	St3gal5	2.51E-07	8.0	All Tumors up
A_44_P346882	S100a8	0.000165148	8.0	All Tumors up
A_44_P805851	Rasgrf2	4.03E-05	8.0	Control Normal Tissue up
A_42_P479160	Tcea3	1.34E-05	8.0	Control Normal Tissue up
A_44_P768625	Mmp13	0.00967822	8.0	All Tumors up
A_44_P823749	Rarres1	0.00307582	8.0	All Tumors up
A_44_P1050200	Tnfrsf1b	1.14E-05	8.0	All Tumors up
A_44_P426638	RGD1565406_predicted	8.01E-06	8.0	Control Normal Tissue up
A_44_P664495	RGD1564335_predicted	0.00650455	8.0	Control Normal Tissue up
A_44_P452245	RGD1566243_predicted	6.84E-06	8.0	Control Normal Tissue up
A_44_P792030	Cyr61	0.000368668	7.9	All Tumors up
A_44_P247281	Mycn	1.01E-05	7.9	All Tumors up
A_44_P399249	A_44_P661776	0.000126672	7.9	Control Normal Tissue up
A_44_P285681	XM_234755	0.0114422	7.9	All Tumors up
A_44_P884867	Angpt2	0.00111075	7.9	All Tumors up
A_44_P253157	Angpt2	0.000108745	7.9	All Tumors up
A_43_P13189	CO566330	1.02E-06	7.9	Control Normal Tissue up
A_44_P321605	Cbs	8.30E-08	7.9	Control Normal Tissue up

Probe ID	Gene Symbol	p-value	Fold Change	Direction of Change
A_44_P612762	AA859536	0.000905884	7.9	All Tumors up
A_42_P820657	TC618445	0.000112057	7.8	Control Normal Tissue up
A_44_P123381	Sfrs5	5.25E-05	7.8	Control Normal Tissue up
A_44_P414087	5-Sep	0.000234226	7.8	All Tumors up
A_44_P701209	ENSRNOT00000040952	1.21E-05	7.8	All Tumors up
A_44_P788634	RGD1562103_predicted	2.68E-07	7.8	Control Normal Tissue up
A_43_P19727	AI029786	0.000297729	7.8	All Tumors up
A_44_P443751	Tnfrsf12a	5.74E-06	7.8	All Tumors up
A_44_P1053951	DV715514	4.33E-05	7.8	All Tumors up
A_44_P531129	TC599821	0.00018003	7.8	All Tumors up
A_43_P12508	LOC497860	0.00306206	7.8	All Tumors up
A_44_P1034950	M33313	1.52E-06	7.8	All Tumors up
A_44_P653221	AA963477	0.00336217	7.8	All Tumors up
A_43_P14622	Fbp1	5.63E-06	7.8	Control Normal Tissue up
A_44_P438117	M84148	0.00148351	7.8	All Tumors up
A_42_P458530	LOC497859	8.26E-06	7.7	All Tumors up
A_44_P518085	AI043579	7.95E-06	7.7	Control Normal Tissue up
A_44_P147496	Fxyd5	4.01E-06	7.7	All Tumors up
A_42_P784614	AI385133	7.50E-06	7.7	All Tumors up
A_44_P304220	LOC679921	9.26E-05	7.7	All Tumors up
A_44_P618288	TC611320	5.78E-05	7.7	Control Normal Tissue up
A_43_P13931	RGD1305351	0.000118929	7.7	Control Normal Tissue up
A_44_P489366	BF544728	0.0030349	7.7	All Tumors up
A_43_P23187	Ces1	3.87E-05	7.7	Control Normal Tissue up
A_44_P219628	XM_216699	6.43E-07	7.7	Control Normal Tissue up
A_44_P101700	Tnfaip6	0.00173608	7.6	All Tumors up
A_44_P652768	CO394414	3.60E-05	7.6	Control Normal Tissue up
A_44_P421820	Msn	0.00776403	7.6	All Tumors up
A_44_P1004324	TC609403	1.39E-06	7.6	Control Normal Tissue up
A_43_P12626	AI031053	0.00251971	7.6	All Tumors up
A_44_P199806	Aox1	6.83E-05	7.6	Control Normal Tissue up
A_43_P10033	AW918833	0.000114633	7.6	All Tumors up
A_44_P224614	TC623018	5.40E-05	7.6	All Tumors up
A_44_P840118	Ogfr1l	4.81E-08	7.6	All Tumors up
A_44_P404836	BE117700	0.000532058	7.5	Control Normal Tissue up
A_44_P187111	TC617128	0.000447061	7.5	Control Normal Tissue up
A_43_P19628	LOC287938	7.81E-08	7.5	All Tumors up
A_44_P180012	DQ402472	0.000104809	7.5	All Tumors up
A_44_P653493	XM_214014	1.03E-05	7.5	All Tumors up
A_44_P859004	TC622371	0.0001225	7.5	Control Normal Tissue up
A_42_P529711	Tff3	0.000105642	7.5	Control Normal Tissue up
A_44_P699821	Col9a3_predicted	0.000769653	7.5	All Tumors up
A_44_P1004323	TC624195	7.46E-05	7.5	Control Normal Tissue up
A_44_P335564	Tacstd2	8.79E-06	7.5	All Tumors up
A_44_P924698	AW921320	0.000194773	7.4	Control Normal Tissue up
A_44_P762016	Cspg2	0.000536744	7.4	All Tumors up
A_44_P167407	Gpm6b	0.00179048	7.4	All Tumors up
A_43_P19776	AW143180	0.000178964	7.4	Control Normal Tissue up
A_44_P959890	C1s	1.88E-05	7.4	All Tumors up
A_42_P675853	Nr1h4	0.000150196	7.4	Control Normal Tissue up
A_44_P119658	RGD1562855_predicted	0.00129327	7.4	All Tumors up
A_44_P125025	TC640745	0.0120806	7.3	All Tumors up
A_44_P776556	A_44_P944159	0.000236835	7.3	Control Normal Tissue up
A_43_P15023	ENSRNOT00000028262	0.000382796	7.3	All Tumors up
A_43_P19999	TC615892	7.74E-06	7.3	All Tumors up
A_42_P544135	AA998098	0.0120135	7.3	All Tumors up
A_44_P589209	Slc12a8	0.000122962	7.3	Control Normal Tissue up
A_44_P178252	Nefl	0.00187775	7.3	All Tumors up
A_43_P12159	Myh10	4.14E-05	7.2	All Tumors up
A_44_P127337	Grip1	0.00285507	7.2	All Tumors up
A_44_P920111	BI282744	6.67E-06	7.2	Control Normal Tissue up
A_44_P638274	TC620934	5.86E-06	7.2	Control Normal Tissue up
A_44_P892720	Tspan9_predicted	0.000311351	7.2	All Tumors up
A_44_P654444	L17080	0.00431291	7.2	All Tumors up
A_43_P14371	ENSRNOT00000013014	6.49E-05	7.2	Control Normal Tissue up

Probe ID	Gene Symbol	p-value	Fold Change	Direction of Change
A_44_P480696	TC596063	2.64E-06	7.2	Control Normal Tissue up
A_44_P175364	LOC500590	7.18E-06	7.2	All Tumors up
A_44_P838920	BE117700	0.000453779	7.2	Control Normal Tissue up
A_42_P623688	ENSRNOT00000012525	1.25E-05	7.2	All Tumors up
A_44_P309979	Akr1b8	6.55E-06	7.2	All Tumors up
A_44_P427346	Gna14	0.00110305	7.1	Control Normal Tissue up
A_44_P1004868	Col5a2	2.22E-05	7.1	All Tumors up
A_44_P372002	Slc2a5	0.00217539	7.1	Control Normal Tissue up
A_44_P791005	M33313	2.24E-06	7.1	All Tumors up
A_44_P304190	Nkd1_predicted	1.53E-05	7.1	All Tumors up
A_44_P246947	TC641380	1.74E-06	7.1	All Tumors up
A_44_P260036	RGD1305351	0.000135605	7.1	Control Normal Tissue up
A_44_P822447	Sftpd	0.00262778	7.1	Control Normal Tissue up
A_44_P208699	TC595994	1.08E-05	7.1	Control Normal Tissue up
A_44_P866810	Dnah1	0.0106202	7.1	Control Normal Tissue up
A_44_P459144	TC616052	0.000875057	7.1	Control Normal Tissue up
A_44_P937542	Adams5	0.00334155	7.1	All Tumors up
A_44_P461187	BF400026	0.00847802	7.1	Control Normal Tissue up
A_44_P461165	Igfbp4	7.76E-05	7.1	All Tumors up
A_44_P366723	Lrg1	8.40E-07	7.1	All Tumors up
A_44_P197064	Snx10	1.86E-05	7.0	All Tumors up
A_44_P281035	TC601187	8.77E-06	7.0	Control Normal Tissue up
A_43_P12855	TC582343	0.000142463	7.0	Control Normal Tissue up
A_44_P881918	AW915309	3.77E-05	7.0	All Tumors up
A_44_P497121	TC578855	0.000136654	7.0	All Tumors up
A_44_P133581	RGD1562533_predicted	6.91E-05	7.0	All Tumors up
A_44_P319080	Bst1	3.90E-05	7.0	All Tumors up
A_44_P1058055	Ptger3	0.000856762	7.0	Control Normal Tissue up
A_44_P110972	Myo5c_predicted	1.55E-06	6.9	Control Normal Tissue up
A_44_P630174	C3	0.000185027	6.9	All Tumors up
A_42_P549786	LOC683313	1.12E-05	6.9	All Tumors up
A_42_P577136	ENSRNOT00000040507	2.12E-05	6.9	All Tumors up
A_44_P900672	BF566249	1.98E-05	6.9	All Tumors up
A_44_P531758	LOC690657	0.00345136	6.9	All Tumors up
A_44_P199028	TC591122	0.000206679	6.9	Control Normal Tissue up
A_44_P242694	TC612255	3.78E-05	6.9	Control Normal Tissue up
A_44_P508066	Gpr116	0.000125704	6.9	All Tumors up
A_44_P164848	Bcl2a1	3.24E-05	6.9	All Tumors up
A_44_P304880	Ca5b	4.04E-05	6.9	All Tumors up
A_44_P253208	BG671334	7.52E-05	6.9	All Tumors up
A_43_P15427	Ms4a4a_predicted	1.97E-07	6.9	All Tumors up
A_44_P1071663	Pex2	5.06E-05	6.9	Control Normal Tissue up
A_44_P108504	Rab31	4.44E-08	6.9	All Tumors up
A_44_P452222	RGD1562705_predicted	0.000111613	6.9	All Tumors up
A_43_P16413	TC599199	3.18E-05	6.9	Control Normal Tissue up
A_42_P574719	Unc13d	2.84E-06	6.9	All Tumors up
A_44_P803684	AW917931	0.00110813	6.9	Control Normal Tissue up
A_42_P572521	AW920967	5.60E-05	6.8	All Tumors up
A_44_P946518	Col5a2	1.87E-05	6.8	All Tumors up
A_44_P213320	Il18	2.28E-05	6.8	Control Normal Tissue up
A_44_P456444	XM_228184	0.0104373	6.8	All Tumors up
A_44_P223978	Pyy	3.34E-06	6.8	Control Normal Tissue up
A_44_P606490	RGD1309085_predicted	7.11E-05	6.8	All Tumors up
A_43_P12029	Lyz	5.65E-06	6.8	All Tumors up
A_44_P454728	TC599266	4.68E-05	6.8	Control Normal Tissue up
A_44_P366902	Ugt2b10_predicted	5.07E-05	6.8	Control Normal Tissue up
A_43_P22638	LOC287992	4.06E-05	6.8	All Tumors up
A_44_P147560	RGD1305604_predicted	0.00205524	6.8	Control Normal Tissue up
A_42_P499158	DV722942	7.81E-06	6.8	Control Normal Tissue up
A_44_P932384	Aldob	2.71E-07	6.8	Control Normal Tissue up
A_44_P743669	Dmn	9.15E-06	6.8	All Tumors up
A_43_P10931	Tnfsf15	0.000706657	6.8	Control Normal Tissue up
A_44_P832194	Dgat2	7.47E-06	6.8	All Tumors up
A_43_P11683	Tnfsf9	1.84E-05	6.7	All Tumors up
A_44_P828142	Ndrp2	0.000166538	6.7	Control Normal Tissue up

Probe ID	Gene Symbol	p-value	Fold Change	Direction of Change
A_44_P746420	Zg16	2.76E-05	6.7	Control Normal Tissue up
A_44_P419064	BF553172	0.00799347	6.7	All Tumors up
A_44_P1048474	XM_221198	0.000595592	6.7	All Tumors up
A_44_P105899	AF217590	4.01E-05	6.7	All Tumors up
A_44_P207403	DV723748	8.00E-08	6.7	All Tumors up
A_43_P19907	S81289	0.00136136	6.7	All Tumors up
A_44_P208711	Mmd	3.67E-05	6.7	All Tumors up
A_44_P432432	CB614494	2.20E-05	6.7	Control Normal Tissue up
A_44_P747182	RGD1565695_predicted	9.35E-07	6.7	All Tumors up
A_42_P708060	AI060246	0.00103241	6.7	Control Normal Tissue up
A_44_P149847	CA509267	0.000583658	6.7	All Tumors up
A_44_P354062	TC633124	1.72E-05	6.7	Control Normal Tissue up
A_44_P806889	TC597507	7.95E-05	6.7	Control Normal Tissue up
A_44_P129749	Prdm7_predicted	8.40E-06	6.7	Control Normal Tissue up
A_44_P264694	Olfml2b_predicted	5.25E-06	6.7	All Tumors up
A_44_P289922	AI547924	0.000860763	6.7	All Tumors up
A_43_P11127	M16406	8.32E-05	6.7	Control Normal Tissue up
A_44_P262798	TC642140	0.000639545	6.7	Control Normal Tissue up
A_44_P805841	Ptpv	0.000349475	6.7	All Tumors up
A_44_P412427	Mmp9	0.00196084	6.7	All Tumors up
A_44_P281482	AW918729	6.88E-06	6.6	Control Normal Tissue up
A_42_P756334	Neto2_predicted	0.000713233	6.6	All Tumors up
A_44_P158235	Slc15a1	0.000599127	6.6	Control Normal Tissue up
A_44_P212850	RGD1311307	8.99E-08	6.6	All Tumors up
A_44_P513385	Amn_predicted	4.63E-07	6.6	Control Normal Tissue up
A_44_P443916	BU758404	0.000227469	6.6	All Tumors up
A_44_P260272	Igj	0.00255591	6.6	All Tumors up
A_44_P351209	Bhlhb8	5.81E-05	6.6	All Tumors up
A_42_P619403	RGD1563888_predicted	8.22E-09	6.6	All Tumors up
A_44_P401131	RGD1564703_predicted	3.13E-05	6.6	Control Normal Tissue up
A_44_P739541	A_44_P976406	1.86E-06	6.6	All Tumors up
A_44_P686427	Cilp_predicted	0.000952154	6.5	All Tumors up
A_44_P461842	TC613623	0.000154163	6.5	Control Normal Tissue up
A_44_P161868	Stc1	0.00349059	6.5	All Tumors up
A_44_P748601	Wnt10a_predicted	0.0094851	6.5	All Tumors up
A_44_P160877	Cp	0.0040035	6.5	All Tumors up
A_42_P641962	RGD1306105_predicted	6.82E-05	6.5	Control Normal Tissue up
A_44_P151708	TC630172	1.97E-05	6.5	Control Normal Tissue up
A_44_P147558	BE120761	0.000210509	6.5	All Tumors up
A_44_P714784	AW917984	0.00664989	6.5	All Tumors up
A_44_P346913	Pled1	6.79E-05	6.5	Control Normal Tissue up
A_44_P218896	Atp2a3	0.00425305	6.5	Control Normal Tissue up
A_43_P12791	Dpp4	1.07E-05	6.5	Control Normal Tissue up
A_44_P431685	AW917120	7.89E-07	6.5	Control Normal Tissue up
A_44_P714927	BC091425	2.62E-05	6.5	Control Normal Tissue up
A_44_P638230	Rimbp2	9.44E-07	6.5	Control Normal Tissue up
A_42_P804387	BG663107	0.00253283	6.5	Control Normal Tissue up
A_44_P144557	Z93363	0.00347554	6.5	All Tumors up
A_44_P676347	Spink1	4.55E-05	6.4	Control Normal Tissue up
A_44_P636897	LOC687523	0.000403557	6.4	Control Normal Tissue up
A_44_P558821	Wnt5a	3.27E-05	6.4	All Tumors up
A_44_P1042360	ENSRNOT00000057971	0.00057378	6.4	All Tumors up
A_43_P12658	Fn1	2.32E-05	6.4	All Tumors up
A_44_P175530	AA850402	1.65E-05	6.4	All Tumors up
A_44_P898953	Galnt14_predicted	0.000222181	6.4	Control Normal Tissue up
A_44_P359188	LOC299339	4.29E-06	6.4	All Tumors up
A_44_P277876	CO566833	0.000170306	6.4	All Tumors up
A_44_P598999	TC622521	2.24E-05	6.4	Control Normal Tissue up
A_44_P194230	TC613867	0.000106728	6.4	Control Normal Tissue up
A_44_P248248	AW916017	2.27E-05	6.4	Control Normal Tissue up
A_43_P10874	Prss12	8.47E-05	6.4	All Tumors up
A_44_P210173	BP483652	0.000119644	6.4	Control Normal Tissue up
A_44_P550662	Lhx2_predicted	3.22E-05	6.4	All Tumors up
A_44_P185243	XM_213999	4.45E-05	6.4	All Tumors up
A_43_P11540	TC589280	0.00066727	6.3	Control Normal Tissue up

Probe ID	Gene Symbol	p-value	Fold Change	Direction of Change
A_44_P901471	TC615769	0.000257307	6.3	Control Normal Tissue up
A_44_P344487	AF217598	0.00719155	6.3	All Tumors up
A_43_P14503	Ceacam10	0.000345567	6.3	Control Normal Tissue up
A_44_P169623	TC603120	0.000157822	6.3	Control Normal Tissue up
A_44_P114692	Pth	0.000276875	6.3	Control Normal Tissue up
A_44_P809279	Wnt2b	0.000241479	6.3	All Tumors up
A_44_P525969	Ifit1_predicted	0.000455546	6.3	All Tumors up
A_44_P1039128	TC603103	3.49E-05	6.3	All Tumors up
A_42_P509923	RGD1307059_predicted	8.64E-05	6.3	All Tumors up
A_44_P256003	Osmr	6.08E-05	6.3	All Tumors up
A_44_P441339	Prickle1	2.87E-07	6.3	All Tumors up
A_44_P132960	Serpine1	1.88E-05	6.3	All Tumors up
A_44_P637322	TC589777	0.00996862	6.3	All Tumors up
A_44_P135592	A_44_P904775	4.98E-05	6.3	Control Normal Tissue up
A_44_P487021	TC615769	0.000191678	6.3	Control Normal Tissue up
A_44_P130333	Nr1i3	5.61E-06	6.3	Control Normal Tissue up
A_44_P550748	AI043862	1.35E-06	6.3	All Tumors up
A_44_P579594	Tgm1	1.88E-06	6.3	All Tumors up
A_44_P520159	Plg	0.00541141	6.2	All Tumors up
A_44_P1013314	TC621613	0.00107326	6.2	All Tumors up
A_44_P489608	TC613996	9.28E-06	6.2	Control Normal Tissue up
A_42_P566079	LOC314964	2.57E-05	6.2	Control Normal Tissue up
A_44_P233502	Senn1b	0.000183615	6.2	Control Normal Tissue up
A_43_P12955	Gnal	0.000745185	6.2	Control Normal Tissue up
A_44_P917115	RGD1562551_predicted	0.000116077	6.2	All Tumors up
A_44_P463262	Ppp1r14c	2.45E-07	6.2	All Tumors up
A_44_P993370	LOC501089	1.72E-06	6.2	All Tumors up
A_42_P461794	Lrrc8c	9.79E-06	6.2	All Tumors up
A_44_P320292	CB547734	0.00366073	6.2	Control Normal Tissue up
A_44_P484889	Il1r2	2.74E-05	6.2	All Tumors up
A_44_P600376	Prkg2	1.42E-05	6.2	All Tumors up
A_42_P549321	AA818205	2.68E-06	6.2	All Tumors up
A_43_P14852	DV728455	0.000168622	6.2	All Tumors up
A_44_P358235	RGD1565148_predicted	0.0100567	6.2	All Tumors up
A_44_P215689	Slit1	1.97E-05	6.2	Control Normal Tissue up
A_44_P1029956	TC600862	0.00143294	6.2	Control Normal Tissue up
A_44_P414066	Tnfrsf19l_predicted	2.45E-05	6.2	All Tumors up
A_44_P132464	CX570325	3.56E-06	6.2	Control Normal Tissue up
A_44_P666098	Pdpn	0.000393426	6.2	All Tumors up
A_44_P147572	Ier5l	2.13E-05	6.2	All Tumors up
A_44_P898364	Dpp4	6.40E-06	6.2	Control Normal Tissue up
A_44_P517392	RGD1561144_predicted	0.000440304	6.1	Control Normal Tissue up
A_44_P457578	TC595239	1.81E-06	6.1	Control Normal Tissue up
A_44_P966141	M12822	0.00135779	6.1	All Tumors up
A_42_P735417	Dio1	5.62E-06	6.1	Control Normal Tissue up
A_44_P382979	Ptger2	0.000298824	6.1	All Tumors up
A_44_P556989	Adora2a	8.59E-05	6.1	All Tumors up
A_44_P321719	CA511571	9.48E-05	6.1	All Tumors up
A_44_P249508	Cybrd1	3.74E-05	6.1	All Tumors up
A_44_P525235	Rgs1	0.000120857	6.1	All Tumors up
A_44_P577274	Ripk3	2.46E-05	6.1	All Tumors up
A_44_P231867	Adamdec1_predicted	0.000209722	6.1	All Tumors up
A_44_P608078	Hexb	2.06E-05	6.1	Control Normal Tissue up
A_44_P367465	TC607870	4.63E-06	6.1	Control Normal Tissue up
A_44_P653272	XM_346135	9.08E-05	6.1	All Tumors up
A_44_P555271	TC600344	0.000137636	6.1	Control Normal Tissue up
A_44_P154513	Cyp2d22	3.07E-06	6.1	Control Normal Tissue up
A_44_P686269	Htra1	7.67E-06	6.1	All Tumors up
A_44_P1007965	Emb	0.00026129	6.1	All Tumors up
A_43_P22437	AW916327	4.27E-05	6.1	All Tumors up
A_44_P961911	TC594574	0.00755038	6.1	All Tumors up
A_44_P792446	Oit3	0.0030134	6.0	All Tumors up
A_44_P152219	RGD1560851_predicted	1.94E-05	6.0	All Tumors up
A_44_P170919	Tff3	4.43E-05	6.0	Control Normal Tissue up
A_44_P363116	Cd302	0.000187502	6.0	Control Normal Tissue up

Probe ID	Gene Symbol	p-value	Fold Change	Direction of Change
A_44_P1021644	AA962967	4.18E-05	6.0	Control Normal Tissue up
A_44_P541276	Ggt1	0.00267171	6.0	All Tumors up
A_44_P527060	Stx11	0.003849	6.0	All Tumors up
A_44_P125733	Nr1i3	0.000284915	6.0	Control Normal Tissue up
A_44_P439292	TC618339	2.36E-05	6.0	Control Normal Tissue up
A_42_P751720	CX570642	2.03E-06	6.0	All Tumors up
A_44_P295673	Slc37a2_predicted	0.000152299	6.0	Control Normal Tissue up
A_44_P1040685	ENSRNOT00000049620	4.04E-05	6.0	Control Normal Tissue up
A_44_P221077	Tnfrsf26_predicted	0.000351759	6.0	All Tumors up
A_44_P411954	TC614121	1.03E-05	6.0	Control Normal Tissue up
A_44_P195619	L04739	1.12E-06	6.0	Control Normal Tissue up
A_44_P503022	Col18a1	2.49E-05	6.0	All Tumors up
A_43_P17235	AI231033	0.000298098	6.0	Control Normal Tissue up
A_44_P560973	Ccl28	8.48E-05	6.0	Control Normal Tissue up
A_44_P203878	Cyp2j4	0.000313818	6.0	Control Normal Tissue up
A_43_P15791	TC605245	0.000430591	6.0	Control Normal Tissue up
A_42_P843692	Cldn15_predicted	8.42E-05	6.0	Control Normal Tissue up
A_44_P222030	Msln	0.00695976	6.0	All Tumors up
A_44_P833626	Ceacam10	0.000346535	6.0	Control Normal Tissue up
A_44_P267013	Cdh23	0.0017458	6.0	Control Normal Tissue up
A_44_P886246	TC591439	0.000408862	6.0	Control Normal Tissue up
A_42_P689357	Pcdh7	0.00203719	6.0	All Tumors up
A_44_P190838	Apobec2_predicted	1.18E-05	6.0	All Tumors up
A_44_P412290	Tcf21	6.21E-05	6.0	All Tumors up
A_44_P504724	BF561546	0.000505658	6.0	Control Normal Tissue up
A_44_P506514	TC644908	9.65E-05	5.9	All Tumors up
A_44_P943285	Cp	0.0124458	5.9	All Tumors up
A_44_P960435	TC621644	0.000188294	5.9	Control Normal Tissue up
A_44_P699964	TC625599	7.74E-06	5.9	Control Normal Tissue up
A_44_P447650	M62828	0.000892386	5.9	All Tumors up
A_42_P693964	RGD1560084_predicted	0.000221373	5.9	All Tumors up
A_44_P818459	A_44_P643573	0.000446323	5.9	Control Normal Tissue up
A_44_P956203	Dgat2	3.20E-06	5.9	All Tumors up
A_44_P669553	XM_224972	3.73E-05	5.9	Control Normal Tissue up
A_44_P158599	TC581550	0.00052509	5.9	All Tumors up
A_42_P606890	TC622561	0.00497684	5.9	All Tumors up
A_44_P117100	Btm3	8.94E-05	5.9	Control Normal Tissue up
A_44_P635423	BF554994	1.34E-05	5.9	All Tumors up
A_42_P763522	TC608310	3.44E-05	5.9	All Tumors up
A_44_P997578	Lrrc48	1.10E-07	5.9	Control Normal Tissue up
A_44_P513059	Col18a1	1.48E-05	5.9	All Tumors up
A_43_P16043	Il12a	0.000256134	5.9	Control Normal Tissue up
A_44_P230320	TC593009	3.37E-05	5.9	Control Normal Tissue up
A_42_P824217	ENSRNOT00000048256	3.11E-07	5.9	All Tumors up
A_44_P537480	AI407991	4.65E-05	5.9	All Tumors up
A_43_P14871	TC606533	3.98E-05	5.9	Control Normal Tissue up
A_43_P10498	Sult1c2a	0.000196042	5.8	Control Normal Tissue up
A_44_P436280	DV727678	9.12E-05	5.8	All Tumors up
A_44_P607842	RGD1308581_predicted	1.85E-05	5.8	Control Normal Tissue up
A_44_P158533	AA875633	0.000797403	5.8	All Tumors up
A_44_P125623	LOC682243	0.00491411	5.8	All Tumors up
A_44_P717610	AABR03000060	6.93E-06	5.8	All Tumors up
A_44_P778966	Rhoj	0.00016224	5.8	All Tumors up
A_44_P342047	Dusp14_predicted	1.94E-06	5.8	All Tumors up
A_44_P381917	Tgfb3	0.000110793	5.8	All Tumors up
A_44_P347283	LOC683733	5.91E-05	5.8	Control Normal Tissue up
A_44_P197786	BF559333	0.000228613	5.8	Control Normal Tissue up
A_44_P532270	Chac1_predicted	2.24E-06	5.8	All Tumors up
A_44_P359052	TC601364	1.56E-05	5.8	Control Normal Tissue up
A_44_P429453	Thbd	5.80E-05	5.8	All Tumors up
A_44_P342550	Msr2_predicted	3.26E-07	5.8	All Tumors up
A_43_P18464	TC606304	8.86E-07	5.8	Control Normal Tissue up
A_44_P296057	TC603491	3.81E-05	5.8	All Tumors up
A_44_P837764	DV728925	4.78E-06	5.8	All Tumors up
A_44_P608892	TC635252	1.53E-06	5.8	Control Normal Tissue up

Probe ID	Gene Symbol	p-value	Fold Change	Direction of Change
A_44_P552533	TC603764	8.24E-06	5.7	Control Normal Tissue up
A_44_P702052	TC608741	8.34E-05	5.7	Control Normal Tissue up
A_44_P427134	Ccl21b	8.35E-05	5.7	All Tumors up
A_44_P880441	Egf	9.54E-05	5.7	Control Normal Tissue up
A_44_P744113	Cxcr4	1.10E-05	5.7	All Tumors up
A_44_P270157	RGD1561067_predicted	2.06E-05	5.7	All Tumors up
A_42_P463754	CF107866	8.11E-05	5.7	All Tumors up
A_44_P700209	TC590186	2.27E-06	5.7	All Tumors up
A_42_P591344	A_44_P892720	5.98E-06	5.7	All Tumors up
A_44_P248090	Nr4a3	0.00336847	5.7	All Tumors up
A_44_P452176	Anxa13_predicted	9.15E-05	5.7	Control Normal Tissue up
A_44_P463899	LOC688553	0.000139179	5.7	Control Normal Tissue up
A_42_P621642	Smpx	0.000988289	5.7	All Tumors up
A_44_P212470	Ap1s2_predicted	0.000590959	5.7	All Tumors up
A_44_P458021	Mafb	0.000516881	5.7	All Tumors up
A_44_P746333	TC590823	0.00236431	5.7	All Tumors up
A_44_P325508	Cyp2d22	7.18E-06	5.7	Control Normal Tissue up
A_44_P573545	LOC362477	0.000221899	5.7	Control Normal Tissue up
A_44_P358548	K02813	0.000369874	5.7	Control Normal Tissue up
A_44_P151138	Gatm	0.000149773	5.7	All Tumors up
A_42_P636232	Sst	2.02E-08	5.7	Control Normal Tissue up
A_44_P448138	BF551342	0.000199302	5.7	All Tumors up
A_44_P289080	Sulfl	1.87E-05	5.7	All Tumors up
A_43_P11985	AW920845	8.09E-05	5.7	Control Normal Tissue up
A_44_P1057403	RGD1310681_predicted	3.42E-06	5.7	All Tumors up
A_44_P164027	AW143756	0.0124595	5.7	All Tumors up
A_43_P14522	TC612592	8.04E-05	5.7	Control Normal Tissue up
A_44_P1042473	ENSRNOT00000040102	0.00332807	5.6	All Tumors up
A_44_P541213	LOC310877	2.72E-06	5.6	All Tumors up
A_43_P13418	TC617367	0.000114246	5.6	Control Normal Tissue up
A_42_P638511	Rimbp2	7.78E-07	5.6	Control Normal Tissue up
A_44_P173355	Slc25a4	6.02E-06	5.6	All Tumors up
A_44_P978172	AA899254	0.00020517	5.6	Control Normal Tissue up
A_44_P116870	Plau	2.95E-06	5.6	All Tumors up
A_44_P864923	CO393293	0.00352235	5.6	Control Normal Tissue up
A_44_P594136	RGD1565540_predicted	1.67E-07	5.6	All Tumors up
A_42_P749550	TC595600	2.63E-05	5.6	Control Normal Tissue up
A_44_P383874	Col15a1	6.92E-06	5.6	All Tumors up
A_44_P425027	Ttc6_predicted	3.16E-06	5.6	Control Normal Tissue up
A_44_P776182	Ret	0.000431813	5.6	Control Normal Tissue up
A_44_P393822	Tead2	4.90E-05	5.6	All Tumors up
A_43_P14310	Inhba	0.00290098	5.6	All Tumors up
A_44_P684242	TC635129	3.77E-06	5.6	Control Normal Tissue up
A_44_P315085	Rln3	9.38E-06	5.6	Control Normal Tissue up
A_44_P485948	TC618928	1.66E-05	5.6	Control Normal Tissue up
A_44_P482519	TC596249	2.99E-05	5.6	All Tumors up
A_44_P321032	St3gal4	3.07E-06	5.6	All Tumors up
A_44_P545686	Samsn1	1.98E-05	5.6	All Tumors up
A_44_P566811	Muc1	9.29E-05	5.5	Control Normal Tissue up
A_44_P355013	Igfl	0.000115191	5.5	All Tumors up
A_44_P281481	AI547698	7.81E-06	5.5	Control Normal Tissue up
A_44_P402948	Tmem63c_predicted	0.000319918	5.5	All Tumors up
A_44_P409605	Nr3c2	0.000160111	5.5	Control Normal Tissue up
A_44_P1019291	Uchl1	4.66E-06	5.5	All Tumors up
A_44_P454450	Ofml	0.000178467	5.5	All Tumors up
A_42_P467630	CF110019	3.21E-05	5.5	All Tumors up
A_44_P916132	RGD1308967_predicted	0.000372881	5.5	All Tumors up
A_44_P318861	TC612212	2.19E-05	5.5	Control Normal Tissue up
A_42_P817417	RGD1560736_predicted	0.00141303	5.5	All Tumors up
A_42_P736812	BM391518	1.98E-05	5.5	Control Normal Tissue up
A_44_P382683	Rasgrp1	0.000489269	5.5	Control Normal Tissue up
A_44_P102235	Aqp8	4.82E-05	5.5	Control Normal Tissue up
A_44_P414484	Car8	1.06E-05	5.5	All Tumors up
A_44_P119519	Cttnbp2	0.00304683	5.5	Control Normal Tissue up
A_43_P13100	ENSRNOT00000016262	0.000511108	5.5	All Tumors up



Probe ID	Gene Symbol	p-value	Fold Change	Direction of Change
A_42_P701855	Gpr176	0.000122789	5.5	All Tumors up
A_44_P1057585	AI234967	1.64E-05	5.5	All Tumors up
A_44_P1018865	B3gat2	0.00238243	5.5	All Tumors up
A_43_P12832	RGD1561255_predicted	0.00314216	5.5	Control Normal Tissue up
A_44_P426529	Fcer2a	2.05E-05	5.5	All Tumors up
A_44_P341910	Cyp17a1	9.06E-06	5.5	Control Normal Tissue up
A_44_P797293	TC619023	2.88E-05	5.5	Control Normal Tissue up
A_44_P965553	Robo2	1.87E-05	5.5	All Tumors up
A_44_P559239	Bche	0.00075998	5.5	Control Normal Tissue up
A_44_P114308	Nmu	4.12E-05	5.5	Control Normal Tissue up
A_44_P849592	TC604845	0.000105288	5.5	Control Normal Tissue up
A_44_P681660	Rab40b_predicted	3.54E-05	5.5	Control Normal Tissue up
A_44_P792507	Cryab	0.000102732	5.4	All Tumors up
A_42_P841017	CF111207	0.000540708	5.4	Control Normal Tissue up
A_44_P824642	Slco2b1	3.93E-05	5.4	Control Normal Tissue up
A_44_P378845	Gzma	0.00096225	5.4	Control Normal Tissue up
A_44_P227983	ENSRNOT00000004009	0.0075516	5.4	Control Normal Tissue up
A_43_P19751	Edg2	0.000259113	5.4	Control Normal Tissue up
A_44_P347118	Tex15_predicted	0.000364087	5.4	Control Normal Tissue up
A_44_P824143	Scn7a	0.000442175	5.4	Control Normal Tissue up
A_44_P758339	Dkk1_predicted	0.00366311	5.4	All Tumors up
A_44_P306344	AW915807	1.26E-05	5.4	Control Normal Tissue up
A_44_P144649	AI071874	9.62E-05	5.4	All Tumors up
A_44_P979645	RGD1307981_predicted	7.86E-06	5.4	Control Normal Tissue up
A_44_P472994	Nnat	0.00135624	5.4	All Tumors up
A_44_P433923	AW142951	1.28E-05	5.4	All Tumors up
A_44_P124355	CO393484	0.000648689	5.4	Control Normal Tissue up
A_44_P372710	BQ196242	2.17E-05	5.4	Control Normal Tissue up
A_44_P135339	TC600409	5.85E-06	5.4	Control Normal Tissue up
A_44_P1001551	LOC366473	0.00190399	5.4	All Tumors up
A_44_P434724	TC600669	4.39E-05	5.4	Control Normal Tissue up
A_44_P491976	ENSRNOT00000054730	3.22E-06	5.4	Control Normal Tissue up
A_44_P374138	Udpgr2	0.000822228	5.4	Control Normal Tissue up
A_44_P669616	Adams9_predicted	0.00118163	5.4	All Tumors up
A_43_P12451	Sct	9.37E-08	5.4	All Tumors up
A_42_P728032	TC628898	0.00470721	5.4	Control Normal Tissue up
A_43_P17697	Gsta2	0.000347977	5.4	Control Normal Tissue up
A_44_P775952	Gnb4	7.07E-05	5.4	All Tumors up
A_44_P168405	CB545011	9.93E-06	5.4	All Tumors up
A_44_P419882	Guca2a	2.80E-05	5.4	Control Normal Tissue up
A_44_P247956	Itgal	0.00014634	5.4	All Tumors up
A_44_P312166	CB614160	0.00141283	5.4	Control Normal Tissue up
A_44_P301936	RGD1561521_predicted	0.00345387	5.4	All Tumors up
A_44_P316898	Chga	6.59E-05	5.4	Control Normal Tissue up
A_42_P832728	Gsta2	0.000380004	5.4	Control Normal Tissue up
A_44_P356636	CF109910	3.69E-06	5.4	Control Normal Tissue up
A_43_P19944	TC583715	0.00226003	5.4	Control Normal Tissue up
A_44_P562860	Slc25a4	3.84E-06	5.4	All Tumors up
A_44_P282843	AA801133	0.00246255	5.3	All Tumors up
A_43_P22351	C5r1	2.55E-05	5.3	All Tumors up
A_44_P874053	TC613666	4.65E-05	5.3	Control Normal Tissue up
A_44_P411756	TC626126	0.00394282	5.3	All Tumors up
A_44_P425580	TC626054	1.62E-06	5.3	Control Normal Tissue up
A_44_P292934	DV716894	9.60E-07	5.3	Control Normal Tissue up
A_42_P588738	Mettl7b	2.44E-06	5.3	Control Normal Tissue up
A_43_P12467	Tcfep211_predicted	0.00112088	5.3	Control Normal Tissue up
A_44_P384404	LOC688956	1.22E-06	5.3	All Tumors up
A_44_P247286	Nid2	0.000356214	5.3	All Tumors up
A_42_P801379	Cdkn1c	0.000150819	5.3	All Tumors up
A_44_P901088	RGD1563347_predicted	6.24E-06	5.3	All Tumors up
A_44_P669786	Rgs5	5.52E-05	5.3	All Tumors up
A_44_P711401	Klk8	7.16E-05	5.3	Control Normal Tissue up
A_44_P464145	ENSRNOT00000042721	0.00361656	5.3	All Tumors up
A_42_P596024	TC602984	1.67E-05	5.3	Control Normal Tissue up
A_43_P19157	RGD1562373_predicted	7.86E-05	5.3	Control Normal Tissue up

Probe ID	Gene Symbol	p-value	Fold Change	Direction of Change
A_44_P252483	LOC360932	7.08E-06	5.3	All Tumors up
A_44_P620966	AA923898	0.00254523	5.3	Control Normal Tissue up
A_44_P487530	Mapre3	0.000475175	5.3	Control Normal Tissue up
A_44_P549847	Pappa_predicted	0.000472527	5.3	All Tumors up
A_44_P436655	Slc5a2	0.000505212	5.3	Control Normal Tissue up
A_44_P971371	ENSRNOT00000008229	6.09E-06	5.3	All Tumors up
A_43_P15900	TC608781	0.00206622	5.3	Control Normal Tissue up
A_42_P520349	Tacr1	6.96E-05	5.3	Control Normal Tissue up
A_44_P508924	A_44_P951387	0.00314363	5.3	Control Normal Tissue up
A_44_P966220	Vcam1	0.000299944	5.3	All Tumors up
A_44_P477819	Btnl8	0.00324122	5.3	Control Normal Tissue up
A_44_P731356	RGD1559807_predicted	0.00107697	5.3	Control Normal Tissue up
A_44_P602851	TC636180	1.25E-05	5.2	Control Normal Tissue up
A_44_P429455	Plxnc1_predicted	4.99E-06	5.2	All Tumors up
A_44_P803553	A_44_P394291	6.18E-05	5.2	Control Normal Tissue up
A_44_P930999	DV716578	3.45E-05	5.2	All Tumors up
A_44_P298331	Gpr68_predicted	9.04E-06	5.2	All Tumors up
A_44_P371317	AB072252	0.000597525	5.2	Control Normal Tissue up
A_44_P839581	TC591217	2.80E-06	5.2	Control Normal Tissue up
A_42_P743682	TC613256	4.36E-05	5.2	Control Normal Tissue up
A_44_P730661	Krt20	0.00414658	5.2	Control Normal Tissue up
A_44_P858611	TC609375	3.59E-05	5.2	All Tumors up
A_44_P128848	TC626593	3.30E-06	5.2	Control Normal Tissue up
A_44_P209149	F3	6.21E-06	5.2	All Tumors up
A_44_P504192	TC642089	0.00204658	5.2	Control Normal Tissue up
A_44_P308398	TC634082	7.87E-06	5.2	Control Normal Tissue up
A_44_P247081	TC635649	2.12E-05	5.2	All Tumors up
A_44_P362749	TC607638	0.000277515	5.2	Control Normal Tissue up
A_44_P336489	CO386194	7.60E-05	5.2	Control Normal Tissue up
A_43_P19763	Arl11	0.000139744	5.2	All Tumors up
A_44_P369612	Cfb	0.000699255	5.2	All Tumors up
A_44_P472996	Camp	0.000154184	5.2	All Tumors up
A_43_P14553	Neurod1	0.000219602	5.2	Control Normal Tissue up
A_44_P457169	BI289678	0.000386809	5.2	All Tumors up
A_44_P338864	AA998473	0.00657274	5.2	All Tumors up
A_44_P440178	TC618126	1.09E-05	5.2	Control Normal Tissue up
A_42_P559737	Edn2	8.66E-07	5.2	Control Normal Tissue up
A_44_P506043	Fut4	0.000180164	5.2	Control Normal Tissue up
A_44_P438060	Loxl1	2.27E-06	5.2	All Tumors up
A_44_P243708	ENSRNOT000000048256	0.000361596	5.2	All Tumors up
A_44_P442802	Pgap1	0.000165681	5.2	Control Normal Tissue up
A_44_P395374	TC637304	0.000750292	5.2	Control Normal Tissue up
A_44_P294015	LOC679861	0.000489565	5.2	Control Normal Tissue up
A_42_P512838	TC601137	0.000201406	5.1	Control Normal Tissue up
A_43_P10133	TC587211	0.000364218	5.1	Control Normal Tissue up
A_43_P17494	Plat	1.89E-06	5.1	All Tumors up
A_44_P181548	TC613308	0.000298424	5.1	Control Normal Tissue up
A_44_P718765	TC603962	2.04E-05	5.1	Control Normal Tissue up
A_44_P234212	TC627511	0.00756081	5.1	All Tumors up
A_44_P427702	Gpc1	3.16E-05	5.1	All Tumors up
A_44_P176053	LOC312831	7.12E-06	5.1	All Tumors up
A_44_P192406	St3gal1	0.00206584	5.1	Control Normal Tissue up
A_42_P799390	XM_214905	0.000146353	5.1	Control Normal Tissue up
A_44_P510949	TC583130	8.64E-05	5.1	Control Normal Tissue up
A_42_P457003	TC598388	3.45E-05	5.1	Control Normal Tissue up
A_44_P1042783	AJ224441	0.0015413	5.1	Control Normal Tissue up
A_44_P395885	Tram111_predicted	0.000580993	5.1	All Tumors up
A_44_P900229	A_44_P806889	2.61E-05	5.1	All Tumors up
A_43_P10016	AW142969	0.000731709	5.1	Control Normal Tissue up
A_44_P656312	TC607133	4.31E-06	5.1	Control Normal Tissue up
A_44_P419757	Crabp2	0.00117513	5.1	All Tumors up
A_44_P325791	ENSRNOT000000024832	0.00100227	5.1	All Tumors up
A_42_P807866	Cd48	2.16E-06	5.1	All Tumors up
A_42_P828695	BI298356	0.000120415	5.1	Control Normal Tissue up
A_42_P666951	TC623350	0.000523765	5.1	All Tumors up

Probe ID	Gene Symbol	p-value	Fold Change	Direction of Change
A_43_P12651	Col9a3_predicted	0.00827108	5.1	All Tumors up
A_44_P248484	M77364	0.00669448	5.1	All Tumors up
A_44_P217726	RGD1311475_predicted	1.19E-06	5.1	All Tumors up
A_44_P421375	ENSRNOT00000041850	0.00273349	5.1	Control Normal Tissue up
A_44_P337365	Chchd6_predicted	2.08E-07	5.1	All Tumors up
A_44_P107370	Myh6	6.69E-05	5.1	All Tumors up
A_44_P238738	TC635322	0.000107939	5.1	Control Normal Tissue up
A_44_P945215	AA996957	2.00E-05	5.1	All Tumors up
A_44_P416938	Fgf2	0.00405104	5.1	All Tumors up
A_44_P363208	TC614577	0.000753911	5.0	Control Normal Tissue up
A_44_P959775	DV718343	0.000140038	5.0	Control Normal Tissue up
A_44_P400591	Dab2	4.00E-05	5.0	All Tumors up
A_44_P458074	Scg2	4.67E-05	5.0	Control Normal Tissue up
A_42_P604331	AY387069	0.00976782	5.0	Control Normal Tissue up
A_44_P890330	BG673684	0.0016285	5.0	All Tumors up
A_43_P15253	XM_344379	0.00837097	5.0	All Tumors up
A_44_P691232	Phlda1	1.79E-06	5.0	All Tumors up
A_44_P117744	Gp2	0.000161621	5.0	Control Normal Tissue up
A_44_P685554	BP504249	9.89E-07	5.0	Control Normal Tissue up
A_44_P306439	CX569614	0.000383143	5.0	Control Normal Tissue up
A_44_P226263	Hoxa2	0.000671054	5.0	Control Normal Tissue up
A_43_P11537	TC621744	1.67E-05	5.0	Control Normal Tissue up
A_44_P939143	RGD1309879	4.44E-07	5.0	All Tumors up
A_44_P342671	Gnb5	2.15E-06	5.0	Control Normal Tissue up
A_44_P173706	AI072466	0.000126106	5.0	Control Normal Tissue up
A_44_P667693	TC601788	1.76E-05	5.0	Control Normal Tissue up
A_44_P941068	BE110944	0.00714917	5.0	Control Normal Tissue up
A_44_P229670	Noxo1_predicted	1.02E-06	5.0	All Tumors up
A_44_P367688	A_44_P739541	0.000112007	5.0	All Tumors up
A_42_P643622	TC616851	0.0031412	5.0	All Tumors up
A_44_P1035058	XM_231999	0.00367967	5.0	All Tumors up
A_44_P670133	Bace2	2.52E-05	5.0	Control Normal Tissue up
A_44_P790449	ENSRNOT00000059002	0.00379904	5.0	Control Normal Tissue up
A_44_P562350	BF542413	1.24E-05	5.0	All Tumors up
A_44_P679072	Dd25	2.75E-07	5.0	All Tumors up
A_44_P715240	Cfh	9.49E-06	5.0	All Tumors up
A_42_P683634	TC615231	6.09E-06	5.0	Control Normal Tissue up
A_44_P652447	Pcsk6	1.00E-07	5.0	All Tumors up
A_43_P10468	S82585	0.00291758	5.0	All Tumors up
A_44_P681227	AA997941	0.000246205	5.0	Control Normal Tissue up
A_42_P547856	A_44_P966657	0.00175491	5.0	Control Normal Tissue up
A_44_P384688	TC615694	0.00140458	5.0	Control Normal Tissue up
A_43_P12783	ENSRNOT00000008229	7.83E-07	5.0	All Tumors up
A_44_P386693	Arhgef9	0.00303979	5.0	Control Normal Tissue up
A_44_P513635	Tmem45b	0.000136205	5.0	Control Normal Tissue up
A_44_P716769	BF289878	4.65E-06	5.0	All Tumors up
A_44_P340236	RGD1563402_predicted	0.000119594	5.0	All Tumors up
A_43_P10690	BF563060	0.000295967	5.0	Control Normal Tissue up

**Supplementary Table S-2. Genes differentially expressed between untreated normal colonic tissue and DSS-treated colonic tissue**

Probe ID	Gene Symbol	p-value	Fold Change	Direction of Change
A_44_P276538	Gp49b	0.00198874	353.8	DSS Normal Tissue up
A_43_P11086	Upk1b	1.94E-05	228.9	DSS Normal Tissue up
A_44_P241070	RGD1565786_predicted	0.00208908	128.1	DSS Normal Tissue up
A_43_P11684	Alpl	7.94E-05	83.2	DSS Normal Tissue up
A_44_P668888	TC585449	0.000773298	56.2	DSS Normal Tissue up
A_42_P534882	Vsnl1	0.000871214	43.2	DSS Normal Tissue up
A_43_P10156	AW143833	0.000261374	39.0	DSS Normal Tissue up
A_44_P734459	DV718231	2.44E-06	38.8	DSS Normal Tissue up
A_44_P362981	Fabp5	5.49E-06	36.4	DSS Normal Tissue up
A_43_P15819	Prss22_predicted	2.14E-08	34.6	DSS Normal Tissue up
A_44_P219628	Ggt1	6.68E-05	34.6	DSS Normal Tissue up
A_44_P384974	Upk1b	8.27E-05	30.2	DSS Normal Tissue up
A_44_P1029697	Chl1	6.49E-06	28.6	DSS Normal Tissue up
A_44_P536676	B3galt3	0.000100577	28.3	DSS Normal Tissue up
A_44_P592667	Spink5_predicted	0.000896615	27.8	DSS Normal Tissue up
A_44_P859004	TC622561	0.000231406	27.7	DSS Normal Tissue up
A_44_P450496	ENSRNOT00000047751	0.000106358	26.7	DSS Normal Tissue up
A_44_P837709	CF112941	2.05E-05	25.7	DSS Normal Tissue up
A_44_P256301	Grem1	0.000709522	25.2	DSS Normal Tissue up
A_43_P15961	Rbclca2	0.000498443	25.1	DSS Normal Tissue up
A_43_P14796	LOC682861	2.07E-05	24.9	DSS Normal Tissue up
A_44_P592221	TC598512	2.62E-05	24.2	DSS Normal Tissue up
A_44_P212985	ENSRNOT00000028262	3.81E-05	24.0	DSS Normal Tissue up
A_42_P544135	TC603491	1.05E-06	23.2	DSS Normal Tissue up
A_42_P552681	Cmah	1.06E-09	23.1	Control Normal Tissue up
A_44_P820062	AI029786	4.23E-05	23.0	DSS Normal Tissue up
A_44_P326133	LOC296723	1.15E-06	22.8	DSS Normal Tissue up
A_44_P879764	B4galt1_predicted	6.04E-08	22.7	DSS Normal Tissue up
A_44_P869362	LOC688150	1.12E-05	22.6	DSS Normal Tissue up
A_42_P773945	B4galt1_predicted	3.35E-09	22.5	DSS Normal Tissue up
A_42_P832417	Vsnl1	0.000311878	22.1	DSS Normal Tissue up
A_42_P575104	Sostdc1	0.000261517	21.9	DSS Normal Tissue up
A_44_P1054324	Csta_predicted	0.000788256	21.9	DSS Normal Tissue up
A_44_P960435	TC613177	7.88E-05	21.9	DSS Normal Tissue up
A_44_P506817	BF287204	0.000734273	21.5	DSS Normal Tissue up
A_42_P626895	LOC689256	0.000439864	21.3	DSS Normal Tissue up
A_44_P377432	RGD1562101_predicted	1.09E-05	21.1	DSS Normal Tissue up
A_44_P496643	LOC503340	4.42E-06	20.5	DSS Normal Tissue up
A_44_P256188	LOC497860	0.000825047	20.4	DSS Normal Tissue up
A_44_P129749	Crabp2	4.03E-05	20.4	DSS Normal Tissue up
A_44_P837716	TC587898	0.000105988	20.2	DSS Normal Tissue up
A_44_P294675	Slfn3	0.000523157	20.1	DSS Normal Tissue up
A_42_P541872	B3galt3	0.000103158	19.7	DSS Normal Tissue up
A_42_P472274	Slurp1_predicted	3.75E-05	19.4	DSS Normal Tissue up
A_44_P256921	Elov14_predicted	0.00014675	18.8	DSS Normal Tissue up
A_44_P563447	Wnt10a_predicted	0.00100739	18.5	DSS Normal Tissue up
A_44_P672002	TC606854	6.16E-06	18.4	DSS Normal Tissue up
A_43_P11590	Mmp7	2.78E-08	17.9	DSS Normal Tissue up
A_42_P786010	Ggta1	0.0006706	17.8	DSS Normal Tissue up
A_43_P22577	RGD1563091_predicted	0.000640231	17.8	DSS Normal Tissue up
A_44_P463425	AW917764	0.00020227	17.2	DSS Normal Tissue up
A_44_P171098	Gsg1	7.20E-06	17.1	DSS Normal Tissue up
A_44_P562582	TC599455	0.000816291	17.0	DSS Normal Tissue up
A_44_P1023977	Sh3kbp1	1.08E-05	17.0	DSS Normal Tissue up
A_43_P11881	Bcat1	3.08E-07	16.4	DSS Normal Tissue up
A_44_P1036943	AA900293	1.06E-05	16.4	DSS Normal Tissue up
A_44_P161470	Defa6	6.51E-06	16.3	DSS Normal Tissue up
A_44_P393551	Gja1	0.000188558	15.6	DSS Normal Tissue up
A_43_P11804	Ptn	0.00108843	15.5	DSS Normal Tissue up

Probe ID	Gene Symbol	p-value	Fold Change	Direction of Change
A_44_P950925	A_44_P950925	0.000763583	15.5	DSS Normal Tissue up
A_43_P13924	Emp2	7.10E-05	15.5	DSS Normal Tissue up
A_44_P975250	LOC683313	2.57E-06	15.4	DSS Normal Tissue up
A_44_P288287	RGD1307724_predicted	0.00115608	15.2	DSS Normal Tissue up
A_44_P674708	S100a8	8.45E-05	15.1	DSS Normal Tissue up
A_44_P157314	BF558825	0.000983981	15.1	DSS Normal Tissue up
A_44_P999845	Sh3kbp1	6.84E-07	15.0	DSS Normal Tissue up
A_43_P12641	Cldn1	0.00123675	14.8	DSS Normal Tissue up
A_44_P550768	TC596680	0.000166948	14.6	DSS Normal Tissue up
A_44_P125273	AA858448	0.00126934	14.6	DSS Normal Tissue up
A_44_P579071	TC614795	0.000127201	14.6	DSS Normal Tissue up
A_44_P818459	AW915396	0.000753878	14.5	DSS Normal Tissue up
A_43_P12786	Fabp4	0.000248494	14.5	DSS Normal Tissue up
A_44_P170266	BF401675	0.00191292	14.4	DSS Normal Tissue up
A_44_P151459	Gp1bb	0.000102645	14.3	DSS Normal Tissue up
A_44_P992908	Hspb1	6.25E-05	14.1	DSS Normal Tissue up
A_44_P494662	RGD1560851_predicted	1.33E-05	14.0	DSS Normal Tissue up
A_44_P622992	LOC500377	8.11E-07	13.8	DSS Normal Tissue up
A_44_P461025	BF287062	3.37E-05	13.7	Control Normal Tissue up
A_42_P693964	Cyp26b1	0.000564298	13.7	DSS Normal Tissue up
A_42_P464974	Ly6d_predicted	0.0006368	13.4	DSS Normal Tissue up
A_44_P527060	Klk10	0.000583086	13.3	DSS Normal Tissue up
A_42_P627998	Igfbp3	0.000643176	13.1	DSS Normal Tissue up
A_44_P668373	LOC679921	6.27E-05	13.0	DSS Normal Tissue up
A_44_P330143	Rhcg	0.00171704	12.9	DSS Normal Tissue up
A_42_P489764	Gjb2	0.000109555	12.6	DSS Normal Tissue up
A_44_P518127	MGC116096	2.62E-09	12.1	DSS Normal Tissue up
A_44_P687400	TC609088	0.0017226	12.1	DSS Normal Tissue up
A_42_P799702	Aard	1.32E-07	12.0	Control Normal Tissue up
A_44_P173960	S68944	0.00203439	11.9	DSS Normal Tissue up
A_44_P147062	Moxd1	1.25E-05	11.8	DSS Normal Tissue up
A_44_P640345	TC600025	0.00219199	11.7	Control Normal Tissue up
A_44_P1043278	XM_213470	0.000926428	11.7	DSS Normal Tissue up
A_42_P839593	AW142999	0.00127689	11.6	DSS Normal Tissue up
A_44_P1007347	Tgm2	0.00038019	11.6	DSS Normal Tissue up
A_44_P451244	5-Sep	0.000121065	11.6	DSS Normal Tissue up
A_44_P353778	LOC364706	0.000272184	11.5	DSS Normal Tissue up
A_42_P759444	TC587465	9.06E-06	11.4	DSS Normal Tissue up
A_43_P11499	Rbp2	0.000274066	11.4	DSS Normal Tissue up
A_42_P461794	Clic3	0.0010957	11.4	DSS Normal Tissue up
A_44_P288291	Phlda3	2.94E-06	11.3	DSS Normal Tissue up
A_44_P1015754	Slc22a3	3.78E-06	11.2	Control Normal Tissue up
A_42_P473398	Cxcl1	1.29E-07	11.1	DSS Normal Tissue up
A_43_P10201	BG665180	3.81E-05	11.0	DSS Normal Tissue up
A_44_P377337	Cox6b_predicted	4.74E-05	10.8	DSS Normal Tissue up
A_44_P561395	LOC683263	0.000205927	10.8	DSS Normal Tissue up
A_42_P588944	Mgp	0.000175267	10.7	DSS Normal Tissue up
A_42_P559414	Wnt4	7.91E-05	10.7	DSS Normal Tissue up
A_44_P361327	ENSRNOT0000051707	0.000766539	10.7	DSS Normal Tissue up
A_44_P180127	Igfbp3	0.000423967	10.7	DSS Normal Tissue up
A_44_P365286	Aldh1a1	0.00057264	10.7	Control Normal Tissue up
A_44_P294838	Il1a	2.12E-07	10.6	DSS Normal Tissue up
A_44_P319322	Krt1-12	0.000722607	10.6	DSS Normal Tissue up
A_44_P922150	RGD1562855_predicted	0.00143324	10.5	DSS Normal Tissue up
A_44_P562607	RGD1306592_predicted	0.000215598	10.5	Control Normal Tissue up
A_43_P15638	Tnc	1.27E-05	10.5	DSS Normal Tissue up
A_44_P236433	Slitrk6_predicted	0.000889373	10.4	DSS Normal Tissue up
A_42_P566079	MGC109519	6.26E-05	10.4	DSS Normal Tissue up
A_42_P660129	Casp12	0.00018578	10.2	DSS Normal Tissue up
A_44_P1055780	S100a8	0.000260319	10.1	DSS Normal Tissue up
A_44_P530060	XM_346120	0.000158575	10.1	Control Normal Tissue up
A_44_P106456	Pdlim2	4.69E-05	10.1	DSS Normal Tissue up
A_44_P125733	Madcam1	8.30E-05	10.0	DSS Normal Tissue up
A_43_P16413	RGD1561521_predicted	0.001527	9.8	DSS Normal Tissue up
A_44_P1005051	Ca5b	4.53E-05	9.8	DSS Normal Tissue up

Probe ID	Gene Symbol	p-value	Fold Change	Direction of Change
A_44_P638176	LOC500152	0.000347819	9.8	DSS Normal Tissue up
A_42_P712801	Entpd3	0.000366818	9.7	DSS Normal Tissue up
A_44_P421405	Sh3kbp1	1.25E-05	9.6	DSS Normal Tissue up
A_43_P11621	Cd44	7.46E-07	9.6	DSS Normal Tissue up
A_44_P443751	Pdpn	0.0003078	9.5	DSS Normal Tissue up
A_44_P885679	Bnc1_predicted	0.000838144	9.5	DSS Normal Tissue up
A_44_P776556	Chac1_predicted	1.27E-06	9.4	DSS Normal Tissue up
A_44_P105899	BI289678	8.55E-05	9.4	DSS Normal Tissue up
A_44_P920111	CF107866	4.63E-05	9.4	DSS Normal Tissue up
A_43_P11512	Spink1	3.80E-05	9.4	Control Normal Tissue up
A_44_P119658	Dusp14_predicted	1.13E-06	9.4	DSS Normal Tissue up
A_43_P14911	Il1b	0.00084482	9.3	DSS Normal Tissue up
A_44_P559239	AW921223	0.00049877	9.3	DSS Normal Tissue up
A_43_P10874	MGC109519	0.000195562	9.2	DSS Normal Tissue up
A_43_P13237	Gpha2	0.00135695	9.2	DSS Normal Tissue up
A_44_P515197	Cxcl2	0.000134366	9.1	DSS Normal Tissue up
A_44_P191632	Odz2	0.000696117	9.1	DSS Normal Tissue up
A_44_P729428	A_44_P729428	8.54E-06	9.1	DSS Normal Tissue up
A_44_P618288	AW916327	3.72E-05	9.0	DSS Normal Tissue up
A_44_P288401	RGD1559887_predicted	0.00150286	9.0	DSS Normal Tissue up
A_44_P849592	BF545957	3.80E-05	8.9	DSS Normal Tissue up
A_44_P975868	TC575730	2.67E-07	8.8	DSS Normal Tissue up
A_42_P457756	Pkib	9.80E-05	8.8	DSS Normal Tissue up
A_44_P171155	LOC363337	9.27E-05	8.7	DSS Normal Tissue up
A_44_P1022458	Tubb6	4.16E-08	8.5	DSS Normal Tissue up
A_44_P991335	LOC679870	0.00166277	8.5	DSS Normal Tissue up
A_44_P484889	Ifitm3	6.54E-05	8.5	DSS Normal Tissue up
A_42_P518462	Hmgn3	0.00135132	8.4	DSS Normal Tissue up
A_44_P264240	Igfbp5	0.000415223	8.4	DSS Normal Tissue up
A_42_P647599	Dcn	0.000314801	8.4	DSS Normal Tissue up
A_42_P475885	Ptprz1	0.000145609	8.3	DSS Normal Tissue up
A_44_P202318	AW917204	8.87E-05	8.3	DSS Normal Tissue up
A_42_P751720	LOC683720	0.000228377	8.2	DSS Normal Tissue up
A_44_P447650	Adarb1	8.25E-05	8.0	DSS Normal Tissue up
A_44_P637322	LOC499022	0.000661879	7.9	DSS Normal Tissue up
A_44_P928163	DY472205	0.000111409	7.9	DSS Normal Tissue up
A_44_P178252	Ccl21b	9.26E-05	7.9	DSS Normal Tissue up
A_44_P1033521	AA875280	0.00222668	7.9	DSS Normal Tissue up
A_44_P290022	Lrg1	2.70E-06	7.9	DSS Normal Tissue up
A_44_P274242	Siglec10_predicted	8.13E-05	7.8	DSS Normal Tissue up
A_42_P688604	Ces1	0.000163498	7.7	Control Normal Tissue up
A_44_P428739	Shc3	0.000800087	7.7	Control Normal Tissue up
A_44_P144557	LOC499660	0.000278562	7.7	DSS Normal Tissue up
A_44_P699964	TC598748	0.00111544	7.7	DSS Normal Tissue up
A_42_P621642	Lsp1	0.00027381	7.7	DSS Normal Tissue up
A_44_P588315	Xlkd1_predicted	0.000333943	7.7	DSS Normal Tissue up
A_44_P1042783	MGC109519	0.000170574	7.7	DSS Normal Tissue up
A_44_P428405	Slc4a9	0.000526276	7.7	DSS Normal Tissue up
A_43_P11614	Anxa1	0.000450609	7.6	DSS Normal Tissue up
A_44_P276317	Ptger3	0.00220507	7.6	Control Normal Tissue up
A_44_P654106	BM422817	4.64E-05	7.6	Control Normal Tissue up
A_44_P288241	RGD1307396_predicted	0.00134497	7.5	DSS Normal Tissue up
A_44_P122912	Es2	0.000941833	7.5	Control Normal Tissue up
A_44_P309473	XM_228778	0.00068274	7.4	Control Normal Tissue up
A_44_P392004	TC613432	7.97E-05	7.4	DSS Normal Tissue up
A_44_P399249	Tgm1	4.45E-06	7.4	DSS Normal Tissue up
A_44_P379520	Sdro	5.68E-05	7.4	DSS Normal Tissue up
A_44_P241616	Ogfr11	3.08E-07	7.4	DSS Normal Tissue up
A_44_P406636	CB557036	0.000815255	7.3	Control Normal Tissue up
A_42_P468712	Tacstd2	4.53E-05	7.3	DSS Normal Tissue up
A_44_P812604	TC599592	0.00174413	7.3	DSS Normal Tissue up
A_42_P804387	Lypd3	0.000256811	7.3	DSS Normal Tissue up
A_43_P23187	RGD1560851_predicted	3.89E-05	7.3	DSS Normal Tissue up
A_44_P203401	RatNP-3b	6.84E-06	7.3	DSS Normal Tissue up
A_43_P14871	Ltbp1	0.000374498	7.2	DSS Normal Tissue up

Probe ID	Gene Symbol	p-value	Fold Change	Direction of Change
A_42_P807866	Ril	4.98E-05	7.2	DSS Normal Tissue up
A_44_P167849	RGD1562968_predicted	0.000204281	7.2	DSS Normal Tissue up
A_44_P898953	LOC499022	0.000165104	7.1	DSS Normal Tissue up
A_42_P621872	Gcgr	0.000182162	7.1	Control Normal Tissue up
A_44_P477819	Nrg1	0.00211007	7.0	DSS Normal Tissue up
A_44_P182136	AI556689	0.000686108	7.0	DSS Normal Tissue up
A_44_P426638	Osmr	5.64E-05	7.0	DSS Normal Tissue up
A_44_P273468	Slc25a4	8.80E-06	7.0	DSS Normal Tissue up
A_44_P508466	Jundp2	0.00222563	6.9	DSS Normal Tissue up
A_44_P1059903	Lzts1	0.00191455	6.9	DSS Normal Tissue up
A_44_P1048789	AA859536	0.00168118	6.9	DSS Normal Tissue up
A_44_P966141	CO399145	0.000716598	6.9	DSS Normal Tissue up
A_44_P520159	P2ry2	4.36E-05	6.9	DSS Normal Tissue up
A_44_P1018957	Hsd11b1	0.000185043	6.9	DSS Normal Tissue up
A_44_P353618	S100a9	0.000153283	6.9	DSS Normal Tissue up
A_44_P555072	MGC94782	0.000378222	6.9	DSS Normal Tissue up
A_44_P699523	TC587634	0.000491963	6.8	DSS Normal Tissue up
A_44_P637195	TC603750	0.00206286	6.8	Control Normal Tissue up
A_44_P746333	TC605464	1.58E-05	6.7	DSS Normal Tissue up
A_44_P142925	RGD1306226_predicted	0.000120933	6.7	DSS Normal Tissue up
A_44_P309913	CB547989	0.000420603	6.7	DSS Normal Tissue up
A_44_P297777	Flna_predicted	0.00053937	6.7	DSS Normal Tissue up
A_44_P288881	ENSRNOT00000040211	0.00153241	6.7	DSS Normal Tissue up
A_44_P191672	Ka17	0.000365791	6.7	DSS Normal Tissue up
A_43_P22638	Pappa_predicted	0.000699574	6.6	DSS Normal Tissue up
A_44_P158798	ENSRNOT00000040952	0.000116312	6.6	DSS Normal Tissue up
A_44_P127337	RGD1561067_predicted	5.08E-05	6.6	DSS Normal Tissue up
A_44_P925373	AA997357	0.000390622	6.5	DSS Normal Tissue up
A_44_P442802	Rassf5	0.000433376	6.5	DSS Normal Tissue up
A_42_P518855	Bcl2a1	0.000188018	6.5	DSS Normal Tissue up
A_42_P820657	Il1r2	0.000103018	6.5	DSS Normal Tissue up
A_44_P494869	Guca1a_predicted	3.09E-05	6.4	DSS Normal Tissue up
A_44_P395885	Cdkn2a	9.27E-06	6.4	DSS Normal Tissue up
A_42_P509923	Defcr4	0.000156622	6.4	DSS Normal Tissue up
A_42_P620975	Apeg1	0.000200907	6.3	Control Normal Tissue up
A_44_P564274	RGD1559473_predicted	0.00174592	6.3	DSS Normal Tissue up
A_44_P229677	LOC363337	0.00114233	6.3	DSS Normal Tissue up
A_44_P396090	XM_345181	0.0004863	6.3	DSS Normal Tissue up
A_44_P485515	RGD1308422	0.00220298	6.3	DSS Normal Tissue up
A_44_P351209	Phlda1	3.04E-06	6.2	DSS Normal Tissue up
A_42_P775217	Ly6g6c	0.000876019	6.2	DSS Normal Tissue up
A_44_P961164	TC583657	0.00114172	6.2	DSS Normal Tissue up
A_44_P157781	AA858875	0.000240291	6.1	DSS Normal Tissue up
A_44_P497121	RGD1308967_predicted	0.000913457	6.1	DSS Normal Tissue up
A_44_P764622	TC600845	0.000527996	6.1	Control Normal Tissue up
A_44_P1057403	Ptrf_predicted	9.82E-05	6.0	DSS Normal Tissue up
A_44_P154513	LOC680858	7.78E-06	5.9	DSS Normal Tissue up
A_42_P607026	Lysmd2_predicted	6.49E-07	5.9	DSS Normal Tissue up
A_44_P231448	ENSRNOT00000000449	0.000308833	5.9	DSS Normal Tissue up
A_44_P398574	Prdm1_predicted	0.000807708	5.9	DSS Normal Tissue up
A_44_P1056603	TC627177	0.000198933	5.9	DSS Normal Tissue up
A_44_P332422	C1s	0.000224507	5.9	DSS Normal Tissue up
A_42_P575398	Aadac	0.000408747	5.9	Control Normal Tissue up
A_42_P841193	Ddit4l	1.92E-05	5.9	Control Normal Tissue up
A_43_P12070	Ly6c	0.00047089	5.9	DSS Normal Tissue up
A_44_P438060	Gna15	5.91E-05	5.9	DSS Normal Tissue up
A_44_P399224	CB545206	0.000745415	5.8	Control Normal Tissue up
A_44_P425027	BF420642	0.000214652	5.8	DSS Normal Tissue up
A_44_P437721	CO566833	0.00105758	5.7	DSS Normal Tissue up
A_42_P499158	Vcam1	0.000793601	5.7	DSS Normal Tissue up
A_43_P23209	Dync2li1	0.00144225	5.7	DSS Normal Tissue up
A_44_P870068	TC627363	0.000190296	5.7	Control Normal Tissue up
A_44_P1016884	BF566249	0.000207454	5.7	DSS Normal Tissue up
A_44_P427006	Emp2	0.000731397	5.7	DSS Normal Tissue up
A_43_P12955	Fcgr3	5.99E-05	5.7	DSS Normal Tissue up

Probe ID	Gene Symbol	p-value	Fold Change	Direction of Change
A_44_P295408	ENSRNOT00000041850	1.81E-05	5.6	Control Normal Tissue up
A_42_P663722	Slc30a2	0.000216631	5.6	DSS Normal Tissue up
A_44_P623856	Dkk4_predicted	0.00122656	5.6	DSS Normal Tissue up
A_44_P869337	TC591217	9.69E-06	5.6	Control Normal Tissue up
A_44_P1041460	Rragd_predicted	1.68E-05	5.6	Control Normal Tissue up
A_44_P901471	TC594336	0.000577678	5.6	DSS Normal Tissue up
A_44_P461130	Krt2-5	0.000332044	5.6	DSS Normal Tissue up
A_44_P739541	A_44_P739541	0.000280214	5.6	DSS Normal Tissue up
A_44_P160841	Calcb	0.00155937	5.5	DSS Normal Tissue up
A_42_P596024	Spnb3	0.000306466	5.5	DSS Normal Tissue up
A_44_P429298	LOC500590	4.53E-05	5.5	DSS Normal Tissue up
A_42_P758222	Arg1	0.00045194	5.5	DSS Normal Tissue up
A_44_P426345	Hsd11b1	0.000361969	5.5	DSS Normal Tissue up
A_44_P828772	BE096652	0.000177957	5.5	DSS Normal Tissue up
A_44_P363116	Gm1960	3.95E-07	5.5	DSS Normal Tissue up
A_44_P283985	LOC689802	1.02E-05	5.5	Control Normal Tissue up
A_44_P359040	RGD1309051	4.26E-06	5.5	DSS Normal Tissue up
A_44_P558821	CK601507	0.00124089	5.4	DSS Normal Tissue up
A_44_P931730	TC619737	0.000186357	5.4	Control Normal Tissue up
A_43_P21977	RGD1566394_predicted	0.000210154	5.4	DSS Normal Tissue up
A_44_P866659	RGD1566394_predicted	3.26E-06	5.4	DSS Normal Tissue up
A_42_P470649	Dio1	5.11E-05	5.4	Control Normal Tissue up
A_43_P12227	Crip2	0.000471432	5.4	DSS Normal Tissue up
A_44_P781967	A_44_P781967	4.04E-05	5.4	DSS Normal Tissue up
A_44_P491976	Kcnmb4	0.000411178	5.4	DSS Normal Tissue up
A_44_P929787	A_44_P929787	0.00106683	5.4	Control Normal Tissue up
A_44_P330847	LOC683973	0.00031439	5.3	Control Normal Tissue up
A_44_P779143	TC617347	0.00181821	5.3	Control Normal Tissue up
A_43_P10020	Lyz	8.90E-05	5.3	DSS Normal Tissue up
A_44_P730817	TC603905	0.000355415	5.3	DSS Normal Tissue up
A_44_P311126	Clu	0.000237423	5.3	DSS Normal Tissue up
A_44_P513059	Sfrp1	0.00171989	5.3	DSS Normal Tissue up
A_44_P391426	Klk11_predicted	0.000691894	5.3	DSS Normal Tissue up
A_43_P13105	Serpinb7	3.77E-05	5.3	DSS Normal Tissue up
A_44_P314295	Zmynd12_predicted	7.33E-05	5.2	Control Normal Tissue up
A_43_P16767	Igfbp4	0.00110246	5.2	DSS Normal Tissue up
A_44_P1050480	Ecm1	2.66E-05	5.2	DSS Normal Tissue up
A_44_P375102	XM_214014	0.000239439	5.2	DSS Normal Tissue up
A_43_P10498	XM_237039	0.000693235	5.2	DSS Normal Tissue up
A_44_P547771	Cited1	0.00179245	5.1	DSS Normal Tissue up
A_44_P673326	CB718208	0.000930972	5.1	Control Normal Tissue up
A_44_P214900	Pzp	0.00022178	5.1	DSS Normal Tissue up
A_44_P247081	Pla2g2a	2.91E-05	5.1	DSS Normal Tissue up
A_44_P1004790	Slc30a2	0.000179072	5.1	DSS Normal Tissue up
A_44_P111881	ENSRNOT00000002836	0.00222236	5.1	DSS Normal Tissue up
A_44_P432432	Plat	1.06E-05	5.0	DSS Normal Tissue up
A_44_P193945	Bst1	0.000700984	5.0	DSS Normal Tissue up
A_44_P587550	AW915632	3.67E-05	5.0	DSS Normal Tissue up
A_43_P17609	Pdlim2	0.000517164	5.0	DSS Normal Tissue up
A_43_P10333	Efemp1	0.000149454	5.0	DSS Normal Tissue up
A_44_P490308	Muc20_predicted	0.00113654	5.0	DSS Normal Tissue up
A_43_P11818	Crp	0.000989462	5.0	Control Normal Tissue up
A_43_P11489	S100a4	0.000229308	5.0	DSS Normal Tissue up
A_44_P353872	RGD1305932_predicted	0.000546457	4.9	DSS Normal Tissue up
A_44_P375995	BI282744	0.000186158	4.9	Control Normal Tissue up
A_44_P398033	Prnp	0.00111789	4.9	DSS Normal Tissue up
A_44_P479157	AI045067	0.0019877	4.9	DSS Normal Tissue up
A_44_P283385	Gip	2.40E-05	4.9	DSS Normal Tissue up
A_44_P260036	Plau	2.98E-05	4.9	DSS Normal Tissue up
A_42_P507566	LOC299339	7.86E-05	4.9	DSS Normal Tissue up
A_44_P533794	Tnfrsf1b	0.000450308	4.9	DSS Normal Tissue up
A_43_P22351	RGD1307594	0.000835805	4.9	DSS Normal Tissue up
A_44_P457578	AA858732	0.000338233	4.9	DSS Normal Tissue up
A_44_P251064	Krt1-14	0.000337534	4.9	DSS Normal Tissue up
A_44_P290966	Pcdh19_predicted	0.000409956	4.9	DSS Normal Tissue up



Probe ID	Gene Symbol	p-value	Fold Change	Direction of Change
A_44_P239205	Rwdd2_predicted	0.000549099	4.9	Control Normal Tissue up
A_44_P199447	Elk3_predicted	0.000185192	4.9	DSS Normal Tissue up
A_42_P537501	Dpp4	9.90E-05	4.9	Control Normal Tissue up
A_44_P523028	LOC689312	5.40E-05	4.9	Control Normal Tissue up
A_44_P233502	AI236833	0.000764801	4.9	DSS Normal Tissue up
A_44_P914382	RGD1559432_predicted	4.16E-06	4.8	DSS Normal Tissue up
A_44_P245314	Cacnb3	1.23E-05	4.8	Control Normal Tissue up
A_44_P1040642	Mafb	0.0014528	4.8	DSS Normal Tissue up
A_44_P171440	Apoe	4.84E-05	4.8	DSS Normal Tissue up
A_44_P835675	CF110937	0.000178771	4.8	DSS Normal Tissue up
A_44_P197064	Tmem63c_predicted	0.0021829	4.8	DSS Normal Tissue up
A_43_P15296	Slit1	0.000300357	4.8	Control Normal Tissue up
A_43_P15023	Thbd	0.000584954	4.8	DSS Normal Tissue up
A_44_P1004840	Tnfsf9	0.000407419	4.8	DSS Normal Tissue up
A_44_P191762	ENSRNOT00000044127	0.00153789	4.8	DSS Normal Tissue up
A_44_P845503	LOC689088	0.00101569	4.7	Control Normal Tissue up
A_42_P799208	DV726678	0.000178003	4.7	DSS Normal Tissue up
A_44_P976358	TC604433	2.47E-05	4.7	Control Normal Tissue up
A_44_P423662	Sh3bp5	0.000335279	4.7	DSS Normal Tissue up
A_42_P556829	Wif1	0.00219703	4.7	DSS Normal Tissue up
A_43_P15507	Indo	0.000158044	4.7	DSS Normal Tissue up
A_44_P638093	TC596726	0.00181505	4.7	Control Normal Tissue up
A_42_P562617	Irf5_predicted	7.83E-05	4.7	DSS Normal Tissue up
A_44_P422134	ENSRNOT00000041850	0.000220135	4.7	Control Normal Tissue up
A_44_P828123	CO393245	1.48E-05	4.7	Control Normal Tissue up
A_44_P886888	TC601338	0.000890041	4.6	Control Normal Tissue up
A_44_P997755	Slc27a2	0.00123349	4.6	Control Normal Tissue up
A_44_P853647	Wasf1	0.00188788	4.6	Control Normal Tissue up
A_44_P303009	CB605594	0.00192607	4.6	DSS Normal Tissue up
A_44_P620941	RGD1564024_predicted	0.00140516	4.6	Control Normal Tissue up
A_44_P269055	Ly6b	0.00182546	4.6	DSS Normal Tissue up
A_44_P480455	Efs_predicted	0.000377916	4.6	DSS Normal Tissue up
A_42_P733209	Dgat2	0.00022986	4.6	DSS Normal Tissue up
A_42_P704429	Fgfl3	0.000231927	4.6	DSS Normal Tissue up
A_44_P473715	RGD1563002_predicted	5.76E-05	4.6	Control Normal Tissue up
A_44_P423651	Prss12	0.00150699	4.5	DSS Normal Tissue up
A_43_P21180	Elmod1_predicted	0.0014041	4.5	DSS Normal Tissue up
A_44_P298331	LOC360619	0.000234014	4.5	DSS Normal Tissue up
A_44_P461187	St3gal4	4.58E-05	4.5	DSS Normal Tissue up
A_44_P1038028	Tnfrsf12a	0.000348194	4.5	DSS Normal Tissue up
A_44_P135238	Wnt7a	0.000635085	4.5	DSS Normal Tissue up
A_44_P246947	Slc25a4	9.48E-05	4.5	DSS Normal Tissue up
A_44_P194274	Dio1	0.000175778	4.5	Control Normal Tissue up
A_44_P961032	TC599726	9.31E-06	4.5	Control Normal Tissue up
A_44_P730298	DV715525	0.0020239	4.4	DSS Normal Tissue up
A_44_P392845	Col5a2	0.000627988	4.4	DSS Normal Tissue up
A_44_P636857	ENSRNOT00000038550	0.000146776	4.4	Control Normal Tissue up
A_44_P630174	AI234967	0.000231146	4.4	DSS Normal Tissue up
A_44_P799454	BF550650	1.79E-05	4.4	Control Normal Tissue up
A_44_P381917	Sphk1	0.000279748	4.4	DSS Normal Tissue up
A_44_P463749	Rasd1	2.79E-05	4.4	Control Normal Tissue up
A_44_P392849	Col5a2	0.000892552	4.4	DSS Normal Tissue up
A_42_P574719	Slc25a4	5.70E-05	4.4	DSS Normal Tissue up
A_44_P316898	Higd1b_predicted	0.000482674	4.4	DSS Normal Tissue up
A_43_P10133	TC605283	0.000183259	4.3	DSS Normal Tissue up
A_44_P540511	Pkib	0.000597749	4.3	DSS Normal Tissue up
A_44_P338207	Selt	0.00117202	4.3	DSS Normal Tissue up
A_44_P980916	Kirrel3_predicted	0.000243104	4.3	DSS Normal Tissue up
A_44_P640313	TC588645	0.00128559	4.3	Control Normal Tissue up
A_44_P579594	Sart2_predicted	5.70E-05	4.3	DSS Normal Tissue up
A_42_P703548	Kynu	7.39E-05	4.3	Control Normal Tissue up
A_42_P753675	Arhgdig_predicted	6.97E-05	4.3	DSS Normal Tissue up
A_42_P499767	Padi2	4.40E-05	4.3	Control Normal Tissue up
A_44_P392846	ENSRNOT00000040507	0.000870304	4.3	DSS Normal Tissue up
A_44_P638915	TC610692	0.000426284	4.2	DSS Normal Tissue up

Probe ID	Gene Symbol	p-value	Fold Change	Direction of Change
A_44_P762624	TC595316	0.000606073	4.2	Control Normal Tissue up
A_43_P19005	RGD1566426_predicted	1.15E-05	4.2	DSS Normal Tissue up
A_44_P977499	TC611761	0.00183231	4.2	Control Normal Tissue up
A_44_P845409	AW913993	0.000288196	4.2	DSS Normal Tissue up
A_43_P15339	Pitx1	0.000662805	4.2	DSS Normal Tissue up
A_44_P180012	Dgat2	9.88E-05	4.2	DSS Normal Tissue up
A_42_P696084	Cspg4	0.000444889	4.2	DSS Normal Tissue up
A_43_P14249	CF110190	0.000223175	4.2	DSS Normal Tissue up
A_44_P239306	LOC287938	1.02E-05	4.2	DSS Normal Tissue up
A_43_P11589	Bhlhb8	0.00128883	4.2	DSS Normal Tissue up
A_44_P1004323	Col18a1	0.000382901	4.2	DSS Normal Tissue up
A_44_P822061	ENSRNOT00000041850	0.000751552	4.1	Control Normal Tissue up
A_42_P458530	Ripk3	0.000702632	4.1	DSS Normal Tissue up
A_44_P486914	Fgf9	0.000384802	4.1	Control Normal Tissue up
A_44_P358703	Spetex-2D	0.00126757	4.1	DSS Normal Tissue up
A_43_P13189	Ppp1r14c	1.34E-05	4.1	DSS Normal Tissue up
A_44_P888860	TC618359	0.000183099	4.1	Control Normal Tissue up
A_44_P243534	RGD1311307	7.36E-06	4.1	DSS Normal Tissue up
A_44_P527544	RGD1308818_predicted	0.000174435	4.1	Control Normal Tissue up
A_43_P16967	Snx10	0.00103905	4.1	DSS Normal Tissue up
A_44_P1060286	S100a4	0.000374966	4.1	DSS Normal Tissue up
A_44_P166581	Ifitm7_predicted	0.000196492	4.0	DSS Normal Tissue up
A_44_P578061	TC639482	0.00223273	4.0	DSS Normal Tissue up
A_44_P606441	TC576288	0.00221221	4.0	DSS Normal Tissue up
A_44_P358227	Mapk15	0.000877785	4.0	Control Normal Tissue up
A_44_P1004324	Col18a1	0.000790833	4.0	DSS Normal Tissue up
A_44_P405847	RGD1564168_predicted	0.00185798	4.0	Control Normal Tissue up
A_44_P409605	Habp2	0.0019831	4.0	DSS Normal Tissue up
A_44_P1040685	Ier5l	0.000184607	4.0	DSS Normal Tissue up
A_44_P932768	TC615892	0.000671346	4.0	DSS Normal Tissue up
A_44_P485208	Crnn_predicted	0.00096437	4.0	DSS Normal Tissue up
A_43_P21810	RGD1309288	0.00106407	4.0	Control Normal Tissue up
A_42_P526712	CX570116	0.000552952	4.0	DSS Normal Tissue up

**Supplementary Table S-3. Genes differentially expressed between DSS-treated colonic tissue and all colonic tumors**

Probe ID	Gene Symbol	p-value	Fold Change	Direction of Change
A_44_P421985	ENSRNOT00000012568	0.00139838	294.9	DSS Normal Tissue up
A_43_P11086	Upk1b	4.11E-06	262.4	DSS Normal Tissue up
A_44_P335794	RGD1310935_predicted	7.92E-07	148.7	DSS Normal Tissue up
A_44_P450496	ENSRNOT00000047751	1.25E-06	110.2	DSS Normal Tissue up
A_43_P12689	Defb1	0.00157943	103.5	DSS Normal Tissue up
A_42_P640792	Gjb6	0.00156411	71.5	DSS Normal Tissue up
A_44_P1049097	Krtdap	2.25E-05	67.5	DSS Normal Tissue up
A_44_P428724	Stfa3_predicted	5.48E-05	66.4	DSS Normal Tissue up
A_44_P592667	Spink5_predicted	5.66E-05	65.2	DSS Normal Tissue up
A_42_P472274	Slurp1_predicted	6.64E-07	55.2	DSS Normal Tissue up
A_42_P464974	Ly6d_predicted	5.22E-06	54.8	DSS Normal Tissue up
A_44_P278960	Sprr3_predicted	0.000134567	45.7	DSS Normal Tissue up
A_42_P534882	Vsn1l	0.000516393	43.6	DSS Normal Tissue up
A_44_P486312	Fmo2	0.000565219	31.4	DSS Normal Tissue up
A_43_P23458	Klk12_predicted	6.59E-05	27.4	DSS Normal Tissue up
A_44_P684180	Lrrn1	1.74E-05	26.8	All Tumors up
A_44_P224769	Klk13_predicted	0.00101792	26.0	DSS Normal Tissue up
A_44_P115142	Mycn	5.13E-06	24.7	All Tumors up
A_44_P344791	RGD1563060_predicted	0.000471679	23.5	DSS Normal Tissue up
A_43_P14604	AW143134	7.26E-05	23.4	All Tumors up
A_44_P384974	Upk1b	4.97E-05	22.9	DSS Normal Tissue up
A_44_P133239	Rptn_predicted	0.000316484	22.0	DSS Normal Tissue up
A_44_P330584	Lix1_predicted	2.79E-05	21.2	All Tumors up
A_42_P489764	Gjb2	6.75E-06	20.6	DSS Normal Tissue up
A_42_P686756	BC087706	9.16E-05	20.0	DSS Normal Tissue up
A_44_P1017035	Slc26a4	3.18E-05	19.6	All Tumors up
A_44_P256921	Elovl4_predicted	4.07E-05	19.1	DSS Normal Tissue up
A_44_P551081	Kb4	0.00185346	18.7	DSS Normal Tissue up
A_44_P445575	Irx2	0.00158555	18.5	DSS Normal Tissue up
A_44_P492122	Lip13_predicted	0.00183515	18.0	DSS Normal Tissue up
A_44_P358194	Fmo3	0.000155748	17.8	DSS Normal Tissue up
A_44_P975889	TC585827	7.41E-07	17.4	All Tumors up
A_42_P832417	Vsn1l	0.000156856	17.0	DSS Normal Tissue up
A_44_P178408	RGD1308195_predicted	0.0037183	17.0	DSS Normal Tissue up
A_44_P511114	Spink5_predicted	0.00193518	16.8	DSS Normal Tissue up
A_44_P1054324	Csta_predicted	0.000520286	16.6	DSS Normal Tissue up
A_44_P991335	LOC679870	0.000145242	16.5	DSS Normal Tissue up
A_44_P497310	RGD1306927_predicted	0.00352288	15.9	DSS Normal Tissue up
A_43_P23375	Dsg1c_predicted	0.00144218	15.9	DSS Normal Tissue up
A_44_P192000	RGD1562305_predicted	9.22E-05	15.4	DSS Normal Tissue up
A_44_P335974	Aldh1a7	7.45E-05	15.0	DSS Normal Tissue up
A_42_P501233	Adra1d	7.04E-05	14.9	All Tumors up
A_44_P562582	TC599455	0.000384337	14.8	DSS Normal Tissue up
A_44_P231448	ENSRNOT00000000449	2.55E-06	14.8	DSS Normal Tissue up
A_44_P518414	LOC685312	0.0022227	14.7	All Tumors up
A_43_P23317	Rsnl2	0.00289353	14.7	DSS Normal Tissue up
A_44_P622992	LOC500377	1.63E-07	14.6	DSS Normal Tissue up
A_42_P597626	Slc26a3	0.000496115	14.3	DSS Normal Tissue up
A_44_P691593	AI072466	2.22E-06	14.1	DSS Normal Tissue up
A_43_P17795	RGD1559565_predicted	3.00E-06	13.8	All Tumors up
A_44_P869362	LOC688150	1.35E-05	13.8	All Tumors up
A_44_P836100	Stfa3_predicted	0.0016101	13.8	DSS Normal Tissue up
A_44_P104140	LOC679949	0.000267834	13.7	All Tumors up
A_44_P147300	Cla2_predicted	1.70E-05	13.6	DSS Normal Tissue up
A_42_P646213	ENSRNOT00000030609	0.000751846	13.4	All Tumors up
A_44_P236187	Lgals7	3.13E-05	13.2	DSS Normal Tissue up
A_44_P191762	ENSRNOT00000044127	8.90E-06	13.1	DSS Normal Tissue up
A_44_P1004886	MGC72614	0.000247605	13.1	All Tumors up

A_44_P837716	TC587898	0.0001116	13.0	DSS Normal Tissue up
A_44_P550785	Gbp5_predicted	0.000108989	13.0	All Tumors up
A_44_P444632	CFI10930	0.000188018	12.4	All Tumors up
A_44_P227243	RGD1309610_predicted	4.91E-06	12.4	DSS Normal Tissue up
A_44_P175495	Cxcl11	6.60E-06	12.1	All Tumors up
A_44_P245835	RGD1310110_predicted	2.99E-05	11.9	All Tumors up
A_44_P990998	Klk8	3.13E-06	11.8	DSS Normal Tissue up
A_44_P265066	Calml3	0.000561819	11.8	DSS Normal Tissue up
A_42_P775217	Ly6g6c	2.55E-05	11.6	DSS Normal Tissue up
A_44_P745749	A_44_P745749	4.25E-06	11.6	All Tumors up
A_42_P786010	Ggtal1	0.000738624	11.5	DSS Normal Tissue up
A_44_P665685	AW142871	0.00133225	11.5	DSS Normal Tissue up
A_44_P839032	TC626563	0.00296735	11.4	DSS Normal Tissue up
A_43_P15596	ENSRNOT00000021832	0.000901809	11.2	DSS Normal Tissue up
A_44_P549004	BG372060	0.00261446	11.2	DSS Normal Tissue up
A_42_P638166	RGD1560368_predicted	0.00331368	11.2	All Tumors up
A_44_P730004	TC596605	7.16E-06	10.8	All Tumors up
A_44_P353778	LOC364706	9.73E-05	10.8	DSS Normal Tissue up
A_44_P226658	Scnn1g	0.00318864	10.7	DSS Normal Tissue up
A_43_P13418	Kcnk2	1.76E-06	10.6	All Tumors up
A_44_P614539	CK475991	0.000734119	10.5	DSS Normal Tissue up
A_44_P282443	AW920715	0.000101422	10.5	All Tumors up
A_44_P1047441	Lrp2	0.000417383	10.3	All Tumors up
A_44_P552738	Dmbt1	0.000224297	10.2	DSS Normal Tissue up
A_42_P773675	Edg8	0.00277195	10.2	DSS Normal Tissue up
A_44_P382482	Atp6v1c2	0.00226703	10.2	DSS Normal Tissue up
A_44_P242397	Ppp2r2b	1.92E-05	10.1	All Tumors up
A_44_P142867	ENSRNOT00000012203	0.000351744	10.1	DSS Normal Tissue up
A_44_P623856	Dkk4_predicted	4.23E-05	9.9	All Tumors up
A_44_P1051894	LOC363915	1.94E-05	9.9	All Tumors up
A_44_P353872	RGD1305932_predicted	1.05E-05	9.8	DSS Normal Tissue up
A_44_P1043278	XM_213470	0.000552052	9.7	DSS Normal Tissue up
A_43_P12162	Ppp2r2b	3.84E-05	9.7	All Tumors up
A_44_P377337	Cox6b_predicted	1.97E-05	9.7	DSS Normal Tissue up
A_43_P11152	Tm4sf1_predicted	0.000228663	9.6	All Tumors up
A_44_P503251	Nov	0.00129436	9.6	DSS Normal Tissue up
A_42_P828757	Tm4sf4	3.26E-05	9.5	All Tumors up
A_42_P508921	Aqp3	0.000172743	9.5	DSS Normal Tissue up
A_43_P15756	Muc2	0.00200633	9.5	DSS Normal Tissue up
A_42_P803673	LOC360228	0.00217616	9.5	All Tumors up
A_42_P549321	TC590532	2.23E-05	9.5	All Tumors up
A_42_P693096	AI454457	1.06E-05	9.5	All Tumors up
A_44_P147062	Moxd1	7.62E-06	9.5	DSS Normal Tissue up
A_44_P165870	Cdo1	4.55E-05	9.4	DSS Normal Tissue up
A_42_P573412	RGD1307150_predicted	3.51E-05	9.4	All Tumors up
A_44_P145283	Krtap14_predicted	0.000394288	9.4	DSS Normal Tissue up
A_44_P263777	AW916070	0.0012255	9.3	DSS Normal Tissue up
A_44_P499177	ENSRNOT00000029771	0.000355674	9.3	DSS Normal Tissue up
A_44_P144857	Enpep	2.80E-06	9.2	All Tumors up
A_44_P787524	Col9a3_predicted	0.000473877	9.2	All Tumors up
A_42_P804822	Scn7a	6.64E-05	9.2	DSS Normal Tissue up
A_44_P405022	Kb1	1.42E-05	9.1	DSS Normal Tissue up
A_43_P12641	Cldn1	0.000588736	9.0	DSS Normal Tissue up
A_44_P193904	Dlgh2	0.00183322	9.0	DSS Normal Tissue up
A_44_P209788	Enpep	1.62E-06	8.8	All Tumors up
A_44_P828772	BE096652	6.23E-06	8.8	DSS Normal Tissue up
A_44_P491796	Spp1	0.000302083	8.7	All Tumors up
A_42_P465601	Myh10	2.59E-05	8.6	All Tumors up
A_44_P747182	TC627511	0.00158371	8.6	All Tumors up
A_44_P471294	A_44_P471294	0.00020729	8.6	All Tumors up
A_44_P829197	AW921479	0.00118189	8.6	DSS Normal Tissue up
A_43_P15507	Indo	2.61E-06	8.6	DSS Normal Tissue up
A_44_P404836	Cp	0.00274035	8.5	All Tumors up
A_44_P929992	ENSRNOT00000006696	0.00327902	8.4	DSS Normal Tissue up
A_44_P1034926	BF281925	1.69E-05	8.4	All Tumors up
A_44_P253157	RGD1562551_predicted	0.000837191	8.3	All Tumors up
A_43_P22696	A_43_P22696	3.69E-05	8.3	All Tumors up

A_42_P550360	Klk6_predicted	0.00254154	8.2	DSS Normal Tissue up
A_44_P506024	RGD1565646_predicted	0.000489437	8.1	DSS Normal Tissue up
A_42_P575104	Sostdc1	0.00148567	8.1	DSS Normal Tissue up
A_44_P399414	Klk7	0.00174912	8.1	DSS Normal Tissue up
A_42_P571433	Msx1	0.000131603	8.0	All Tumors up
A_44_P769703	Nrep	3.99E-05	7.9	All Tumors up
A_44_P360767	Spink1	0.00236267	7.9	DSS Normal Tissue up
A_44_P323765	RGD1307443_predicted	5.17E-05	7.9	DSS Normal Tissue up
A_44_P149370	Cyp2b13	0.00169741	7.7	DSS Normal Tissue up
A_43_P12467	Pde1a	0.000432077	7.7	All Tumors up
A_44_P1034879	RGD1564865_predicted	0.00312676	7.7	DSS Normal Tissue up
A_44_P925373	AA997357	6.28E-05	7.6	All Tumors up
A_44_P391426	Klk11_predicted	4.87E-05	7.6	DSS Normal Tissue up
A_44_P447373	Ass	0.000239142	7.6	All Tumors up
A_44_P428405	Slc4a9	0.00017411	7.6	DSS Normal Tissue up
A_44_P781967	A_44_P781967	2.10E-06	7.6	DSS Normal Tissue up
A_44_P590984	ENSRNOT00000042464	0.000335066	7.6	All Tumors up
A_44_P330143	Rhcg	0.00291168	7.4	DSS Normal Tissue up
A_44_P566811	BG669273	0.0010842	7.4	All Tumors up
A_44_P132325	AW531866	0.000121155	7.4	All Tumors up
A_44_P653053	LOC498335	0.000390582	7.3	DSS Normal Tissue up
A_44_P412570	Ilf5_predicted	0.000362615	7.3	DSS Normal Tissue up
A_44_P163243	Klks3	0.00322443	7.3	DSS Normal Tissue up
A_43_P14371	Smpx	0.000482107	7.3	All Tumors up
A_44_P746247	TC606539	4.58E-05	7.2	DSS Normal Tissue up
A_44_P868581	RGD1562095_predicted	0.00376032	7.2	All Tumors up
A_44_P548426	RGD1305527_predicted	0.000350933	7.2	DSS Normal Tissue up
A_44_P476810	ENSRNOT00000001372	0.00046591	7.2	DSS Normal Tissue up
A_44_P127749	RGD1306105_predicted	0.000743232	7.2	DSS Normal Tissue up
A_44_P208133	ENSRNOT00000056464	0.00253689	7.2	DSS Normal Tissue up
A_44_P481915	Id4	6.65E-05	7.2	DSS Normal Tissue up
A_44_P479157	AI045067	0.000136517	7.2	DSS Normal Tissue up
A_42_P684885	Atp12a	0.000606983	7.1	DSS Normal Tissue up
A_43_P11776	Gstm1	1.69E-07	7.1	DSS Normal Tissue up
A_44_P102588	Ces2	0.00020044	7.1	DSS Normal Tissue up
A_44_P127869	Id4	4.00E-06	7.1	DSS Normal Tissue up
A_43_P21461	Zfp319_predicted	0.0019354	7.1	DSS Normal Tissue up
A_44_P142925	RGD1306226_predicted	2.77E-05	7.1	DSS Normal Tissue up
A_44_P480696	Ap1s2_predicted	0.000314733	7.0	All Tumors up
A_44_P272453	Cldn17_predicted	0.00127562	6.9	DSS Normal Tissue up
A_44_P949804	BU758404	0.0002422	6.9	All Tumors up
A_44_P1011716	Adora2b	0.000865984	6.9	DSS Normal Tissue up
A_43_P14558	Ngfg	0.00215795	6.9	DSS Normal Tissue up
A_44_P219598	Unc5c	0.00062932	6.9	All Tumors up
A_44_P1053321	Gbp2	5.81E-05	6.8	All Tumors up
A_44_P661776	A_44_P661776	0.000294942	6.8	DSS Normal Tissue up
A_43_P11464	Fgg	0.000213144	6.8	All Tumors up
A_44_P196909	Wfdc5_predicted	0.00178466	6.7	DSS Normal Tissue up
A_44_P374823	ENSRNOT00000056448	0.00280005	6.6	DSS Normal Tissue up
A_44_P191632	Odz2	0.000729943	6.6	DSS Normal Tissue up
A_44_P182195	Ton	0.00228832	6.6	DSS Normal Tissue up
A_44_P607972	TC593692	3.84E-05	6.6	DSS Normal Tissue up
A_44_P261473	BC089934	0.000375715	6.6	DSS Normal Tissue up
A_44_P841532	TC584998	4.35E-05	6.5	DSS Normal Tissue up
A_44_P364859	Lypd2_predicted	0.000157092	6.5	DSS Normal Tissue up
A_42_P628981	Prss23	1.25E-06	6.5	All Tumors up
A_44_P374824	ENSRNOT00000056448	0.000636918	6.5	DSS Normal Tissue up
A_44_P743669	DV716578	1.57E-05	6.5	All Tumors up
A_44_P257893	Gbp4_predicted	0.00269214	6.5	All Tumors up
A_43_P11499	Rbp2	0.000667269	6.4	DSS Normal Tissue up
A_44_P994500	CF111094	1.53E-05	6.4	All Tumors up
A_44_P149300	Muc4	0.00114012	6.3	DSS Normal Tissue up
A_44_P130333	Mmp11	0.000239474	6.3	All Tumors up
A_44_P931389	CA509267	0.000912727	6.3	All Tumors up
A_43_P17494	RGD1305269_predicted	0.000190237	6.3	All Tumors up
A_44_P714784	BF289878	1.78E-06	6.3	All Tumors up
A_44_P578700	TC642004	3.91E-05	6.2	DSS Normal Tissue up

A_43_P13924	Emp2	0.000526416	6.2	DSS Normal Tissue up
A_44_P313810	Dync1l1	0.00312723	6.2	DSS Normal Tissue up
A_44_P220533	Vsig2_predicted	0.00219617	6.1	DSS Normal Tissue up
A_42_P518462	Hmgn3	0.00143411	6.1	DSS Normal Tissue up
A_43_P11558	Apod	8.92E-05	6.1	All Tumors up
A_44_P961496	TC615769	0.000379011	6.1	DSS Normal Tissue up
A_44_P562884	TC619135	3.70E-05	6.1	DSS Normal Tissue up
A_44_P976747	TC613633	3.22E-05	6.1	DSS Normal Tissue up
A_44_P182479	Kcnk4	0.000492332	6.1	DSS Normal Tissue up
A_44_P557626	Klk9_predicted	0.000456343	6.1	DSS Normal Tissue up
A_44_P396772	Lrrn1	0.000732152	6.1	All Tumors up
A_44_P237664	AW141875	5.99E-05	6.0	All Tumors up
A_43_P12374	Edg7	0.000360116	6.0	DSS Normal Tissue up
A_44_P823561	TC603553	0.000929473	6.0	All Tumors up
A_44_P182136	AI556689	0.000414494	6.0	DSS Normal Tissue up
A_44_P107680	Gpr87_predicted	0.00225758	6.0	DSS Normal Tissue up
A_42_P559414	Wnt4	0.00023097	6.0	DSS Normal Tissue up
A_44_P294914	RGD1562499_predicted	0.00194735	6.0	DSS Normal Tissue up
A_44_P799807	BF398472	1.04E-05	5.9	DSS Normal Tissue up
A_44_P533877	Gk11	0.00189918	5.9	DSS Normal Tissue up
A_44_P635239	Nrep	1.52E-05	5.9	All Tumors up
A_44_P961499	TC615769	0.000318645	5.9	DSS Normal Tissue up
A_44_P934649	TC613996	1.60E-05	5.9	DSS Normal Tissue up
A_44_P656737	TC613867	0.00019773	5.9	DSS Normal Tissue up
A_44_P1014619	Katnal1	0.00162994	5.9	All Tumors up
A_44_P960804	TC601767	2.32E-05	5.9	DSS Normal Tissue up
A_44_P461130	Krt2-5	8.23E-05	5.8	DSS Normal Tissue up
A_44_P230410	Ptprn2	0.000126004	5.8	DSS Normal Tissue up
A_44_P1033435	Ka13	0.000355222	5.8	DSS Normal Tissue up
A_44_P199028	Dkk1_predicted	0.00144944	5.8	All Tumors up
A_44_P391982	Mmd	9.22E-05	5.8	All Tumors up
A_44_P717610	TC611311	3.18E-06	5.8	All Tumors up
A_44_P751844	TC635556	2.15E-05	5.8	DSS Normal Tissue up
A_43_P14969	Fbp1	0.000517286	5.8	DSS Normal Tissue up
A_44_P458021	Tnfrsf11b	0.000266958	5.8	All Tumors up
A_44_P684732	A_44_P684732	0.000192708	5.7	All Tumors up
A_44_P1048795	Dst_predicted	0.000924463	5.7	DSS Normal Tissue up
A_44_P784011	TC639313	6.06E-05	5.7	DSS Normal Tissue up
A_44_P545654	Slc1a2	0.002179	5.7	All Tumors up
A_42_P761225	Lypd2_predicted	7.76E-06	5.7	DSS Normal Tissue up
A_42_P663722	Slc30a2	5.97E-05	5.7	All Tumors up
A_44_P653272	TC589935	0.000140802	5.7	All Tumors up
A_42_P577677	Tnni1	1.18E-05	5.7	All Tumors up
A_42_P756334	Myh6	4.74E-05	5.7	All Tumors up
A_44_P917115	TC607376	0.000195491	5.7	All Tumors up
A_44_P812604	TC599592	0.00158425	5.7	DSS Normal Tissue up
A_44_P1039128	Cxcl10	0.00260259	5.7	All Tumors up
A_44_P685985	TC611320	0.000266369	5.7	DSS Normal Tissue up
A_44_P638274	TC590186	3.10E-06	5.7	All Tumors up
A_44_P700820	TC593009	5.18E-05	5.7	DSS Normal Tissue up
A_44_P886240	TC606783	0.000201487	5.7	DSS Normal Tissue up
A_44_P702082	TC595994	4.13E-05	5.6	DSS Normal Tissue up
A_44_P313542	Sgk	0.00141699	5.6	DSS Normal Tissue up
A_44_P886035	TC601364	2.36E-05	5.6	DSS Normal Tissue up
A_44_P730116	TC601834	0.00112697	5.6	DSS Normal Tissue up
A_44_P124355	BE107098	4.21E-05	5.6	All Tumors up
A_42_P602570	Bex1	0.000281057	5.6	All Tumors up
A_44_P808602	TC591609	0.000887887	5.6	DSS Normal Tissue up
A_42_P499767	Padi2	2.69E-06	5.6	All Tumors up
A_44_P106581	AW143880	9.28E-07	5.6	DSS Normal Tissue up
A_44_P171155	LOC363337	0.000174818	5.6	DSS Normal Tissue up
A_44_P690669	AW921140	0.00278804	5.6	DSS Normal Tissue up
A_44_P550768	TC596680	0.00148478	5.5	DSS Normal Tissue up
A_44_P337843	LOC311984	0.00370725	5.5	All Tumors up
A_44_P793670	TC603202	0.000335708	5.5	All Tumors up
A_44_P354062	Tram1ll1_predicted	0.000503017	5.5	All Tumors up
A_44_P244668	Aqp8	6.16E-05	5.5	DSS Normal Tissue up

A_43_P12356	Tmeff1	6.37E-05	5.5	All Tumors up
A_44_P916583	CB614494	7.17E-05	5.5	DSS Normal Tissue up
A_44_P1000653	Serpina3n	0.000102761	5.5	DSS Normal Tissue up
A_43_P14622	Cybrd1	8.44E-05	5.4	All Tumors up
A_44_P170111	Al102927	0.000716208	5.4	DSS Normal Tissue up
A_44_P151459	Gp1bb	0.000999914	5.4	DSS Normal Tissue up
A_44_P1013713	LOC683733	0.00010527	5.4	DSS Normal Tissue up
A_42_P759444	TC587465	5.83E-05	5.4	DSS Normal Tissue up
A_44_P245941	Il1f6_predicted	0.000178365	5.4	DSS Normal Tissue up
A_42_P549786	B3gat2	0.00320951	5.3	All Tumors up
A_43_P10033	Apobec2_predicted	2.70E-05	5.3	All Tumors up
A_44_P482485	ENSRNOT00000059002	0.00356136	5.3	DSS Normal Tissue up
A_44_P171098	Gsg1	0.000176036	5.3	DSS Normal Tissue up
A_44_P1009656	ENSRNOT00000057120	0.000522016	5.3	DSS Normal Tissue up
A_44_P866810	Tead2	8.07E-05	5.3	All Tumors up
A_44_P283385	Gip	4.21E-06	5.3	DSS Normal Tissue up
A_44_P578452	TC630385	5.19E-05	5.3	DSS Normal Tissue up
A_44_P810573	TC615685	0.00149758	5.3	DSS Normal Tissue up
A_44_P758422	AW143472	0.000115612	5.2	DSS Normal Tissue up
A_42_P843692	Cadps	3.13E-05	5.2	All Tumors up
A_43_P15489	Il24	0.00121547	5.2	DSS Normal Tissue up
A_44_P112222	LOC685912	0.00237036	5.2	DSS Normal Tissue up
A_44_P700598	BP483652	0.000372613	5.2	DSS Normal Tissue up
A_44_P745269	Ak311	0.00173404	5.2	All Tumors up
A_44_P311326	ENSRNOT00000028196	1.44E-05	5.2	DSS Normal Tissue up
A_44_P976406	A_44_P976406	8.12E-06	5.2	All Tumors up
A_44_P761505	TC583715	0.00311188	5.2	DSS Normal Tissue up
A_44_P901264	TC607281	0.000197663	5.2	DSS Normal Tissue up
A_44_P311816	Tmed6_predicted	0.000431779	5.2	All Tumors up
A_44_P531245	S57440	0.0025546	5.1	DSS Normal Tissue up
A_42_P791512	Mep1a	0.001887	5.1	DSS Normal Tissue up
A_44_P464960	RGD1561950_predicted	0.000737753	5.1	All Tumors up
A_43_P20474	Ptprb_predicted	0.00163171	5.1	DSS Normal Tissue up
A_44_P234663	LOC683626	0.00373567	5.1	DSS Normal Tissue up
A_44_P1047467	RGD1305614_predicted	5.18E-06	5.1	All Tumors up
A_44_P165986	Klk7_predicted	0.000564435	5.1	DSS Normal Tissue up
A_44_P637872	TC597010	0.00218047	5.1	DSS Normal Tissue up
A_44_P131470	Hexb	6.50E-05	5.1	DSS Normal Tissue up
A_43_P16045	AB072252	0.00084083	5.1	DSS Normal Tissue up
A_43_P13105	Serpib7	1.23E-05	5.1	DSS Normal Tissue up
A_44_P426529	Me3_predicted	8.24E-07	5.1	All Tumors up
A_43_P16398	Z29072	0.00164566	5.1	DSS Normal Tissue up
A_44_P960435	TC613177	0.00295645	5.0	DSS Normal Tissue up
A_44_P685385	TC597507	0.000361019	5.0	DSS Normal Tissue up
A_44_P1008753	Fhl1	0.00261505	5.0	DSS Normal Tissue up
A_44_P119160	Papss2_predicted	0.000984329	5.0	DSS Normal Tissue up
A_44_P449108	AI043579	7.87E-05	5.0	DSS Normal Tissue up
A_44_P129288	CO394414	0.00030181	5.0	DSS Normal Tissue up
A_42_P688422	Egfl9_predicted	0.00168915	5.0	DSS Normal Tissue up
A_44_P185015	Spetex-2B	5.66E-05	5.0	All Tumors up
A_44_P319322	Krt1-12	0.0016901	5.0	DSS Normal Tissue up
A_44_P123537	Capn9	0.000849603	5.0	DSS Normal Tissue up

**Supplementary Table S-4.** Genes differentially expressed between untreated and DSS-treated colonic tissue in wild type rats

Probe ID	GeneName	p-value	Fold-Change	Fold-Change
A_44_P196849	Calm4	6.21E-05	202.4	DSS Normal Tissue up
A_44_P791908	RGD1560859	0.00175313	144.2	DSS Normal Tissue up
A_64_P140437	Cxcl2	0.000249096	98.8	DSS Normal Tissue up
A_42_P473398	Cxcl1	5.24E-05	34.7	DSS Normal Tissue up
A_64_P105226	Defb14	0.00138779	32.1	DSS Normal Tissue up
A_64_P131573	Defa8	2.25E-05	25.2	Control Normal Tissue up
A_42_P714311	Ccl3	0.000939088	24.6	DSS Normal Tissue up
A_64_P113798	A_64_P113798	0.00039143	23.1	Control Normal Tissue up
A_44_P273783	Aldh1a3	1.91E-06	23.1	DSS Normal Tissue up
A_44_P269055	Ly6b	0.000458467	23.0	DSS Normal Tissue up
A_43_P14911	Il1b	0.000969323	21.4	DSS Normal Tissue up
A_64_P025016	Bcat1	8.01E-05	19.2	DSS Normal Tissue up
A_64_P150623	LOC689756	9.27E-06	18.0	DSS Normal Tissue up
A_64_P089555	Steap4	7.41E-05	17.7	DSS Normal Tissue up
A_43_P12786	Fabp4	0.000239857	16.3	DSS Normal Tissue up
A_64_P038872	A2m	0.000837079	16.3	DSS Normal Tissue up
A_64_P126995	Lrrc15	0.000142158	16.1	DSS Normal Tissue up
A_42_P466706	PCOLCE2	0.000657218	15.6	DSS Normal Tissue up
A_64_P038873	A2m	0.00066264	15.1	DSS Normal Tissue up
A_64_P127026	Cmah	3.41E-05	14.1	Control Normal Tissue up
A_42_P575398	Aadac	8.31E-06	13.7	Control Normal Tissue up
A_42_P736530	RGD1563091	4.84E-05	13.6	DSS Normal Tissue up
A_44_P142925	Tprg1	0.00057248	13.5	DSS Normal Tissue up
A_44_P879764	B4galt1	1.51E-05	13.3	DSS Normal Tissue up
A_64_P137075	Col7a1	0.000276829	13.0	DSS Normal Tissue up
A_43_P15638	Tnc	0.000318946	13.0	DSS Normal Tissue up
A_64_P047478	Igfbp5	0.00187234	12.9	DSS Normal Tissue up
A_42_P508921	Aqp3	0.000645552	12.9	DSS Normal Tissue up
A_44_P362981	Fabp5	0.000603053	12.8	DSS Normal Tissue up
A_42_P695401	Ccl2	0.000450449	12.1	DSS Normal Tissue up
A_42_P595653	Sh3kbp1	2.19E-05	12.1	DSS Normal Tissue up
A_42_P641004	Il1a	0.00136407	11.9	DSS Normal Tissue up
A_64_P013243	A_64_P013243	0.00075855	11.6	DSS Normal Tissue up
A_64_P006608	LOC100362200	1.98E-06	11.1	DSS Normal Tissue up
A_64_P065091	Vcan	0.000136746	10.8	DSS Normal Tissue up
A_43_P14796	LOC682861	0.000309855	10.6	DSS Normal Tissue up
A_64_P016978	Ccl11	0.00204797	10.5	DSS Normal Tissue up
A_64_P103724	Alox12	1.15E-05	9.9	DSS Normal Tissue up
A_44_P326133	XM_231258	0.00137289	9.8	DSS Normal Tissue up
A_64_P059728	TC597252	0.00011222	9.7	DSS Normal Tissue up
A_64_P057227	Fer114	0.000585316	9.4	DSS Normal Tissue up
A_64_P129855	Meis1	0.00052737	9.4	DSS Normal Tissue up
A_64_P104247	TC630808	0.00010664	9.2	DSS Normal Tissue up
A_64_P046990	Srsf12	1.29E-05	9.1	DSS Normal Tissue up
A_44_P1018957	Hsd11b1	0.000122505	9.0	DSS Normal Tissue up
A_42_P740370	Cpxm2	2.09E-05	8.9	DSS Normal Tissue up
A_44_P238556	Mcpt2	7.05E-05	8.9	DSS Normal Tissue up
A_64_P096096	RGD1562551	0.000236455	8.8	DSS Normal Tissue up
A_64_P281840	Nrg1	7.35E-06	8.6	DSS Normal Tissue up
A_44_P393551	Gja1	0.000264146	8.6	DSS Normal Tissue up
A_43_P16767	Igfbp4	8.47E-05	8.2	DSS Normal Tissue up
A_64_P035291	Gsta5	8.55E-05	8.2	Control Normal Tissue up
A_64_P077560	Sh3kbp1	2.61E-05	8.0	DSS Normal Tissue up
A_42_P641517	ENSRNOT00000028012	0.000102372	8.0	DSS Normal Tissue up
A_64_P036955	Mmp2	8.59E-05	8.0	DSS Normal Tissue up
A_42_P499158	Vcam1	0.00158646	8.0	DSS Normal Tissue up
A_44_P496643	A_44_P496643	0.00174689	7.9	DSS Normal Tissue up
A_44_P122912	Ces1c	5.02E-05	7.8	Control Normal Tissue up
A_42_P724510	Epdr1	6.93E-07	7.8	DSS Normal Tissue up



Probe ID	GeneName	p-value	Fold-Change	Fold-Change
A_64_P082067	Ifit3	0.00185388	7.7	DSS Normal Tissue up
A_44_P332422	C1s	0.000371676	7.7	DSS Normal Tissue up
A_64_P009857	Tbx1	0.000227475	7.6	DSS Normal Tissue up
A_43_P10102	Spry4	0.000794682	7.6	DSS Normal Tissue up
A_44_P209788	Enpep	0.00183708	7.6	Control Normal Tissue up
A_64_P115157	Ces1e	0.000396372	7.5	Control Normal Tissue up
A_64_P060662	Tcf21	0.00182017	7.3	DSS Normal Tissue up
A_64_P152154	Aldh1b1	0.000450343	7.3	Control Normal Tissue up
A_44_P299565	Mcpt1	0.000446707	7.3	DSS Normal Tissue up
A_42_P626433	Scara5	0.000747879	7.3	DSS Normal Tissue up
A_64_P158975	Ptx3	0.00163231	7.2	DSS Normal Tissue up
A_64_P026316	C4b	3.72E-05	7.2	DSS Normal Tissue up
A_44_P555271	Mmp12	0.000329008	7.2	DSS Normal Tissue up
A_42_P559831	Ces1c	3.48E-05	7.2	Control Normal Tissue up
A_64_P105338	A_64_P105338	0.000295737	7.1	DSS Normal Tissue up
A_44_P133485	Bend5	6.27E-07	7.1	Control Normal Tissue up
A_44_P996729	Mmp2	5.74E-05	7.0	DSS Normal Tissue up
A_64_P029327	A_64_P029327	0.00147816	6.9	DSS Normal Tissue up
A_42_P535644	Adamts1	0.000926017	6.8	DSS Normal Tissue up
A_64_P056841	A_64_P056841	6.83E-05	6.7	Control Normal Tissue up
A_64_P051307	Runx2	0.00177259	6.7	DSS Normal Tissue up
A_44_P845503	A_44_P845503	5.58E-05	6.7	Control Normal Tissue up
A_44_P393343	St3gal6	2.37E-05	6.5	Control Normal Tissue up
A_64_P131577	Defa9	0.000622971	6.5	Control Normal Tissue up
A_44_P171440	Apoe	4.33E-06	6.5	DSS Normal Tissue up
A_64_P018761	Calca	0.0019223	6.5	Control Normal Tissue up
A_43_P22629	A_43_P22629	2.55E-05	6.4	DSS Normal Tissue up
A_44_P612762	Lrrc8c	2.03E-05	6.4	DSS Normal Tissue up
A_64_P052765	Cdh16	0.00123921	6.3	DSS Normal Tissue up
A_44_P258031	Efhc2	0.000732608	6.3	Control Normal Tissue up
A_42_P756334	Myh6	0.000365575	6.2	DSS Normal Tissue up
A_42_P625157	Zfp503	5.60E-05	6.2	Control Normal Tissue up
A_42_P637122	Sertad4	2.33E-05	6.2	DSS Normal Tissue up
A_64_P087643	RGD1561282	0.000611582	6.2	Control Normal Tissue up
A_42_P820657	Il1r2	0.00106873	6.1	DSS Normal Tissue up
A_44_P835847	C1qtnf3	0.00136912	6.1	DSS Normal Tissue up
A_43_P11590	Mmp7	0.000356005	6.1	DSS Normal Tissue up
A_64_P144879	Rarres1	7.06E-05	6.0	DSS Normal Tissue up
A_64_P146507	A_64_P146507	0.000304606	5.9	DSS Normal Tissue up
A_44_P247081	Pla2g2a	9.94E-05	5.9	DSS Normal Tissue up
A_44_P1004323	Col18a1	0.000156148	5.9	DSS Normal Tissue up
A_64_P024356	Sh2b2	0.000601383	5.8	DSS Normal Tissue up
A_44_P787848	Jam2	0.00117347	5.8	DSS Normal Tissue up
A_64_P109657	Ednra	5.50E-05	5.8	DSS Normal Tissue up
A_64_P148413	Ces1d	0.000716585	5.8	Control Normal Tissue up
A_64_P172851	RGD1562667	0.000440876	5.8	DSS Normal Tissue up
A_42_P518855	Bcl2a1d	9.69E-05	5.8	DSS Normal Tissue up
A_42_P541872	B3galnt1	6.25E-05	5.7	DSS Normal Tissue up
A_44_P125733	Madcaml	0.000718919	5.6	DSS Normal Tissue up
A_42_P602724	Ubd	0.00116321	5.6	DSS Normal Tissue up
A_64_P119777	Pxdn	0.000730583	5.6	DSS Normal Tissue up
A_42_P717175	Pla2g2d	5.72E-05	5.6	DSS Normal Tissue up
A_44_P588315	Lyve1	0.00140341	5.5	DSS Normal Tissue up
A_64_P215398	Lyc2	0.000264348	5.5	DSS Normal Tissue up
A_64_P116949	Plxdc2	0.000135574	5.4	DSS Normal Tissue up
A_64_P110941	Cndp1	7.81E-06	5.4	DSS Normal Tissue up
A_64_P064695	ENSRNOT00000043269	0.000494111	5.4	DSS Normal Tissue up
A_64_P051121	Pdpn	0.000312209	5.4	DSS Normal Tissue up
A_44_P438863	Serpine2	0.00141325	5.4	DSS Normal Tissue up
A_64_P138919	Eln	0.000225902	5.4	DSS Normal Tissue up
A_64_P077420	Kb23	0.00164356	5.3	Control Normal Tissue up
A_64_P034414	Tnf	0.00160132	5.3	DSS Normal Tissue up
A_44_P992908	Hspb1	0.000131119	5.2	DSS Normal Tissue up
A_43_P15023	Thbd	0.00189065	5.2	DSS Normal Tissue up
A_64_P004974	Ednrb	3.21E-05	5.2	DSS Normal Tissue up

Probe ID	GeneName	p-value	Fold-Change	Fold-Change
A_43_P12070	Ly6c	0.000374616	5.2	DSS Normal Tissue up
A_64_P083600	Fxyd5	0.0001014	5.1	DSS Normal Tissue up
A_64_P119633	Plat	0.00147591	5.1	DSS Normal Tissue up
A_44_P1022002	Ccl7	4.62E-05	5.1	DSS Normal Tissue up
A_64_P107589	LOC685067	0.00108707	5.1	DSS Normal Tissue up
A_44_P248090	Thbs2	0.000422999	5.1	DSS Normal Tissue up
A_64_P088836	Gpr98	0.000101271	5.1	DSS Normal Tissue up
A_64_P105988	Mcpt114	0.000262921	5.0	DSS Normal Tissue up
A_43_P15507	Ido1	1.30E-05	5.0	DSS Normal Tissue up
A_64_P042495	Cbln1	0.000843293	5.0	DSS Normal Tissue up
A_44_P502287	B4galt6	8.93E-05	5.0	DSS Normal Tissue up
A_44_P529904	Bend7	1.06E-06	5.0	Control Normal Tissue up
A_42_P577677	Tnni1	0.0016342	5.0	Control Normal Tissue up
A_42_P508984	Pf4	0.000555442	5.0	DSS Normal Tissue up
A_43_P11804	Ptn	0.00144788	5.0	DSS Normal Tissue up
A_64_P012846	ENSRNOT00000041800	1.60E-06	4.9	Control Normal Tissue up
A_64_P025286	Lyz2	0.000259272	4.9	DSS Normal Tissue up
A_64_P003572	Lgr5	0.000699758	4.9	Control Normal Tissue up
A_64_P026517	Parvg	0.00171676	4.8	DSS Normal Tissue up
A_64_P050079	LOC100188984	4.40E-05	4.8	Control Normal Tissue up
A_64_P006498	Ces1e	5.38E-05	4.8	Control Normal Tissue up
A_43_P10689	Synm	0.00091647	4.8	DSS Normal Tissue up
A_64_P067923	RGD1564149	6.21E-05	4.8	DSS Normal Tissue up
A_42_P481167	Gucy1a3	1.09E-05	4.7	Control Normal Tissue up
A_64_P092414	Col5a2	0.00136216	4.7	DSS Normal Tissue up
A_42_P591344	Itgb2	0.000270183	4.7	DSS Normal Tissue up
A_64_P077692	Ly49si1	0.000374935	4.6	DSS Normal Tissue up
A_64_P010748	A_64_P010748	0.000605588	4.6	DSS Normal Tissue up
A_42_P655047	Prrx2	0.00138654	4.6	DSS Normal Tissue up
A_64_P054692	Tmem212	0.000213603	4.6	DSS Normal Tissue up
A_64_P084059	ENSRNOT00000049208	0.000302726	4.5	Control Normal Tissue up
A_64_P031741	A_64_P031741	0.000543365	4.5	DSS Normal Tissue up
A_44_P366723	Igfl	0.00068475	4.5	DSS Normal Tissue up
A_64_P080025	Serping1	0.000191514	4.5	DSS Normal Tissue up
A_44_P451357	Sparc	0.00190452	4.5	DSS Normal Tissue up
A_44_P513385	Dab2	0.000276	4.4	DSS Normal Tissue up
A_64_P052825	Fcer1a	0.000139245	4.4	DSS Normal Tissue up
A_64_P022746	Srpx	0.00195288	4.4	DSS Normal Tissue up
A_43_P19776	LOC681325	0.00155305	4.4	DSS Normal Tissue up
A_64_P138470	Ifi204	2.92E-05	4.4	DSS Normal Tissue up
A_43_P11489	S100a4	0.000261597	4.4	DSS Normal Tissue up
A_44_P337351	Cxcl12	0.000761743	4.4	DSS Normal Tissue up
A_64_P163653	LOC681325	0.00115465	4.3	DSS Normal Tissue up
A_44_P372998	Cpa6	0.00107555	4.3	DSS Normal Tissue up
A_64_P157691	RGD1559482	0.000145113	4.3	DSS Normal Tissue up
A_44_P126061	Oasl2	0.00013301	4.3	DSS Normal Tissue up
A_44_P290656	ENSRNOT00000055066	0.000213155	4.3	DSS Normal Tissue up
A_44_P360926	Nlrp5	9.30E-05	4.3	DSS Normal Tissue up
A_44_P445070	Lgals1	0.00160308	4.3	DSS Normal Tissue up
A_44_P1053951	TC603458	0.000762197	4.3	DSS Normal Tissue up
A_64_P039826	LOC680236	0.000693749	4.3	DSS Normal Tissue up
A_64_P164240	LOC301193	0.000312488	4.3	DSS Normal Tissue up
A_44_P337365	Fcer2	0.000571132	4.2	DSS Normal Tissue up
A_44_P172601	Icos	0.00101873	4.2	DSS Normal Tissue up
A_44_P192406	Dusp9	0.00182988	4.2	DSS Normal Tissue up
A_44_P297777	Flna	0.000692306	4.2	DSS Normal Tissue up
A_44_P280954	Klk1c10	1.14E-05	4.2	Control Normal Tissue up
A_44_P1005051	Car5b	0.000967015	4.2	DSS Normal Tissue up
A_44_P325666	Cyp2d2	0.00113018	4.2	Control Normal Tissue up
A_44_P1050480	Ecm1	0.00111039	4.2	DSS Normal Tissue up
A_44_P1013314	Isg15	0.000633798	4.1	DSS Normal Tissue up
A_64_P026122	Mak	0.00175366	4.1	Control Normal Tissue up
A_43_P11812	Bgn	0.00198699	4.1	DSS Normal Tissue up
A_44_P472994	Anxa5	0.000140189	4.1	DSS Normal Tissue up
A_44_P555689	LOC291863	3.58E-05	4.1	Control Normal Tissue up

<b>Probe ID</b>	<b>GeneName</b>	<b>p-value</b>	<b>Fold-Change</b>	<b>Fold-Change</b>
A_44_P1052046	RGD1562717	0.00113837	4.1	DSS Normal Tissue up
A_64_P084058	LOC685125	0.000541143	4.0	Control Normal Tissue up
A_44_P1053321	Gbp2	0.000889467	4.0	DSS Normal Tissue up
A_44_P428739	Shc3	0.000903938	4.0	Control Normal Tissue up
A_64_P109754	Epgn	6.73E-06	4.0	DSS Normal Tissue up

**Supplementary Table S-5.** Genes differentially expressed between untreated and DSS-treated colonic tumors

Probe ID	Gene Symbol	p-value	Fold Change	Direction of Change
A_44_P369080	AI177761	0.00428728	11.4	DSS Tumor up
A_44_P776708	TC616959	0.0106115	10.3	DSS Tumor up
A_44_P288916	CB544899	0.000197027	7.5	Control Tumor up
A_42_P675879	Cyp4f4	0.00778895	7.5	DSS Tumor up
A_44_P517293	BF284313	0.00466903	6.6	DSS Tumor up
A_44_P113088	Slc34a2	4.24E-05	6.0	Control Tumor up
A_44_P207752	AW527592	0.00304673	5.5	DSS Tumor up
A_44_P306524	Slc30a3	0.012879	4.6	Control Tumor up
A_44_P876244	CK839878	0.0139567	4.5	DSS Tumor up
A_44_P169124	BF558918	0.000207985	4.5	Control Tumor up
A_44_P349277	RGD1562653_predicted	0.0090653	4.4	DSS Tumor up
A_42_P691339	ENSRNOT00000018076	0.00438147	4.3	Control Tumor up
A_44_P330565	XM_341050	0.00424961	4.2	Control Tumor up
A_44_P360767	Spink1	0.000847638	4.2	Control Tumor up
A_44_P450583	BF410961	0.010487	4.1	DSS Tumor up
A_44_P662803	A_44_P662803	0.000255741	3.9	Control Tumor up
A_44_P788404	BG670091	0.0108574	3.8	DSS Tumor up
A_44_P172601	Icos	0.00401718	3.7	Control Tumor up
A_44_P439843	AA818116	0.00479433	3.7	DSS Tumor up
A_44_P378742	Flrt3_predicted	0.00672601	3.7	Control Tumor up
A_44_P176906	BE110453	0.00519128	3.6	DSS Tumor up
A_43_P16391	Adam5	0.005401	3.6	Control Tumor up
A_43_P15907	RGD1564811_predicted	0.00862405	3.5	DSS Tumor up
A_43_P15596	ENSRNOT00000021832	0.0082345	3.5	Control Tumor up
A_44_P1057309	Lphn3	0.0118139	3.5	DSS Tumor up
A_44_P624280	TC598890	0.0030291	3.5	Control Tumor up
A_43_P13056	Il10ra	0.00611274	3.4	DSS Tumor up
A_44_P505488	BI288152	0.000206235	3.4	DSS Tumor up
A_44_P604893	CB584111	0.00889187	3.4	DSS Tumor up
A_44_P413679	AI013540	0.00177957	3.3	Control Tumor up
A_44_P307939	AI236404	0.00382547	3.3	DSS Tumor up
A_44_P285794	XM_345753	0.0109691	3.3	DSS Tumor up
A_44_P246799	CB547862	0.0113769	3.3	Control Tumor up
A_44_P368153	RGD1561831_predicted	0.00195341	3.3	Control Tumor up
A_44_P179373	AA818488	0.00906589	3.3	Control Tumor up
A_44_P951387	A_44_P951387	0.00220254	3.2	Control Tumor up
A_44_P275313	CB557013	0.00337643	3.1	DSS Tumor up
A_44_P468224	Olr1394_predicted	0.010525	3.1	Control Tumor up
A_44_P324806	AI103119	0.00674521	3.0	Control Tumor up
A_44_P289526	AI168950	0.000647597	3.0	DSS Tumor up
A_44_P251241	AA923942	0.00679271	3.0	Control Tumor up
A_44_P481398	Unc13a	0.00339891	3.0	Control Tumor up
A_44_P328136	Mx1	0.0125957	2.9	DSS Tumor up
A_44_P943917	Pirb	0.0110895	2.9	Control Tumor up
A_43_P23455	Dhx33_predicted	0.00448119	2.9	DSS Tumor up
A_44_P354415	Trem1_predicted	0.0117197	2.9	Control Tumor up
A_44_P838920	TC590823	0.00913886	2.9	Control Tumor up
A_44_P749490	DV723974	0.0039061	2.9	DSS Tumor up
A_44_P562092	Gng11	0.00716901	2.9	Control Tumor up

Probe ID	Gene Symbol	p-value	Fold Change	Direction of Change
A_42_P679814	Cyp3a18	0.005038	2.8	Control Tumor up
A_44_P653053	LOC498335	0.00155323	2.8	Control Tumor up
A_44_P468468	Lbp	0.0104176	2.8	Control Tumor up
A_44_P961602	Rasl12_predicted	0.000438737	2.8	Control Tumor up
A_44_P128916	Centb1_predicted	0.00821664	2.8	Control Tumor up
A_44_P458227	Nphs2	0.000822298	2.8	DSS Tumor up
A_44_P676285	TC632060	0.00424787	2.8	Control Tumor up
A_44_P525187	Rnase9	0.0117392	2.7	Control Tumor up
A_44_P184057	BE102354	0.0120198	2.7	DSS Tumor up
A_43_P15262	Ahr	0.00352215	2.7	Control Tumor up
A_44_P445136	Olr13_predicted	0.0133385	2.7	Control Tumor up
A_44_P670435	TC605849	0.00883789	2.6	DSS Tumor up
A_44_P335079	Tff3	0.00038513	2.6	Control Tumor up
A_44_P326430	ENSRNOT00000056114	0.00506741	2.6	DSS Tumor up
A_44_P244506	AA946181	0.00206406	2.6	DSS Tumor up
A_44_P136027	BQ199246	0.00206954	2.6	DSS Tumor up
A_44_P669786	ENSRNOT00000005187	0.00319747	2.6	Control Tumor up
A_44_P157881	AI555968	0.0119597	2.6	DSS Tumor up
A_44_P1007347	Tgm2	0.0112529	2.6	Control Tumor up
A_44_P515211	Tnfsf15	0.0133481	2.6	Control Tumor up
A_44_P115774	AI105429	0.00631519	2.6	Control Tumor up
A_44_P219972	Nt5e	0.00609486	2.6	Control Tumor up
A_44_P156774	LOC681198	0.00271144	2.6	Control Tumor up
A_44_P526978	Bmp3	0.0110674	2.5	Control Tumor up
A_44_P508066	Nnat	0.0121074	2.5	DSS Tumor up
A_44_P242958	Ttpa	0.00300959	2.5	Control Tumor up
A_44_P961496	TC615769	0.00218545	2.5	Control Tumor up
A_44_P669124	DV722696	0.0110583	2.5	Control Tumor up
A_44_P365318	Olr1313_predicted	0.0108728	2.5	Control Tumor up
A_44_P397836	Npc111	0.0025301	2.5	Control Tumor up
A_44_P926626	AA800429	0.0104658	2.5	Control Tumor up
A_44_P115142	Mycn	0.00750047	2.4	Control Tumor up
A_44_P319322	Krt1-12	0.00623736	2.4	DSS Tumor up
A_44_P337843	LOC311984	0.0127196	2.4	Control Tumor up
A_43_P13363	Tmem37	9.28E-05	2.4	Control Tumor up
A_44_P269070	Omacs	0.0102802	2.4	DSS Tumor up
A_44_P202470	AA955742	0.0131214	2.4	DSS Tumor up
A_42_P771337	Lamp3	0.0053058	2.4	Control Tumor up
A_44_P946892	TC639110	0.00440642	2.4	Control Tumor up
A_44_P454580	RGD1310835_predicted	0.00366186	2.4	Control Tumor up
A_44_P681872	AW141628	0.0089968	2.4	Control Tumor up
A_44_P494196	S79307	0.00790939	2.4	Control Tumor up
A_44_P870880	BF555751	0.0137546	2.4	Control Tumor up
A_44_P311552	A_44_P311552	0.00787683	2.3	DSS Tumor up
A_44_P1017206	RGD1307753_predicted	0.00907007	2.3	Control Tumor up
A_43_P13779	AA819135	0.00159466	2.3	DSS Tumor up
A_44_P562292	TC599327	0.00465974	2.3	Control Tumor up
A_44_P900333	TC624655	0.00107139	2.3	Control Tumor up
A_44_P541640	RGD1566137_predicted	0.0101968	2.3	Control Tumor up
A_44_P511375	TC642638	0.00665458	2.3	DSS Tumor up
A_44_P562669	DV718178	0.00687371	2.3	Control Tumor up
A_44_P521163	LOC680726	0.00731028	2.3	DSS Tumor up
A_44_P961499	TC615769	0.00552057	2.3	Control Tumor up
A_44_P757197	CB557736	0.00181376	2.3	DSS Tumor up

Probe ID	Gene Symbol	p-value	Fold Change	Direction of Change
A_44_P727817	AW917233	0.00236552	2.3	Control Tumor up
A_44_P236770	TC595776	0.00637937	2.3	Control Tumor up
A_44_P229118	Muc1	0.000182024	2.3	Control Tumor up
A_44_P516137	Syngn3_predicted	0.00392534	2.3	Control Tumor up
A_42_P648652	Clca6	0.00137556	2.3	Control Tumor up
A_42_P792497	Cyp2j4	0.0114074	2.3	Control Tumor up
A_44_P156673	LOC289334	0.00907462	2.2	DSS Tumor up
A_44_P180229	RGD1565457_predicted	0.00480726	2.2	Control Tumor up
A_44_P936139	CK358538	0.0064021	2.2	Control Tumor up
A_43_P22739	RGD1565785_predicted	0.00958312	2.2	Control Tumor up
A_44_P291189	Hspb9_predicted	0.0070416	2.2	DSS Tumor up
A_44_P130740	CV112435	0.00848032	2.2	Control Tumor up
A_43_P18725	RGD1560168_predicted	0.014237	2.2	DSS Tumor up
A_44_P321686	ENSRNOT00000002188	0.0143287	2.2	DSS Tumor up
A_43_P21913	Usp53_predicted	0.000136732	2.2	Control Tumor up
A_44_P515029	Map1b	0.00737465	2.2	DSS Tumor up
A_44_P356658	Pdzd4_predicted	4.98E-05	2.2	DSS Tumor up
A_44_P819401	AA957643	0.000984584	2.2	Control Tumor up
A_44_P382291	Cbfa2t2_predicted	0.0141694	2.2	DSS Tumor up
A_42_P774527	Gzmc	0.0137355	2.2	Control Tumor up
A_44_P852957	TC592692	0.00608359	2.1	Control Tumor up
A_43_P22696	A_43_P22696	0.00529268	2.1	DSS Tumor up
A_43_P15475	Tpc1808	0.00711809	2.1	Control Tumor up
A_44_P672438	TC633528	0.0116248	2.1	DSS Tumor up
A_44_P1038716	RGD1565166_predicted	3.51E-05	2.1	Control Tumor up
A_44_P529645	RGD1565374_predicted	0.00264828	2.1	Control Tumor up
A_44_P203640	Klhl25	0.00331441	2.1	DSS Tumor up
A_42_P619056	Gent2	0.00464837	2.1	Control Tumor up
A_44_P838681	ENSRNOT00000028551	0.00525435	2.1	Control Tumor up
A_44_P120002	Gtf2i	0.00080901	2.1	DSS Tumor up
A_44_P219752	Bpi	0.00412672	2.1	Control Tumor up
A_44_P608910	TC600389	0.00251891	2.1	Control Tumor up
A_44_P548649	LOC691332	0.00675791	2.1	Control Tumor up
A_44_P502171	BQ202512	0.0106012	2.1	DSS Tumor up
A_44_P575872	ENSRNOT00000049735	0.00830661	2.1	Control Tumor up
A_44_P225129	LOC309292	0.00241916	2.1	DSS Tumor up
A_43_P11879	Htr2b	0.0106182	2.1	Control Tumor up
A_44_P824441	TC607190	0.00147808	2.1	Control Tumor up
A_44_P491759	Ka24	0.0119946	2.1	DSS Tumor up
A_44_P152317	A_44_P152317	0.00756651	2.1	Control Tumor up
A_44_P228820	AA946250	0.000107075	2.1	Control Tumor up
A_42_P703647	Cda_predicted	0.00202212	2.1	Control Tumor up
A_44_P355212	BQ196445	0.00600253	2.1	Control Tumor up
A_44_P698626	ENSRNOT00000055514	0.00554807	2.0	DSS Tumor up
A_44_P334736	Edn1	0.00262551	2.0	Control Tumor up
A_43_P16372	Olr737	0.0028322	2.0	Control Tumor up
A_44_P482538	Mcm4	0.00545262	2.0	DSS Tumor up
A_44_P316883	RGD1304728_predicted	0.00152562	2.0	DSS Tumor up
A_44_P391498	LOC305806	0.000656439	2.0	Control Tumor up
A_44_P614425	BQ035298	0.0126108	2.0	Control Tumor up
A_44_P307978	Cited2	0.00241979	2.0	Control Tumor up
A_44_P395771	Tie1	0.00661096	2.0	DSS Tumor up
A_44_P514658	AW533219	0.0125775	2.0	Control Tumor up
A_44_P344197	Olr1410_predicted	0.00253977	2.0	Control Tumor up

<b>Probe ID</b>	<b>Gene Symbol</b>	<b>p-value</b>	<b>Fold Change</b>	<b>Direction of Change</b>
A_44_P882995	RGD1561950_predicted	0.00900656	2.0	DSS Tumor up
A_44_P476024	LOC362652	0.00617447	2.0	Control Tumor up
A_43_P15444	Smo	0.0042347	2.0	DSS Tumor up

**Supplementary Table S-6.** Genes differentially expressed in untreated normal colonic tissue between Pirc and wild type rats

<b>Probe ID</b>	<b>Gene Symbol</b>	<b>p-value</b>	<b>Fold Change</b>	<b>Direction of Change</b>
A_64_P150623	LOC689756	4.01E-05	11.8	Pirc Normal Tissue up
A_44_P247081	Pla2g2a	5.09E-05	6.8	Pirc Normal Tissue up
A_64_P013164	A_64_P013164	5.44E-05	2.8	Wild Type Normal Tissue up
A_64_P034952	Vom2r50	5.17E-05	2.6	Wild Type Normal Tissue up
A_64_P022615	Vamp5	0.000129518	2.4	Wild Type Normal Tissue up
A_64_P137233	Sec14l2	2.14E-05	2.2	Wild Type Normal Tissue up
A_64_P039949	LOC679119	6.92E-05	2.1	Wild Type Normal Tissue up



**Supplementary Table S-7. Genes differentially expressed in DSS-treated normal colonic tissue between Pirc and wild type rats**

Probe ID	Gene Symbol	p-value	Fold Change	Direction of Change
A_44_P161470	Defa6	1.00E-07	4031.8	Pirc DSS Normal Tissue up
A_64_P124105	Defa24	2.54E-06	2438.6	Pirc DSS Normal Tissue up
A_64_P131573	Defa8	5.43E-09	1655.3	Pirc DSS Normal Tissue up
A_64_P031394	Defa-rs1	2.52E-06	1634.4	Pirc DSS Normal Tissue up
A_64_P131577	Defa9	9.13E-09	429.3	Pirc DSS Normal Tissue up
A_44_P203401	RatNP-3b	1.08E-07	296.4	Pirc DSS Normal Tissue up
A_64_P054112	T	2.11E-08	258.3	Pirc DSS Normal Tissue up
A_64_P009999	Tac1	9.15E-12	231.3	Pirc DSS Normal Tissue up
A_64_P053431	Cxcl17	2.72E-05	155.9	Pirc DSS Normal Tissue up
A_64_P125531	Defa10	1.15E-07	127.7	Pirc DSS Normal Tissue up
A_64_P025305	Clca4l	0.00097984	104.3	Pirc DSS Normal Tissue up
A_64_P155311	Prss22	0.00019443	74.4	Pirc DSS Normal Tissue up
A_64_P009996	Tac1	3.24E-08	68.1	Pirc DSS Normal Tissue up
A_64_P064134	Prss27	0.00077118	66.9	Pirc DSS Normal Tissue up
A_43_P11684	Alpl	0.000287703	60.8	Pirc DSS Normal Tissue up
A_64_P052017	Cxcl3	0.000233972	42.6	Pirc DSS Normal Tissue up
A_44_P1012017	ENSRNOT00000035058	0.000197078	40.3	Pirc DSS Normal Tissue up
A_64_P034472	A_64_P034472	3.89E-05	36.3	Pirc DSS Normal Tissue up
A_64_P043837	A_64_P043837	2.14E-05	32.8	Pirc DSS Normal Tissue up
A_64_P062168	RGD1306446	0.00106847	29.6	Pirc DSS Normal Tissue up
A_44_P1004757	Serpib10	0.0027514	28.0	Pirc DSS Normal Tissue up
A_64_P047947	S100a7a	0.000797992	26.2	Pirc DSS Normal Tissue up
A_43_P11086	Upk1b	0.00178396	26.1	Pirc DSS Normal Tissue up
A_64_P072128	Cxcl5	0.000117098	26.0	Pirc DSS Normal Tissue up
A_64_P167065	ENSRNOT00000046465	2.78E-05	25.5	Pirc DSS Normal Tissue up
A_44_P416695	Krt15	0.00290923	25.4	Pirc DSS Normal Tissue up
A_44_P121417	RGD1565787	0.00345282	23.8	Pirc DSS Normal Tissue up
A_42_P475871	Prss27	0.00021014	23.1	Pirc DSS Normal Tissue up
A_44_P219628	Ggt1	0.000125862	22.8	Pirc DSS Normal Tissue up
A_43_P11590	Mmp7	2.67E-06	22.5	Pirc DSS Normal Tissue up
A_64_P132482	Gpr87	0.00130823	22.3	Pirc DSS Normal Tissue up
A_43_P15281	Tp63	0.0105174	22.2	Pirc DSS Normal Tissue up
A_44_P247081	Pla2g2a	5.29E-07	21.9	Pirc DSS Normal Tissue up
A_64_P141384	Habp2	0.00199428	21.7	Pirc DSS Normal Tissue up
A_43_P12689	Defb1	0.00697652	21.6	Pirc DSS Normal Tissue up
A_42_P472699	Amn	5.68E-06	20.6	WT DSS Normal Tissue up
A_64_P150884	Scel	0.00661394	20.4	Pirc DSS Normal Tissue up
A_44_P515627	ENSRNOT00000004866	0.0023658	19.7	Pirc DSS Normal Tissue up
A_44_P255912	RGD1308564	0.00127608	18.9	Pirc DSS Normal Tissue up
A_42_P638494	Nppb	0.000930987	18.5	Pirc DSS Normal Tissue up
A_64_P140437	Cxcl2	0.00659992	18.0	Pirc DSS Normal Tissue up
A_44_P465329	Mal	0.000311945	17.8	Pirc DSS Normal Tissue up
A_64_P161306	ENSRNOT00000007422	6.68E-05	17.8	Pirc DSS Normal Tissue up
A_64_P124968	S100a7a	0.00136384	17.7	Pirc DSS Normal Tissue up
A_44_P438313	Serpib11	0.00241097	15.9	Pirc DSS Normal Tissue up
A_42_P778330	Sox2	0.00485974	15.9	Pirc DSS Normal Tissue up
A_42_P473398	Cxcl1	0.000431864	15.7	Pirc DSS Normal Tissue up
A_44_P129749	Crabp2	0.00832983	15.5	Pirc DSS Normal Tissue up
A_44_P563447	Wnt10a	0.00634017	15.4	Pirc DSS Normal Tissue up
A_64_P096412	Krt23	0.000317282	14.9	Pirc DSS Normal Tissue up
A_64_P150879	Scel	0.00571203	14.8	Pirc DSS Normal Tissue up
A_64_P105389	Krt4	0.00391379	14.6	Pirc DSS Normal Tissue up
A_44_P497121	Fam46b	0.00251055	14.4	Pirc DSS Normal Tissue up
A_44_P147572	ENSRNOT00000006888	0.000610821	14.2	Pirc DSS Normal Tissue up
A_44_P109876	Slc30a10	4.19E-05	14.2	WT DSS Normal Tissue up
A_64_P032504	Np4	2.34E-05	14.1	Pirc DSS Normal Tissue up
A_64_P015758	ENSRNOT00000050106	0.000519105	14.1	Pirc DSS Normal Tissue up
A_64_P018832	A_64_P018832	1.49E-06	14.0	Pirc DSS Normal Tissue up
A_64_P032337	A_64_P032337	0.000745941	13.9	Pirc DSS Normal Tissue up

Probe ID	Gene Symbol	p-value	Fold Change	Direction of Change
A_64_P132261	LOC687842	0.000247383	13.7	Pirc DSS Normal Tissue up
A_64_P086235	Irx1	0.000340742	13.4	Pirc DSS Normal Tissue up
A_64_P020621	Dlk2	0.00719081	13.4	Pirc DSS Normal Tissue up
A_64_P007880	LOC689709	6.27E-05	13.4	WT DSS Normal Tissue up
A_64_P005626	Anxa9	0.00180444	12.9	Pirc DSS Normal Tissue up
A_64_P078894	Ii23a	0.000141355	12.9	Pirc DSS Normal Tissue up
A_64_P366033	ENSRNOT00000046630	0.000999071	12.4	Pirc DSS Normal Tissue up
A_64_P162810	RGD1310110	1.13E-05	12.3	Pirc DSS Normal Tissue up
A_42_P719607	Ppbp	4.05E-05	12.1	Pirc DSS Normal Tissue up
A_44_P352951	Slc46a1	3.70E-05	12.0	WT DSS Normal Tissue up
A_64_P091953	Spink4	0.00147947	12.0	Pirc DSS Normal Tissue up
A_44_P288881	ENSRNOT00000040211	0.00887507	11.9	Pirc DSS Normal Tissue up
A_64_P090040	Sult1c3	0.000882539	11.8	Pirc DSS Normal Tissue up
A_64_P131414	A_64_P131414	0.00748124	11.7	Pirc DSS Normal Tissue up
A_44_P294675	Slfn3	1.80E-05	11.6	Pirc DSS Normal Tissue up
A_64_P023619	Ggta1p	0.000440209	11.3	Pirc DSS Normal Tissue up
A_64_P122382	Ii10	0.000107717	11.3	Pirc DSS Normal Tissue up
A_44_P294838	Ii1a	0.00123343	11.0	Pirc DSS Normal Tissue up
A_64_P135634	Tpd52i1	3.35E-05	11.0	Pirc DSS Normal Tissue up
A_64_P118532	Casr	3.39E-05	11.0	WT DSS Normal Tissue up
A_42_P556829	Wif1	0.000335924	11.0	Pirc DSS Normal Tissue up
A_43_P13127	Slc38a4	0.00184627	10.9	Pirc DSS Normal Tissue up
A_64_P161399	Slfn3	5.71E-05	10.9	Pirc DSS Normal Tissue up
A_42_P641004	Ii1a	0.00192806	10.5	Pirc DSS Normal Tissue up
A_64_P022155	Slc2a5	0.000691784	10.4	WT DSS Normal Tissue up
A_64_P125551	RGD1559884	0.00124451	10.2	Pirc DSS Normal Tissue up
A_64_P108054	A_64_P108054	3.44E-05	10.2	Pirc DSS Normal Tissue up
A_44_P508466	Jdp2	0.00029772	10.2	Pirc DSS Normal Tissue up
A_64_P030504	A_64_P030504	0.000239138	10.1	Pirc DSS Normal Tissue up
A_44_P665685	Krtap13-2	0.00211921	9.9	Pirc DSS Normal Tissue up
A_44_P399249	Tgm1	0.00328922	9.9	Pirc DSS Normal Tissue up
A_44_P1004790	Slc30a2	2.97E-06	9.6	Pirc DSS Normal Tissue up
A_64_P130280	Upk1a	2.29E-05	9.5	Pirc DSS Normal Tissue up
A_44_P304190	Tifa	3.79E-07	9.3	Pirc DSS Normal Tissue up
A_64_P067654	Aldh3a1	0.000242407	9.3	Pirc DSS Normal Tissue up
A_64_P095413	Slc4a9	0.00154466	8.9	Pirc DSS Normal Tissue up
A_44_P353618	S100a9	7.55E-05	8.9	Pirc DSS Normal Tissue up
A_44_P547771	Cited1	0.000321822	8.7	Pirc DSS Normal Tissue up
A_43_P15590	Fmod	0.00122694	8.7	WT DSS Normal Tissue up
A_64_P053785	Adra2a	0.00199972	8.6	Pirc DSS Normal Tissue up
A_43_P12051	Cyp4f1	0.00622332	8.6	Pirc DSS Normal Tissue up
A_64_P083309	TC586401	4.59E-05	8.5	WT DSS Normal Tissue up
A_64_P104568	A_64_P104568	0.00376199	8.5	Pirc DSS Normal Tissue up
A_64_P155193	Dio1	1.50E-06	8.4	WT DSS Normal Tissue up
A_42_P534882	Vsnl1	0.00580195	8.4	Pirc DSS Normal Tissue up
A_42_P826853	Tnfrsf17	0.00170329	8.4	Pirc DSS Normal Tissue up
A_44_P490308	Muc20	0.000142734	8.0	Pirc DSS Normal Tissue up
A_64_P034414	Tnf	0.000307953	8.0	Pirc DSS Normal Tissue up
A_64_P366035	ENSRNOT00000046630	0.000397715	7.8	Pirc DSS Normal Tissue up
A_64_P014982	Habp2	0.00313203	7.8	Pirc DSS Normal Tissue up
A_64_P366031	LOC100360169	0.000722552	7.8	Pirc DSS Normal Tissue up
A_64_P082317	Car13	0.00208223	7.7	Pirc DSS Normal Tissue up
A_64_P035291	Gsta5	0.000106734	7.7	Pirc DSS Normal Tissue up
A_44_P486914	Fgf9	0.000933128	7.7	WT DSS Normal Tissue up
A_43_P19751	RGD1565975	0.0039934	7.6	Pirc DSS Normal Tissue up
A_64_P133167	Duoxa2	7.69E-06	7.5	Pirc DSS Normal Tissue up
A_64_P034749	RGD1560859	0.00271833	7.5	Pirc DSS Normal Tissue up
A_64_P079326	Tp73	0.00734383	7.5	Pirc DSS Normal Tissue up
A_44_P592221	Sox7	0.00120775	7.5	Pirc DSS Normal Tissue up
A_64_P156682	Hmgn3	2.64E-05	7.5	Pirc DSS Normal Tissue up
A_64_P111630	Gsg1	0.00436152	7.5	Pirc DSS Normal Tissue up
A_64_P139559	Foxo6	3.78E-06	7.4	WT DSS Normal Tissue up
A_42_P775217	Ly6g6c	0.00907066	7.3	Pirc DSS Normal Tissue up
A_64_P117891	Adamts15	1.43E-05	7.3	WT DSS Normal Tissue up
A_64_P118444	Ii22	0.000202845	7.3	Pirc DSS Normal Tissue up

Probe ID	Gene Symbol	p-value	Fold Change	Direction of Change
A_64_P087539	Dusp14	0.00230682	7.2	Pirc DSS Normal Tissue up
A_64_P054074	Tgm3	3.53E-05	7.2	WT DSS Normal Tissue up
A_64_P048637	Cnfn	0.00811057	7.2	Pirc DSS Normal Tissue up
A_64_P014090	TC610252	5.38E-05	7.1	Pirc DSS Normal Tissue up
A_44_P447373	Ass1	9.85E-05	7.1	Pirc DSS Normal Tissue up
A_44_P1055780	S100a8	0.00182346	7.0	Pirc DSS Normal Tissue up
A_44_P194230	Slit2	0.00217369	6.9	Pirc DSS Normal Tissue up
A_64_P079609	Tpd521l	4.93E-05	6.9	Pirc DSS Normal Tissue up
A_44_P820062	Aif1l	0.00101463	6.9	Pirc DSS Normal Tissue up
A_64_P018761	Calca	0.00152999	6.9	Pirc DSS Normal Tissue up
A_64_P006608	LOC100362200	1.69E-05	6.8	WT DSS Normal Tissue up
A_42_P826221	Dpysl4	6.10E-06	6.8	WT DSS Normal Tissue up
A_42_P762829	Cebpd	6.86E-07	6.8	Pirc DSS Normal Tissue up
A_44_P1007841	ENSRNOT00000057971	0.00263494	6.8	Pirc DSS Normal Tissue up
A_64_P034884	Syce1	0.0103975	6.7	WT DSS Normal Tissue up
A_43_P14424	Pax9	0.00181349	6.7	Pirc DSS Normal Tissue up
A_64_P150623	LOC689756	0.000390078	6.6	Pirc DSS Normal Tissue up
A_44_P150112	Pigz1l	0.00103365	6.6	Pirc DSS Normal Tissue up
A_64_P146692	Slc22a1	9.17E-06	6.6	Pirc DSS Normal Tissue up
A_64_P119633	Plat	0.00052879	6.5	Pirc DSS Normal Tissue up
A_64_P074157	XM_223305	0.0105261	6.5	Pirc DSS Normal Tissue up
A_44_P518127	Wwtr1	6.38E-05	6.5	Pirc DSS Normal Tissue up
A_64_P112579	Slc16a1l	4.30E-05	6.4	Pirc DSS Normal Tissue up
A_43_P20484	Slc39a2	0.000138174	6.3	WT DSS Normal Tissue up
A_64_P091728	Slc22a1	8.15E-06	6.3	Pirc DSS Normal Tissue up
A_64_P054376	Gpr4	0.00027822	6.3	Pirc DSS Normal Tissue up
A_44_P327799	Apoc3	0.00299641	6.2	WT DSS Normal Tissue up
A_42_P518462	Hmgn3	5.39E-05	6.2	Pirc DSS Normal Tissue up
A_64_P129263	Ptprz1	0.00405507	6.2	Pirc DSS Normal Tissue up
A_64_P095554	ENSRNOT00000066209	5.28E-05	6.2	Pirc DSS Normal Tissue up
A_64_P048230	Tmem72	0.000579548	6.2	Pirc DSS Normal Tissue up
A_64_P112305	LOC497860	3.03E-05	6.2	Pirc DSS Normal Tissue up
A_64_P007268	Gpr77	0.000105057	6.2	Pirc DSS Normal Tissue up
A_44_P980916	Kirrel3	1.05E-06	6.1	Pirc DSS Normal Tissue up
A_64_P045661	Lrrc48	5.38E-06	6.0	WT DSS Normal Tissue up
A_44_P1023538	C3	0.000325486	6.0	Pirc DSS Normal Tissue up
A_43_P15426	Trpc3	0.000774369	6.0	WT DSS Normal Tissue up
A_64_P062275	LOC100360919	4.15E-06	6.0	Pirc DSS Normal Tissue up
A_44_P668373	Vasn	0.00373612	6.0	Pirc DSS Normal Tissue up
A_64_P035362	ENSRNOT00000043148	0.00467999	5.9	Pirc DSS Normal Tissue up
A_64_P366012	LOC100359793	0.00710975	5.9	Pirc DSS Normal Tissue up
A_64_P026993	Tmprss11e	5.76E-05	5.9	Pirc DSS Normal Tissue up
A_64_P012962	ENSRNOT00000039417	0.00510668	5.9	Pirc DSS Normal Tissue up
A_64_P108993	Klk11	0.00342956	5.9	Pirc DSS Normal Tissue up
A_64_P129780	Il17a	0.0019984	5.8	Pirc DSS Normal Tissue up
A_43_P17022	RGD1562552	1.18E-06	5.8	Pirc DSS Normal Tissue up
A_44_P404591	Hopx	3.30E-06	5.8	Pirc DSS Normal Tissue up
A_44_P352055	ENSRNOT00000042159	1.26E-05	5.7	WT DSS Normal Tissue up
A_64_P148498	Tacstd2	0.00274248	5.7	Pirc DSS Normal Tissue up
A_64_P032792	Alpi	0.000429246	5.7	WT DSS Normal Tissue up
A_64_P137481	St3gal2	4.47E-05	5.7	WT DSS Normal Tissue up
A_42_P665039	Col17a1	0.00751695	5.7	Pirc DSS Normal Tissue up
A_43_P14796	LOC682861	0.00295758	5.7	Pirc DSS Normal Tissue up
A_64_P039949	LOC679119	2.03E-08	5.6	WT DSS Normal Tissue up
A_64_P136036	Ankk1	2.49E-05	5.6	Pirc DSS Normal Tissue up
A_42_P521086	RGD1310587	0.000119158	5.6	WT DSS Normal Tissue up
A_64_P016352	Macc1	0.000184996	5.6	Pirc DSS Normal Tissue up
A_44_P273468	Slc25a4	3.59E-06	5.5	Pirc DSS Normal Tissue up
A_64_P014153	ENSRNOT00000060957	0.000499234	5.5	Pirc DSS Normal Tissue up
A_44_P269930	Mfsd2a	6.09E-05	5.5	Pirc DSS Normal Tissue up
A_64_P130999	Cd44	0.000285553	5.5	Pirc DSS Normal Tissue up
A_64_P088382	Angptl4	7.30E-05	5.4	Pirc DSS Normal Tissue up
A_64_P130189	Trpv3	3.49E-05	5.4	WT DSS Normal Tissue up
A_42_P669779	Cldn1	0.00621212	5.4	Pirc DSS Normal Tissue up
A_42_P756334	Myh6	0.000704489	5.3	WT DSS Normal Tissue up

Probe ID	Gene Symbol	p-value	Fold Change	Direction of Change
A_64_P079523	Ahnak2	1.32E-05	5.3	WT DSS Normal Tissue up
A_44_P298331	Gsdma	0.00247668	5.3	Pirc DSS Normal Tissue up
A_64_P007879	LOC689709	0.00513186	5.3	WT DSS Normal Tissue up
A_64_P086784	Runx1t1	4.30E-05	5.3	Pirc DSS Normal Tissue up
A_44_P198535	Akap12	0.00809479	5.3	WT DSS Normal Tissue up
A_42_P753675	Arhgdig	4.30E-05	5.3	Pirc DSS Normal Tissue up
A_64_P107948	ENSRNOT00000061403	0.000148271	5.2	WT DSS Normal Tissue up
A_44_P1056309	Snx8	0.00481667	5.2	Pirc DSS Normal Tissue up
A_44_P130856	LOC100360801	2.51E-05	5.2	WT DSS Normal Tissue up
A_64_P002809	A_64_P002809	0.00238961	5.2	Pirc DSS Normal Tissue up
A_43_P11444	S100g	0.00318799	5.1	WT DSS Normal Tissue up
A_64_P153702	Rnase1	0.00414448	5.1	Pirc DSS Normal Tissue up
A_64_P018751	Aqp4	4.85E-07	5.1	Pirc DSS Normal Tissue up
A_44_P183784	Akap12	0.00586965	5.1	WT DSS Normal Tissue up
A_44_P476810	Kctd4	0.00498931	5.1	Pirc DSS Normal Tissue up
A_64_P042917	FQ230482	3.44E-06	5.1	WT DSS Normal Tissue up
A_64_P016069	Krt1-5	4.16E-06	5.1	Pirc DSS Normal Tissue up
A_43_P23363	Spata22	1.08E-05	5.1	WT DSS Normal Tissue up
A_64_P061735	A_64_P061735	0.00112246	5.1	Pirc DSS Normal Tissue up
A_64_P126969	Cyp1b1	2.84E-07	5.0	Pirc DSS Normal Tissue up
A_44_P1013006	Steap1	0.00299384	5.0	Pirc DSS Normal Tissue up
A_43_P18469	Syt13	0.000618398	5.0	WT DSS Normal Tissue up
A_64_P051307	Runx2	0.00527545	5.0	Pirc DSS Normal Tissue up
A_44_P504133	Agmo	2.98E-06	5.0	WT DSS Normal Tissue up
A_64_P083730	ENSRNOT00000061042	0.000746215	5.0	Pirc DSS Normal Tissue up
A_44_P377432	Gpr98	0.000250746	5.0	Pirc DSS Normal Tissue up
A_64_P083474	Ttc9	2.84E-05	5.0	Pirc DSS Normal Tissue up
A_64_P124041	Ddx60	1.20E-06	5.0	WT DSS Normal Tissue up
A_64_P025016	Bcat1	0.00725285	4.9	Pirc DSS Normal Tissue up
A_64_P089316	Syt15	0.00700067	4.9	WT DSS Normal Tissue up
A_64_P096096	RGD1562551	0.00242921	4.9	Pirc DSS Normal Tissue up
A_44_P154513	Tmem40	0.000869091	4.9	Pirc DSS Normal Tissue up
A_44_P517258	Pck1	0.00109282	4.9	WT DSS Normal Tissue up
A_44_P1051894	Tmem132c	6.54E-05	4.9	Pirc DSS Normal Tissue up
A_64_P012709	Slc26a3	4.71E-05	4.8	WT DSS Normal Tissue up
A_64_P280765	Cd44	0.000133995	4.8	Pirc DSS Normal Tissue up
A_64_P009823	Slc39a4l	1.39E-05	4.8	Pirc DSS Normal Tissue up
A_44_P182402	Cnksr3	8.34E-06	4.7	WT DSS Normal Tissue up
A_64_P062163	RGD1306446	0.000406171	4.7	Pirc DSS Normal Tissue up
A_64_P003572	Lgr5	0.000837137	4.7	Pirc DSS Normal Tissue up
A_64_P084891	Serpib8	1.42E-05	4.7	Pirc DSS Normal Tissue up
A_44_P175041	Nr1d1	0.00683234	4.7	WT DSS Normal Tissue up
A_64_P158345	Ddx60	1.09E-05	4.6	WT DSS Normal Tissue up
A_64_P006628	Tac4	0.00237319	4.6	Pirc DSS Normal Tissue up
A_44_P482325	Fhl1	5.17E-06	4.6	WT DSS Normal Tissue up
A_64_P096822	A_64_P096822	0.00845322	4.6	Pirc DSS Normal Tissue up
A_64_P104583	Sstr2	1.89E-05	4.6	WT DSS Normal Tissue up
A_44_P961164	Rhbdl3	0.000371395	4.6	Pirc DSS Normal Tissue up
A_64_P128022	RGD1565367	0.000144281	4.6	Pirc DSS Normal Tissue up
A_64_P103936	Acot5	4.98E-05	4.6	Pirc DSS Normal Tissue up
A_44_P335974	Aldh1a7	0.00457573	4.6	Pirc DSS Normal Tissue up
A_64_P054692	Tmem212	0.000221176	4.5	WT DSS Normal Tissue up
A_43_P23187	Rimklb	0.000153287	4.5	Pirc DSS Normal Tissue up
A_64_P128833	Wnt3	0.000252597	4.5	Pirc DSS Normal Tissue up
A_44_P260036	Plau	0.000761639	4.5	Pirc DSS Normal Tissue up
A_64_P058784	Olr803	0.000570444	4.5	Pirc DSS Normal Tissue up
A_64_P055537	ENSRNOT00000048555	0.000465987	4.5	WT DSS Normal Tissue up
A_64_P022125	Gzmc	0.00516993	4.4	WT DSS Normal Tissue up
A_44_P436604	Leprel1	0.00559912	4.4	WT DSS Normal Tissue up
A_64_P061765	Fam89a	5.54E-05	4.4	Pirc DSS Normal Tissue up
A_64_P049515	Tmem45a	0.00126951	4.4	WT DSS Normal Tissue up
A_44_P309643	Trps1	0.0034398	4.4	Pirc DSS Normal Tissue up
A_64_P158148	Cnksr3	3.62E-06	4.4	WT DSS Normal Tissue up
A_44_P311917	LOC680758	4.48E-05	4.4	Pirc DSS Normal Tissue up
A_64_P166203	XM_341720	5.80E-05	4.3	Pirc DSS Normal Tissue up

Probe ID	Gene Symbol	p-value	Fold Change	Direction of Change
A_64_P049371	Gpha2	0.0023565	4.3	Pirc DSS Normal Tissue up
A_64_P075734	TC603221	0.0032012	4.3	Pirc DSS Normal Tissue up
A_64_P112141	Ptpn13	0.00161544	4.3	Pirc DSS Normal Tissue up
A_44_P525270	RGD1308544	6.13E-05	4.3	WT DSS Normal Tissue up
A_44_P286341	Grhl1	0.00692464	4.3	Pirc DSS Normal Tissue up
A_64_P038926	Prodh	4.08E-09	4.3	Pirc DSS Normal Tissue up
A_64_P068333	Zc3h12a	0.000111577	4.3	Pirc DSS Normal Tissue up
A_64_P070628	ENSRNOT00000009196	0.00325231	4.3	WT DSS Normal Tissue up
A_64_P124354	Car8	1.39E-05	4.3	Pirc DSS Normal Tissue up
A_64_P013164	A_64_P013164	2.46E-06	4.3	WT DSS Normal Tissue up
A_44_P445044	Apold1	0.00903718	4.3	WT DSS Normal Tissue up
A_43_P16403	Clca1	0.00145192	4.3	WT DSS Normal Tissue up
A_44_P127337	Rbpms	0.00251579	4.3	Pirc DSS Normal Tissue up
A_64_P054923	LOC680029	0.00269264	4.2	Pirc DSS Normal Tissue up
A_64_P033895	Mt4	0.00471438	4.2	WT DSS Normal Tissue up
A_64_P062670	Chst8	0.00083398	4.2	WT DSS Normal Tissue up
A_64_P048972	Tmtc1	0.00128071	4.2	WT DSS Normal Tissue up
A_64_P013758	Hp	0.000646627	4.2	Pirc DSS Normal Tissue up
A_64_P022015	Sstr2	4.89E-06	4.2	WT DSS Normal Tissue up
A_44_P233569	Gnb5	3.88E-06	4.2	WT DSS Normal Tissue up
A_64_P092782	Wnt16	0.00301614	4.2	Pirc DSS Normal Tissue up
A_42_P476474	Fhl1	4.84E-05	4.1	WT DSS Normal Tissue up
A_64_P151259	A_64_P151259	0.000227685	4.1	Pirc DSS Normal Tissue up
A_64_P397292	Prdm4	0.00267831	4.1	Pirc DSS Normal Tissue up
A_44_P1020311	RGD1562629	0.000567071	4.1	WT DSS Normal Tissue up
A_64_P125973	Tnfrsf1b	0.000177617	4.1	Pirc DSS Normal Tissue up
A_64_P070942	Ankk1	0.000127778	4.1	Pirc DSS Normal Tissue up
A_64_P100078	Cd274	0.00577504	4.1	Pirc DSS Normal Tissue up
A_43_P12032	Slc14a2	0.000140444	4.1	WT DSS Normal Tissue up
A_44_P508066	Nnat	0.0003137	4.1	Pirc DSS Normal Tissue up
A_64_P012907	Mep1a	8.67E-06	4.1	WT DSS Normal Tissue up
A_64_P067923	RGD1564149	0.000148248	4.1	WT DSS Normal Tissue up
A_64_P061740	Trpv1	0.00025864	4.1	WT DSS Normal Tissue up
A_64_P142395	Zc3h7b	1.17E-06	4.1	Pirc DSS Normal Tissue up
A_64_P050999	Sema7a	0.00975471	4.0	Pirc DSS Normal Tissue up
A_43_P12374	Lpar3	0.000648467	4.0	Pirc DSS Normal Tissue up
A_64_P012471	LOC689740	0.000820903	4.0	Pirc DSS Normal Tissue up
A_44_P328062	Edn3	0.00118479	4.0	WT DSS Normal Tissue up
A_44_P433147	Gnat3	1.30E-05	4.0	WT DSS Normal Tissue up
A_44_P326259	Iffo1	8.28E-05	4.0	WT DSS Normal Tissue up
A_64_P150509	Ccr10	0.000126461	4.0	Pirc DSS Normal Tissue up
A_44_P252441	St3gal2	0.00225099	4.0	WT DSS Normal Tissue up

**Supplementary Table S-8.** Genes differentially expressed in normal colonic tissue between tumor-free and tumor-positive Pirc rats

Probe ID	Gene Symbol	p-value	Fold Change	Direction of Change
A_64_P110708	XM_341286	0.4488	5.4	tumor-positive up versus tumor-free
A_44_P231628	Snpc2	0.2247	4.7	tumor-positive up versus tumor-free
A_44_P456769	Ncr1	0.4766	4.6	tumor-positive up versus tumor-free
A_44_P137893	Ptpn20b	0.3150	4.3	tumor-positive up versus tumor-free
A_64_P027477	Olr89	0.4911	4.2	tumor-positive up versus tumor-free
A_64_P007183	RGD1563842	0.0002	3.8	tumor-positive up versus tumor-free
A_44_P304759	A_44_P304759	0.0553	3.7	tumor-free up versus tumor-positive
A_64_P127576	Mpz	0.0433	3.6	tumor-free up versus tumor-positive
A_64_P021921	A_64_P021921	0.0463	3.5	tumor-free up versus tumor-positive
A_64_P139024	ENSRNOT00000021857	0.0273	3.4	tumor-positive up versus tumor-free
A_64_P297256	LOC498752	0.0415	3.3	tumor-free up versus tumor-positive
A_44_P126498	Klhdc1	0.0853	3.3	tumor-positive up versus tumor-free
A_44_P180731	Zfpm2	0.2027	3.3	tumor-positive up versus tumor-free
A_44_PP360767	Spink3	0.2397	3.3	tumor-free up versus tumor-positive
A_64_P088665	Olr898	0.4391	3.2	tumor-positive up versus tumor-free
A_64_P152753	RGD1566380	0.0284	3.1	tumor-free up versus tumor-positive
A_43_P15498	Chrng	0.0822	3.1	tumor-free up versus tumor-positive
A_64_P053756	A_64_P053756	0.0182	3.0	tumor-positive up versus tumor-free